

ABSTRACT

KAMRATH, BROCK JACOB WATSON. Improving Performance and Examining Expansion of Constructed Wetlands for Tertiary Treatment of Nitrogen Removal from Domestic and Municipal Wastewater (Under the direction of Dr. Michael R. Burchell II).

Constructed wetlands have the potential to be an invaluable tool to reduce nitrogen loads to downstream waterbodies. However, for this tool to be effective, it must be maintained. The studies conducted as part of this dissertation demonstrate the need to maintain free water surface (FWS) constructed wetlands (CWs) to sustain their treatment efficiency over time, help to address the knowledge gap in long-term or late-stage nitrogen removal performance in FWS CWs, and evaluate the potential for FWS CWs to provide nitrogen removal at minor wastewater treatment plants (WWTPs) across the state of North Carolina (NC).

Water quality sampling and flow monitoring were conducted for thirty-five months (September 2018 – May 2021) at the two 20+ year old parallel FWS CWs within the Walnut Cove WWTP (one of three WWTPs with currently operational treatment wetlands in NC). Over the first seven months of monitoring, TN loads were reduced by 11% or less and nominal TN removal rates were only $0.1 \text{ g-N m}^{-2} \text{ d}^{-1}$ in both cells, which demonstrated that nitrogen removal in the aging wetland cells was well below what has been observed at other FWS CWs treating nitrogen-enriched wastewater. The results of the study suggested that poor performance was linked to unfavorable inlet nitrogen speciation and the accumulation of a substantial detritus substrate that had developed over time.

A laboratory experiment was conducted to quantify and model $\text{NH}_4\text{-N}$ release from the accumulated detritus substrate. A simple first-order kinetic model using two parameters, the porewater $\text{NH}_4\text{-N}$ concentration (C_{pw}) and the rate constant (k_u), was proposed to represent the upward diffusion of $\text{NH}_4\text{-N}$ from the substrate porewater to the overlying water column.

Parameter values were calibrated for 23 of the 27 wetland microcosms (mean $R^2 = 0.85$). Values ranged from 4.7 to 21.5 mg-N L⁻¹ for C_{pw} and 0.004 to 0.13 m d⁻¹ (1.5 to 47.4 m yr⁻¹) for k_u . The potential areal ammonium release rates (J_{UF}) from the detritus substrate at an overlying water column concentration of 4 and 6 mg L⁻¹ were 0.21 and 0.14 g-N m⁻² d⁻¹ (70 and 50 g-N m⁻² yr⁻¹), respectively. At these rates, NH₄-N diffusion from the detritus substrate would substantially influence N removal performance in lightly loaded systems (TKN load < 120 g-N m⁻² yr⁻¹). These results provided both an initial estimate of the magnitude of N release from an accumulated detritus substrate and evidence to support regular FWS CW maintenance.

To improve nitrogen removal at the site, a detritus removal and revegetation was conducted in wetland cell 1. The detritus removal was conducted at a relatively low cost (less than 15,000\$ per ha) and in a relatively low amount of time (~ 5 days). Continued monitoring over the next 24 months found that the detritus removal improved the hydraulic efficiency and the nitrogen removal performance in cell 1 (TN removal efficiency of 19%) relative to the non-cleaned out cell 2 (TN removal efficiency of -9%). This improved performance provided the first evidence for the use of a detritus removal to improve nitrogen removal.

To evaluate if increased pretreatment could enhance nitrogen removal at the site, a one month long in-situ NO₃-N dosing study was conducted in spring 2021. On a nominal area basis, the NO₃-N mass removal rates in both cells were approximately 0.2 g-N m⁻² d⁻¹ (75 g-N m⁻² d⁻¹). This substantial NO₃-N removal improved the total dissolved nitrogen (TDN) removal efficiency and indicated that improved pretreatment could be used improve nitrogen removal in FWS CWs receiving non-nitrified wastewater. It also suggested that the influence of operational age on nitrogen removal may be a function of inlet nitrogen speciation in FWS CWs.

To assess the total amount of nitrogen released from package plant type minor WWTPs in NC, water quality samples were collected from the effluent of the Danbury WWTP (a minor WWTP in Danbury, NC) biweekly in 2019. The annual effluent TN load for that year indicated that an additional 755 kg of unaccounted-for nitrogen, mostly in the form of NO₃-N, were released from the minor WWTP. Because of the potential for these plants to release substantial NO₃-N loads, the targeted use of relatively small FWS CWs for tertiary treatment at these WWTPs could provide an opportunity for improved nitrogen removal in NC. For example, a small 0.2 ha (0.5 acre) FWS CW could remove 50% (~400 kg yr⁻¹) of effluent NO₃-N load at the Danbury WWTP effluent.

© Copyright 2021 by Brock Jacob Watson Kamrath

All Rights Reserved

Improving Performance and Examining Expansion of Constructed Wetlands for Tertiary
Treatment of Nitrogen Removal from Domestic and Municipal Wastewater

by
Brock Jacob Watson Kamrath

A dissertation submitted to the Graduate Faculty of
North Carolina State University
in partial fulfillment of the
requirements for the degree of
Doctor of Philosophy

Biological and Agricultural Engineering

Raleigh, North Carolina
2021

APPROVED BY:

Dr. Michael R. Burchell II
Committee Chair

Dr. Tarek Aziz

Dr. Ashley Beck

Dr. François Birgand

Dr. Natalie Nelson

DEDICATION

To Audrey,
You are my rock. This dissertation could not have been completed without your love, patience,
ideas, kindness, support, and humor.

I Love You.

To Mom, Dad, and Bill
Thank you for your unconditional love and support.

To Nick,
Thanks for being my guiding light along the way, Go Hawks!

BIOGRAPHY

Brock Jacob Watson Kamrath was born on May 22nd, 1993, in Springfield, IL to Stuart Kamrath and Angela Kamrath-Hodson. He grew up just north of Springfield in Sherman, IL with his parents and his older brother, Nick.

He graduated from Williamsville High School in 2011. After high school, Brock attended the University of Iowa where he pursued a civil engineering degree with a focus in water quality. In 2015, He received his B.S.E in Civil Engineering with an emphasis in environmental engineering. During his time at Iowa, his interest in research was sparked by his work as an undergraduate research assistant in Dr. Keri Hornbuckle's laboratory. After graduation, he accepted an engineering position at Andrews Engineering, Inc., where he worked on a variety of projects focused on landfill construction and remediation projects. After working at Andrews for a little over one year, Brock accepted an offer to study under Dr. Michael Burchell II in the Department of Biological and Agricultural Engineering at North Carolina State University.

Following the completion of his Master's degree in the June 2018, Brock continued to expand his focus on water quality treatment systems in his Ph.D. His Ph.D. research focused on improving the nitrogen removal performance of aging FWS CWs and evaluating management and maintenance techniques that could be used to extend their design life. Upon completion of his Ph.D., Brock will be accepting an ORISE post-doctoral fellowship at the U.S. EPA at the RTP Campus in Durham, NC. In this position, he will begin research in environmental pollutant fate and transport modeling with a focus on identifying the most effective alternative practices for minimizing the environmental impacts of different anthropogenic activities.

ACKNOWLEDGMENTS

It is often said that nothing great is ever accomplished alone and I could not have completed this project without all the people that assisted me in my time at North Carolina State University. First and foremost, I would like to give special thanks my advisor, Dr. Mike Burchell. Your decision to offer me a position in your lab 5 years ago started my journey through grad school and provided me with a fantastic opportunity to pursue my career goals. You have provided guidance when needed, patience as I worked to improve my research and writing skills, and perhaps most importantly, you helped me slow down when I get ahead of myself and pushed me when I started to drag my feet.

In addition to my advisor, I am particularly indebted my initial colleague in Dr. Burchell's research team, Jack Kurki-Fox. He deserves an enormous thanks for helping me in the lab, in the field, in the office, in life, and on the intramural fields. You "showed me the ropes" in research and my graduate career would not have been nearly as successful without your help and guidance. I would also like to thank my committee members, Dr. François Birgand, Dr. Natalie Nelson, Dr. Tarek Aziz, and Dr. Beck, for their assistance in keeping me on the right track and providing additional understanding on topics that were new to me. An additional thanks to Fred Summers, Tommy Stephenson, Jay Campbell, Justin Macialek, Jonathan Lewis, Jerry Yu, and the Walnut Cove Public Works Department for their help in the field and the laboratory. I would like to thank all the fellow graduate students that I got to work with over these last 5 years. It has been an honor to share the halls of Weaver with you and I have made several lifelong friends in the process. I would also like to thank the officemates I've had the pleasure of working with during my five years in Weaver, Alex Geddie, Rebecca Purvis, Russell Smith, and Piyush Patil.

You have all allowed me to work through ideas aloud and put up with my occasional foot tapping and desk drumming.

In general, I would like to thank all the friends who have helped make this process easier and my life better. I would like to give another special thanks to my wonderful wife Audrey. You have been incredibly supportive during my pursuit of this degree. Thank you for listening to me go on and on about wetlands, nitrogen pollution, bad field days, and water quality sampling. You have always been there to say that I can do it, I love you. Finally, I would like to thank my family for their support in my decisions, the guidance they have given to me, and for allowing me the opportunity to focus on my goals throughout my life.

In addition to the help and guidance of many gracious individuals in my quest to complete my research projects, I also wish to acknowledge and thank both the Water Resources Research Institute (WRRI) and NC Sea Grant for providing the funding to make this research possible.

TABLE OF CONTENTS

CHAPTER 1: Introduction	1
Motivation: Improving nitrogen removal in North Carolina	1
Treatment wetlands	3
Mechanisms for nitrogen removal within FWS CWs	5
Knowledge gaps in long-term and late-stage performance data	7
Limited monitoring data undermines late-stage management and operational optimization....	10
State of FWS CWs treating wastewater in NC	12
Objectives and hypothesis	13
Overall Objectives	13
Specific Objectives:	14
Dissertation Overview	15
References	17
CHAPTER 2: Nitrogen removal in an aging free water surface wetland receiving ammonia-dominated lagoon effluent	23
Abstract	23
Introduction	24
Methods and materials	29
Site Description	29
Data Collection	32
Data Analysis	35
Nitrogen dynamics	45
Results	48
Hydraulics	48
Hydrology	52
Water quality analysis	55
Nitrogen removal performance	60
Nitrogen dynamics	62
Discussion	64
Age influences treatment through detritus accumulation	64
Study Limitations	65
Conclusion	68
References	70

CHAPTER 3: Estimating ammonium-release from accumulated detritus in a free water surface constructed wetland	75
Abstract.....	75
Introduction.....	76
Methods and Materials	80
Experimental design	80
Water quality analysis	83
Nitrogen dynamics	84
Statistical analysis	87
Results	88
NH ₄ -N concentration changes.....	88
Water quality parameters.....	90
Model calibration	91
Statistical analysis	94
Modeled internal nitrogen release at the Walnut Cove WWTP.....	97
Discussion.....	99
The potential for an accumulated detritus substrate to be an internal nitrogen source in constructed wetlands	99
Nitrogen dynamics model validation	100
Potential application of results.....	102
Conclusion	104
References.....	106
CHAPTER 4: Detritus removal to improve nitrogen removal and extend the useful life of a free water surface constructed wetland in NC.....	108
Abstract.....	108
Introduction.....	109
Methods and materials.....	112
Site description.....	112
Detritus Removal.....	113
Hydrology	115
Internal hydraulics.....	117
Water quality sampling.....	121
Nitrogen removal performance	123
Results & Discussion	125
Detritus removal.....	125

Hydrology	127
Internal hydraulics.....	129
Water quality parameters.....	132
Nitrogen concentrations.....	137
Load removal	142
Mass removal rates.....	143
Influence of seasonality	144
Future for detritus removal to improve nitrogen removal	147
Study limitations	148
Conclusion	149
References.....	151
CHAPTER 5: In-situ nitrate dosing to evaluate the influence of pretreatment and age on nitrogen removal in treatment wetlands	154
Abstract.....	154
Introduction.....	155
Materials and methods.....	158
Site monitoring.....	158
Nitrate Dosing	159
Data Collection.....	162
Nitrogen removal performance	166
Results	168
Site Conditions.....	168
Nitrogen removal performance	174
Discussion.....	179
Improved pretreatment to improve nitrogen removal	179
Operational age as an influence on NO ₃ -N removal	180
The influence of age on total nitrogen removal	183
Conclusion	184
References.....	185
CHAPTER 6: Assessment of nitrogen release from a minor WWTP and potential for FWS CW implementation to improve nitrate removal	188
Abstract.....	188
Introduction.....	189
Methods and Materials	191
Site Description.....	191

Data Collection.....	193
Data Analysis	194
Results	197
Danbury WWTP Effluent	197
Wetland Design.....	202
Discussion.....	205
Unaccounted-for nitrogen load from a minor WWTP	205
Potential Danbury WWTP wetland.....	206
Widespread implementation of FWS CWs for tertiary treatment at minor WWTPs enhances NO ₃ -N removal.	208
Future Work.....	208
Conclusion	209
References.....	211
CHAPTER 7: Summary and Conclusions.....	214
Summary.....	214
Major Conclusions	215
Areas of Future Work.....	217
The effectiveness and frequency of maintenance methods (Maintain to sustain)	217
Detailed estimate of nitrogen release from minor WWTPs and cost to implement FWS CWs across NC	220
Treatment Wetland Database.....	221
Overall Conclusion.....	221
References.....	222
APPENDICES	223
Appendix A: Hydraulic Analysis.....	224
Appendix B: Evapotranspiration Calculation.....	240
Appendix C: Linear relationships between Q _{in} and Q _{out} at both outlets	245
Appendix D: Chapter III Supplemental Information	258
Appendix E: Chapter IV Supplemental Information	286
Appendix F: Chapter V Supplemental Information	305
Appendix G: Chapter VI Supplemental Information	312

LIST OF TABLES

Table 2.1: Ranges of performance for the three evaluated hydraulic indexes. Ranges modified from thresholds presented in Liu et al. (2020) and Persson et al. (1999). ...	41
Table 2.2: Results from the inert tracer tests performed in March 2019. These results represent the average of two tests run in cell 1 and the one test run in cell 2 during this period. Values of e , τ , N , λ_e are averages of the values derived from both the moments and gamma distribution methods for analyzing a residence time distribution (RTD).	50
Table 2.3: Average hydraulic indices for both cells over the study period. The three dimensionless parameters (λ_e , t_{10} , $\sigma\Phi^2$), were averaged over both the moment and gamma fit analysis.	51
Table 2.4: The water budget for both cells. Inflow and outflow rates are the sum of the daily flow rates at each location. Precipitation and evapotranspiration were assumed to be the same for both cells. Both cumulative volumes and depths of precipitation and evapotranspiration were reported. A positive error indicated inflow was greater than outflow for the period. Residual term includes possible water lost to infiltration and errors in flow estimates and climatic measurements.	54
Table 2.5: Nominal hydraulic residence time (HRT), mean residence time (τ), nominal hydraulic loading rate (HLR), and effective HLR using the median inflow to both cells. Nominal values are based on design volumes and design surface areas for the cells. Mean residence time and effective HLR use the effective volumes and areas of the cells based on the tracer test data.	55
Table 2.6: Average values of mid-day water quality parameters measured during the period from 9/1/2018 to 3/31/2019. No measurements were taken in November, December, or January. The inlet sampling station samples the influent waste stream immediately before it enters the two wetland cells and therefore can be assumed to represent the influent to both cells.....	56
Table 2.7: Average concentrations of nitrogen species at each sampling location during the period from 9/1/2018 to 3/31/2019. The inlet sampling station samples the influent waste stream immediately before it enters the two wetland cells and therefore represents the influent to both cells.	57
Table 2.8: Concentration change through the wetland based on mean concentrations during the study period. A positive change indicated a decrease through the wetland and a negative change indicated an increase through the wetland.	58
Table 2.9: Influent and effluent loads for each nitrogen during the period from 11/1/2018 to 3/31/2019 (151 days).	60
Table 2.10: Areal mass removal rate of nitrogen species within each wetland during the period from 11/1/2018 to 3/31/2019 (n = 151 days). A positive areal mass removal rate indicated a retention, and a negative areal mass removal rate indicated an internal release. J_{nom} was the nominal removal rate and J_{eff} was the effective removal rate.	61

Table 3.1: The initial NH ₄ concentrations in the source water relative to the target initial NH ₄ concentrations for each experimental run.	82
Table 3.2: The mean NH ₄ -N concentrations on each sampling day for each initial NH ₄ -N concentration in each experimental run. Day 0 represented the NH ₄ -N concentrations approximately 1 hour after the microcosms were prepared. The high increase in NH ₄ -N concentrations in this short period was likely due to the mixing associated with creating the wetland microcosms.	89
Table 3.3: Two-way ANOVA results. Treatment (initial NH ₄ concentration) and block (experimental run) were evaluated for their effect on areal NH ₄ release rate (J _{UF}). These rates represent ammonium release over a seven-day.....	92
Table 3.4: Two-way ANOVA results. Treatment (initial NH ₄ concentration) and block (experimental run) were evaluated for their effect on areal NH ₄ release rate (J _{UF}). These rates represent ammonium release over a seven-day.....	93
Table 3.5: One-way ANOVA results. Experimental runs (Run) were evaluated for their effect on the calibrated C _{pw} values.....	94
Table 3.6: One-way ANOVA results. Experimental runs (Run) were evaluated for their effect on the calibrated k _u values.....	95
Table 3.7: Upward flux (J _{UF}) ranges expected in the wetland using modeling results from the microcosm experiments. The values are reported in g-N m ⁻² d ⁻¹ and the interval corresponded to the expected range of influent NH ₄ -N concentrations to the Walnut Cove wetland cells.....	98
Table 4.1: Overview of tracer experimental setup. Period is broken down into pre-wetland (Pre) and post-wetland rejuvenation (Post). Time interval is the sampling time interval. Sampling start refers to the time at which sampling was initiated after tracer injection (t ₀). Note that variable time interval indicates variable sampling frequency used to better capture changes in tracer breakthrough.	119
Table 4.2: Ranges of performance for the three evaluated hydraulic indexes. Ranges modified from thresholds presented in Liu et al. (2020) and Persson et al. (1999). This table refers back to Table 2.1.....	120
Table 4.3: Results from heavy metal analysis of detritus sample. All values are in units of mg/kg DW.....	126
Table 4.4: Summary of median monthly hydrology for both wetland cells at the Walnut Cove WWTP during the monitoring period (June 2019 through May 2021). Inflow, precipitation, and evapotranspiration were assumed to be equal in both cells. Median and mean residuals based on the monthly volumes for each term in the water budget.....	127
Table 4.5: Results from tracer test RTD analysis. Values represent averages by cell, period, and capacity. Cells were maintained at a nominal pool depth of 0.3 m for the duration of the study, except Cell 1, which was held at half-capacity (HC) until August 2019 after detritus removal. Values from both RTD analysis methods were included in the averages.	131

Table 4.6: Average hydraulic indices for both wetland cells over the study period. The three dimensionless parameters (λ_e , t_{10} , σ_{ϕ^2}) were averaged over both the moment and gamma fit analysis.	131
Table 4.7: Central tendencies and ranges of mean monthly temperature, dissolved oxygen, pH, and specific conductivity during the study period. Values calculated from measurements taken during site visits.....	135
Table 4.8: Mean (SD) of monthly nitrogen concentrations from June 2019 through May 2021. Percent reduction derived from median values reported here. Continuous data was not collected from March 2020 through August 2020. Site wide floods removed February, November, and December 2020 from analysis. Nitrate dosing study in April 2021 was removed from analysis. All concentrations in mg-N L^{-1}	138
Table 4.9: Cumulative loading from June 2019 through May 2021, excluding April 2021. April 2021 was excluded because that was the $\text{NO}_3\text{-N}$ dosing period, which was explored in-depth in chapter 5. Data were filled using linear interpolation for March 2020 through August 2020 for TDN and TN. All loads are in $\text{kg (kg d}^{-1}\text{)}$	143
Table 4.10: The average daily nominal and effective areal mass removal rates (J_{nom} and J_{eff} , respectively) for each nitrogen species within each wetland from June 2019 through May 2021, excluding April 2021. A positive mass removal rate indicated a retention, and a negative mass removal rate indicated an internal release.....	144
Table 5.1: Mean values for daytime temperature, dissolved oxygen, and pH for the dosing run, which ran from March 21 st , 2021 to April 20 th , 2021.....	168
Table 5.2: Hydraulic conditions within the two FWS CW cells at the Walnut Cove WWTP during the nitrate dosing period. The number of tanks (N) and the volumetric efficiency (e) were used as part of equations 5.5 and 5.6 to estimate a nitrate removal rate constant for each wetland cell.	174
Table 5.3: Flow-weighted average concentrations of nitrogen species at each sampling location during the period from 3/21/2021 to 4/21/2021. The inlet sampling station represents influent to both cells.....	175
Table 5.4: Concentration change through the wetland based on flow weighted mean concentrations during the study period. A positive change indicated a decrease through the wetland and a negative change indicated an increase through the wetland.	175
Table 5.5: Influent and effluent loads for each nitrogen species during the dosing run 3/21/2021 to 4/21/2021 ($n = 31$ days). Loads were presented in kg , with kg d^{-1} reported in parentheses. The load reduction and removal efficiency were bolded. ..	177
Table 5.6: Areal mass removal rates of nitrogen species within each wetland during the period from 3/21/2021 to 4/21/2021 ($n = 31$ days). A positive removal rate indicated a retention, and a negative removal rate indicated an internal release. J_{nom} was the nominal areal mass removal rates and J_{eff} was the effective areal mass removal rate.....	178

Table 5.7: Three scenarios to examine effect of improved pretreatment on nitrogen removal in the Walnut Cove wetlands. The influent nitrogen speciation was based on the general values observed in this chapter, along with chapters 2 and 4. The no change scenario included no improvement in upstream pretreatment. Scenarios 2 & 3 included improved upstream pretreatment, at 25% or 75% of the influent NH ₄ -N was nitrified before entering the two wetland cells.	180
Table 6.1: Annual effluent NH ₄ -N loads (in kg and lbs.) from the Danbury WWTP for 2016-2019 as reported in the ECHO database.	199
Table 6.2: Statistical summary of monthly effluent nitrogen data from grab samples in 2019 (n = 12). Concentrations are shown in units of mg L ⁻¹	200
Table 6.3: Comparison of the nitrogen removal (in kg yr ⁻¹), capital costs, and potential nitrogen credits for both the 50% and the 90% removal options.	207

LIST OF FIGURES

Figure 2.1: Monthly mean NH₄-N concentrations, TN concentrations, and effluent flow rates from 1996 through 2017 at the Walnut Cove WWTP. The blue lines represent the trend in the data using a local polynomial regression (loess) fitting. The red dashed line in the NH₄-N plot represents the discharge limit (10 mg-N L⁻¹) for NH₄-N in the plant effluent. Please note that while the red line is continuous in this plot, the limit is only in effect from April through October each year.26

Figure 2.2: Changes in NH₄-N and TN concentrations in the plant effluent between the first decade of operation (1996-2006) and the second decade of operation (2007-2017).26

Figure 2.3: Top: Aerial photograph of the WWTP (Image modified from Google Maps). Arrows indicate flow direction. Raw IN is the location of the raw wastewater inlet. The primary and secondary lagoons are labeled lagoon 1 and lagoon 2, respectively. Duckweed raceway is labeled as such, and the duckweed collector is outlined by a dashed line. FWS CW cells are labeled as Cell 1 and Cell 2. Bottom: Closer look at wetland configuration. Sampling stations are shown with red circles and the weather station is shown with a blue star.30

Figure 2.4: Left: External view of a sampling station. The 30 W solar panel visible on top of station. Right: Internal view of a sampling station. The 6712 Portable Teledyne ISCO automated sampler integrated with 730 Bubbler Flow Module and two 12-volt deep cycle batteries are visible.32

Figure 2.5: An example of a submerged weir caused by a flow blockage at the outlet of cell 2 on September 18, 2018.34

Figure 2.6: Results and analysis of the experiment initiated on March 8th, 2019. This experiment was a pilot test for site and only cell 1 was investigated. Vertical lines represent mean actual residence time (τ) and nominal residence time based on plug-flow characteristics (t_{nom}). The blue line represents the RTD built from the method of moments. The red line represents the RTD built from fitting a gamma distribution.48

Figure 2.7: Results and analysis of the experiment initiated on March 23rd, 2019. Vertical lines represent mean actual residence time (τ) and nominal residence time based on plug-flow characteristics (t_{nom}). The blue line represents the RTD built from the method of moments. The red line represents the RTD built from fitting a gamma distribution.49

Figure 2.8: Areal view of the tracer tests initiated on March 23rd, 2019. Limited vegetation coverage is apparent in this photograph. This photo was taken approximately 6 hours after the dye was released. Preferential flow paths are visible in cell 1 (left). The preferential flow paths for cell 2 (right) did not begin until the last half of the cell.51

Figure 2.9: Observations of detritus substrate in the FWS CWs. The pictures show detritus substrate above the water level in some places with channelized flow paths cutting through the detritus. Although the cells are vegetated, the vegetation was

not in contact with the wastewater, but was instead growing on the accumulated detritus.	52
Figure 2.10: Average daily flow rates at the inlet and outlet of both cells over the study period.....	53
Figure 2.11: Cumulative daily flow rates at the inlet and outlet of both cells over the study period.....	53
Figure 2.12: Concentrations of ON, NH ₄ -N, NO ₃ -N, and TN in composite samples collected from the sampling stations (inlet, outlet 1, and outlet 2). Boxplots indicate the median and interquartile range.....	58
Figure 2.13: Estimated effective removal rates for nitrogen in the two FWS CWs at the Walnut Cove WWTP from November 2018 through March 2019. All values are in g-N m ⁻² d ⁻¹	63
Figure 3.1: Diagram nitrogen processing in the detritus impacted FWS CW wetlands. 30 cm of accumulated detritus has greatly reduced the depth of the water column. The aerobic zone has been expanded to better present nitrogen processing. The actual aerobic or oxidized zone would only be less than 1 cm in depth. Diagram modified from nitrogen cycling presented in Kadlec and Wallace (2009).	77
Figure 3.2: NH ₄ -N concentrations in the porewater experiments a) installed on October 25th, 2019, b) installed on January 10th, 2020.	79
Figure 3.3: Top left: Microcosms from run 1 after detritus substrate addition. Note that the depth of the detritus is approximately 9 cm (0.3 ft). Top right: A microcosm from run 3 after detritus and source water addition. Bottom: a picture of the nine microcosms covered by a black tarp to limit light penetration.	81
Figure 3.4: Experimental setup for each run. Nine microcosms were created from a new batch of detritus for each run. In each run, three target initial NH ₄ -N concentrations were applied in triplicate.	82
Figure 3.5: Return of NH ₄ -N produced within the detritus substrate to the overlying water column.	85
Figure 3.6: The measured NH ₄ -N concentrations over time for each experimental unit. The plots are split by experimental run. The x-axis represented days since the microcosms were started. The y-axis represented the NH ₄ -N concentrations in the overlying water column.	90
Figure 3.7: Changes in water quality parameters (Temperature, pH, DO (%), and Specific Conductivity) over the study period. Units are different for each parameter and noted on the y-axis label.	91
Figure 3.8: Density plots of calibrated parameter values C _{pw} and k _u for every experimental unit (n = 27). The plots show the relative distribution of calibrated values. Density estimate was scaled to maximum of 1.	93

Figure 3.9: Density plots of calibrated parameter values C_{pw} and k_u for the remaining experimental units ($n = 24$). The plots show the relative distribution of calibrated values. Density estimate was scaled to maximum of 1.	94
Figure 3.10: Calibrated C_{pw} values (in, $mg-N L^{-1}$) for each experimental run ($n = 23$). Solid dots represent the mean for each run and error bars represent the standard error. Each run was compared using post-hoc Tukey's HSD. <i>ns</i> indicated no significant difference. ** indicated a p-value < 0.01	95
Figure 3.11: Calibrated k_u values (in, $m d^{-1}$) for each remaining experimental run ($n=23$). Solid dots represent the mean value for each run and error bars represent the standard error. Each run was compared using post-hoc Tukey's HSD. <i>ns</i> indicated no significant difference. * indicated a p-value < 0.05	96
Figure 3.12: Calculated upward flux (J_{UF}) values for each run (1, 2, and 3) and each water column NH_4-N concentration (2, 4, 6, 8, and $10 mg L^{-1}$) ($n = 23$). The black dot represented the mean J_{UF} value, and the error bars represented the standard error. ..	98
Figure 4.1: Left: thickness of accumulated detritus in cell 1. Right: View of wetland cell 1 immediately prior to clean out. Unvegetated short-circuit paths were evident.	111
Figure 4.2: Aerial photograph of the two wetland cells (Image modified from Google Maps). The arrows indicate flow direction. Sampling stations are shown with red circles and the weather station is shown with a blue star.	113
Figure 4.3: Left: the excavator removing detritus from the first half of cell 1. Right: An areal view of both wetland cells during the detritus removal of cell 1. Cell 1 is the top cell in this picture.....	114
Figure 4.4: View of the cell 1, taken from the inlet, shows the removed detritus placed on the cell side slopes and the replanted cattail clumps within the FWS CW basin. ...	114
Figure 4.5: Left: view of cell 1, taken from just to the right of the cell inlet, soon after the cell was brought back online in mid-May 2019. Right: View of cell 1, taken from the cell inlet, at the start of the July 26 th , 2019, tracer tests with vegetation reestablished.....	115
Figure 4.6: Hydrologic data from the study site during the monitoring period (June 2019 through May 2021). Top: the monthly median inflow and outflow of both cells during the period. Note the inlet flows were the same to both cells. Middle: the monthly precipitation and ET depths (mm) at the site. These were assumed to be the same for both cells. Bottom: Cumulative monthly volumes (m^3) for each term in the water budget.	128
Figure 4.7: Results from the experiment initiated on January 31st, 2020. Vertical lines represent mean actual residence time (τ) and nominal residence time (t_n). The blue line represents the method of moments RTD, while the red line represents the gamma distribution RTD.	130
Figure 4.8: Mean monthly water quality parameter measurements (temperature, dissolved oxygen (DO), pH, and specific conductivity) during the monitoring period. IN, OUT1, and OUT2 refer to measurements taken at the inlet splitter box, the cell 1 outlet, and the cell 2 outlet, respectively.	136

Figure 4.9: Mean monthly concentrations of NO ₃ -N and NH ₄ -N in grab samples collected at OUT1 (cell 1 outlet or detritus removal treatment) and OUT2 (cell 2 outlet or control) during weekly site visits. Within the boxplots, the lines connected mean monthly outlet concentrations for each month.....	139
Figure 4.10: Mean monthly concentrations of DON and ON from weekly composite samples collected at OUT1 (cell 1 outlet or detritus removal treatment) and OUT2 (cell 2 outlet or control). Within the boxplots, the lines connected mean monthly outlet concentrations for each month.....	139
Figure 4.11: Mean monthly concentrations of TDN and TN in weekly composite samples collected at OUT1 (cell 1 outlet or detritus removal treatment) and OUT2 (cell 2 outlet or control). Within the boxplots, the lines connected mean monthly outlet concentrations for each month.	140
Figure 4.12: Average NH ₄ -N and NO ₃ -N concentrations over the 24-month study period. Spring data were limited by the lack of grab sampling in April and May 2020 due to the COVID 19 pandemic and the removal of April 2021 data which included the nitrate dosing study discussed in chapter 5. Here spring is April-June, summer was July-September, fall was October-December, and winter was January-March.....	146
Figure 5.1: Aerial photograph of the two wetland cells (Image modified from Google Maps). The arrows indicate flow direction. Sampling stations are shown with red circles and the weather station is shown with a blue star.	158
Figure 5.2: A schematic of the continuous dosing setup. Arrows represent the flow direction..	161
Figure 5.3: Top Left: Filling tank #3 with Ca(NO ₃) ₂ fertilizer and source water being added. Top Right: All three tanks connected and tarped with the distribution container visible in the foreground. Bottom Left: The dosing setup with the 0.25” PEX pipe running from the container to wetland influent pipe. Bottom Right: The 0.25” PEX pipe and ball valve used to release the NO ₃ -N enriched water into the wetland influent.	161
Figure 5.4: Water quality parameter (pH, dissolved oxygen (DO), and temperature) measurements during the dosing period. Measurements were taken at each site visit during daylight hours (between 8:00 and 14:00). IN, OUT1, and OUT2 refer to measurements taken at the inlet splitter box, the cell 1 outlet, and the cell 2 outlet, respectively. Boxplots represent the median and interquartile ranges.....	169
Figure 5.5: Areal view of wetland cells 1 (left) and 2 (right) taken on April 23 rd , 2021, approximately 6 hours after the initiation of the tracer test. Cell 1 was nearly 100% with vegetation (mostly duckweed) made it difficult to visually trace the progression of the tracer from the air. Cell 2 was nearly all open water. Channels through the detritus substrate can be seen in the right half of cell 2.....	169
Figure 5.6: Photographs of the duckweed clarifier, just upstream of the inlet splitter box on April 8, 2021. The cloudy green water was indicative of an algal bloom. The photos also show that there was no shading of the nutrient-rich water upstream of the wetland cells during this period.	171

Figure 5.7: Dissolved oxygen (DO) concentrations at the outlet of each FWS CW cell. Concentrations were recorded every 30 minutes by U26 HOBO DO data loggers (Onset Computer Corporation, Bourne, MA).....	171
Figure 5.8: Mean hourly DO concentrations (in Eastern Standard Time) at each cell outlet for the period between 3/21/21 and 4/3/21. The diurnal pattern suggested by the data in Figure 5.7 is clearly visible.	172
Figure 5.9: DO concentrations and pH during the dosing period at each sampling location. The substantial reduction of DO and pH after April 5th at the cell 1 outlet (OUT1) highlighted the influence of shading on algal activity. Shading did not occur to the same extent in cell 2.	172
Figure 5.10: NO ₃ -N concentrations for each daily sample during the monitoring period. Sampling stations are labelled as IN (inlet), OUT1 (outlet 1), and OUT2 (outlet 2).....	176
Figure 5.11: Cumulative daily NO ₃ -N loads (in, kg) during the monitoring period. Sampling stations are labelled as IN (inlet), OUT1 (outlet 1), and OUT2 (outlet 2).....	177
Figure 6.1: A photograph of the Danbury WWTP. The flow direction is away from the photographer.	192
Figure 6.2: Monthly maximum NH ₄ -N concentrations in Danbury WWTP effluent in 2019 based on reported NPDES data obtained from the ECHO database.	198
Figure 6.3: Cumulative NH ₄ -N effluent load from Danbury WWTP in 2019 based on reported NPDES data obtained from the ECHO database.	198
Figure 6.4: Mean monthly NH ₄ -N, NO ₃ -N, and TN concentrations in 2019 for the NCSU grab sampling data. Note the increase in NH ₄ -N in the 3 rd and 4 th months (March and April), which shows when the aerators malfunctioned and how long it took the system to bring working properly again.....	200
Figure 6.5: Comparison of monthly mean NH ₄ -N concentrations estimated from grab sampling program with monthly maximum NH ₄ -N concentrations estimated from samples collected by site operator.	201
Figure 6.6: Cumulative loads for NH ₄ -N based on monthly maximum concentrations in the ECHO database (NPDES NH ₄ -N) and NH ₄ -N, NO ₃ -N, and TN based on the grab sampling program.	201
Figure 6.7: Relationship between $\ln(A_{50}^1)$ and temperature (in °C) for the 5000 iterations of the Monte Carlo uncertainty analysis. The regression was represented using the blue line. This relationship was used to predict monthly A_{50}^1 values at the Danbury WWTP.....	203
Figure 6.8: Relationship between $\ln(A_{90}^1)$ and temperature (in °C) for the 5000 iterations of the Monte Carlo uncertainty analysis. The regression was represented using the blue line. This relationship was used to predict monthly A_{90}^1 values at the Danbury WWTP.	203

Figure 6.9: Initial estimate of the required wetland area (in ha MGD⁻¹) necessary for 50% and 90% NO₃-N removal from minor WWTPs in NC. The solid blue line represents a LOESS regression through area required for 90% NO₃-N removal (A₉₀¹). The dashed black line represents a LOESS regression through area required for 50% NO₃-N removal (A₉₀¹). For both regressions, the shaded area represents the 95% standard error.204

Figure 6.10: Required wetland area (in ha) necessary for 50% and 90% NO₃-N removal from the Danbury WWTP effluent based on monthly data from 2016-2020 (n = 52). The solid blue line represents a LOESS regression through area required for 90% NO₃-N removal (A₉₀). The dashed black line represents a LOESS regression through area required for 50% NO₃-N removal (A₉₀). For both regressions, the shaded area represents the 95% standard error.204

Figure 7.1: Two potential life cycles for treatment wetlands. A. The life cycle of an unmaintained wetland, where the system eventually begins to fail and must be replaced. B. The treatment wetland life cycle when a wetland rejuvenation is performed. If active management is employed, the operational age at which declining performance becomes a problem will be increased.218

CHAPTER 1: INTRODUCTION

MOTIVATION: IMPROVING NITROGEN REMOVAL IN NORTH CAROLINA

Across the globe, excessive nutrient loadings, derived from anthropogenic inputs, led to cultural eutrophication that stresses the aquatic environment (Howarth et al., 2011; McCrackin et al., 2017; Rabalais, 2002; Sobota et al., 2013). Eutrophication leads to a variety of adverse effects: including, but not limited to, algal blooms, hypoxic conditions, fish and shellfish kills, changes in aquatic community structure, and ecosystem degradation. (Anderson et al., 2002; Beman et al., 2005; Bricker et al., 2008; Diaz & Rosenberg, 2008; Paerl et al., 2006). In terms of cost to society, eutrophication can produce depleted fisheries, stymie tourism, and lead to adverse human health conditions; all of which negatively impact an area's economy and wellbeing (Bowen & Valiela, 2001; Hoagland et al., 2002; Lipton & Hicks, 2003). In 2018, tourism contributed 3.7 billion dollars to the economies of the coastal counties of North Carolina (NC) (Economic Development Partnership of North Carolina, 2019). In the same year, coastal recreational and commercial fishing in the state had economic impacts of 4.6 billion and 0.4 billion dollars, respectively (NC DMF, 2019). The high environmental and economic value of NC's coastal environment reinforces the necessity for protection from cultural eutrophication. Because several major river basins in NC drain into this coastal environment (Tar-Pamlico, Cape Fear, Roanoke, and Neuse), protection from eutrophication must occur not only in the coastal plain region, but also in the piedmont region, where these watersheds originate.

The need to protect water resources against cultural eutrophication was made clear in the latter half of the 20th century when the negative impacts of coastal eutrophication were observed in both the Pamlico River Estuary and the Neuse River Estuary (Copeland & Gray, 1991). To curtail excess nutrient loadings and limit eutrophication, the two estuaries were classified as

nutrient sensitive waters (NSW) (15A NCAC 02B .0710 & .0730). To protect these NSWs, the Environmental Management Commission established both nutrient management rules (to reduce significant nutrient sources in the watersheds that discharged to estuaries) and nutrient reduction goals (to provide a framework for success). In both basins, nitrogen (N) reduction goals were set at a 30% reduction in total nitrogen (TN) relative to an early 1990s baseline TN load. In the Neuse River basin, nutrient management rules were enacted in 1998 and the baseline TN load, by which reduction goals were to be compared, was set to the average annual TN load discharged from the basin between 1991 and 1995 (Lebo et al., 2012; NC DWQ, 2009; Rothenberger et al., 2009). Meanwhile, in the Tar-Pamlico River basin, nutrient management rules were enacted by 2001, and the baseline TN load, by which reduction goals were to be compared, was set at the TN load discharged to the estuary in 1991 (NC DWQ, 2010, 2015).

Despite nominal success in implementing nutrient management practices for both point and nonpoint pollution sources, neither river basin has achieved the 30% TN reduction goal (NC DWQ, 2015; NCDA&CS, 2019a, 2019b). If the two watersheds targeted specifically for N reduction have not met their reduction goals, it is unlikely that other NC watersheds have substantially reduced N loads in the 21st century. The continued effects of eutrophication in NC can be seen in part by the 288 algal blooms documented in natural waterways from 2012 to 2019 (NC DWR, 2019). The lack of success in TN reduction, considering nominally sufficient nutrient management practice implementation, likely stems from legacy N in the watershed, overestimates of BMP performance, intensifying N sources, and previously unaccounted for N sources. To further protect the valuable environmental resources of NC, intensifying or previously unaccounted for N sources must be mitigated with new or existing water management strategies. One potential strategy to increase N removal in NC is the widespread implementation

of small free water surface (FWS) constructed wetlands (CWs) to provide tertiary treatment at minor wastewater treatment plants (WWTPs) across the state.

TREATMENT WETLANDS

Humans have, directly or indirectly, released wastewater to natural wetlands since the beginning of civilization. In North America, documented piping of municipal or domestic wastewater to natural wetlands has been occurring since the beginning of centralized wastewater collection systems in the early 20th century, with several of these initial sites identified in Kadlec and Wallace (2009). Beginning in the early 1970s, studies of natural wetlands used to polish pre-treated sewage were initiated and the nutrient removal capabilities of these environments were documented (Kadlec, 2009; Mitsch & Gosselink, 2015; Odum et al., 1975).

Water quality improvement observed in these treatment wetlands was determined to be the product of complex biological and physical interactions unique to the saturated conditions in the wetland environment (Kadlec & Wallace, 2009; Keddy, 2010; Mitsch & Gosselink, 2015). The observed connection between the unique hydrologic conditions of the wetland environment and water quality improvement sparked an idea that similar water quality improvements could be produced in upland environments through the introduction of wetland hydrology. This idea led to the development of constructed wetlands (CWs): engineered systems built to imitate wetland hydrology and remove pollutants from wastewater via the biological, chemical, and physical processes found natural wetland ecosystems (Vymazal, 2007).

While CW treatment systems were not developed in the United States until the 1970s, the oldest documented constructed wetland system is thought to stem from a note handwritten in 1904 (Brix, 1997; Kadlec & Wallace, 2009). The note describes the channeling and release of domestic wastewater from a residence to several dug-out gardens in Hornsby, Australia. A more

scientific approach to natural pollutant removal systems began in Germany in the early 1950s. The most notable of these early scientists was Dr. Kathe Seidel, who initiated several experiments at the Max Plank Institute to investigate the potential of artificial beds planted with macrophytes to treat wastewater (Seidel, 1976; Vymazal, 2010).

In the 1960s, Dr. Seidel expanded her experiments to the field scale to improve decentralized wastewater treatment, including septic systems and lagoons, by routing the discharge through artificial ditches containing gravel or sand and various macrophyte species. This “hydrobotanical” method proved effective, and the first large-scale (1-ha) CW to treat domestic wastewater was built in the Netherlands in 1967 (at the time, this new practice was identified as a “rush pond”) (De Jong, 1976; Vymazal, 2010). This initial system was followed in 1968 by several more rush ponds built in Hungary (Vymazal, 2010). Back in the United States, the first CWs were built in 1973 (Kadlec & Wallace, 2009). Three systems built in that year have the potential to claim the title of “1st constructed wetlands in North America”: a subsurface wetland built near Seymour, Wisconsin, a single 8.5 ha marsh built by the Mt. View Sanitary District (California), and a pilot scale system built at the Brookhaven National Laboratory (New York). Since these initial attempts, CWs have been successfully implemented worldwide, and these systems have proven to be effective in improving the water quality from several different types of wastewaters, including municipal and domestic wastewater, CAFO wastewater, acid mine drainage, food processing wastewaters, landfill leachates, stormwater runoff, and agricultural runoff (Kadlec & Wallace, 2009; Vymazal, 2010).

Variable wastewater characteristics derived from the different wastewater sources led to the development of specialized CW configurations. The different CW configurations were first classified by flow direction, with additional sub-classifications for flow location and vegetation

(Kadlec & Wallace, 2009; Mitsch & Gosselink, 2015; Vymazal, 2010). Generally, there are two types of CW; free water surface (FWS) CWs and sub-surface (SSF) CWs (Kadlec & Wallace, 2009; Mitsch & Gosselink, 2015; Vymazal, 2001, 2010). A FWS CW has standing water that moves horizontally through the basin with emergent herbaceous macrophytes and minimal infiltration, resembling a natural marsh. Alternatively, in a SSF CW, water flows either horizontally or vertically through a porous medium with little to no standing water. This porous medium is often also planted with herbaceous macrophytes. A detailed description of each system can be found in Vymazal (2010). This dissertation will focus primarily on the FWS CW, since it is the most common type of CW for treating municipal or domestic wastewater in North America and in North Carolina (Burchell et al., 2016; Kadlec & Wallace, 2009).

MECHANISMS FOR NITROGEN REMOVAL WITHIN FWS CWS

Nitrogen removal in CWs is driven by biological N transformations, including algal or plant uptake (assimilation) and microbial processing (Vymazal, 2007). The microbial processes critical for complete N cycling include mineralization (ammonification), nitrification, and denitrification. Collectively, these microbial processes breakdown organic material to produce reduced inorganic nitrogen (NH_4^+) (ammonification), convert NH_4^+ to oxidized nitrogen (NO_2^- & NO_3^-) (nitrification), and convert NO_3^- to nitrogen gas (N_2) (denitrification). The final transformation of NO_3^- to N_2 gas (denitrification) completely removes N from the water column and releases it to the atmosphere. Additional microbial processes, dissimilatory nitrate reduction to ammonium (DNRA), nitrogen fixation, and anammox have the potential to transform nitrogen. However, these additional processes often occur at low rates in most treatment wetland environments and can be considered negligible relative to the other nitrogen transformations (Vymazal, 2007).

Of these transformations, N removal through microbial denitrification (the production and release of N gas (N_2) from nitrate (NO_3^-)) has been identified as the core sustainable N removal process in the wetland environment (Bachand & Horne, 1999a; Bastviken et al., 2005; Burchell et al., 2007; Drake et al., 2018; Ingersoll & Baker, 1998; Jasper et al., 2014; Kadlec & Wallace, 2009; Messer et al., 2017; Mitsch & Gosselink, 2015). Denitrification is common in the wetland environment, where long periods of saturation result in anaerobic conditions within the wetland substrate. In denitrification, denitrifying bacteria under anaerobic conditions use NO_3^- as the terminal electron acceptor in respiration, thereby reducing the NO_3^- to nitrogen gases (NO , N_2O and N_2), with complete denitrification ending in the production of N_2 gas (Reddy et al., 1984). A concentration gradient then develops, and diffusion transports the N gases from the subsurface to the atmosphere. As the principal gas in Earth's atmosphere, N_2 is a harmless by-product of the complete N cycle. However, incomplete denitrification can result in the production of N_2O , a potent greenhouse gas. Although N_2O is a potent greenhouse gas, the exceedingly small cumulative land area of CWs severely limits the total amount of N_2O produced and CW implementation should not be discouraged based on the scant production of greenhouse gas relative to the total anthropogenic production of greenhouse gases (Søvik et al., 2006).

A prerequisite to denitrification is the presence of an electron donor in the environment (Reddy et al., 1984). With NO_3^- acting as the terminal electron acceptor for respiration, the denitrifying bacteria need an energy/electron source. In the CW environment, this electron source is carbon. The importance of available carbon for N removal was shown in Ingersoll and Baker (1998), which observed a positive correlation between the amount of carbon within the wetland environment and the amount of N removed. This positive correlation was corroborated

by both Hume et al. (2002) and Burchell et al. (2007), both of which observed improved $\text{NO}_3\text{-N}$ removal with increasing organic carbon, likely via increased denitrification rates. To maximize removal of N from the systems through denitrification, it is crucial that the primary source of N entering the wetlands is $\text{NO}_3\text{-N}$. In CWs, NO_3^- either enters the wetland dissolved in the influent water column or must be produced within the CW via nitrification. For FWS CWs aimed at treating wastewater from minor WWTPs, the conventional activated sludge process often used within WWTPs results in an influent to the wetland that contains substantial amounts of dissolved $\text{NO}_3\text{-N}$, reducing the need for internal nitrification (Carey & Migliaccio, 2009).

Microcosm, mesocosm, and field-scale studies have shown that FWS CWs effectively remove N, especially NO_3^- , from wastewater (Crumpton et al., 2020; Gersberg et al., 1983; Ingersoll & Baker, 1998; Iovanna et al., 2008; Kadlec, 2012; Kadlec & Wallace, 2009; Land et al., 2016; Messer et al., 2017). Because of their proven effectiveness in removing N, FWS CWs have the potential to be an ideal method to increase N removal from pretreated wastewater; however, this removal is not guaranteed, and several factors may influence the N removal performance of an individual CW, including but not limited to the amount of N in the influent, the amount of contact with microbial communities (i.e. adequate residence time and surface area), and the site's climate (i.e. temperature) (Crumpton et al., 2006).

KNOWLEDGE GAPS IN LONG-TERM AND LATE-STAGE PERFORMANCE DATA

Although there has been over 50 years of experience with CW design and performance, knowledge gaps in operation persist. One such gap is in the long-term operation of these systems, as only a few studies have evaluated long-term or late-stage nutrient removal in CWs. This lack of late-stage or long-term performance data is not limited to CWs. Liu et al. (2017)

identified a similar shortcoming in most urban and agricultural best management practices used to improve hydrology and water quality.

The Land et al. (2016) meta-analysis highlights the lack of long-term and late-stage performance data for treatment wetlands. This meta-analysis screened over 5,000 articles on the effectiveness of constructed and restored wetlands to remove N and phosphorus. After screening, the group evaluated 93 articles containing monitoring data from 203 treatment wetlands. Within these articles, the median operational age at the start of monitoring was one year old and the median age at the end of monitoring was three years old. Of the 203 wetlands in the study, only four were studied for longer than 10 years.

As of this dissertation, the author was only able to find three treatment wetlands in the United States with over 15 years of reported monitoring data, of which only two are constructed wetlands: the Olentangy River Wetland Research Park and the Orlando Easterly Wetland. The Olentangy River Wetland Research Park treats riverine water in a mixed agricultural/urban watershed, and the Orlando Easterly Wetland polishes pre-treated wastewater from the City of Orlando. Of concern for CW design life and management, both the Olentangy and Orlando Easterly wetlands have shown decreased nutrient removal performance over time (Mitsch et al., 2014; Slayton, 2019; Wang et al., 2006). These performance declines over time suggest that treatment wetlands designed under the assumption of steady-state performance may overestimate late-stage treatment ability. For CWs treating municipal or domestic wastewater under a national pollutant discharge elimination system (NPDES) permit, the potential failure to meet treatment goals after one to two decades of operation could result in unexpected permit violations and disillusionment by practitioners, followed by an aversion to treatment wetlands use.

Outside of the lack of long-term studies, Land et al. (2016) outlined additional difficulties with the data in wetland monitoring studies. These difficulties included incomplete water balances and inadequate meteorological data, which made estimating a water balance impossible and, by extension, limited our full understanding of the effects of CW hydrology on nutrient treatment. Further, many of the studies reviewed in Land et al. (2016) did not report or measure all the individual N species. Instead, studies analyzed samples or provided results for only the N species that heavily impact the system. It was suggested that sampling for specific N species is the preferred approach as it limits sampling cost, which allows for more frequent sampling, longer monitoring periods, or both. However, the failure to measure and report concentrations for the three main N species (TKN, NH₄, and NO₃) makes it difficult to determine the influence of N speciation on N removal.

In addition to the challenges stated above, the two often cited treatment wetland databases, the North American Treatment Wetland Database and the Water Environment Research Foundation Database, are no longer available to researchers. These databases became outdated due to a lack of funding and were taken offline (personal communications with Brad Finney and Scott Wallace). Data from constructed wetlands treating domestic or municipal wastewater is also commonly unavailable, especially for smaller systems, because NPDES permits only require influent untreated wastewater and final plant effluent sampling (US EPA, 2000). As a result, the entire wastewater treatment plant is treated as a black box; treatment wetlands within the treatment train are not monitored separately and thus the treatment wetland performance is unknown. Hence, while there is data on long-term wastewater treatment plant (WWTP) performance, there is limited data on the treatment wetlands within these systems.

The current state of treatment wetland monitoring data, especially for late-stage or long-term monitoring data, is inadequate. Inadequate monitoring data limits our knowledge about long-term temporal variation of N removal performance. When a negative correlation between treatment performance and years of operation is probable, inadequate monitoring data leaves us blind to the timing of declining performance and potential remediation techniques.

LIMITED MONITORING DATA UNDERMINES LATE-STAGE MANAGEMENT AND OPERATIONAL OPTIMIZATION

The focus on short-term, initial monitoring at CW sites severely limits the ability to assess the impacts of operation and management decisions over a CW's design life. One decision that must be made is how to manage vegetation. Gersberg et al. (1986), Bachand and Horne (1999b), Thullen et al. (2005), and Kadlec (2008) agree that the presence of vegetation, along with optimal management of vegetation improves CW N removal performance. Brix (1997) summarizes the role of macrophytes in the treatment potential of FWS CWs. Physically, vegetation reduces current velocities improving retention time, impounds and intercepts suspended solids filtering out debris, minimizes erosion risks maintain the soil structure, and creates a canopy that restricts light to the water surface limiting algal growth. Key for N removal, vegetation can assimilate N from the substrate and the water column, decay to provide a carbon source for denitrification, and it can provide a surface for microbial growth and a conduit to deliver oxygen into the subsurface. Oxygen transfer to the subsurface can create pockets of nitrification in an otherwise anaerobic wetland environment. This is important for wetlands that receive NH_4^+ -dominated wastewater and require nitrification prior to denitrification for effective N removal. Outside of improved treatment, active vegetation management can make a CW aesthetically pleasing.

While established vegetation is necessary to optimize N removal, a variety of problems are associated with poorly maintained vegetation, particularly when biomass builds up to a high level (Thullen et al., 2005). Sartoris et al. (1999) observed low DO concentrations in dense vegetation bands in FWS CW treating NH₄-N dominated wastewater, which suggested that dense vegetation may restrict nitrification. As mentioned earlier, nitrification is a critical step for N removal in CWs receiving non-nitrified wastewater, and Sartoris et al. (1999) noted that limited nitrification due to increased dense vegetation was a likely cause of the low NH₄-N removal observed in their study.

Not only is the density of vegetation important, but the location and pattern of vegetation is also important. Numerical modeling by Jenkins and Greenway (2005) indicated that significant negative influences on treatment efficiency can arise from improperly designed or maintained wetlands, especially in terms of vegetation placement and aspect ratio. Their results showed a decrease in the hydraulic efficiency of a modelled FWS CW when vegetation patterns ran parallel to the flow path (i.e., fringing vegetation). Conversely, Thullen et al. (2002) observed that a banded pattern of emergent wetland vegetation paired with open water areas perpendicular to the flow through the cell enhanced N removal in wetland mesocosms receiving NH₄-N dominated effluent.

Perhaps most importantly, the accumulation of solids can, over the span of a decade or two, produce significant hydraulic inefficiencies in a CW (Kadlec & Wallace, 2009; Wang et al., 2006; White et al., 2008). In the absence of active vegetation management, litterfall from dense stands of emergent vegetation can fill in the wetland basin through a process analogous to bog formation. This accumulation of decaying biomass (i.e., detritus) and filling in of the FWS CW

basin over time can lead to short-circuiting via preferential flow paths and dead zones in areas where flow is blocked by accumulated debris (Kadlec and Wallace, 2009; Wang et al., 2006).

Preferential flow paths restrict the available wetland surface area to area of the flow paths. Wetland surface area is connected to wetland performance through the hydraulic loading rate (HLR) metric, which is defined as the flow (Q , in L³ T⁻¹) divided by the area (A , in L²). Notably for N removal, both Land et al. (2016), a review of data from 203 wetland studies from across the globe, and Crumpton et al. (2020), an analysis of data from 26 constructed wetlands in Iowa spanning 69 wetland years, noted that TN removal efficiency had a significant negative correlation with HLR. Therefore, preferential flow paths effectively decrease the wetland surface area, which in turn causes the HLR to increase and the TN removal efficiency to decrease. Therefore, as a CW ages, these hydraulic inefficiencies may lead to a decline in treatment efficiency and potentially to system failure. However, studies investigating the impact of age (i.e., detritus) on N removal performance have not been undertaken. Subsequently, methods to combat this problem are not widely available in literature and have not been disseminated to operators of CW systems.

STATE OF FWS CWS TREATING WASTEWATER IN NC

Although FWS CWs appear ideal for improved N removal, there were only four such systems providing biological nutrient removal in NC as of 2016 (Burchell et al., 2016). In addition to the dearth of these systems, there are two problems associated with the four currently operating treatment wetlands that need to be addressed prior to renewed recommendations and strategies for more widespread treatment wetland implementation for tertiary biological nutrient removal in North Carolina.

- **Problem 1:** Performance data on these wetlands is unavailable. The lack of data stems from the fact that these systems are located within the treatment train of WWTPs and the entire WWTP is treated as a black box. The lack of data makes it difficult to assess the actual treatment ability of CWs in NC and creates uncertainty around their effectiveness.
- **Problem 2:** Current CWs treating wastewater in NC have been operated for more than 15 years and, according to their operators, sustaining the initial N removal performance of these systems has been difficult in recent years. While numerous studies have documented the N removal capabilities of CWs with less than 10 years of operation (Land et al., 2016), performance data on aging systems, along with techniques to extend their useful life, is largely unavailable. As a result, sustained long-term treatment performance remains a challenge (Wu et al., 2015).

The dearth of systems, shortage of performance data, and concerns over declining performance combine to create an environment of uncertainty regarding the N removal capabilities of these systems. To reduce this uncertainty and address these problems, a research project was initiated to obtain data on the performance of current FWS CWs in NC and to better understand the late-stage management of these systems.

OBJECTIVES AND HYPOTHESIS

Overall Objectives

FWS CWs have the potential to be invaluable tools in the mission to reduce N loads to downstream water bodies in NC. However, to recommend widespread implementation with confidence, it is crucial to understand the design life and late-stage management of these systems and provide long-term maintenance and operational guidance that is often lacking. To provide insights into the N removal performance of a FWS CW in NC and the influence of operational

age on that performance, the water quality and hydrology of two aging FWS CW cells within a minor WWTP in NC were monitored over a three-year period from September 2018 through May 2021. To evaluate the potential for maintenance techniques to sustain or improve N removal over time, a rejuvenation technique was conducted on one of the two aging wetland cells in April 2019. An additional study was also conducted at another minor WWTP to demonstrate the amount of unaccounted-for N currently released from these systems and provide an estimate of the wetland area that would be required to reduce N export from these locations.

Specific Objectives:

Objective 1: Evaluate the N removal efficiency of aging FWS CWs and, if ineffective, identify the cause(s) of the poor performance.

- Hypothesis 1: The two 20+ year old FWS CW cells at the Walnut Cove WWTP will have poor N removal performance due to their operational age.
- Hypothesis 2: Because they are over 20 years old, accumulated detritus substrate will be the major factor that reduces the hydraulic efficiency.

Objective 2: Identify and quantify the internal N source within an aged FWS CW.

- Hypothesis 1: Diffusion alone can transport a substantial amount of $\text{NH}_4\text{-N}$ from the accumulated detritus substrate within an aged FWS CW to the overlying water column and this $\text{NH}_4\text{-N}$ release can be represented using a kinetic model.

Objective 3: Evaluate the potential for detritus removal to be a wetland management strategy to improve N removal.

- Hypothesis 1: Operational age negatively influences wetland N removal by physically reducing the effective areas and volumes of the wetland cell as detritus accumulates.

- Hypothesis 2: The physical removal of this accumulated detritus will increase the effective area, volume, and HRT of the wetland cell.
- Hypothesis 3: Increasing the effective area, especially the submerged surface area through revegetation and increased water depths, will improve N removal.

Objective 4: Evaluate the influence of influent N speciation on temporal changes in N removal performance.

- Hypothesis 1: Increasing operational age will have a negative influence on NO₃-N removal.
- Hypothesis 2: Increasing the upstream conversion of NH₄-N to NO₃-N in the influent of FWS CWs receiving NH₄-N dominated influent will improve N removal.

Objective 5: Quantify N release in a minor WWTP and evaluate the potential for improved N removal through the addition of a FWS CW to these systems.

- Hypothesis 1: Minor WWTPs without NO₃-N monitoring requirements focus on nitrification and release an unaccounted-for NO₃-N load to waterways in NC.
- Hypothesis 2: The NO₃-N enriched effluent from minor WWTPs could be significantly reduced by relatively small FWS CWs.

DISSERTATION OVERVIEW

The following dissertation chapters were structured to address the above objectives and hypotheses. In Chapter II, two full-scale 20+ year old FWS CWs that are the focus of this dissertation were introduced and their initial nitrogen removal performance and internal hydraulics were studied to meet Objective 1 and the associated hypotheses. In Chapter III, a laboratory study focused on quantifying the extent of nitrogen release from the accumulated detritus substrate and its potential influence as an internal nitrogen source was conducted to meet

Objective 2 and the corresponding hypotheses. In Chapter IV, a detritus removal was conducted in one of the two FWS CWs studied in Chapter II and its influence on both internal hydraulics and nitrogen removal performance was evaluated. The work presented in this chapter addressed Objective 3 and the corresponding hypotheses by focusing on detritus removal as a potential method to rejuvenate aging FWS CWs. Both Chapters II and IV focused on FWS CW receiving non-nitrified influent; however, most FWS CWs will receive influent that has been at least partially nitrified. Therefore, in Chapter V, an in-situ $\text{NO}_3\text{-N}$ dosing study was used to evaluate the $\text{NO}_3\text{-N}$ removal performance of the two previously studied full-scale FWS CWs and meet Objective 4 and the corresponding hypotheses. In Chapter VI, the effluent of a minor WWTP in NC was monitored over the span of a year to quantify the amount of nitrogen (especially $\text{NO}_3\text{-N}$) released from these plants. In addition to quantifying the amount of nitrogen release, a preliminary assessment of the wetland area that would be needed to provide adequate nitrogen removal at these minor WWTPs and the potential cost were also conducted. Overall, this chapter assessed Objective 5 and the corresponding hypotheses. Finally, Chapter VII summarized the results and insights gained from the entire research project and provided recommendations about operation, maintenance, and expansion of current and future FWS CWs in NC.

REFERENCES

- Anderson, D. M., Glibert, P. M., & Burkholder, J. M. (2002). Harmful algal blooms and eutrophication: Nutrient sources, composition, and consequences. *Estuaries*, 25(4 B), 704–726. <https://doi.org/10.1007/BF02804901>
- Bachand, P. A. M., & Horne, A. J. (1999a). Denitrification in constructed free-water surface wetlands: I. Very high nitrate removal rates in a macrocosm study. *Ecological Engineering*, 14(1–2), 9–15. [https://doi.org/10.1016/S0925-8574\(99\)00016-6](https://doi.org/10.1016/S0925-8574(99)00016-6)
- Bachand, P. A. M., & Horne, A. J. (1999b). Denitrification in constructed free-water surface wetlands: II. Effects of vegetation and temperature. *Ecological Engineering*, 14(1–2), 17–32. [https://doi.org/10.1016/S0925-8574\(99\)00017-8](https://doi.org/10.1016/S0925-8574(99)00017-8)
- Bastviken, S. K., Eriksson, P. G., Premrov, A., & Tonderski, K. (2005). Potential denitrification in wetland sediments with different plant species detritus. *Ecological Engineering*, 25(2), 183–190. <https://doi.org/10.1016/j.ecoleng.2005.04.013>
- Beman, J. M., Arrigo, K. R., & Matson, P. A. (2005). Agricultural runoff fuels large phytoplankton blooms in vulnerable areas of the ocean. *Nature*, 434(7030), 211–214. <https://doi.org/10.1038/nature03370>
- Bowen, J. L., & Valiela, I. (2001). The ecological effects of urbanization of coastal watersheds: Historical increases in nitrogen loads and eutrophication of Waquoit Bay estuaries. *Canadian Journal of Fisheries and Aquatic Sciences*, 58(8), 1489–1500. <https://doi.org/10.1139/f01-094>
- Bricker, S. B., Longstaff, B., Dennison, W., Jones, A., Boicourt, K., Wicks, C., & Woerner, J. (2008). Effects of nutrient enrichment in the nation's estuaries: A decade of change. *Harmful Algae*, 8(1), 21–32. <https://doi.org/10.1016/j.hal.2008.08.028>
- Brix, H. (1997). Do macrophytes play a role in constructed treatment wetlands? *Water Science and Technology*; London, 35(5), 11–17.
- Burchell, M. R., Skaggs, R. W., Lee, C. R., Broome, S., Chescheir, G. M., & Osborne, J. (2007). Substrate Organic Matter to Improve Nitrate Removal in Surface-Flow Constructed Wetlands. *Journal of Environmental Quality*, 36(1), 194–207. <https://doi.org/10.2134/jeq2006.0022>
- Burchell, M. R., Thompson, T. W., Broome, S. W., Krometis, L. A., & Badgely, B. (2016). Constructed wetlands to polish wastewater in small rural communities—Evaluation of current and potential use to improve water quality trends and protect human health. Final report. (Virginia Tech/ NC State University Regional Collaborative Proposal Planning and Development Grants, p. 29) [Final Report].

- Carey, R. O., & Migliaccio, K. W. (2009). Contribution of Wastewater Treatment Plant Effluents to Nutrient Dynamics in Aquatic Systems: A Review. *Environmental Management*, 44(2), 205–217. <http://dx.doi.org/10.1007/s00267-009-9309-5>
- Copeland, B. J., & Gray, J. (1991). Status and trends of the Albemarle-Pamlico estuaries (Albemarle-Pamlico Estuarine Study Report No. 90–01; p. 422). Department of Environment Health and Natural Resources.
- Crumpton, W. G., Stenback, G. A., Fisher, S. W., Stenback, J. Z., & Green, D. I. S. (2020). Water quality performance of wetlands receiving nonpoint-source nitrogen loads: Nitrate and total nitrogen removal efficiency and controlling factors. *Journal of Environmental Quality*, 49(3), 735–744. <https://doi.org/10.1002/jeq2.20061>
- Crumpton, W. G., Stenback, G., Miller, B., & Helmers, M. (2006). Potential Benefits of Wetland Filters for Tile Drainage Systems: Impact on Nitrate Loads to Mississippi River Subbasins. Agricultural and Biosystems Engineering Technical Reports and White Papers. https://lib.dr.iastate.edu/abe_eng_reports/8
- De Jong, J. (1976). The Purification of Wastewater with the Aid of Rush or Reed Ponds. In *Biological Control of Water Purification* (pp. 133–140). University of Pennsylvania Press.
- Diaz, R. J., & Rosenberg, R. (2008). Spreading dead zones and consequences for marine ecosystems. *Science*, 321(5891), 926–929. <https://doi.org/10.1126/science.1156401>
- Drake, C. W., Jones, C. S., Schilling, K. E., Amado, A. A., & Weber, L. J. (2018). Estimating nitrate-nitrogen retention in a large constructed wetland using high-frequency, continuous monitoring and hydrologic modeling. *Ecological Engineering*, 117, 69–83. <https://doi.org/10.1016/j.ecoleng.2018.03.014>
- Economic Development Partnership of North Carolina. (2019). *Economic Impact Studies* [Company]. Visit North Carolina. <https://partners.visitnc.com/economic-impact-studies>
- Gersberg, R. M., Elkins, B. V., & Goldman, C. R. (1983). Nitrogen removal in artificial wetlands. *Water Research*, 17(9), 1009–1014. [https://doi.org/10.1016/0043-1354\(83\)90041-6](https://doi.org/10.1016/0043-1354(83)90041-6)
- Gersberg, R. M., Elkins, B. V., Lyon, S. R., & Goldman, C. R. (1986). Role of aquatic plants in wastewater treatment by artificial wetlands. *Water Research*, 20(3), 363–368. [https://doi.org/10.1016/0043-1354\(86\)90085-0](https://doi.org/10.1016/0043-1354(86)90085-0)
- Hoagland, P., Anderson, D. M., Kaoru, Y., & White, A. W. (2002). The economic effects of harmful algal blooms in the United States: Estimates, assessment issues, and information needs. *Estuaries*, 25(4 B), 819–837. <https://doi.org/10.1007/BF02804908>
- Howarth, R., Chan, F., Conley, D. J., Garnier, J., Doney, S. C., Marino, R., & Billen, G. (2011). Coupled biogeochemical cycles: Eutrophication and hypoxia in temperate estuaries and

- coastal marine ecosystems. *Frontiers in Ecology and the Environment*, 9(1), 18–26.
<https://doi.org/10.1890/100008>
- Ingersoll, T. L., & Baker, L. A. (1998). Nitrate removal in wetland microcosms. *Water Research*, 32(3), 677–684. [https://doi.org/10.1016/S0043-1354\(97\)00254-6](https://doi.org/10.1016/S0043-1354(97)00254-6)
- Iovanna, R., Hyberg, S., & Crumpton, W. G. (2008). Treatment wetlands: Cost-effective practice for intercepting nitrate before it reaches and adversely impacts surface waters. *Journal of Soil and Water Conservation*, 63(1), 14A-15A. <https://doi.org/10.2489/jswc.63.1.14A>
- Jasper, J. T., Jones, Z. L., Sharp, J. O., & Sedlak, D. L. (2014). Nitrate Removal in Shallow, Open-Water Treatment Wetlands. *Environmental Science & Technology*, 48(19), 11512–11520. <https://doi.org/10.1021/es502785t>
- Jenkins, G. A., & Greenway, M. (2005). The hydraulic efficiency of fringing versus banded vegetation in constructed wetlands. *Ecological Engineering*, 25(1), 61–72.
<https://doi.org/10.1016/j.ecoleng.2005.03.001>
- Kadlec, R. H. (2008). The effects of wetland vegetation and morphology on nitrogen processing. *Ecological Engineering*, 33(2), 126–141. <https://doi.org/10.1016/j.ecoleng.2008.02.012>
- Kadlec, R. H. (2009). Wastewater treatment at the Houghton Lake wetland: Hydrology and water quality. *Ecological Engineering*, 35(9), 1287–1311.
<https://doi.org/10.1016/j.ecoleng.2008.10.001>
- Kadlec, R. H. (2012). Constructed Marshes for Nitrate Removal. *Critical Reviews in Environmental Science and Technology*, 42(9), 934–1005.
<https://doi.org/10.1080/10643389.2010.534711>
- Kadlec, R. H., & Wallace, S. D. (2009). *Treatment Wetlands* (2nd ed.). CRC Press.
- Keddy, P. A. (2010). *Wetland Ecology: Principles and Conservation* (2nd ed.). Cambridge University Press.
https://books.google.com/books/about/Wetland_Ecology.html?id=eVeaSqFy2VgC
- Land, M., Graneli, W., Grimvall, A., Hoffmann, C. C., Mitsch, W. J., Tonderski, K. S., & Verhoeven, J. T. A. (2016). How effective are created or restored freshwater wetlands for nitrogen and phosphorus removal? A systematic review. *Environmental Evidence*; London, 5. <http://dx.doi.org.prox.lib.ncsu.edu/10.1186/s13750-016-0060-0>
- Lebo, M. E., Paerl, H. W., & Peierls, B. L. (2012). Evaluation of progress in achieving TMDL mandated nitrogen reductions in the Neuse river basin, North Carolina. *Environmental Management*, 49(1), 253–266. <https://doi.org/10.1007/s00267-011-9774-5>
- Lipton, D., & Hicks, R. (2003). The cost of stress: Low dissolved oxygen and economic benefits of recreational striped bass (*Morone saxatilis*) fishing in the Patuxent River. *Estuaries*, 26(2 A), 310–315. <https://doi.org/10.1007/bf02695969>

- Liu, Y., Engel, B. A., Flanagan, D. C., Gitau, M. W., McMillan, S. K., & Chaubey, I. (2017). A review on effectiveness of best management practices in improving hydrology and water quality: Needs and opportunities. *Science of The Total Environment*, 601–602, 580–593. <https://doi.org/10.1016/j.scitotenv.2017.05.212>
- McCrackin, M. L., Cooter, E. J., Dennis, R. L., Harrison, J. A., & Compton, J. E. (2017). Alternative futures of dissolved inorganic nitrogen export from the Mississippi River Basin: Influence of crop management, atmospheric deposition, and population growth. *Biogeochemistry*, 133(3), 263–277. <https://doi.org/10.1007/s10533-017-0331-z>
- Messer, T. L., Burchell, M. R., Birgand, F., Broome, S. W., & Chescheir, G. (2017). Nitrate removal potential of restored wetlands loaded with agricultural drainage water: A mesocosm scale experimental approach. *Ecological Engineering*, 106, 541–554. <https://doi.org/10.1016/j.ecoleng.2017.06.022>
- Mitsch, W. J., & Gosselink, J. G. (2015). *Wetlands* (5th ed.). John Wiley & Sons, Inc.
- Mitsch, W. J., Zhang, L., Waletzko, E., & Bernal, B. (2014). Validation of the ecosystem services of created wetlands: Two decades of plant succession, nutrient retention, and carbon sequestration in experimental riverine marshes. *Ecological Engineering*, 72, 11–24. <https://doi.org/10.1016/j.ecoleng.2014.09.108>
- NC DMF. (2019). 2019 License and Statistics Annual Report (p. 430) [Annual Report]. NC DEQ. http://portal.ncdenr.org/c/document_library/get_file?p_l_id=1169848&folderId=33372974&name=DLFE-141802.pdf
- NC DWQ. (2009). Neuse River Basinwide Water Quality Plan. <https://files.nc.gov/ncdeq/Water%20Quality/Planning/BPU/BPU/Neuse/Neuse%20Plans/2009%20Plan/NR%20Basinwide%20Plan%202009%20-%20Final.pdf>
- NC DWQ. (2010). Tar-Pamlico River Basinwide Management Plan 2010. https://files.nc.gov/ncdeq/Water%20Quality/Planning/BPU/BPU/Tar_Pamlico/Tar%20Pamlico%20Plans/2010%20Plan/TarPamlicoBasinPlan2010noappendices.pdf
- NC DWQ. (2015). Tar-Pamlico Nutrient Sensitive Waters Implementation Strategy: <https://files.nc.gov/ncdeq/Water%20Quality/Planning/NPU/Tar%20Pamlico/TarPamPhaseIVAgreementsigned.pdf>
- NC DWR. (2019). Algal Bloom Map [ArcGIS Interactive Map]. NC DEQ. <https://ncdenr.maps.arcgis.com/apps/webappviewer/index.html?id=58e9afca8b724b3f82cc81a8b825f83e>
- NCDA&CS. (2019a). 2019 Annual Progress Report (Crop Year 2018) on the Neuse Agricultural Rule (15 A NCAC 2B.0238)—A Report to the Environmental Management Commission from the Neuse Basin Oversight Committee: Crop Year 2018 (p. 16) [Government]. https://files.nc.gov/ncdeq/Water%20Quality/Planning/NPU/Neuse/Neuse_CY2018_Annual_Report.pdf

- NCDA&CS. (2019b). 2019 Annual Progress Report (Crop Year 2018) on the Tar-Pamlico Agricultural Rule (15A NCAC 02B .0256) A Report to the Environmental Management Commission from the Tar-Pamlico Basin Oversight Committee: Crop Year 2018 (p. 17). https://files.nc.gov/ncdeq/Water%20Quality/Planning/NPU/Tar%20Pamlico/Tar-Pam_CY2018_Annual_Report.pdf
- Odum, H. T., Ewel, K. C., Mitsch, W. J., & Ordway, J. W. (1975). Recycling treated sewage through cypress wetlands in Florida. University of Florida.
- Paerl, H. W., Valdes, L. M., Piehler, M. F., & Stow, C. A. (2006). Assessing the effects of nutrient management in an estuary experiencing climatic change: The Neuse River Estuary, North Carolina. *Environmental Management*, 37(3), 422–436. <https://doi.org/10.1007/s00267-004-0034-9>
- Rabalais, N. N. (2002). Nitrogen in Aquatic Ecosystems. *AMBIO: A Journal of the Human Environment*, 31(2), 102–112. <https://doi.org/10.1579/0044-7447-31.2.102>
- Reddy, K. R., Patrick, W. H., & Broadbent, F. E. (1984). Nitrogen transformations and loss in flooded soils and sediments. *C R C Critical Reviews in Environmental Control*, 13(4), 273–309. <https://doi.org/10.1080/10643388409381709>
- Rothenberger, M. B., Burkholder, J. M., & Brownie, C. (2009). Long-term effects of changing land use practices on surface water quality in a coastal river and lagoonal estuary. *Environmental Management*, 44(3), 505–523. <https://doi.org/10.1007/s00267-009-9330-8>
- Sartoris, J. J., Thullen, J. S., Barber, L. B., & Salas, D. E. (1999). Investigation of nitrogen transformations in a southern California constructed wastewater treatment wetland. *Ecological Engineering*, 14(1), 49–65. [https://doi.org/10.1016/S0925-8574\(99\)00019-1](https://doi.org/10.1016/S0925-8574(99)00019-1)
- Seidel, K. (1976). *Macrophytes and Water Purification*. In *Biological Control of Water Pollution* (pp. 109–122). University of Pennsylvania Press.
- Slayton, K. (2019). Orlando Easterly Wetlands Compliance and Performance Review for the City of Orlando’s Easterly Wetlands Treatment System 2018 Annual Report (p. 43). Public Works Department - Water Reclamation Division. http://www.cityoforlando.net/wetlands/wp-content/uploads/sites/59/2019/05/Annual-Report-2018.pdf?_ga=2.200194598.947842668.1613420029-1039633945.1613420029
- Sobota, D. J., Compton, J. E., & Harrison, J. A. (2013). Reactive nitrogen inputs to US lands and waterways: How certain are we about sources and fluxes? *Frontiers in Ecology and the Environment*, 11(2), 82–90. <https://doi.org/10.1890/110216>
- Søvik, A. K., Augustin, J., Heikkinen, K., Huttunen, J. T., Necki, J. M., Karjalainen, S. M., Kløve, B., Liikanen, A., Mander, Ü., Puustinen, M., Teiter, S., & Wachniew, P. (2006). Emission of the Greenhouse Gases Nitrous Oxide and Methane from Constructed Wetlands in Europe. *Journal of Environmental Quality*, 35(6), 2360–2373. <https://doi.org/10.2134/jeq2006.0038>

- Thullen, J. S., Sartoris, J. J., & Nelson, S. M. (2005). Managing vegetation in surface-flow wastewater-treatment wetlands for optimal treatment performance. *Ecological Engineering*, 25(5), 583–593. <https://doi.org/10.1016/j.ecoleng.2005.07.013>
- Thullen, J. S., Sartoris, J. J., & Walton, W. E. (2002). Effects of vegetation management in constructed wetland treatment cells on water quality and mosquito production. *Ecological Engineering*, 18(4), 441–457. [https://doi.org/10.1016/S0925-8574\(01\)00105-7](https://doi.org/10.1016/S0925-8574(01)00105-7)
- Vymazal, J. (2001). Types of constructed wetlands for wastewater treatment: Their potential for nutrient removal. In *Transformations of nutrients in natural and constructed wetlands* (pp. 1–93). Backhuys Publishers.
- Vymazal, J. (2007). Removal of nutrients in various types of constructed wetlands. *Science of The Total Environment*, 380(1–3), 48–65. <https://doi.org/10.1016/j.scitotenv.2006.09.014>
- Vymazal, J. (2010). Constructed Wetlands for Wastewater Treatment. *Water*, 2(3), 530–549. <https://doi.org/10.3390/w2030530>
- Wang, H., Jawitz, J. W., White, J. R., Martinez, C. J., & Sees, M. D. (2006). Rejuvenating the largest municipal treatment wetland in Florida. *Ecological Engineering*, 26(2), 132–146. <https://doi.org/10.1016/j.ecoleng.2005.07.016>
- White, J. R., Gardner, L. M., Sees, M., & Corstanje, R. (2008). The Short-Term Effects of Prescribed Burning on Biomass Removal and the Release of Nitrogen and Phosphorus in a Treatment Wetland. *Journal of Environmental Quality*, 37(6), 2386–2391. <https://doi.org/10.2134/jeq2008.0019>
- Wu, H., Zhang, J., Ngo, H. H., Guo, W., Hu, Z., Liang, S., Fan, J., & Liu, H. (2015). A review on the sustainability of constructed wetlands for wastewater treatment: Design and operation. *Bioresource Technology*, 175, 594–601. <https://doi.org/10.1016/j.biortech.2014.10.068>

CHAPTER 2: NITROGEN REMOVAL IN AN AGING FREE WATER SURFACE WETLAND RECEIVING AMMONIA-DOMINATED LAGOON EFFLUENT

ABSTRACT

Performance data on aging treatment wetlands, along with techniques to extend their useful life, is largely unavailable. The limited data that we have suggests that there is the potential for treatment efficiency to decline with operational age. With hundreds of treatment wetlands now in their 2nd or 3rd decade of operation, it is crucial to better understand the design life and late-stage performance of these systems. To provide these insights, continuous hydrology and water quality monitoring was initiated at the inlet and outlet of two 20+ year old free water surface (FWS) constructed wetland (CW) cells. The study objectives were to evaluate the nitrogen removal efficiency of aging, potentially ineffective FWS CW cells and, if ineffective, identify the cause(s) of the poor performance. From November 2018 through March 2019, nitrogen removal performance was substandard. Total nitrogen (TN) concentrations were reduced by 2% or less, while loads were reduced by 11%, or less. TN removal rates of 0.1 g-N m⁻² d⁻¹ in each cell (based on the nominal wetland surface area) and overall nitrogen removal was well below what has been observed at other FWS CWs treating nitrogen-enriched wastewater. The poor performance was linked to unfavorable inlet nitrogen speciation and the accumulation of a substantial detritus substrate within the wetlands. Together, these issues limited microbial nitrogen transformations and severely reduced the hydraulic efficiency within the cells.

INTRODUCTION

With over fifty years of study and implementation worldwide, free water surface (FWS) constructed wetlands (CWs), have proven to be effective in reducing excess nitrogen in the water column, especially in the form of nitrate ($\text{NO}_3\text{-N}$) (Crumpton et al., 2020; Gersberg et al., 1983; Ingersoll & Baker, 1998; Iovanna et al., 2008; Kadlec, 2012; Kadlec & Wallace, 2009; Land et al., 2016; Messer et al., 2017; Seidel, 1976). In addition to the proven treatment, the gravity driven hydraulics and self-sustaining removal pathways used in FWS CWs limit anthropogenic energy inputs and operating costs, making them ideal low-cost, environmentally friendly treatment options. Although ideal for improved nitrogen removal, as of 2016 there only three such systems providing tertiary treatment for wastewater treatment plants (WWTPs) in NC (Burchell et al., 2016). And, within these three systems, there were two problems that needed to be addressed prior to recommending a strategy of widespread treatment wetland implementation for improved nitrogen removal in North Carolina.

First, performance data on treatment wetlands in NC is practically unavailable. According to the EPA fact sheet on FWS CWs for wastewater treatment (2000), “Sampling for NPDES monitoring is usually limited to the untreated wastewater and the final system effluent. Since the wetland component is usually preceded by some form of preliminary treatment, the NPDES monitoring program does not document wetland influent characteristics.” In addition to the lack of wetland influent sampling, wetland effluent has also not been directly sampled. Instead, final plant effluent samples are collected, and these are taken after the water has moved through more treatment processes (namely, final clarification and disinfection). As a result, the entire WWTP is treated as a black box and the treatment performance of the CW is unknown.

The lack of data makes it difficult to assess the actual treatment ability of CWs in NC and creates uncertainty around the effectiveness of these systems.

Second, the FWS CWs in NC have been in operation for about 20 years (Burchell et al., 2016). While numerous studies have documented the nitrogen removal capabilities of CWs with less than 10 years of operation (Land et al., 2016), performance data on aging systems, along with techniques to extend their useful life, have been unavailable. As a result, sustained long-term treatment performance remains a challenge (Wu et al., 2015). Operators of each site reinforced this view by expressing concern that their FWS CWs had been exhibiting suboptimal treatment performance in recent years (Burchell et al., 2016). However, as of 2018 there was no performance data on the wetland systems within WWTPs in NC. Therefore, declining wetland performance as a root cause of increasing nitrogen concentrations in WWTP effluent was only a hypothesis.

To test this hypothesis, a study was conducted at one of these sites (the Walnut Cove WWTP), where two 0.7 ha FWS CW cells have received pretreated municipal wastewater since 1996 and have begun to show signs of declining nitrogen removal performance through increased effluent $\text{NH}_4\text{-N}$ and TN concentrations over time (Figure 2.1). During the first decade of operation (1996 - 2006), the WWTP's nitrogen removal performance was satisfactory. The mean $\text{NH}_4\text{-N}$ effluent concentration was 1.6 mg-N L^{-1} , well below the plant's 10 mg-N L^{-1} discharge limit for $\text{NH}_4\text{-N}$, and the mean TN effluent concentration was 3.6 mg-N L^{-1} (Figure 2.2). However, this performance began to wane. From 2007 to 2017, $\text{NH}_4\text{-N}$ and TN effluent concentrations increased to 6.2 mg-N L^{-1} and 7.6 mg-N L^{-1} , with monthly $\text{NH}_4\text{-N}$ concentrations more frequently exceeding 10 mg-N L^{-1} (Burchell et al., 2016) (Figure 2.1 & 2.2).

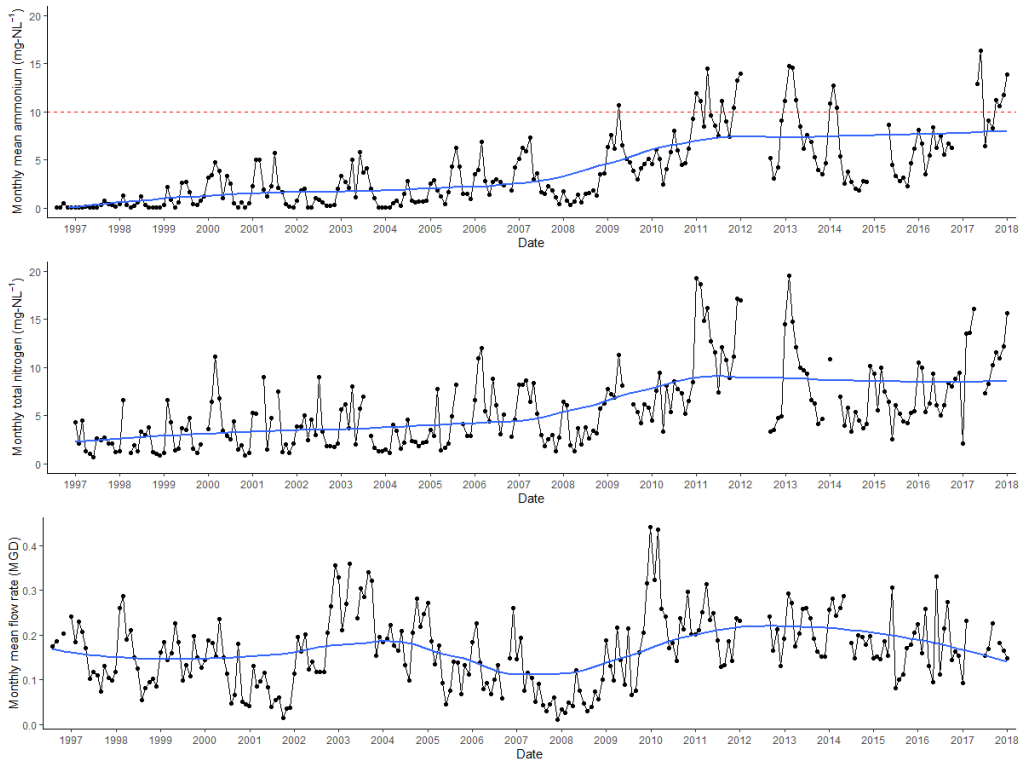


Figure 2.1: Monthly mean NH₄-N concentrations, TN concentrations, and effluent flow rates from 1996 through 2017 at the Walnut Cove WWTP. The blue lines represent the trend in the data using a local polynomial regression (loess) fitting. The red dashed line in the NH₄-N plot represents the discharge limit (10 mg-N L⁻¹) for NH₄-N in the plant effluent. Please note that while the red line is continuous in this plot, the limit is only in effect from April through October each year.

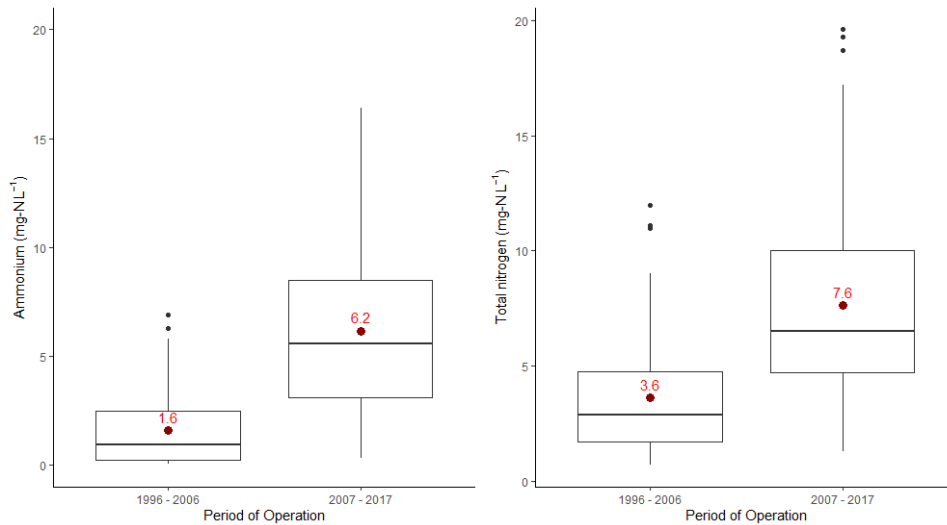


Figure 2.2: Changes in NH₄-N and TN concentrations in the plant effluent between the first decade of operation (1996-2006) and the second decade of operation (2007-2017).

Although effluent nitrogen concentrations increased, flow through the plant was roughly the same for both periods with an average effluent flow rate of 0.16 MGD during the first 10 years and 0.17 during the next 10 years (Figure 2.1). The similarity in flow rates between the two periods suggested that the declining nitrogen removal performance of the entire WWTP was not the result of either decreased residence time caused by increased flow or increased nitrogen loading due to added influent waste streams. Instead, the similarity in flow rates suggested that the plant had received consistent wastewater flows and nitrogen loads over the 20+ year operational period. Therefore, the decline in the nitrogen removal performance was likely caused by either a decline in nitrogen processing or an internal nitrogen source within the WWTP.

In terms of nitrogen processing, the treatment train was designed so the aerated primary and secondary lagoons would partially nitrify the $\text{NH}_4\text{-N}$ in the raw wastewater. This partially nitrified wastewater was then discharged to the anoxic duckweed raceway, where assimilation by the duckweed provided additional $\text{NH}_4\text{-N}$ removal during the growing season. Finally, wastewater was discharged to the FWS CWs, where the previously produced $\text{NO}_3\text{-N}$ could be removed via denitrification and additional $\text{NH}_4\text{-N}$ removal could be provided by macrophyte assimilation and paired nitrification/denitrification (Brix, 1997; Ingersoll & Baker, 1998; Kadlec & Wallace, 2009, 2009; Vymazal, 2007). Because only the plant effluent was monitored, the nitrogen processing decline could have occurred in the lagoons, duckweed raceway, wetland cells, or all three.

To identify the potential location of poor nitrogen processing, Burchell et al. (2016) conducted a month-long preliminary study of one of the FWS CW cells from mid-May to mid-June 2016. During the month-long study, mean TN concentrations decreased from 10.5 to 9.0 mg-N L^{-1} through the wetland cell (14% concentration reduction), with the concentration

reduction derived solely from an organic nitrogen (ON) concentration decline through the cell. Mean ammonium ($\text{NH}_4\text{-N}$) concentrations increased substantially, from 2.6 mg-N L^{-1} to 6.9 mg-N L^{-1} through the wetland cell. Nitrite and nitrate ($\text{NO}_2\text{-N} + \text{NO}_3\text{-N}$, hereafter just $\text{NO}_3\text{-N}$) concentrations were negligible ($< 0.05 \text{ mg-N L}^{-1}$) at both the influent and effluent sampling locations during the study. The negligible $\text{NO}_3\text{-N}$ concentrations were the result of insufficient upstream nitrification caused by the inactive lagoon aerators that had been non-functional for several months according to the site operators. While insufficient upstream aeration was certainly a factor in the poor nitrogen removal observed during the short-term study, it assumed to be a short-term condition and not a main cause of the long-term decline in performance seen in Figure 2.1. Instead, the increase in effluent $\text{NH}_4\text{-N}$ concentrations over time and the $\text{NH}_4\text{-N}$ concentration increase through one of the cells during the short-term study led to the hypothesis that the FWS CW treatment efficiency had declined due to age. To assess this hypothesis, a long-term monitoring study was initiated at both cells to evaluate wetland treatment effectiveness and identify potential cause(s) for the lack of nitrogen removal.

The study objectives were to (1) implement a monitoring setup to collect continuous water quality and hydrology data at the inlet and outlet of each wetland cell; (2) assess the current internal hydraulic performance of the wetland cells; (3) quantify nitrogen removal performance through concentration reductions, removal efficiencies, and areal removal rates; (4) if treatment performance was indeed diminished, identify potential cause(s) of increasing $\text{NH}_4\text{-N}$ and TN concentrations in the plant effluent.

METHODS AND MATERIALS

Site Description

The Walnut Cove WWTP (Permit ID #NC0025526) is a municipal wastewater treatment plant located in Walnut Cove, NC (36°17'38.5"N 80°07'57.3"W). During the study period, the WWTP served an estimated population of 1,820 persons (UNC, 2020). The plant is permitted to discharge a monthly average flow below 2273 m³ d⁻¹ (0.5 MGD). Because the plant is permitted to discharge less than 1.0 MGD, it is classified as a minor WWTP. Within the WWTP, raw sewage is first pumped into the primary aerated lagoon. The primary lagoon then discharges into the secondary aerated lagoon, which is followed by the serpentine *Lemna*-dominated pond (duckweed raceway), circular duckweed collector, inlet splitter box, two parallel *Typha*-dominated FWS CW cells, and a chlorine contact chamber before it is finally discharged into Town Fork Creek (Figure 2.3).

The WWTP was modified to its current configuration in 1996, when the town of Walnut Cove, inspired by Dr. Bill Wolverton's work using natural processes to treat environmental problems, modified their lagoon only WWTP to resemble Dr. Wolverton's aquatic plant/microbial water purification system (Patent #5,137,628). This modification included the addition of the duckweed raceway and the two-cattail dominated FWS CW cells. The duckweed raceway was included to facilitate sedimentation (by creating a quiescent environment), stabilize pH and temperature (by providing widespread shading that prevented algal growth) (Zirschky & Reed, 1988). Meanwhile, the primary function of the two FWS CW cells was to provide BOD, TSS, and nitrogen removal (Wolverton, 1992; Wolverton et al., 1983). This natural treatment train was designed to maintain concentrations of BOD₅, TSS, and NH₄-N well below the effluent discharge limits set in the site's NPDES permit (NC0025526), which required monthly average

BOD₅ and TSS concentrations to be less than 30 mg L⁻¹ all year long and monthly average NH₄-N concentrations to be less than 10 mg-N L⁻¹ from April 1st to October 31st.



Figure 2.3: Top: Aerial photograph of the WWTP (Image modified from Google Maps). Arrows indicate flow direction. Raw IN is the location of the raw wastewater inlet. The primary and secondary lagoons are labeled lagoon 1 and lagoon 2, respectively. Duckweed raceway is labeled as such, and the duckweed collector is outlined by a dashed line. FWS CW cells are labeled as Cell 1 and Cell 2. Bottom: Closer look at wetland configuration. Sampling stations are shown with red circles and the weather station is shown with a blue star.

Both wetland cells 1 and 2 received the same wastewater stream, which was discharged to the wetlands through a concrete splitter box with two contracted sharp crested weirs. The weirs had the same crest length and crest elevation, and therefore released the same influent flow rates to both cells. In addition to the main wastewater stream, both wetland cells received surface runoff from the immediate area surrounding the cell. Both wetland bottoms were underlain by a clay layer, which was assumed to allow negligible groundwater inputs and outputs. Contracted sharp-crested weirs were also installed at each wetland outlet to maintain an operational pool depth of 0.3 m. At a 0.3 m pool depth, the nominal wetland volume (V) would be 2130 m^3 per cell based on the construction plans.

In 2017, the year prior to the start of this study, the average effluent flow rate was $680 \text{ m}^3 \text{ d}^{-1}$ (0.18 MGD). If the plant effluent was assumed to be equivalent to the wetland influent, then each cell would have received an average influent flow (Q) of $340 \text{ m}^3 \text{ d}^{-1}$ (0.09 MGD). At this flow rate, the nominal wetland residence time (t_n) or hydraulic retention time (HRT) (Equation 2.1).

$$t_n = \frac{V}{Q}$$

(Eq. 2.1)

which assumes ideal plug flow hydraulics and 100% volumetric efficiency (i.e., the entire design cell volume is used), would be approximately 6 days. At this same flow rate, the nominal hydraulic loading rate (HLR_n), (Equation 2.2).

$$HLR_n = \frac{Q}{A}$$

(Eq. 2.2)

which assumes the entire nominal cell surface area (A) is used (7200 m^2), would be approximately 5 cm d^{-1} .

Data Collection

Hydrology and water quality monitoring in the CWs were conducted using an upstream/downstream design. Sampling stations were located at the inlet splitter box and both outlet structures (Figure 2.3). Each sampling station consisted of an ISCO 6712 automatic sampler integrated with an ISCO 730 bubbler module (Teledyne ISCO, Lincoln, NE) (Figure 2.4). The automated samplers were powered by two 12-volt deep cycle batteries charged by a 30-W solar panel. Bubbler modules were set to measure stage above the weir crest at 15-minute intervals. Stage measurements were taken in the water column approximately 1 m upstream of the weirs. Stage data were downloaded from automated samplers using an ISCO 581 Rapid Transfer Device (RTD).



Figure 2.4: Left: External view of a sampling station. The 30 W solar panel visible on top of station. Right: Internal view of a sampling station. The 6712 Portable Teledyne ISCO automated sampler integrated with 730 Bubbler Flow Module and two 12-volt deep cycle batteries are visible.

A Campbell-Scientific weather station was installed to gather climatic data at 15-minute intervals, including the barometric pressure (in mmHg), total precipitation (mm), air temperature ($^{\circ}\text{C}$), relative humidity (%), wind speed (m/s), wind direction (degrees), net solar radiation (W m^{-2}), net latent radiation (W m^{-2}), albedo, net radiation up (W m^{-2}), and net radiation down (W m^{-2}). As part of the weather station, an automatic tipping-bucket rain gauge measured rainfall accumulation and intensity. The rain gauge was installed approximately 1 m above the ground, and in a location free from overhead obstruction. Each bucket tip corresponded to 0.25 mm of precipitation. Daily evapotranspiration (ET) losses were estimated using the standardized ASCE Penman-Monteith Reference ET equation and meteorological data gathered from the on-site weather station (Allen et al., 2005) (Appendix B). A U20 HOBO water level sensor (Onset Computer Corporation, Bourne, MA) was placed in the inlet splitter box to measure influent water temperature and provide backup stage measurements for flow calculations.

Sampling stations were installed in July 2018 and water quality monitoring began in August 2018. The weather station was installed one month later, in September 2018. Initial equipment troubleshooting followed by site wide flood caused by precipitation from Hurricane Michael (October 2018) delayed the start of continuous water quality and hydrologic data collection until November 2018. Continuous water quality and hydrology monitoring was maintained through March 2019. Weekly site visits were conducted to download data and perform site maintenance. During site visits, additional water quality parameters including pH, DO, specific conductivity, and temperature were measured with a YSI Pro field probe (Xylem US, Yellow Springs, OH).

Water quality samples were collected using uniform time-based sampling. Daily composite samples were composed of two 300 mL subsamples collected at 12-h intervals.

Uniform time-based sampling was selected instead of flow-based sampling to avoid sampling errors associated with occasional flow blockages, which could alter the stage measurements, and result in overestimates of flow rate and erroneous increases in sampling frequency (Figure 2.5).



Figure 2.5: An example of a submerged weir caused by a flow blockage at the outlet of cell 2 on September 18, 2018.

To preserve the samples in the field, sample bottles were pre-acidified using 25% sulfuric acid to preserve the sample at $\text{pH} < 2$ (Burke et al., 2002). Samples were collected during weekly site visits and composited into 7-day composite weekly samples for each sample location. Composite samples were submitted to the NCSU BAE Environmental Analysis Laboratory (BAE EAL) for analysis. Each composite sample was analyzed for TKN (Standard Methods 4500-Norg B, Bran & Leubbe Autoanalyzer III), $\text{NO}_3\text{-N}$ (standard autoanalyzer techniques, Lachat QuickChem 8000), $\text{NH}_4\text{-N}$ (Standard Methods 4500-NH3 G), and Cl^- (EPA Method 325.2). Concurrent organic nitrogen (ON) concentrations were estimated by subtracting $\text{NH}_4\text{-N}$ from TKN and total nitrogen (TN) concentrations were estimated by adding TKN and $\text{NO}_3\text{-N}$ concentrations.

In addition to water quality and hydrology monitoring, three inert tracer tests were conducted to evaluate the internal hydraulics of the FWS CW cells. A successful pilot tracer test was conducted in cell 1 on March 8, 2019 and led to a paired tracer test conducted in both cells on March 23, 2018. Tracer tests were initiated by adding 150 mL of Rhodamine WT fluorescent dye to the influent waste stream. Rhodamine WT dye was used as the inert tracer because of its ease of use and visibility. To obtain initial background fluorescence, grab samples were collected from the wetland outlets at the start of each experiment. During the tracer tests, both outlet ISCO automatic samplers collected discrete 700 mL samples. All samples were brought back to the NCSU BAE Ecological Restoration Lab for analysis. Rhodamine WT concentrations were measured using a Cyclops-7 Fluorometer and Databank Handheld Datalogger (Turner Designs, San Jose, CA). Samples were run in accordance with the recommended measurement practices in Appendix B of the Cyclops Submersible Sensors User's Manual (2019). Further description of tracer test data analysis and results can be found in Appendix A.

Data Analysis

Internal hydraulics

The duration of time that water spends between the inlet and outlet of the wetland is known as the wetland residence time (residence time is analogous to the wetland hydraulic retention time (HRT) and the terms can be used interchangeably). Residence time is a function of wetland flow dynamics. The most common approach to wetland flow dynamics is to assume that the wetland system acts as an ideal, plug-flow reactor (Carleton, 2002; Kadlec, 2000; Kadlec & Wallace, 2009). Wetland performance can then be predicted using plug-flow chemical reactor models built using principles borrowed from chemical engineering (Bodin et al., 2012; Levenspiel, 1999). Assuming wetlands act as ideal plug-flow reactors, all the influent water at

time t_0 will uniformly pass through the wetland and exit the wetland at a future time, t_n (Equation 2.1). Therefore, t_n can be assumed to be the time required for a complete volume exchange in the wetland (Kadlec & Wallace, 2009; Persson et al., 1999; Wahl et al., 2010). Wetland treatment performance modeled using plug-flow hydraulics represents the best-case scenario for pollutant removal because it assumes the entire wetland basin is utilized for treatment.

However, since the early 1990s, hydraulic performance tests conducted using inert tracers (i.e. tracer tests) have shown that assumption of uniform plug-flow is not appropriate for modeling field-scale CW hydraulics (Kadlec & Wallace, 2009). Short-circuiting, obstructions, and dead zones in the wetland produce nonideal flow patterns. The nonideal flow patterns reduce the efficiency of wetland and cause treatment predictions based on plug-flow conditions to overestimate the wetland treatment ability. In terms of CW implementation, the lack of uniform flow increases the land area required to achieve the same treatment predicted using the plug-flow reactor model (Equation 2.1).

The actual flow through a wetland can be described by a distribution function of residence time represented by a Residence Time Distribution (RTD). An RTD is developed for hydraulic tracer tests by measuring the outflow and outlet concentrations of pulse-injected inert tracers. The developed RTD represents the degree of residence time variability within the system (Persson et al., 1999). RTDs developed from the tracer data are often used to evaluate the hydraulic performance of a wetland cell (Bodin et al., 2012, 2013; Kadlec & Wallace, 2009; Levenspiel, 1999; Martinez & Wise, 2003; Wahl et al., 2010).

The flow represented by a wetland RTD function is somewhere between the distribution of a plug flow system and a single continuously stirred tank reactor (CSTR). As a result, the CW hydraulics can be modeled as a number (N) of CSTRs in series and is known as the tanks-in-

series (TIS) model. Using the TIS model, theoretical plug-flow can be represented by an infinite number of tanks (N) or a single CSTR can be represented by an N value of 1. Because plug-flow is ideal in FWS CW, the greater the value of N, the better the hydraulic performance (Kadlec & Wallace, 2009; Persson et al., 1999).

Furthermore, the departure from ideal, plug flow conditions results in an actual residence time, τ , that is less than the theoretical t_n . The ratio of τ/t_n is referred to as the wetland volumetric efficiency, e , and represents the departure of actual flow from ideal plug flow (Thackston et al., 1987). As the ratio of τ to t_n , the ideal volumetric efficiency would be 1. Because t_n and τ are calculated using the same flow rates, e can be used to calculate the cell's effective volume ($V_e = e \cdot V$), which represents the cell volume actively involved in flow. This effective wetland volume (V_e) can be used to estimate the effective wetland area ($A_e = V_e/h$), where h is the estimated wetland water depth where there was flow (i.e., channel water depth). Hereafter, the term *nominal* will be used to describe values based on the designed size of the wetland cells (i.e., the best estimate of the initial wetland conditions) and the term *effective* will be used to describe values based on the actual wetland conditions (A_e and V_e) estimated from the RTDs.

Tracer data were represented using RTDs, which were then used to evaluate the hydraulic performance of each cell (Bodin et al., 2012, 2013; Kadlec & Wallace, 2009; Levenspiel, 1999; Martinez & Wise, 2003; Wahl et al., 2010). There are two common methods to convert tracer experiment data to an RTD. The first method was the method of moments, which uses numerical integration of measured data. The second method was fitting the observed data to a gamma distribution function by minimizing the sum of squared errors. Both methods were used in the analysis of Walnut Cove tracer experiment data. The theoretical RTD is expressed as a function of time, $E(t)$, shown in equation 2.3 (Martinez & Wise, 2003). For direct comparison of the

RTDs under different experimental conditions, $E(t)$ can be normalized by multiplying by the nominal residence time (t_{nom}).

$$E(t) = \frac{Q(t)C(t)}{\int_0^{\infty} Q(t)C(t)dt} \quad (\text{Eq. 2.3})$$

where $E(t)$ = residence time distribution (d^{-1}), $Q(t)$ = volumetric flow exiting the wetland cell (L/d), $C(t)$ = concentration of tracer exiting the wetland cell (mg/L)

For the method of moments, the RTD for each tracer experiment was estimated using the trapezoid integration rule (equation 5) The zeroth, first, and second moments for the RTD, which correspond to the mass of tracer recovered (M_{rec}), observed mean residence time (τ) and the spread of the RTD curve (σ^2), respectively, can also be estimated using this method (Equations 2.4, 2.5, 2.6, & 2.7).

$$E(t) = \frac{Q(t)C(t)}{\int_0^{\infty} Q(t)C(t)dt} = \frac{Q(t)C(t)}{M_0} \approx \frac{Q(t)C(t)}{\sum_{i=2}^n \left(\frac{(Q(t_i)C(t_i) + Q(t_{i-1})C(t_{i-1}))}{2} \right) (t_i - t_{i-1})} \quad (\text{Eq. 2.4})$$

$$M_{rec} = M_0 = \int_0^{\infty} Q(t)C(t)dt \approx \sum_{i=2}^n \left(\frac{(Q(t_i)C(t_i) + Q(t_{i-1})C(t_{i-1}))}{2} \right) (t_i - t_{i-1}) \quad (\text{Eq. 2.5})$$

$$\tau = M_1 = \int_0^{\infty} tE(t)dt \approx \frac{\sum_{i=2}^n \left(\frac{(t_i Q(t_i)C(t_i) + t_{i-1} Q(t_{i-1})C(t_{i-1}))}{2} \right) (t_i - t_{i-1})}{\sum_{i=2}^n \left(\frac{(Q(t_i)C(t_i) + Q(t_{i-1})C(t_{i-1}))}{2} \right) (t_i - t_{i-1})} \quad (\text{Eq. 2.6})$$

$$\sigma^2 = M_2 = \int_0^{\infty} t^2 E(t) dt - \tau^2 \approx \left[\frac{\sum_{i=2}^n \left(\frac{(t_i^2 Q(t_i) C(t_i) + t_{i-1}^2 Q(t_{i-1}) C(t_{i-1}))}{2} \right) (t_i - t_{i-1})}{\sum_{i=2}^n \left(\frac{(Q(t_i) C(t_i) + Q(t_{i-1}) C(t_{i-1}))}{2} \right) (t_i - t_{i-1})} \right] - \tau^2$$

(Eq. 2.7)

Tracer test results were also analyzed by building an RTD through the fitting the data to the probability density function of the gamma distribution as a function of the parameters (x, α, β) (Equation 2.8).

$$f(x, \alpha, \beta) = \frac{\beta^\alpha}{\Gamma(\alpha)} x^{\alpha-1} e^{-\beta x}$$

(Eq. 2.8)

where x is time, α is the N parameter, and β is N/τ . In the data fitting process, initial values τ and N parameters were set to those estimated using the method of moments. Optimization was completed by minimizing the sum of squared error between the gamma function and the estimated $E(t)$ from the method of moments (Equation 2.9).

$$SSE = \sum_{i=1}^n \left[E(t_i) - f\left(t_i, N, \frac{N}{\tau}\right) \right]^2$$

(Eq. 2.9)

Both methods were used to analyze tracer data and estimate the mass of tracer recovered (M_{rec}), observed mean residence time (τ) and the spread of the RTD curve (σ^2). From the estimates of τ and σ^2 , the number of tanks in series parameter (N), the volumetric efficiency (e), the hydraulic efficiency index (λ_e), and the dimensionless dispersion (σ_ϕ^2) were calculated (Equations 2.10, 2.11, 2.12, & 2.13). The estimates from both methods were averaged together to

provide a single value for each estimate in each cell. The hydraulic efficiency index, developed by Persson et al. (1999), allows for a comparison of hydraulic efficiency between different wetland cells.

$$N = \frac{\tau^2}{\sigma^2}$$

(Eq. 2.10)

$$e = \frac{\tau}{t_n}$$

(Eq. 2.11)

$$\lambda_e = e \left(1 - \frac{1}{N}\right)$$

(Eq. 2.12)

$$\sigma_\phi^2 = \frac{\sigma^2}{\tau^2}$$

(Eq. 2.13)

To evaluate and compare hydraulic indices, the hydraulic efficiency index (λ_e), the dimensionless dispersion (σ_ϕ^2), and the short-circuiting index (dimensionless time at which 10% of recovered tracer mass has left the basin, t_{10}/t_n) were estimated for both the moment and gamma fit methods. The hydraulic efficiency index provides a measure of general hydraulic performance, the dimensionless dispersion provides a measure of mixing between water parcels, and the short-circuiting index provides a measure of preferential flow paths in the wetland. The indices from both methods were averaged together to provide a single index value for each cell. For both the hydraulic efficiency index and the short-circuiting index, greater values represent better hydraulic performance. For the dimensionless dispersion index, lower values represent better hydraulic performance because a mixing of all the water parcels suggests that the wetland

is acting like a single CSTR, which would indicate that N was equal to 1. Using ranges of hydraulic indices given in Liu et al. (2020) and Persson et al. (1999), a qualitative evaluation of hydraulic performance was developed (Table 2.1). The R script used to perform analysis can be found in Appendix A.

Table 2.1: Ranges of performance for the three evaluated hydraulic indexes. Ranges modified from thresholds presented in Liu et al. (2020) and Persson et al. (1999).

Hydraulic Index	Performance Ranges		
	compromised	acceptable	excellent
λ_e	≤ 0.5	$0.5 - 0.75$	> 0.75
σ_{ϕ^2}	> 0.2	$0.1 - 0.2$	$0.0 - 0.1$
t_{10}/t_{nom}	$0 - 0.3$	$0.3 - 0.7$	> 0.7

Hydrology

Flow was estimated from stage measurements taken at 15-minute data intervals. Flow rates were estimated using the Francis (1883) equation as specified for standard fully contracted weirs in the Bureau of Reclamation’s Water Measurement Manual (2001) (Equation 2.14).

$$Q = 3.33(L - 0.2H)(H^{3/2}) \quad (\text{Eq 2.14})$$

where Q = volumetric flow ($\text{ft}^3 \text{ s}^{-1}$), L = length of the weir (ft), and H = head over the weir (ft). The site’s sharp-crested rectangular contracted weirs had a weir length (L) of 1.5 ft (0.45 m). This equation was valid when H/L was less than or equal to 0.33. With L equal to 1.5 ft, the equation was valid for the site when H was less than or equal to 0.5 ft. Under normal conditions, stage was always below the 0.5 ft threshold. Once calculated, flow rate estimates were converted to SI units. However, the entire WWTP was within the 20-year floodplain associated with Town Fork Creek and subject to sitewide flooding. When a site wide flood

occurred, as one did in October 2018, the flow rates were impossible to quantify (all sharp-crested weirs were fully submerged) and omitted from analysis.

To reduce the influence of error-inducing noise in stage measurements, the 15-minute flow estimates were averaged to daily flow estimates. Daily Q_{in} , P , and ET estimates were likely more accurate than outlet flow measurements. Short-term equipment malfunctions and measurement errors caused by flow blockages or debris on the outlet weir plates were more common at the outlet, and occasionally resulted in missing or obviously inaccurate Q_{out} estimates. Therefore, daily Q_{out} values were evaluated for accuracy using the following algorithm, which assumed an acceptable daily water balance accuracy of $\pm 20\%$ (Kadlec & Wallace, 2009; Martinez & Wise, 2003). If Q_{out} was greater than $1.2*(Q_{in} + P*A_d - ET*A_s)$ or less than $0.8*(Q_{in} + P*A_d - ET*A_s)$, then the Q_{out} estimated by the stage measurement was removed and filled using a seasonal linear relationship between Q_{in} and Q_{out} (i.e., a missing or inaccurate data point from February 2019 would be filled using a linear relationship of daily flow estimates from January through March 2019).

The bottoms of both wetland cells were designed to include a clay layer, so infiltration was assumed to be negligible. The wetland cells were not designed to store water; therefore, storage should be near zero over the time periods evaluated. With infiltration and storage set to zero, any remaining residual was deemed to represent slight measurement or estimate error within the water budget.

Using wastewater flow data (both measured and adjusted), weather data, wetland surface runoff area, and infiltration assumptions, a water balance was conducted for the study period (Nov 18 through Mar 19) (Equation 2.15).

$$Residual = V_{in} + (P * A_d) - V_{out} - ET * A_s$$

(Eq. 2.15)

where V_{in} and V_{out} were the cumulative influent and effluent flow for each cell (m^3), respectively, P was cumulative precipitation (m), A_d was the cell nominal surface area plus the drainage area that contributes surface runoff to each cell (m^2), ET was cumulative evapotranspiration (m), A_s was the nominal cell surface area (m^2), and Residual was the unaccounted-for water volume that would produce water balance closure (m^3).

Water quality analysis

Summary statistics were calculated from water quality parameters (water temperature ($^{\circ}C$), pH, dissolved oxygen ($mg\ L^{-1}$), and specific conductivity ($\mu S\ cm^{-1}$)) which were measured at each sampling station during most site visits. However, variable site visit and measurement frequencies during the period caused variable monthly parameter measurement sample sizes. Therefore, measurements were averaged by month and then by period to avoid skewing the central tendency towards times of increased measurement frequency.

Summary statistics were calculated from weekly pollutant concentrations observed at each sampling location from September 2018 through March 2019. Summary statistics (including median, mean, and standard deviation) were computed for each nitrogen species (ON, NO_3-N , NH_4-N , and TN). To provide a measure of statistical significance, student t-tests were performed to evaluate the difference between paired pollutant concentrations at the inlet and outlet 1 (cell 1) and the inlet and outlet 2 (cell 2). The weekly span was longer than the residence times in either cell and therefore deemed long enough to prevent synoptic errors due to travel time differences. A significance level of 0.05 was used for all tests. Using the mean

concentration during the study period, percent change through both wetland cells was calculated for each nitrogen species using equation 2.16.

$$\text{Percent (\%) Change} = \left(\frac{C_{in} - C_{out}}{C_{in}} \right) * 100$$

(Eq. 2.16)

where, C_{in} was the inlet sample pollutant concentration (mg L^{-1}) and C_{out} was the outlet sample pollutant concentration (mg L^{-1}). A positive change indicated an observed decrease in concentration through the wetland cell, while a negative change indicated an observed increase of concentration through the cell.

Pollutant load analysis

For the load analysis, daily influent and effluent loads were estimated for each nitrogen species (ON, $\text{NH}_4\text{-N}$, $\text{NO}_3\text{-N}$, TN) using the linear interpolation of concentration method (Moatar & Meybeck, 2005) (Equation 2.17). This method was selected because it was shown by Moatar & Meybeck (2005) to provide accurate load estimates for seasonally variable nutrient concentrations in monitoring programs with regular sampling. Using this method, daily loads were calculated by multiplying the average daily flow by the daily pollutant concentration. To estimate daily pollutant concentrations, the ON, $\text{NH}_4\text{-N}$, $\text{NO}_3\text{-N}$, and TN concentrations in each composite sample were applied to the days included in that sample. For periods without samples (winter break, tracer tests, and equipment malfunction), daily pollutant concentrations were estimated by interpolating between the last known daily concentration and the next known daily concentration. Influent and effluent loads were estimated by summing the daily loads between 11/1/2018 and 3/31/2019 ($n = 151$ days). The load analysis was conducted in R using method 6 in the RiverLoad package (Nava et al., 2019).

$$Load = \sum_{j=1}^n C_j^{int} Q_j$$

(Eq. 2.17)

where, Load was the mass pollutant load per defined period (in kg d⁻¹), C_j^{int} was the the daily observed or interpolated pollutant concentration on day j (in g m⁻³), and Q_j was the daily flow rate at the sampling location on day j.

Wetland performance was evaluated by calculating the load reduction, removal efficiency, and the removal rate for each nitrogen species. Pollutant load reductions were calculated by subtracting the cumulative outlet loads during the study period from cumulative inlet loads. Wetland removal efficiency was calculated by dividing the cumulative load reduction by the cumulative inlet load. Average daily load reductions (kg-N d⁻¹) were estimated by dividing the cumulative load reduction by the 151 days of the period. To allow for comparison to other wetland studies, average daily load reductions were converted to removal rate estimates (g N m⁻² day⁻¹). Both a nominal removal rate (J_{nom}) and an effective removal rate (J_{eff}) were estimated. The J_{nom} estimate did not consider the internal hydraulics of the cell and assumed the entire nominal cell surface area (7200 m²) was used for treatment. Meanwhile, J_{eff} applied the results of the hydraulic analysis and assumed that treatment only occurred in the effective surface area (A_e) of each cell. J_{nom} was used to compare performance between other wetland studies, while J_{eff} was compared to J_{nom} to assess the influence of hydraulic inefficiencies on cell performance. All analyses were conducted using R software (R Core Team, 2017).

Nitrogen dynamics

A simplified sequential nitrogen model can be used to illustrate the magnitude of different nitrogen conversions within a wetland (Gerke et al., 2001; Kadlec, 2008; Kadlec &

Wallace, 2009). Despite its simplicity, this model can be useful in quantifying the apparent or effective rates of nitrogen conversions and identifying the dominant nitrogen transformations within a wetland. These conversions include settling of particulate ON (PON), ammonification of ON to NH₄-N, volatilization of NH₃-N to the atmosphere, assimilation of NO₃-N and NH₄-N, nitrification of NH₄-N to NO₃-N, and denitrification of NO₃-N to N₂ gas (Kadlec & Wallace, 2009; Martin & Reddy, 1997; Reddy et al., 1984). Assimilation of NO₃-N was likely insignificant due to the low NO₃-N concentrations (see Results) and the preference for NH₄-N as a nitrogen source (Kadlec & Wallace, 2009; Vymazal, 2007). Volatilization was likely insignificant because effluent pH was 7.1 during this period (see Results). The other five mechanisms were used to estimate nitrogen dynamics within the cells (equations 2.18, 2.19, and 2.20).

$$J_{ON} = J_A + J_S \tag{Eq 2.18}$$

$$J_{NH4} = J_{AU} + J_N - J_A \tag{Eq 2.19}$$

$$J_{NO3} = J_D - J_N \tag{Eq 2.20}$$

where J_{ON} , J_{NH4} , and J_{NO3} were the effective removal rates of ON, NH₄-N, and NO₃-N (g-N m⁻² d⁻¹) during the study period. J_S , J_A , J_{AU} , J_N , and J_D were the removal rates caused by sedimentation, ammonification, assimilation, nitrification, and denitrification, respectively. The assimilation removal rate (J_{AU}) was estimated to be 18 g-N m⁻² yr⁻¹ (0.05 g-N m⁻² d⁻¹). This value was estimated by averaging the typical FWS CW assimilation rates reported in Kadlec & Wallace (2009) for November (-50 g-N m⁻² yr⁻¹), December (-10 g-N m⁻² yr⁻¹), January (50 g-N

m⁻² yr⁻¹), February (50 g-N m⁻² yr⁻¹), and March (50 g-N m⁻² yr⁻¹). The negative assimilation rates indicated a release of nitrogen back to the water column. Prior to the investigation in Chapter 3, these negative rates were the only method by which internal nitrogen release could be represented. Ammonification, nitrification, and denitrification were represented using areal first-order removal rates (Equations 2.21, 2.22, and 2.23).

$$J_A = k_a \theta_a^{(T-20)} (C_o - C^*) \quad (\text{Eq 2.21})$$

$$J_N = k_n \theta_n^{(T-20)} C_A \quad (\text{Eq 2.22})$$

$$J_D = k_d \theta_d^{(T-20)} C_N \quad (\text{Eq 2.22})$$

where k_a , k_n , and k_d were the rate constants for ammonification, nitrification, and denitrification, respectively. θ_a , θ_n , and θ_d were the theta values for temperature adjustment for ammonification, nitrification, and denitrification, respectively. C_o , C_A , and C_N were the mean concentrations of ON, NH₄-N, and NO₃-N within the cells during the study, respectively. C^* was the irreducible background ON concentration (set to 1.0 mg-N L⁻¹). T was the average water temperature during the period (set to 10°C). Because the operating conditions and outlet nitrogen concentrations were similar in both cells, nitrogen dynamics were estimated for a general Walnut Cove FWS cell by averaging the outlet concentrations together from both cells.

The nitrogen dynamics in the cells were solved sequentially with ON dynamics being estimated first, followed by NH₄-N and then NO₃-N dynamics. For the ON removal rate, it was assumed that ammonification would occur in a manner similar to other FWS CWs, therefore k_a and θ_a were set to the median FWS CW values of 30 m yr⁻¹, and 1.02, respectively (Kadlec &

Wallace, 2009). J_A was then solved for using equation 2.21 and J_s was then solved for using equation 2.18. The removal rate due to nitrification (J_N) could then be estimated using equation 2.19 and the previously estimated values of J_{NH_4} , J_A , and J_{AU} . Finally, the removal rate due to denitrification (J_D) could then be estimated using the previously estimated values of J_{NO_3} and J_N .

RESULTS

Hydraulics

The data from each tracer test and the subsequent RTDs developed using both the method of moments and the gamma distribution method are shown in Figure 2.6 and 2.7. Tests were conducted at outflows between $354 \text{ m}^3 \text{ d}^{-1}$ (0.09 MGD) and $463 \text{ m}^3 \text{ d}^{-1}$ (0.12 MGD), which were slightly below the median outflow of approximately $560 \text{ m}^3 \text{ d}^{-1}$ (0.15 MGD) during the entire monitoring period (Table 2.5).

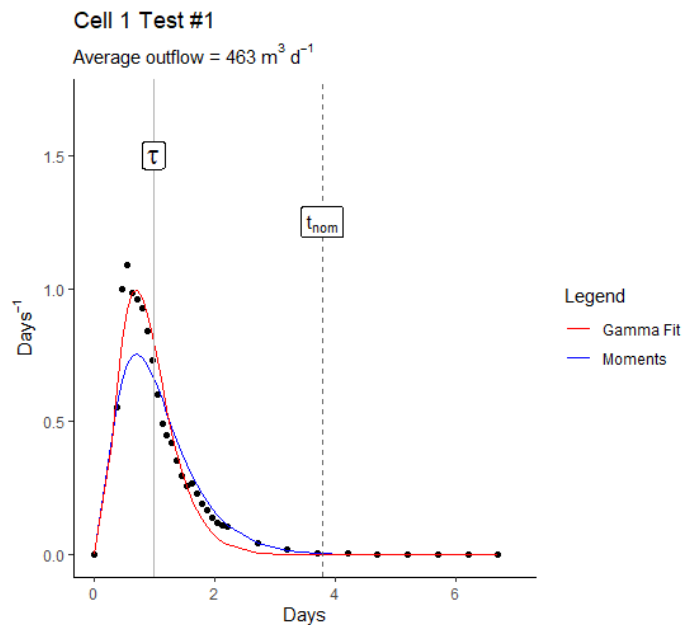


Figure 2.6: Results and analysis of the experiment initiated on March 8th, 2019. This experiment was a pilot test for site and only cell 1 was investigated. Vertical lines represent mean actual residence time (τ) and nominal residence time based on plug-flow characteristics (t_{nom}). The blue line represents the RTD built from the method of moments. The red line represents the RTD built from fitting a gamma distribution.

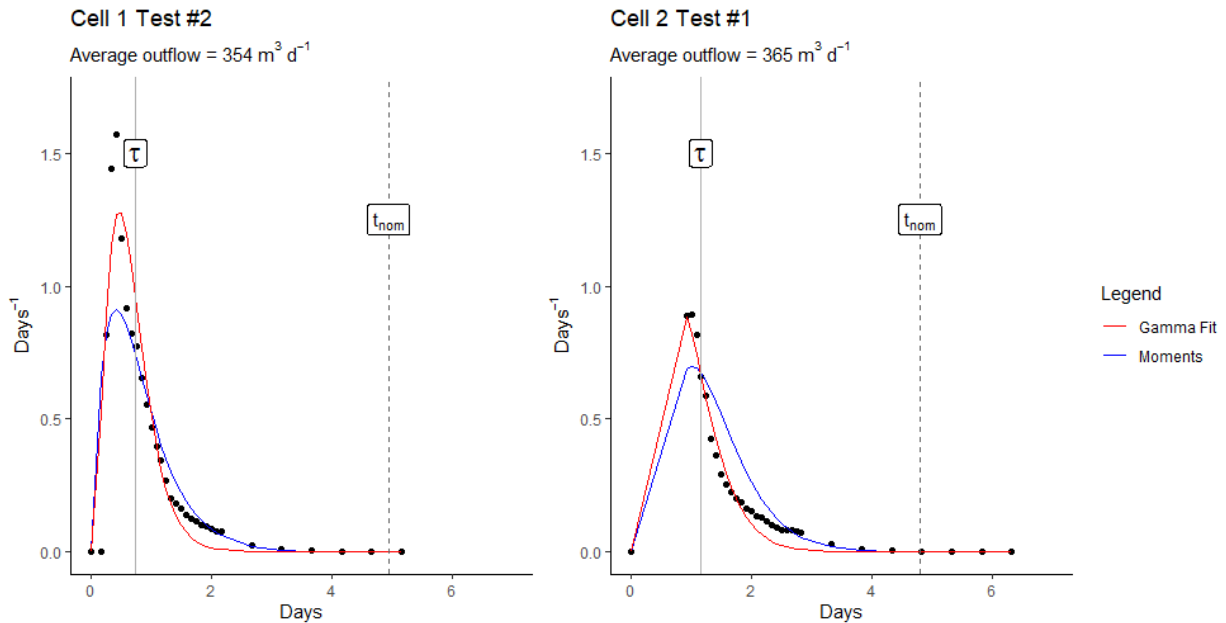


Figure 2.7: Results and analysis of the experiment initiated on March 23rd, 2019. Vertical lines represent mean actual residence time (τ) and nominal residence time based on plug-flow characteristics (t_{nom}). The blue line represents the RTD built from the method of moments. The red line represents the RTD built from fitting a gamma distribution.

For these tests, mass recovered ranged from 51 to 64% of the initial tracer mass added (Table 2.2). These mass recoveries were below the 80% threshold suggested in Headley & Kadlec (2007). Low mass recovery was likely the result of Rhodamine WT dye adsorption to organic material in the highly organic wetland environment (Kadlec & Wallace, 2009; Lin et al., 2003; Williams & Nelson, 2011). Residual Rhodamine WT dye within the cells were not observed during site visits 5 to 7 days after tests were initiated. This indicated that there was not a second peak that could have been missed and provided evidence that the shape of the RTD gathered from the tracer tests accurately represented cell hydraulics, even without closure of the tracer mass balance.

Based on the tracer test results, mean residence times were 0.9 to 1.1 days for cells 1 and 2, respectively (Table 2.2). In comparison, nominal HRTs for the original wetland design should be 4.6 and 5.0 days for cells 1 and 2, respectively. Volumetric efficiencies were similar in both

cells at approximately 0.20 (i.e., only 20% of the nominal treatment volume was being used). Using the e values and estimated water depths, effective surface areas (A_e) were 2840 and 3270 m^2 in cells 1 and 2, respectively. These A_e values were 39 and 45% of the nominal cell surface area, respectively. The number of tanks (N) was 3.1 and 4.3 in cells 1 and 2, respectively. In a review of 170 tracer tests on 106 different FWS CWs, Kadlec (2012) found that the median volumetric efficiency (e) was 0.7 and the median N value was 4.4, with the 10th and 90th percentiles of N values ranging from 1.7 to 8.9, respectively. Based on these median values, both wetland cells had underperforming internal hydraulics with e values well below their expected value and N values slightly below the expected value.

Table 2.2: Results from the inert tracer tests performed in March 2019. These results represent the average of two tests run in cell 1 and the one test run in cell 2 during this period. Values of e , τ , N , λ_e are averages of the values derived from both the moments and gamma distribution methods for analyzing a residence time distribution (RTD).

Wetland cell	Estimated water depth (m)	Recovery (%)	Average Q_{out} ($m^3 d^{-1}$)	Nominal residence time, t_n (d)	Mean residence time, τ (d)	Hydraulic efficiency, e	Effective wetland area, A_e (m^2)	Number of tanks, (N)
Cell 1	0.15	64	408	4.6	0.9	0.20	2840	3.1
Cell 2	0.15	51	364	5.0	1.1	0.23	3270	4.3

Along with the e and N values, several index values were also used to contextualize the hydraulic performance. For both cells, the hydraulic efficiency index (λ_e) was less than 0.2, the short-circuiting index (t_{10}/t_{nom}) was less than 0.1, and the mixing index (σ_ϕ^2) greater than 0.2 (Table 2.3). When compared to the expected index values for poor, adequate, and good hydraulic performance in Table 2.1, it was evident that both wetland cells were hydraulic compromised with poor overall performance.

Table 2.3: Average hydraulic indices for both cells over the study period. The three dimensionless parameters (λ_e , t_{10} , σ_ϕ^2), were averaged over both the moment and gamma fit analysis.

Wetland cell	Tests	Nominal Depth, m	λ_e	t_{10}/t_{nom}	σ_ϕ^2
Cell 1	2	0.3 (12")	0.13	0.09	0.35
Cell 2	1	0.3 (12")	0.18	0.04	0.23

Visual evidence indicated that these hydraulic inefficiencies were caused by substantial detritus accumulation within the FWS CW basin during the 20+ years of operation. The accumulated detritus had formed a new substrate layer within both cells, with the water column no longer in contact with the antecedent wetland soil. Observations in both cells suggested that the detritus depth in both cells ranged from 0.3 to 0.45 m with the surface of the detritus at or above the water level. This substantial accumulation of detritus led to shallow water depths and preferential flow paths through the cell where water flowed through small channels cut into the top of detritus substrate (Figure 2.8 & 2.9).



Figure 2.8: Areal view of the tracer tests initiated on March 23rd, 2019. Limited vegetation coverage is apparent in this photograph. This photo was taken approximately 6 hours after the dye was released. Preferential flow paths are visible in cell 1 (left). The preferential flow paths for cell 2 (right) did not begin until the last half of the cell.



Figure 2.9: Observations of detritus substrate in the FWS CWs. The pictures show detritus substrate above the water level in some places with channelized flow paths cutting through the detritus. Although the cells are vegetated, the vegetation was not in contact with the wastewater, but was instead growing on the accumulated detritus.

Hydrology

Mean daily flow estimates were calculated at the inlet, outlet 1, and outlet 2 for each day (Figures 2.10 & 2.11). 58 days (38%) and 19 days (13%) were filled due to error at outlets 1 and 2, respectively. The median influent and effluent flow rates in cell 1 were 559 and 561 $\text{m}^3 \text{d}^{-1}$, respectively. Meanwhile, the median influent and effluent flow rates in cell 2 were 560 and 559 $\text{m}^3 \text{d}^{-1}$, respectively. The water budget indicated that the residuals in cells 1 and 2 were 2.8 and 3.8% of the inflow of cells 1 and 2, respectively (Table 2.4). This residual was deemed acceptable for use in further analysis.

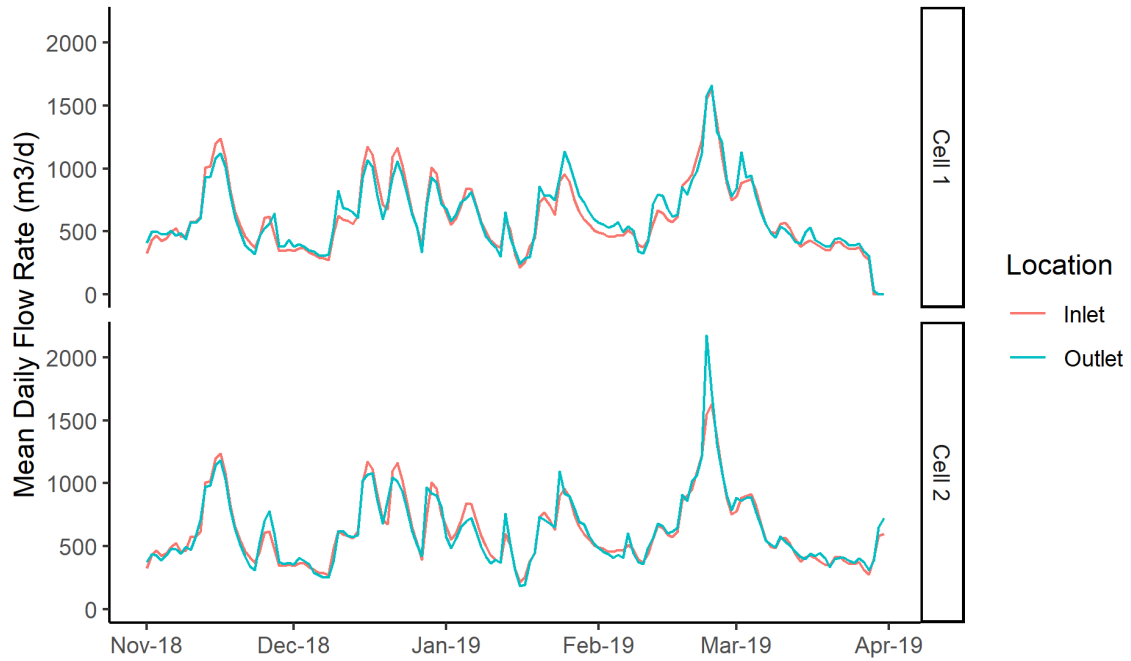


Figure 2.10: Average daily flow rates at the inlet and outlet of both cells over the study period.

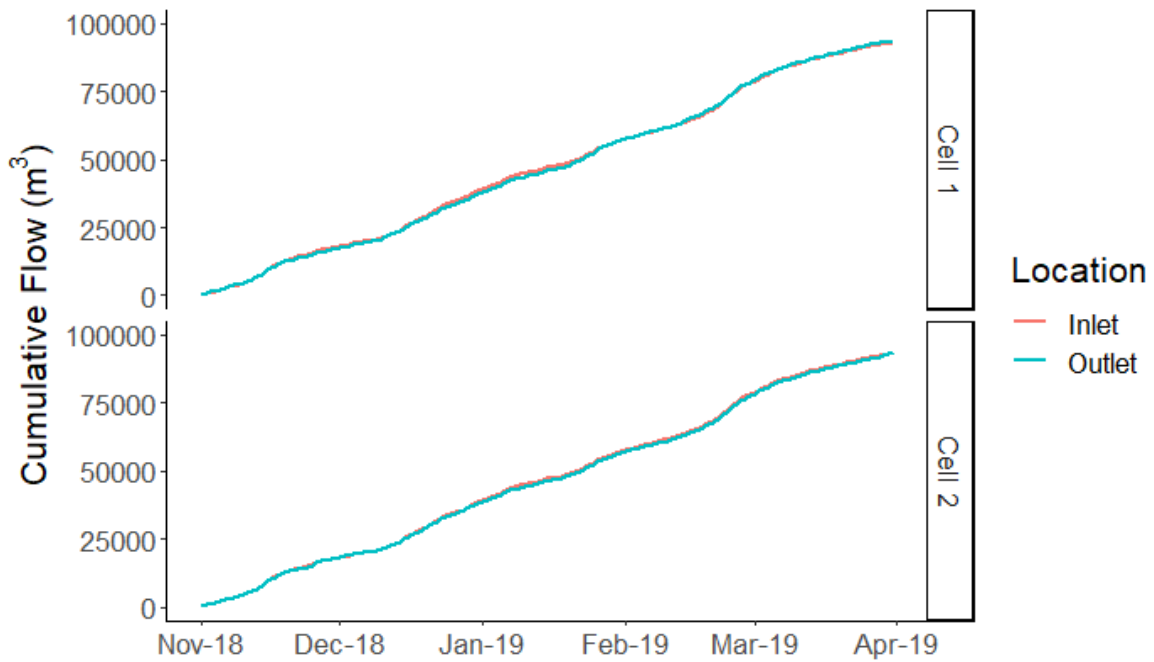


Figure 2.11: Cumulative daily flow rates at the inlet and outlet of both cells over the study period.

Table 2.4: The water budget for both cells. Inflow and outflow rates are the sum of the daily flow rates at each location. Precipitation and evapotranspiration were assumed to be the same for both cells. Both cumulative volumes and depths of precipitation and evapotranspiration were reported. A positive error indicated inflow was greater than outflow for the period. Residual term includes possible water lost to infiltration and errors in flow estimates and climatic measurements.

	Wetland cell 1	Wetland cell 2
Nominal Drainage Area, A_d (m^2)	9800	9800
Nominal Surface Area, A_s (m^2)	7200	7200
Inflow (m^3)	92,340	93,920
Outflow (m^3)	93,020	93,570
Precipitation (m^3, mm)	6130, 625	
Evapotranspiration (m^3, mm)	2850, 395	
Residual (m^3) (% of inflow)	2600 (2.8%)	3640 (3.9%)

Using the hydrologic and hydraulic results, 20+ years of operation and detritus accumulation had decreased the residence time of the cells from over 3 days for both cells to below 1 day at this median inflow rate (Table 2.5). This also increased the HLR from approximately 8 cm d^{-1} , which nearly matches the 8.9 cm d^{-1} average HLR for FWS CWs with TN removal data in the Kadlec and Wallace (2009) database, to an effective HLR of approximately 20 cm d^{-1} .

Table 2.5: Nominal hydraulic residence time (HRT), mean residence time (τ), nominal hydraulic loading rate (HLR), and effective HLR using the median inflow to both cells. Nominal values are based on design volumes and design surface areas for the cells. Mean residence time and effective HLR use the effective volumes and areas of the cells based on the tracer test data.

	Cell 1	Cell 2
Median Q_{in} ($m^3 d^{-1}$)	560	560
Nominal HRT (d)	3.3	3.3
Mean residence time, τ (d)	0.7	0.8
Nominal HLR ($cm d^{-1}$)	7.8	7.8
Effective HLR ($cm d^{-1}$)	20	17

Water quality analysis

Water quality parameters were measured 16 times from August 2018 through March 2019. Because measurements were taken during site visits, all measurements were recorded during the daytime. Water quality measurements were taken after Hurricane Michael in October 2018 until February 2019. Mean values during the period can be found in Table 2.6. Daytime measurements paired with the lack of data from November, December, and January indicated these mean values were an overestimate of water temperatures during the period. A better measure for temperature during this period was the HOBO data logger in the inlet spitter box. Using the data logger data, which measured temperature every 15 minutes, the mean inlet water temperature over the monitoring period was 10°C.

Table 2.6: Average values of mid-day water quality parameters measured during the period from 9/1/2018 to 3/31/2019. No measurements were taken in November, December, or January. The inlet sampling station samples the influent waste stream immediately before it enters the two wetland cells and therefore can be assumed to represent the influent to both cells.

Sampling Station	Average concentrations (mg-N L ⁻¹)			
	Temperature (°C)	Dissolved Oxygen (mg L ⁻¹)	pH	Specific Conductivity (µS cm ⁻¹)
Inlet	16.5	1.0	7.2	365
Outlet 1	16.4	0.9	7.1	372
Outlet 2	16.6	0.9	7.1	367

Nitrogen concentration analysis spanned from 9/1/2018 to 3/31/2019, which resulted in 28, 24, and 27 weekly composite samples collected at the inlet, outlet 1, and outlet 2, respectively (Figure 2.12). The number of samples collected were not equal because outlet composite samples could not be collected during tracer tests and there were a few instances of mid-week equipment malfunctions. Mean (\pm standard deviation) and median concentrations for each nitrogen species were calculated and reported in Table 2.7. The average difference between mean and median concentrations for each nitrogen species was less than 0.5 mg-N L⁻¹; therefore, only means were reported.

Mean ON concentrations were 2.8, 2.4, and 2.3 mg-N L⁻¹ at the inlet, outlet 1, and outlet 2, respectively. ON concentration dynamics were similar in both cells with 0.4 and 0.3 mg-N L⁻¹ reductions in cells 1 and 2, respectively. Mean NH₄-N concentrations were 8.0, 8.2 and 8.4 mg-N L⁻¹ at the inlet, outlet 1, and outlet 2, respectively, an increase through both cells. Mean NO₃-N concentrations decreased through the cells, and were 0.13, 0.09, and 0.05 mg-N L⁻¹ at the inlet, outlet 1, and outlet 2, respectively. Notably, these NO₃-N concentrations were well below those of the reduced nitrogen species (ON and NH₄-N). Relative to the inlet mean concentrations at other FWS CWs wetlands reported by Kadlec and Wallace (2009), mean inlet ON and NO₃-N

concentrations were below or near the minimum concentrations observed in other FWS CW treatment wetlands. Overall, TN concentrations were slightly reduced through each cell, with mean TN concentrations of 10.9, 10.7, and 10.8 mg-N L⁻¹ at the inlet, outlet 1, and outlet 2, respectively.

Overall, no mean concentration reductions were greater than 0.5 mg-N L⁻¹ for any nitrogen species and NH₄-N concentrations increased through both wetland cells (Table 2.7 & 2.8). Of the 21 paired sampling periods, there were no significant differences between inlet and outlet concentrations of ON, NH₄-N, or TN in either cell at the p=0.05 level. For NO₃-N concentrations, there was a significant decrease between inlet and outlet concentrations in both cells. However, this significant difference was irrelevant in terms of nitrogen load removal, due to the very low NO₃-N concentrations. Based on concentration data, there appeared to be minimal nitrogen processing through the cell; this can be seen most clearly in the 2 and 1% TN concentration reductions for cells 1 and 2, respectively (Table 2.8).

Table 2.7: Average concentrations of nitrogen species at each sampling location during the period from 9/1/2018 to 3/31/2019. The inlet sampling station samples the influent waste stream immediately before it enters the two wetland cells and therefore represents the influent to both cells.

Sampling Station	Average concentrations (mg-N L ⁻¹)			
	ON	NH ₄ -N	NO ₃ -N	TN
Inlet	2.8 ± 1.2	8.0 ± 2.0	0.13 ± 0.08	10.9 ± 2.3
Outlet 1	2.4 ± 1.6	8.2 ± 1.5	0.09 ± 0.06	10.7 ± 2.2
Outlet 2	2.3 ± 1.6	8.4 ± 1.6	0.05 ± 0.03	10.8 ± 2.5

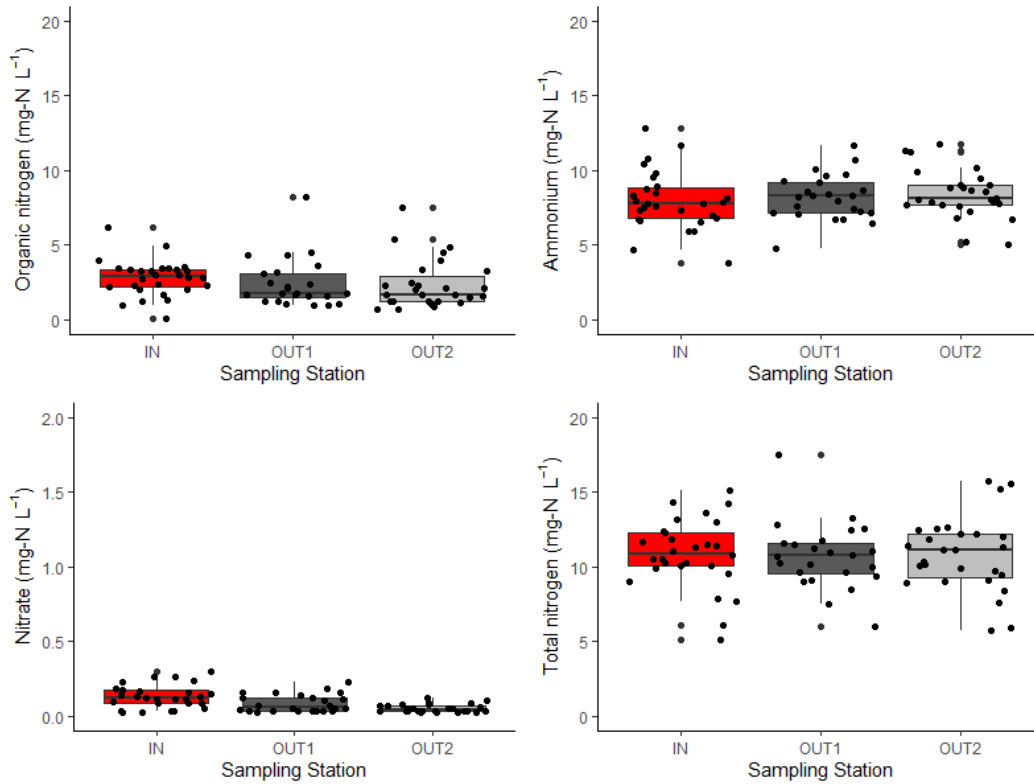


Figure 2.12: Concentrations of ON, NH₄-N, NO₃-N, and TN in composite samples collected from the sampling stations (inlet, outlet 1, and outlet 2). Boxplots indicate the median and interquartile range.

Table 2.8: Concentration change through the wetland based on mean concentrations during the study period. A positive change indicated a decrease through the wetland and a negative change indicated an increase through the wetland.

Wetland	Concentration change through cell, in mg-N L ⁻¹ (%)			
	ON	NH ₄ -N	NO ₃ -N	TN
Cell 1	0.4 (14%)	-0.2 (-2%)	0.04 (31%)	0.2 (2%)
Cell 2	0.5 (21%)	-0.4 (-5%)	0.08 (89%)	0.1 (1%)

Because concentration changes did not consider dilution or infiltration, conclusions about nitrogen processing and treatment performance within the cells should not be made using concentration changes alone. However, two notable trends were observed in the concentration results. One was the lack of $\text{NO}_3\text{-N}$ in the influent waste stream. $\text{NO}_3\text{-N}$ concentrations were never greater than 0.5 mg-N L^{-1} in the influent, which was dominated by $\text{NH}_4\text{-N}$ (inlet $\text{NH}_4\text{-N}$ concentrations were, on average, greater than 70% of the inlet TN concentrations). This lack of $\text{NO}_3\text{-N}$ was concerning because without $\text{NO}_3\text{-N}$ entering the system, denitrification and therefore complete nitrogen removal were likely to be limited. Additionally, the continuation of the low influent $\text{NO}_3\text{-N}$ concentrations suggested that the lack of upstream aeration (i.e., pretreatment) was not a short-term condition and may have been influencing nitrogen processing for longer than what was previously understood.

The other key takeaway was the increase in $\text{NH}_4\text{-N}$ concentration through both wetland cells. An increase in $\text{NH}_4\text{-N}$ concentrations also occurred during the short study in the summer of 2016 (Burchell et al., 2016), and this continued observation of $\text{NH}_4\text{-N}$ increases suggested an internal $\text{NH}_4\text{-N}$ source was present in both cells (through ammonification of water column ON, release of $\text{NH}_4\text{-N}$ from the substrate, or both). Additionally, this increase suggested that $\text{NH}_4\text{-N}$ removal processes (i.e., assimilation and nitrification) were limited during the study period. While assimilation was expected to be minimal during the non-growing season (fall and winter months), Gerke et al (2001) showed that substantial nitrification could occur in a FWS CW at mean water temperatures of only 11°C . This site had a slightly lower mean water temperature (9.8°C) during the study period, but this slight change should not have severely impacted nitrification.

Nitrogen removal performance

The load analysis spanned from 11/1/2018 to 3/31/2019 for a total of 151 days. The inlet TN load during this period was approximately 1100 kg (7.4 kg-N d⁻¹) for both cells. Most of this TN load entered the cells as TKN (7.3 kg-N d⁻¹, or 99% of the TN), and more specifically as NH₄-N (5.4 kg-N d⁻¹). During this period, there was a slight export of NH₄-N in cell 2 and a slight removal in cell 1 (Table 2.9). Unlike NH₄-N, ON and NO₃-N were retained within both cells. Roughly 100 kg of ON were retained in both cells, which equated to a removal efficiency of approximately 35%. NO₃-N removal efficiency was substantial (29% in cell 1 and 57% in cell 2), but actual NO₃-N removal was small relative to the TN removal in the cells (~100 kg-N), because the influent NO₃-N load was only 14 kg-N. When evaluated as TN, neither cell performed well (8 and 11% removal), and ON retention contributed the most to overall nitrogen retention within either cell. Note, loads were not calculated for September and October due to flow measurement issues, so load removal efficiencies are somewhat different than the concentration changes.

Table 2.9: Influent and effluent loads for each nitrogen during the period from 11/1/2018 to 3/31/2019 (151 days).

Wetland	Sampling Station	Load, in kg (kg/d)			
		ON	NH ₄ -N	NO ₃ -N	TN
Cell 1	Inlet	278 (1.8)	819 (5.4)	14 (0.1)	1111 (7.4)
	Outlet	175 (1.2)	811 (5.3)	10 (0.1)	996 (6.6)
	Removal efficiency	37%	1%	29%	11%
Cell 2	Inlet	281 (1.9)	828 (5.5)	14 (0.1)	1123 (7.5)
	Outlet	188 (1.2)	838 (5.5)	6 (0.04)	1031 (6.8)
	Removal efficiency	33%	-1%	57%	8%

The removal rate for each nitrogen species was estimated over the period for both the nominal area and the effective area (Table 2.10). The nominal ON removal rate was approximately $0.1 \text{ g-N m}^{-2} \text{ d}^{-1}$ for each cell. With $\text{NH}_4\text{-N}$ mass release and $\text{NO}_3\text{-N}$ mass retention values at essentially $0 \text{ g-N m}^{-2} \text{ d}^{-1}$, the nominal TN removal rates for both cells were also approximately $0.1 \text{ g-N m}^{-2} \text{ d}^{-1}$ for each cell.

This value was well below the $0.35 \text{ g-N m}^{-2} \text{ d}^{-1}$ median annual TN removal rate estimated from 116 FWS wetlands by Kadlec and Wallace (2009). In fact, the TN removal rate in the wetland cells was in the bottom 10th percentile of the 116 wetlands evaluated. At $0.1 \text{ g-N m}^{-2} \text{ d}^{-1}$, the TN removal rate was also less than half of the $0.24 \text{ g-N m}^{-2} \text{ d}^{-1}$ of TN retained in a comparable FWS CW in California, which received an influent TN load of $0.98 \text{ g-N m}^{-2} \text{ d}^{-1}$ ($0.75 \text{ g-N m}^{-2} \text{ d}^{-1}$ from $\text{NH}_4\text{-N}$) from 9/16/1996 to 5/6/1997 (Sartoris et al., 1999). To further illustrate the poor nitrogen removal performance of the cells, the $0.1 \text{ g-N m}^{-2} \text{ d}^{-1}$ TN removal rate was below the median TN removal rate of $0.25 \text{ g-N m}^{-2} \text{ d}^{-1}$ determined from a meta-analysis of 203 wetlands by Land et al. (2016) and the average TN removal rate of $0.40 \text{ g-N m}^{-2} \text{ d}^{-1}$ observed in 26 restored wetlands in Iowa receiving nitrate-enriched agricultural drainage by Crumpton et al. (2020).

Table 2.10: Areal mass removal rate of nitrogen species within each wetland during the period from 11/1/2018 to 3/31/2019 (n = 151 days). A positive areal mass removal rate indicated a retention, and a negative areal mass removal rate indicated an internal release. J_{nom} was the nominal removal rate and J_{eff} was the effective removal rate.

Wetland	Surface Area (m ²)		Pollutant areal mass removal rate (g-N m ⁻² d ⁻¹)			
			ON	NH ₄ -N	NO ₃ -N	TN
Cell 1	7200	J_{nom}	0.09	0.01	0.00	0.11
	2840	J_{eff}	0.24	0.03	0.01	0.28
Cell 2	7200	J_{nom}	0.08	-0.01	0.01	0.08
	3270	J_{eff}	0.19	-0.02	0.02	0.18

When only the effective wetland cell area was considered (e.g., the reduced wetland cell area due to detritus buildup), the TN removal rate increased to 0.28 and 0.18 g-N m⁻² d⁻¹ in cells 1 and 2, respectively. These removal rates were near the central tendency of TN removal rates for each of the previously stated studies (Kadlec & Wallace, 2009; Land et al., 2016; Sartoris et al., 1999). The near expected nitrogen removal rate when only the effective areas were considered demonstrated how nitrogen removal was at least in part limited by the poor hydraulic efficiency within the cells. Therefore, if the effective area of the cells were restored to the original dimensions, nitrogen load removal would likely improve. However, this increase in the TN removal rate when only the effective area was considered may not be sustainable when the cell is cleaned out for two reasons. One, overloaded systems have been shown to produce greater areal removal rates, likely because nitrogen availability is not an issue (Ingersoll & Baker, 1998). Two, the wetland environment (i.e., the amount of organic carbon, water depth, vegetation cover, shading, etc.) of the wetland cell following clean-out will be different from the previous detritus-filled conditions.

Nitrogen dynamics

Although they are difficult to accurately quantify given the data collected in this study, it was important to attempt to explain the overall N dynamics that may occur in these wetlands. The estimated effective nitrogen removal rates attributed to each nitrogen transformation are shown in Figure 2.13. Effective removal rates for ammonification, nitrification and denitrification were estimated to be 0.1, 0.05, and 0.08 g-N m⁻² d⁻¹ (36, 18, and 30 g-N m⁻² yr⁻¹), respectively (values are based on the reduced areas of active treatment discovered in this study). The apparent nitrification rate of 0.05 g-N m⁻² d⁻¹ was similar to the mean wetland nitrification rate of 0.048 g-N m⁻² d⁻¹, provided by Vymazal (2007); but it was well below the 0.1 to 0.3 g-N

$\text{m}^{-2} \text{d}^{-1}$ nitrification rate range estimated in other FWS CW studies (Kadlec, 2008; Kadlec et al., 2010, 2012; Kadlec & Wallace, 2009; Sartoris et al., 1999).

The $0.07 \text{ g-N m}^{-2} \text{ d}^{-1}$ denitrification rate was also on the lower end of the expected range (0.003 to $1.02 \text{ g-N m}^{-2} \text{ d}^{-1}$) provided by Vymazal (2007) and well below the denitrification rates observed in FWS CWs receiving $\text{NO}_3\text{-N}$ -dominated influent which typically ranged from 0.1 to $0.3 \text{ g-N m}^{-2} \text{ d}^{-1}$ (Bachand & Horne, 1999; Drake et al., 2018; Kadlec, 2012; Messer et al., 2017). The relatively low $0.07 \text{ g-N m}^{-2} \text{ d}^{-1}$ denitrification rate suggested that the denitrification was limited by the $0.08 \text{ g-N m}^{-2} \text{ d}^{-1}$ of available $\text{NO}_3\text{-N}$.

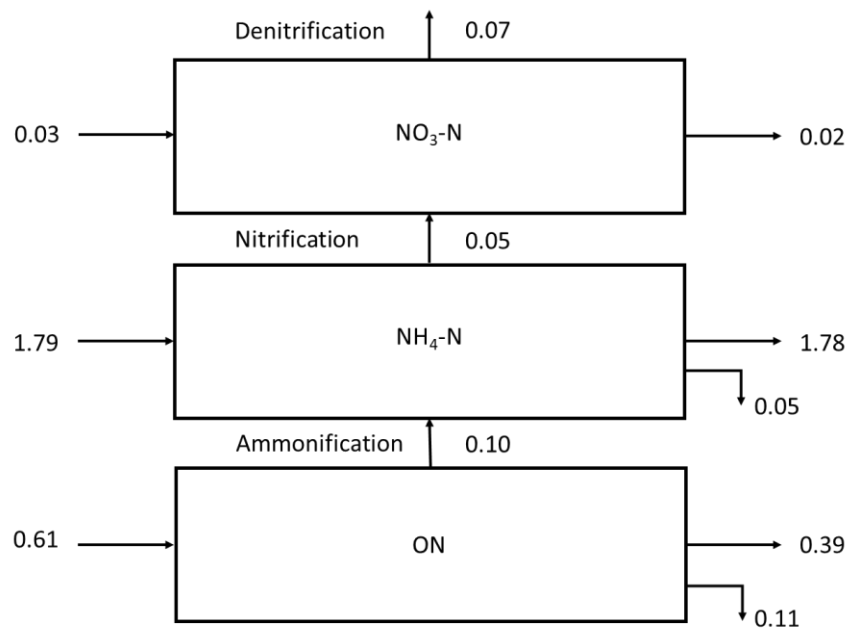


Figure 2.13: Estimated effective removal rates for nitrogen in the two FWS CWs at the Walnut Cove WWTP from November 2018 through March 2019. All values are in $\text{g-N m}^{-2} \text{ d}^{-1}$.

DISCUSSION

Age influences treatment through detritus accumulation

The lack of nitrogen removal in the aging wetland cells indicated that operational age, particularly due to lack of maintenance and excessive detritus build-up, does influence nitrogen removal. From the data gathered, the poor nitrogen removal was due, at least in part, to the reduced residence times and surface areas caused by the poor internal hydraulics. The reduced surface area is of particular importance because it results an increase in HLR based on equation 2.2. HLR has been negatively correlated with TN removal in FWS CWs (Crumpton et al., 2020; Ingersoll & Baker, 1998; Land et al., 2016). Thus, while the initial nitrogen removal in the FWS CWs was unknown, it can be inferred that the reduction in surface area due to hydraulic inefficiencies has diminished the nitrogen removal performance.

The poor internal hydraulics were the product of 20+ years of accumulated detritus that had formed into a 0.3 to 0.45 m deep substrate overlying the FWS CW bottom. Not only did this accumulated detritus substrate limit the wetland cell treatment area, but it also had the potential to be an internal nitrogen source. Table 2.7 showed that $\text{NH}_4\text{-N}$ concentrations increased through both cells, and Table 2.9 confirmed a small export of $\text{NH}_4\text{-N}$ from cell 2. The $\text{NH}_4\text{-N}$ export was caused by either ammonification in the water column or ammonification in the detritus and the subsequent diffusion of $\text{NH}_4\text{-N}$ from the detritus substrate porewater to the water column. The regeneration of $\text{NH}_4\text{-N}$ from decaying vegetation within a FWS CW was suggested by Sartoris et al. (1999), and, while not addressed in this chapter, its influence on nitrogen dynamics at Walnut Cove and other FWS CWs will be the subject of Chapter 3.

Of note, this accumulated detritus and the accompanying hydraulic inefficiencies were found to be the main cause of diminished phosphorus removal performance over time at the

Orlando Easterly Wetlands (Martinez & Wise, 2003; Wang et al., 2006). The connection between age and accumulated detritus in both studies suggested that the underlying cause of diminished performance with age is the physical process of the FWS CW basin filling in with decaying biomass. As a physical process, the accumulation of detritus over time has the potential to be universal for FWS CWs with macrophyte vegetation, which suggests that managing vegetation or detritus will be critical for sustaining FWS CW treatment effectiveness over time.

One method to reduce the accumulated detritus and improve wetland treatment effectiveness is a wetland rejuvenation (i.e., detritus removal or prescribed burning). The only examples of wetland rejuvenation available in the literature were also observed at the Orlando Easterly Wetland (Wang et al., 2006; White et al., 2008). At the site both detritus removal and prescribed burns have been employed to successfully reduce the amount of biomass in the basin and remediate age-related declines in total phosphorus removal. Although the Orlando Easterly Wetland studies are excellent case studies, further evidence of their effectiveness is needed before widespread use of wetland rejuvenation in CWs of variable size, wastewater source, location, and treatment goals.

Study Limitations

A critical limitation in the determination of overall nitrogen removal and assessment of nitrogen removal potential was the lack of $\text{NO}_3\text{-N}$ in the wetland influent. This lack of influent $\text{NO}_3\text{-N}$ was the product of poor upstream pretreatment at the facility. The lagoons were designed to have five aerators running constantly (two 3.5 hp surface aerators in the primary lagoon and three 7.5 hp surface aerators in the secondary lagoon). However, only one of these aerators (a 7.5 hp aerator in the secondary lagoon) was operational during the study. This observation suggested that the lack of aeration was not a temporary condition (as initially proposed), but that the

number of aerators running in the upstream lagoons had gradually declined as the maintenance required to sustain the aerators and electrical infrastructure increased with operational age. Under this assumption, the decline in nitrogen removal due to wetland aging was likely compounded by a gradual reduction in upstream pretreatment.

Without influent $\text{NO}_3\text{-N}$, denitrification (the main route for complete nitrogen removal in heavily loaded FWS CWs) was restricted to the amount of $\text{NO}_3\text{-N}$ that could be internally produced via nitrification (Bachand & Horne, 1999; Bastviken et al., 2005; Kadlec, 2012; Kadlec & Wallace, 2009; Mitsch & Gosselink, 2015; van Oostrom & Russell, 1994; Vymazal, 2007). Using the estimated nitrification rate and the nominal surface area, nitrification could have only converted 54 kg-N (7%) of the influent $\text{NH}_4\text{-N}$ load to $\text{NO}_3\text{-N}$. While this value is low, the amount of $\text{NH}_4\text{-N}$ converted to $\text{NO}_3\text{-N}$ drops to 23 kg-N (3%) when calculated using the effective surface area.

Other factors, such as DO, alkalinity, and pH, were relatively constant over the four-year period, which suggested that the lack of vegetation and the reduced amount of submerged surface area for microbial growth may have played a crucial role in the decline of the nitrification rates. In both cells, the accumulated detritus substrate constricted the water column to narrow channels that flowed around the wetland vegetation. These narrow channels minimized the submerged surface area for microbial growth and likely limited the potential for oxygen to be transferred to the substrate by vegetation (Figure 2.9). The importance of submerged stems and litter on nitrification was noted in a study of nitrogen dynamics following a vegetation die off in two FWS CW cells at the Tres Rios Wetlands (Kadlec, 2008). During the two years prior to the vegetation die off, nitrification rates in the wetlands were estimated to be $0.22 \text{ g-N m}^{-2} \text{ d}^{-1}$; however, in the two years after the vegetation die off, the nitrification rates dropped to -0.01 g-N

$\text{m}^{-2} \text{d}^{-1}$ in one cell and $0.02 \text{ g-N m}^{-2} \text{ d}^{-1}$ in the other cell. Taken together, it was likely that both influent nitrogen speciation and the accumulated detritus combined to restrict nitrogen removal in the cells during the monitoring period.

There were also limitations on the simplified sequential nitrogen process model used to provide estimates of nitrogen transformations within the wetland cells. For example, it was suspected that there was an upward flux of $\text{NH}_4\text{-N}$ from the accumulated detritus substrate to the water column, but there was no generally accepted method to represent this process in the model at the time this chapter was written. To include this process, negative assimilation rates were used during winter months (when nitrogen removal via assimilation would not outdo this nitrogen release). An attempt to fill this knowledge gap was conducted during this research project and reported in Chapter 3.

The other study limitation was the length of monitoring time for this baseline study. Often, studies to evaluate wetland performance are conducted on annual time scales to account for the seasonality of nutrient removal performance. However, the clear lack of nitrogen removal observed (measured during the summer of 2016 and the six months during this study) and particularly poor hydraulic performance in both cells was enough evidence to develop the conclusions presented herein. The decision was made to cut this initial baseline monitoring study short because the data supported expedited detritus removal in cell 1, which was initiated in April 2019. However, monitoring was continued after the detritus removal, with the objective to compare nitrogen removal between the rejuvenated and non-rejuvenated cell (Chapter 4). In this continued monitoring, cell 2 remained in its initial aged condition. Data in Chapter 4 will show that the reduced nitrogen removal performance observed in cell 2 during this next period of monitoring was consistent with the observations presented in this chapter.

CONCLUSION

The study found that nitrogen removal in aging FWS CW cells was substandard. TN removal efficiencies were 11% and 8%, in cells 1 and 2, respectively. TN concentration reduction were worse at 2% and 1% in cells 1 and 2, respectively. Additionally, the TN removal rate was $0.1 \text{ g-N m}^{-2} \text{ d}^{-1}$ in each cell (based on nominal cell volumes), which was well below what has been observed at other FWS CWs treating nitrogen-enriched wastewater. Based on estimated nitrogen dynamics, most nitrogen removal was the product of ON sedimentation. This general lack of TN removal matched the lack of nitrogen removal observed by Burchell et al. (2016) in cell 1 in the spring 2016, which suggested that this poor nitrogen removal performance had been consistent in the cells.

The lack of nitrogen removal was linked to the poor internal hydraulics of both cells. The volumetric efficiency of each cell was less than 0.25, with residences near 1 day and effective surface areas less than 50% of the nominal surface areas. This poor hydraulic performance was most likely caused by an accumulated detritus substrate between 0.3 and 0.45 m in depth. The accumulated detritus not only limited the magnitude of every nitrogen transformation, but it also had the potential to provide an internal nitrogen source, further reducing treatment effectiveness. While the poor nitrogen removal was at least partially a product of the accumulated detritus substrate, the lack of influent $\text{NO}_3\text{-N}$ made it difficult to assess whether the poor performance was due solely to the age-related accumulated detritus substrate or if it was a combination of both the detritus and reduced availability of $\text{NO}_3\text{-N}$.

Based on these observations, wetland nitrogen removal could be improved by either removing the detritus substrate or by increasing upstream nitrification, or both. Furthermore, the increase in $\text{NH}_4\text{-N}$ through the cells indicated that the detritus should be evaluated to determine

whether it is a considerable internal nitrogen source. If the accumulated detritus is a substantial nitrogen source, then detritus removal would not only increase the effective surface areas and volumes of a wetland cells, but would also remove an internal source, and therefore provide an additional benefit to the cleaning out the cells.

REFERENCES

- Allen, R. G., Walter, I. A., Elliott, R. L., Howell, T. A., Itenfisu, D., Jensen, M. E., & Snyder, R. L. (2005). The ASCE Standardized Reference Evapotranspiration Equation. American Society of Civil Engineers.
- Bachand, P. A. M., & Horne, A. J. (1999). Denitrification in constructed free-water surface wetlands: I. Very high nitrate removal rates in a macrocosm study. *Ecological Engineering*, 14(1–2), 9–15. [https://doi.org/10.1016/S0925-8574\(99\)00016-6](https://doi.org/10.1016/S0925-8574(99)00016-6)
- Bastviken, S. K., Eriksson, P. G., Premrov, A., & Tonderski, K. (2005). Potential denitrification in wetland sediments with different plant species detritus. *Ecological Engineering*, 25(2), 183–190. <https://doi.org/10.1016/j.ecoleng.2005.04.013>
- Bodin, H., Mietto, A., Ehde, P. M., Persson, J., & Weisner, S. E. B. (2012). Tracer behaviour and analysis of hydraulics in experimental free water surface wetlands. *Ecological Engineering*, 49, 201–211. <https://doi.org/10.1016/j.ecoleng.2012.07.009>
- Bodin, H., Persson, J., Englund, J.-E., & Milberg, P. (2013). Influence of residence time analyses on estimates of wetland hydraulics and pollutant removal. *Journal of Hydrology*, 501, 1–12. <https://doi.org/10.1016/j.jhydrol.2013.07.022>
- Brix, H. (1997). Do macrophytes play a role in constructed treatment wetlands? *Water Science and Technology*; London, 35(5), 11–17.
- Burchell, M. R., Thompson, T. W., Broome, S. W., Krometis, L. A., & Badgely, B. (2016). Constructed wetlands to polish wastewater in small rural communities—Evaluation of current and potential use to improve water quality trends and protect human health. Final report. (Virginia Tech/ NC State University Regional Collaborative Proposal Planning and Development Grants, p. 29) [Final Report].
- Burke, P. M., Hill, S., Iricanin, N., Douglas, C., Essex, P., & Tharin, D. (2002). Evaluation of Preservation Methods for Nutrient Species Collected by Automatic Samplers. *Environmental Monitoring and Assessment*, 80(2), 149–173. <https://doi.org/10.1023/A:1020660124582>
- Carleton, J. N. (2002). Damköhler number distributions and constituent removal in treatment wetlands. *Ecological Engineering*, 19(4), 233–248. [https://doi.org/10.1016/S0925-8574\(02\)00094-0](https://doi.org/10.1016/S0925-8574(02)00094-0)
- Crumpton, W. G., Stenback, G. A., Fisher, S. W., Stenback, J. Z., & Green, D. I. S. (2020). Water quality performance of wetlands receiving nonpoint-source nitrogen loads: Nitrate and total nitrogen removal efficiency and controlling factors. *Journal of Environmental Quality*, 49(3), 735–744. <https://doi.org/10.1002/jeq2.20061>
- Drake, C. W., Jones, C. S., Schilling, K. E., Amado, A. A., & Weber, L. J. (2018). Estimating nitrate-nitrogen retention in a large constructed wetland using high-frequency, continuous

- monitoring and hydrologic modeling. *Ecological Engineering*, 117, 69–83.
<https://doi.org/10.1016/j.ecoleng.2018.03.014>
- Francis, J. B. (1883). *Lowell Hydraulics Experiments* (fourth). D. Van Nostrand.
- Gerke, S., Baker, L. A., & Xu, Y. (2001). Nitrogen Transformations in a Wetland Receiving Lagoon Effluent: Sequential Model and Implications for Water Reuse. *Water Research*, 35(16), 3857–3866. [https://doi.org/10.1016/S0043-1354\(01\)00121-X](https://doi.org/10.1016/S0043-1354(01)00121-X)
- Gersberg, R. M., Elkins, B. V., & Goldman, C. R. (1983). Nitrogen removal in artificial wetlands. *Water Research*, 17(9), 1009–1014. [https://doi.org/10.1016/0043-1354\(83\)90041-6](https://doi.org/10.1016/0043-1354(83)90041-6)
- Headley, T. R., & Kadlec, R. H. (2007). Conducting hydraulic tracer studies of constructed wetlands: A practical guide. *Ecology & Hydrobiology*, 7(3), 269–282.
[https://doi.org/10.1016/S1642-3593\(07\)70110-6](https://doi.org/10.1016/S1642-3593(07)70110-6)
- Ingersoll, T. L., & Baker, L. A. (1998). Nitrate removal in wetland microcosms. *Water Research*, 32(3), 677–684. [https://doi.org/10.1016/S0043-1354\(97\)00254-6](https://doi.org/10.1016/S0043-1354(97)00254-6)
- Iovanna, R., Hyberg, S., & Crumpton, W. G. (2008). Treatment wetlands: Cost-effective practice for intercepting nitrate before it reaches and adversely impacts surface waters. *Journal of Soil and Water Conservation*, 63(1), 14A–15A. <https://doi.org/10.2489/jswc.63.1.14A>
- Kadlec, R. H. (2000). The inadequacy of first-order treatment wetland models. *Ecological Engineering*, 15(1–2), 105–119. [https://doi.org/10.1016/S0925-8574\(99\)00039-7](https://doi.org/10.1016/S0925-8574(99)00039-7)
- Kadlec, R. H. (2008). The effects of wetland vegetation and morphology on nitrogen processing. *Ecological Engineering*, 33(2), 126–141. <https://doi.org/10.1016/j.ecoleng.2008.02.012>
- Kadlec, R. H. (2012). Constructed Marshes for Nitrate Removal. *Critical Reviews in Environmental Science and Technology*, 42(9), 934–1005.
<https://doi.org/10.1080/10643389.2010.534711>
- Kadlec, R. H., Cuvellier, C., & Stober, T. (2010). Performance of the Columbia, Missouri, treatment wetland. *Ecological Engineering*, 36(5), 672–684.
<https://doi.org/10.1016/j.ecoleng.2009.12.009>
- Kadlec, R. H., Pries, J., & Lee, K. (2012). The Brighton treatment wetlands. *Ecological Engineering*, 47, 56–70. <https://doi.org/10.1016/j.ecoleng.2012.06.042>
- Kadlec, R. H., & Wallace, S. D. (2009). *Treatment Wetlands* (2nd ed.). CRC Press.
- Land, M., Graneli, W., Grimvall, A., Hoffmann, C. C., Mitsch, W. J., Tonderski, K. S., & Verhoeven, J. T. A. (2016). How effective are created or restored freshwater wetlands for nitrogen and phosphorus removal? A systematic review. *Environmental Evidence*; London, 5. <http://dx.doi.org/prox.lib.ncsu.edu/10.1186/s13750-016-0060-0>

- Levenspiel, O. (1999). *Chemical Reaction Engineering* (3rd ed.). Wiley.
- Lin, A. Y.-C., Debroux, J.-F., Cunningham, J. A., & Reinhard, M. (2003). Comparison of rhodamine WT and bromide in the determination of hydraulic characteristics of constructed wetlands. *Ecological Engineering*, 20(1), 75–88. [https://doi.org/10.1016/S0925-8574\(03\)00005-3](https://doi.org/10.1016/S0925-8574(03)00005-3)
- Liu, J., Dong, B., Zhou, W., & Qian, Z. (2020). Optimal selection of hydraulic indexes with classical test theory to compare hydraulic performance of constructed wetlands. *Ecological Engineering*, 143, 105687. <https://doi.org/10.1016/j.ecoleng.2019.105687>
- Martin, J. F., & Reddy, K. R. (1997). Interaction and spatial distribution of wetland nitrogen processes. *Ecological Modelling*, 105(1), 1–21. [https://doi.org/10.1016/S0304-3800\(97\)00122-1](https://doi.org/10.1016/S0304-3800(97)00122-1)
- Martinez, C. J., & Wise, W. R. (2003). Hydraulic Analysis of Orlando Easterly Wetland. *Journal of Environmental Engineering*, 129(6), 553–560. [https://doi.org/10.1061/\(ASCE\)0733-9372\(2003\)129:6\(553\)](https://doi.org/10.1061/(ASCE)0733-9372(2003)129:6(553))
- Messer, T. L., Burchell, M. R., Birgand, F., Broome, S. W., & Chescheir, G. (2017). Nitrate removal potential of restored wetlands loaded with agricultural drainage water: A mesocosm scale experimental approach. *Ecological Engineering*, 106, 541–554. <https://doi.org/10.1016/j.ecoleng.2017.06.022>
- Mitsch, W. J., & Gosselink, J. G. (2015). *Wetlands* (5th ed.). John Wiley & Sons, Inc.
- Moatar, F., & Meybeck, M. (2005). Compared performances of different algorithms for estimating annual nutrient loads discharged by the eutrophic River Loire. *Hydrological Processes*, 19(2), 429–444. <https://doi.org/10.1002/hyp.5541>
- Nava, V., Patelli, M., Rotiroti, M., & Leoni, B. (2019). An R package for estimating river compound load using different methods. *Environmental Modelling and Software*, 117, 100–108.
- Persson, J., Somes, N. L. G., & Wong, T. H. F. (1999). Hydraulic Efficiency of Constructed Wetlands and Ponds. *Water Science and Technology*; London, 40(3), 291–300.
- Reddy, K. R., Patrick, W. H., & Broadbent, F. E. (1984). Nitrogen transformations and loss in flooded soils and sediments. *C R C Critical Reviews in Environmental Control*, 13(4), 273–309. <https://doi.org/10.1080/10643388409381709>
- Sartoris, J. J., Thullen, J. S., Barber, L. B., & Salas, D. E. (1999). Investigation of nitrogen transformations in a southern California constructed wastewater treatment wetland. *Ecological Engineering*, 14(1), 49–65. [https://doi.org/10.1016/S0925-8574\(99\)00019-1](https://doi.org/10.1016/S0925-8574(99)00019-1)
- Seidel, K. (1976). Macrophytes and Water Purification. In *Biological Control of Water Pollution* (pp. 109–122). University of Pennsylvania Press.

- Thackston, E. L., Shields, F. D., & Schroeder, P. R. (1987). Residence Time Distributions of Shallow Basins. *Journal of Environmental Engineering*, 113(6), 1319–1332. [https://doi.org/10.1061/\(ASCE\)0733-9372\(1987\)113:6\(1319\)](https://doi.org/10.1061/(ASCE)0733-9372(1987)113:6(1319))
- Turner Designs. (2019). Cyclops Submersible Sensors User's Manual. Turner Designs. <http://docs.turnerdesigns.com/t2/doc/manuals/998-2100.pdf>
- UNC. (2020). North Carolina Water and Wastewater Rates Dashboard [Governmental]. UNC School of Government Environmental Finance Center. </resource/north-carolina-water-and-wastewater-rates-dashboard>
- US Department of the Interior. (2001). *Water Measurement Manual* (3rd ed.). US Department of the Interior, Bureau of Reclamation.
- US EPA. (2000). *Wastewater Technology Fact Sheet: Free Water Surface Wetlands* (EPA 832-F-00-024). Office of Water.
- van Oostrom, A. J., & Russell, J. M. (1994). Denitrification in Constructed Wastewater Wetlands Receiving High Concentrations of Nitrate. *Water Science and Technology*, 29(4), 7–14.
- Vymazal, J. (2007). Removal of nutrients in various types of constructed wetlands. *Science of The Total Environment*, 380(1–3), 48–65. <https://doi.org/10.1016/j.scitotenv.2006.09.014>
- Wahl, M. D., Brown, L. C., Soboyejo, A. O., Martin, J., & Dong, B. (2010). Quantifying the hydraulic performance of treatment wetlands using the moment index. *Ecological Engineering*, 36(12), 1691–1699. <https://doi.org/10.1016/j.ecoleng.2010.07.014>
- Wang, H., Jawitz, J. W., White, J. R., Martinez, C. J., & Sees, M. D. (2006). Rejuvenating the largest municipal treatment wetland in Florida. *Ecological Engineering*, 26(2), 132–146. <https://doi.org/10.1016/j.ecoleng.2005.07.016>
- White, J. R., Gardner, L. M., Sees, M., & Corstanje, R. (2008). The Short-Term Effects of Prescribed Burning on Biomass Removal and the Release of Nitrogen and Phosphorus in a Treatment Wetland. *Journal of Environmental Quality*, 37(6), 2386–2391. <https://doi.org/10.2134/jeq2008.0019>
- Williams, C. F., & Nelson, S. D. (2011). Comparison of Rhodamine-WT and bromide as a tracer for elucidating internal wetland flow dynamics. *Ecological Engineering*, 37(10), 1492–1498. <https://doi.org/10.1016/j.ecoleng.2011.05.003>
- Wolverton, B. C. (1992). *Aquatic Plant/Microbial Water Purification System* (United States Patent Office Patent No. 5137625).
- Wolverton, B. C., Donald, R. C. M., & Duffer, W. R. (1983). Microorganisms and Higher Plants for Waste Water Treatment. *Journal of Environmental Quality*, 12(2), 236–242. <https://doi.org/10.2134/jeq1983.00472425001200020018x>

Wu, H., Zhang, J., Ngo, H. H., Guo, W., Hu, Z., Liang, S., Fan, J., & Liu, H. (2015). A review on the sustainability of constructed wetlands for wastewater treatment: Design and operation. *Bioresource Technology*, 175, 594–601.
<https://doi.org/10.1016/j.biortech.2014.10.068>

Zirschky, J., & Reed, S. C. (1988). The Use of Duckweed for Wastewater Treatment. *Journal (Water Pollution Control Federation)*, 60(7), 1253–1258.

CHAPTER 3: ESTIMATING AMMONIUM-RELEASE FROM ACCUMULATED DETRITUS IN A FREE WATER SURFACE CONSTRUCTED WETLAND

ABSTRACT

One potential cause of declining performance in free water surface constructed wetlands (FWS CW) is the accretion of decaying biomass, or detritus. Over time (10-20 years), this detritus can form a new substrate above the antecedent wetland soil. As FWS CWs continue to age across the country, we need to better understand the influence of this accumulated detritus substrate on nitrogen (N) removal and inform operators about the importance of detritus management and removal. A laboratory study was conducted to quantify the ammonium ($\text{NH}_4\text{-N}$) released from an accumulated detritus substrate and provide a kinetic model that would represent this release. In this study, three experimental runs were conducted, each using nine wetland microcosms loaded with detritus (mainly from *Typha* spp.) from a 20+ year old FWS CW. Each run was conducted with three variable initial $\text{NH}_4\text{-N}$ concentrations in the water column (0 mg L^{-1} , 5 mg L^{-1} , and 10 mg L^{-1}). Each initial concentration was triplicated and randomly assigned. The release was reasonably represented using first order kinetics (mean $R^2 = 0.77$). Modeled porewater $\text{NH}_4\text{-N}$ concentration (C_{pw}) and the rate constant (k_u), values ranged from 4.7 to 21.5 mg-N L^{-1} and 0.004 to 0.13 d^{-1} (1.5 to 47.4 m yr^{-1}), respectively. The potential areal ammonium release rates (J_{UF}) from the detritus substrate at an overlying water column concentration of 4 and 6 mg L^{-1} were 0.21 and 0.14 $\text{g-N m}^{-2} \text{ d}^{-1}$ (70 and 50 $\text{g-N m}^{-2} \text{ yr}^{-1}$), respectively. At these rates, $\text{NH}_4\text{-N}$ diffusion from the detritus substrate would substantially influence N removal performance in lightly loaded systems (TKN load $< 120 \text{ g-N m}^{-2} \text{ yr}^{-1}$).

These results provide both an initial estimate of the magnitude of N release from an accumulated detritus substrate and evidence to support regular FWS CW maintenance to remove the internal source.

INTRODUCTION

Within free water surface (FWS) constructed wetlands (CW), the accumulation of decaying biomass (i.e., detritus) has the potential to negatively influence treatment performance (Kadlec & Wallace, 2009; Martinez & Wise, 2003; Thullen et al., 2005; Wang et al., 2006). The problem of accumulated detritus begins with the stands of macrophyte vegetation that thrive in FWS CWs treating wastewaters with high nutrient levels. This vegetation is necessary for optimal wetland performance because it intercepts suspended solids, assimilates nutrients, contributes a carbon source for denitrification, and provides a surface biofilm growth (Brix, 1997; Kadlec & Wallace, 2009; Mitsch & Gosselink, 2015; Thullen et al., 2005). However, at the end of each growing season, the detritus from this vegetation falls back into the FWS CW basin. Because saturated conditions are maintained in these systems, this detritus decays slowly, allowing for a buildup over time (similar to the process of bog formation) (Kadlec et al., 2010; Kadlec & Wallace, 2009; Mitsch et al., 2012; Thullen et al., 2005). Detritus accumulation rates have been observed to be between 1-3 cm yr⁻¹ in depth in high nutrient environments (Kadlec et al., 2010; Kadlec & Wallace, 2009). While, some detrital material enhances wetland treatment, at these accumulation rates, detritus can severely reduce water depths, effective areas, basin volume, and hydraulic retention time after only 10 to 20 years of operation, thereby decreasing treatment efficiency (Kadlec et al., 2010; Kadlec & Wallace, 2009; Martinez & Wise, 2003; Wang et al., 2006). In addition to its negative influence on internal hydraulics, an accumulated

detritus substrate has also been identified as a potential internal nitrogen source (Reddy et al., 1984; Sartoris et al., 1999; Thullen et al., 2002).

The potential internal nitrogen source is the product of soil diagenetic processes that lead to an accumulation of $\text{NH}_4\text{-N}$ within the substrate porewater. This accumulation is due to the production of $\text{NH}_4\text{-N}$ as a by-product of the microbial respiration, and the inhibition of nitrification (i.e., $\text{NH}_4\text{-N}$ removal) due to the lack of oxygen under the anaerobic soil conditions present in FWS CWs (Reddy et al., 1984). As $\text{NH}_4\text{-N}$ accumulates, the $\text{NH}_4\text{-N}$ concentration increases within the substrate porewater. As the $\text{NH}_4\text{-N}$ concentration increases in the porewater diffusion drives $\text{NH}_4\text{-N}$ upward into the overlying water column (Figure 3.1).

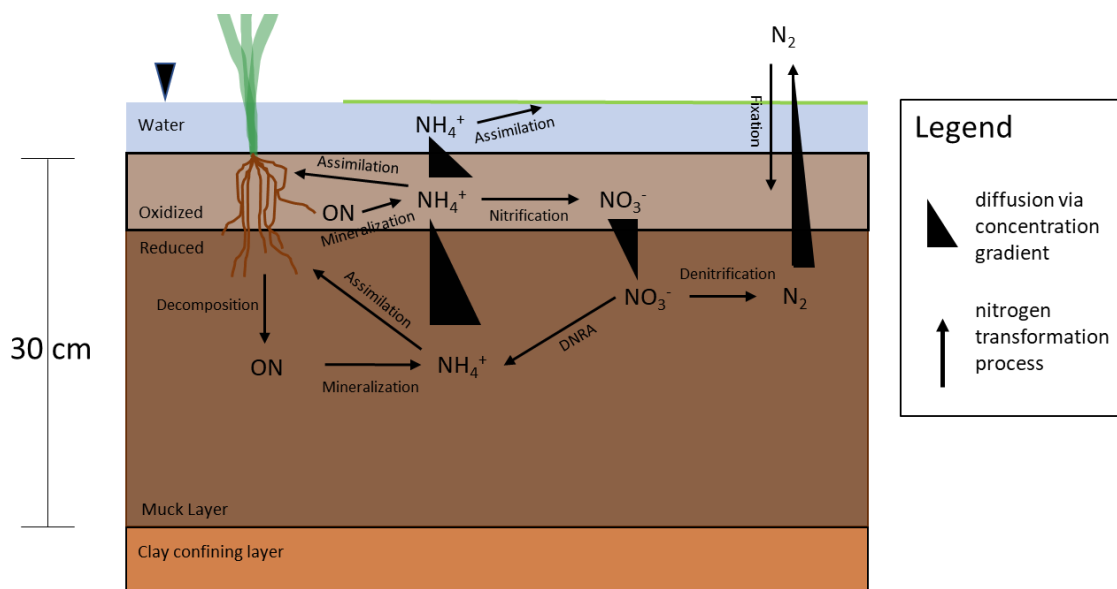


Figure 3.1: Diagram nitrogen processing in the detritus impacted FWS CW wetlands. 30 cm of accumulated detritus has greatly reduced the depth of the water column. The aerobic zone has been expanded to better present nitrogen processing. The actual aerobic or oxidized zone would only be less than 1 cm in depth. Diagram modified from nitrogen cycling presented in Kadlec and Wallace (2009).

While these consequences are known, research to quantify the influence of accumulated detritus on treatment performance is scarce. Because the magnitude of its influence is unknown, this process has not been included in the current FWS CW design models (often the tanks-in-series or TIS model) (Kadlec & Wallace, 2009). The scarcity of research on pollutant return rates

is noted in Kadlec and Wallace (2009), where the authors stated that although chemical return rates from the wetland substrate are likely significant, there was “at present [2009], no scientific study to provide guidance on modeling this transfer.” The two FWS CW cells at the Walnut Cove wastewater treatment plant (WWTP), described in Chapter 2, provided an opportunity to study the influence of an accumulated detritus substrate on nitrogen removal and model the return of nitrogen from the substrate back to the water column.

At the Walnut Cove WWTP, an initial short-term monitoring study in May 2016 revealed that the average daily inlet and outlet ammonium ($\text{NH}_4\text{-N}$) concentrations in the wetland were 2.6 and 6.9 mg-N L^{-1} , respectively, which represented a 4.4 mg-N L^{-1} increase in $\text{NH}_4\text{-N}$ concentrations through the cell (Burchell et al., 2016). This short-term study was followed by a more intensive longer-term study from September 2018 to March 2019, which showed that the average inlet and outlet NH_4 concentrations for both cells were 8.0 and 8.3, respectively (Chapter 2). The general increase in $\text{NH}_4\text{-N}$ concentrations through the cells in both studies suggested that the accumulated detritus substrate within the FWS CW cells produced an internal $\text{NH}_4\text{-N}$ source. Furthermore, the greater increase in $\text{NH}_4\text{-N}$ concentrations through the cells at lower inlet $\text{NH}_4\text{-N}$ concentrations suggested that the internal release of $\text{NH}_4\text{-N}$ from the detritus substrate porewater up to the water column was likely driven by diffusive transport.

To begin examining $\text{NH}_4\text{-N}$ transport between the detritus substrate and the overlying water column, dialysis porewater samplers were installed into the detritus substrate of one of the wetland cells in the fall 2019 and winter 2020. The dialysis porewater samplers were built and used following the description of an in-situ porewater sampler in Hesslein (1976). Details of the methodology were included in Appendix D. The porewater samplers measured elevated levels of $\text{NH}_4\text{-N}$ in the substrate porewater, which resulted in a concentration gradient between the

substrate and the water column that could drive the diffusion of $\text{NH}_4\text{-N}$ from the substrate to the water column (Figure 3.2). Note, that the gradient differed between the two experiments, which suggested that there may be spatial and temporal variability in the magnitude of the upward diffusion of $\text{NH}_4\text{-N}$ from the substrate porewater to the overlying water column.

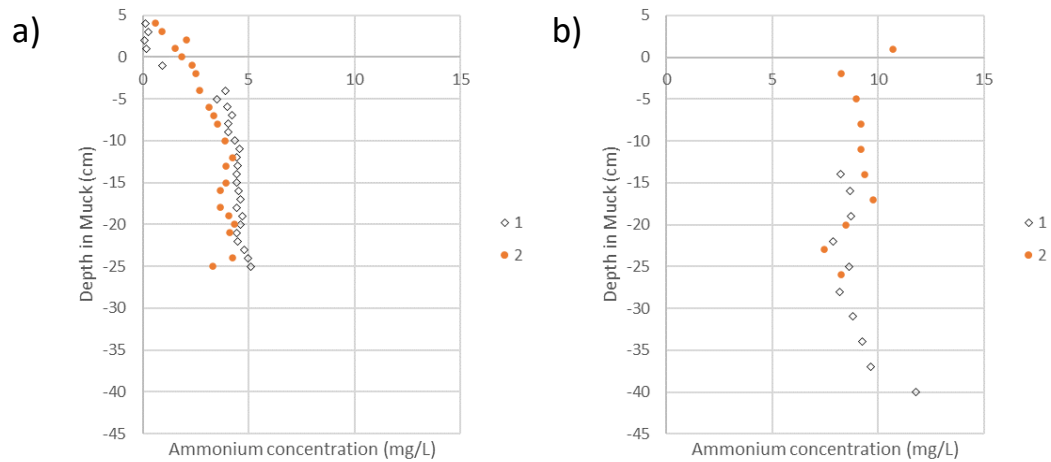


Figure 3.2: $\text{NH}_4\text{-N}$ concentrations in the porewater experiments a) installed on October 25th, 2019, b) installed on January 10th, 2020.

As a first attempt to quantify the magnitude of internal nitrogen source in the FWS CW, and to begin closing the return rate knowledge gap, a laboratory study was initiated to: (1) represent $\text{NH}_4\text{-N}$ release dynamics using a simple kinetic model and (2) estimate the $\text{NH}_4\text{-N}$ release from the accumulated detritus substrate (i.e., the internal nitrogen source) at the Walnut Cove wetlands. To complete these objectives, wetland microcosms were prepared using accumulated detritus from the currently operational 24-year-old FWS CW cells at the Walnut Cove WWTP in North Carolina. The study's practical objectives were to highlight implications of poor wetland maintenance and motivate wetland operators to initiate regular detritus cleanouts to improve long-term nitrogen treatment performance.

METHODS AND MATERIALS

Experimental design

The experiment was performed within Weaver Laboratory at North Carolina State University. Nine experimental units (i.e., microcosms) consisted of 20 cm x 13 cm x 30 cm plastic containers with internal baffles filled with an aged detritus substrate. The detritus substrate was collected from several different locations in a 24-year-old FWS CW cell treating municipal wastewater in Walnut Cove, NC. To collect the detritus, laboratory personnel waded into the cell and shoveled detritus from mixed depths into three 19-L (5-gal) buckets. These buckets were brought back to the lab in Raleigh, NC where they were left undisturbed for at least 24 hours before excess water was poured off and the contents of each bucket were combined in a 66-L (70-qt) muck bucket. The detritus was analyzed for nitrogen content prior to use in the experiment (Appendix D). From the bottom to the top, each microcosm was filled with the detritus substrate (3 kg wet weight; ~9 cm depth) followed by 3-L of source water (~9 cm water column depth) (Figure 3.3). Care was taken to minimize the disturbance of the detritus substrate when adding water. Advective transport was minimized by using batch design instead of a flow through design for the wetland microcosms. The microcosms were then covered with black plastic to limit both light exposure and gas exchange with the atmosphere, both of which had the potential to increase confounding nitrogen conversions (assimilation and nitrification).

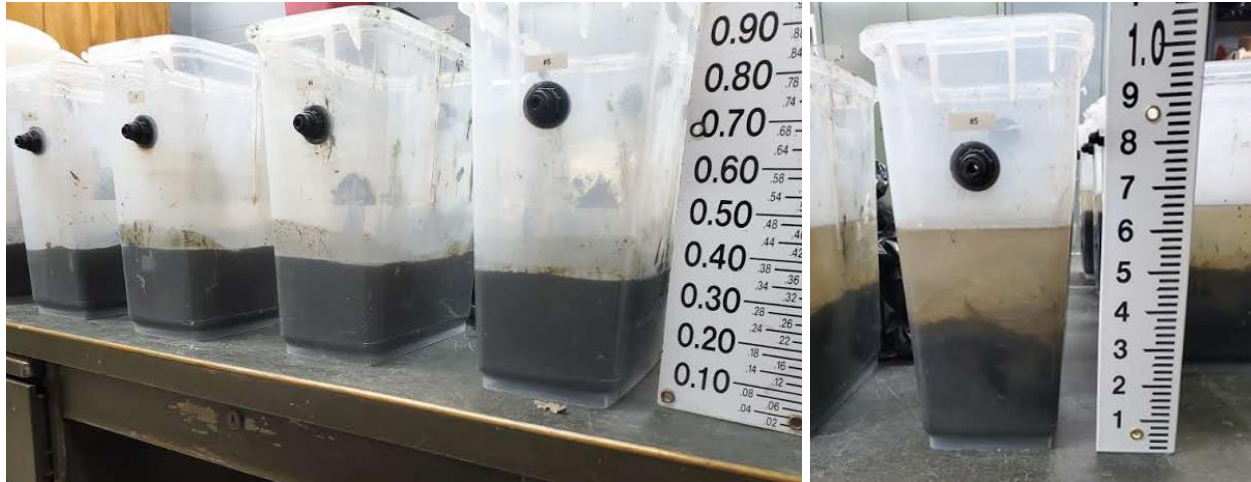


Figure 3.3: Top left: Microcosms from run 1 after detritus substrate addition. Note that the depth of the detritus is approximately 9 cm (0.3 ft). Top right: A microcosm from run 3 after detritus and source water addition. Bottom: a picture of the nine microcosms covered by a black tarp to limit light penetration.

The experiment was run three times. A new batch of detritus was obtained from the Walnut Cove FWS CW cell for each experimental run. Each run lasted approximately 2 weeks. For each experimental run, the initial water column $\text{NH}_4\text{-N}$ concentration was set to one of three target concentrations (0 mg L^{-1} , 5 mg L^{-1} , and 10 mg L^{-1}) (Figure 3.4). These initial values spanned the range of likely influent $\text{NH}_4\text{-N}$ concentrations to the Walnut Cove wetlands. The initial $\text{NH}_4\text{-N}$ concentrations were achieved using powdered standard grade (>99%) ammonium sulfate ($(\text{NH}_4)_2\text{SO}_4$) (Alpha Chemicals, MO) dissolved into a source water reservoir. Each initial

water column $\text{NH}_4\text{-N}$ concentrations were replicated in triplicate and randomly assigned to the nine wetland microcosms.

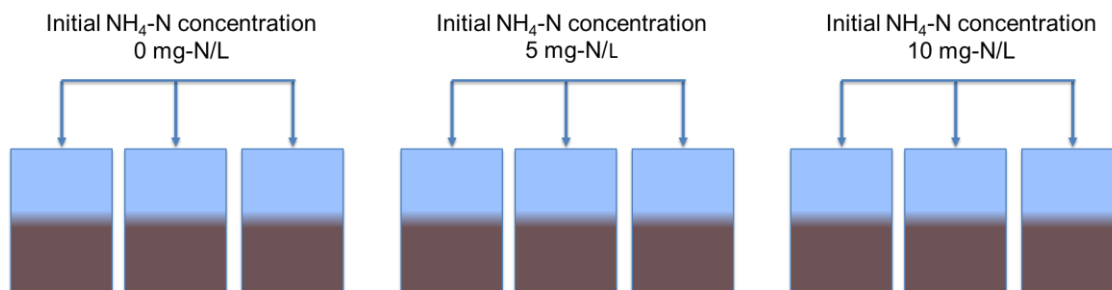


Figure 3.4: Experimental setup for each run. Nine microcosms were created from a new batch of detritus for each run. In each run, three target initial $\text{NH}_4\text{-N}$ concentrations were applied in triplicate.

To create the source water reservoir for each initial $\text{NH}_4\text{-N}$ concentration, three 66-L (70-qt) muck buckets were each filled with ten liters of filtered tap water. The amount of $(\text{NH}_4)_2\text{SO}_4$ added to each mixing bucket was 0 g, 0.24 g, and 0.47 g to the 0 mg-N L^{-1} , 5 mg-N L^{-1} , and 10 mg-N L^{-1} treatments, respectively. After the $(\text{NH}_4)_2\text{SO}_4$ additions, each bucket was mixed for approximately 1 minute. After the source water was mixed, each source water reservoir was sampled and analyzed to obtain the initial $\text{NO}_3\text{-N}$ and $\text{NH}_4\text{-N}$ concentrations. Source water ammonium concentrations were within 1.3 mg N L^{-1} of the target concentrations for each experiment (Table 3.1).

Table 3.1: The initial NH_4 concentrations in the source water relative to the target initial NH_4 concentrations for each experimental run.

Run	Dates	Treatment		
		0 mg-N L^{-1}	5 mg-N L^{-1}	10 mg-N L^{-1}
1	11/12/20 to 11/26/20	0.4	6.2	10.7
2	12/10/20 to 12/21/20	0.4	5.9	11.3
3	1/25/21 to 2/5/21	0.8	5.5	10.2

Water quality analysis

Water quality samples were collected directly from each microcosm water column via a 1000- μ L pipette with Fisherbrand SureOne pipette tips (Thermo Fisher Scientific, Waltham, MA). Initial samples were collected in the first hour after the microcosms were loaded. After this initial sampling, samples were collected on days 1, 2, 3, 5, 7, 8, and 18 for the first experimental run and days 1, 3, 5, 7, and 11 for the final two runs. After each sample was collected, additional water quality parameters including pH, dissolved oxygen (DO), specific conductivity, and temperature were measured in 6 of the 9 microcosms using a YSI Pro field probe (Xylem US, Yellow Springs, OH). Parameters were not measured in all microcosms to provide the potential to evaluate if the mixing from the YSI probe influenced ammonium release. Values for water quality parameters (temperature, DO, pH, and Specific conductivity) on day 1 and day 7 were compared to evaluate the changes in these parameters during the study period.

Water quality samples were analyzed immediately using a HACH DR3900 Spectrophotometer (HACH, Loveland, CO). Samples were analyzed for ammonium concentrations (mg-N L^{-1} or g-N m^{-3}) using TNTplus 832 vials and the USEPA compliant method 10205. Samples were also analyzed for nitrate concentrations (mg-N L^{-1} or g-N m^{-3}), as a check for potential nitrification within the microcosms, using TNTplus 835 vials and the USEPA compliant method 10206.

Although water quality samples were collected over a period longer than 7 days, increasing nitrate concentrations (a sign of nitrification) were observed in samples collected after day 7. The mean $\text{NO}_3\text{-N}$ concentration in all runs for samples taken between day 0 and day 7 was 0.3 mg-N L^{-1} , but the mean $\text{NO}_3\text{-N}$ increased to 1.5 mg-N L^{-1} for samples taken after day 7 (Appendix D). Because nitrification converts $\text{NH}_4\text{-N}$ to $\text{NO}_3\text{-N}$, $\text{NH}_4\text{-N}$ release rates estimated

with data influenced by nitrification would underestimate the actual release rate from the substrate, and instead represent a net or apparent NH₄-N release rate (i.e., the NH₄-N release rate minus the nitrification rate). Therefore, to best estimate NH₄-N release rates and remove the potential nitrification influence, samples taken after day 7 were omitted from analysis. The reduction to a seven-day period was acceptable because the wetland study site had a residence time less than 3 days and the average nominal hydraulic retention time (HRT) in most FWS CWs is approximately 7 days (Gerke et al., 2001; Kadlec & Wallace, 2009).

Nitrogen dynamics

Nitrogen removal in treatment wetlands is often represented using the steady-state first-order k-C* model (Kadlec & Wallace, 2009). To represent the internal hydraulics of a treatment wetland more accurately, this k-C* can be expanded to include the number of tanks-in-series (TIS) derived from the wetland's residence time distribution (RTD). From this baseline, first-order areal conversions for ON, NH₄, and NO₃ can be combined to create a sequential nitrogen dynamics model. A mass balance can then be computed for each tank in the model to produce a model that better represents the entire nitrogen cycle within a wetland (Gerke et al., 2001; Kadlec, 2008; Kadlec & Wallace, 2009). In this model, ammonium production within the wetland is limited to the ammonification of water column organic nitrogen and does not consider the ammonium return from the substrate (Equation 3.1) (Kadlec, 2008).

$$QC_{A,out} = Q_{in}C_{A,in} + (J_A - J_N - J_{AU})A_j \quad (\text{Eq. 3.1})$$

where, the first term ($Q_{in}C_{A,in}$) is the NH₄-N load into the tank (g d⁻¹), the second term ($J_A = k_a C_{O,j}$) is the NH₄-N load added due to ammonification of ON in the water column, the

third term ($J_N = k_n C_{A,j}$) is the $\text{NH}_4\text{-N}$ load removed due to nitrification to $\text{NO}_3\text{-N}$, and the fourth term (J_{AU}) is the $\text{NH}_4\text{-N}$ load removed by plant uptake.

Here we suggest adding a first-order release rate to the model to represent the upward flux of $\text{NH}_4\text{-N}$ from an accumulated detritus substrate (Equation 3.2 & Figure 3.5).

$$V \frac{dC_A}{dt} = J_{UF} A = k_u A (C_{pw} - C_A) \quad (\text{Eq. 3.2})$$

where J_{UF} is the upward flux ($\text{g-N m}^{-2} \text{d}^{-1}$), A is the surface area (m^2), k_u is the rate constant or upward diffusion velocity constant (m d^{-1}), C_{pw} is the $\text{NH}_4\text{-N}$ concentration in the porewater (mg L^{-1}), and C_A is the $\text{NH}_4\text{-N}$ concentration in the water column (mg L^{-1}). Mechanistically, this model describes the diffusive transport of $\text{NH}_4\text{-N}$ from the substrate porewater to the overlying water column by having the upward flux approach zero as C_A approaches C_{pw} . This term could easily be added as a fifth term to the previous sequential model (Equation 3.1). Equation 3.2 was derived analytically to provide an equation that could be used to predict C_A at time t (C_t) (Equation 3.3)

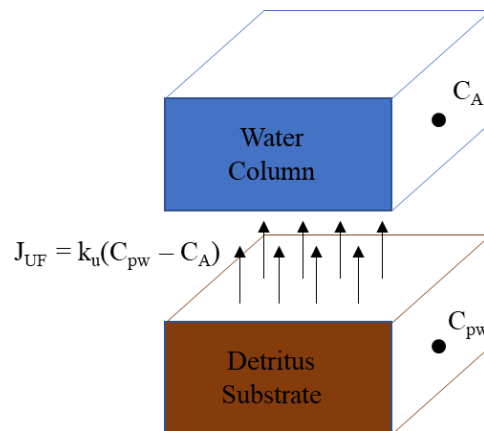


Figure 3.5: Return of $\text{NH}_4\text{-N}$ produced within the detritus substrate to the overlying water column.

For overlying water of area (A) and depth (h), we hypothesize that the accumulation of ammonium in the water column can be approximated by a first order rate and be written as:

$$\frac{dC}{dt} = \frac{k_u}{h} (C_{pw} - C_A)$$

This can be further developed into the following equations:

$$\frac{dC}{(C_{pw} - C_A)} = \frac{k_u}{h} dt$$

$$\int_{C_0}^{C_t} \frac{dC}{(C_{pw} - C_A)} = \int_0^t \frac{k_u}{h} dt$$

Let us make a variable change and introduce u as:

$$u = C_{pw} - C_A$$

$$\frac{d}{dC} [u] = \frac{d}{dC} [C_{pw} - C_A]$$

$$\frac{du}{dC} = -1; du = -dC$$

$$- \int_{(C_{pw}-C_0)}^{(C_{pw}-C_t)} \frac{du}{u} = \int_0^t \frac{k_u}{h} dt$$

$$-(\ln(C_{pw} - C_t) - \ln(C_{pw} - C_0)) = \frac{k_u}{h} t$$

$$\ln(C_{pw} - C_t) - \ln(C_{pw} - C_0) = -\frac{k_u}{h} t$$

$$\ln\left(\frac{C_{pw} - C_t}{C_{pw} - C_0}\right) = -\frac{k_u}{h} t$$

$$\frac{C_{pw} - C_t}{C_{pw} - C_0} = e^{-\frac{k_u}{h} t}$$

$$(C_{pw} - C_t) = (C_{pw} - C_0) * e^{-\frac{k_u}{h} t}$$

$$-C_t = -C_{pw} + (C_{pw} - C_0) * e^{-\frac{k_u}{h} t}$$

$$C_t = C_{pw} - (C_{pw} - C_0) * e^{-\frac{k_u t}{h}} \quad (\text{Eq 3.3})$$

where C_0 is the initial water column NH_4 concentration (g m^{-3}); C_t is the concentration at time, t (g m^{-3}); and d is the distance from the midpoint of the substrate to the midpoint of the water column (m). The experimental data were used to calibrate the model parameters (k_u and C_{pw}) using Eq 3.3.

Model parameters (C_{pw} and k_u) were calibrated to data from each experimental unit ($n = 27$). The “optim” function within the R stats package was used to generate the optimum calibration values (RStudio Team, 2021). Optimization was conducted by using the Nelder-Mead method to minimize the root mean squared error (RMSE) between measured NH_4 concentrations (C_t) and predicted NH_4 concentrations (Nelder & Mead, 1965). The initial k_u value was set to 0.1 m d^{-1} (36 m yr^{-1}) (a value within the range of rate coefficients for ON removal in FWS CWs (Kadlec & Wallace, 2009)), h was set to 0.09 m (based on the depth of the water column), C_{pw} was set to 10 g-N m^{-3} (based on the results from porewater samplers), and C_0 was set to the NH_4 concentration in the source water (Table 3.1). Model performance was evaluated using the coefficient of determination or Nash-Sutcliffe Efficiency (R^2).

Statistical analysis

A one-way ANOVA was used to evaluate differences between experimental runs (Run) (i.e., detritus batches) for each calibrated parameter values (C_{pw}) and (k_u). Differences between runs would suggest variability in $\text{NH}_4\text{-N}$ release relative to both within basin detritus composition and water temperature during sampling. There were nine replicates of each microcosm per experimental run. The statistical model in this analysis is described below (Equation 3.4).

$$Y_{ij} = \mu + \alpha_i + \varepsilon_{ij}$$

(Eq. 3.4)

where, Y_{ij} = parameter value for the i^{th} run, μ = overall mean, α_i = the fixed effect of the i^{th} run, and ε_{ij} = experimental error in j^{th} observation on a response variable at the i^{th} run. The null and alternative hypotheses to be used was given as:

$$H_0: \mu_{\text{run1}} = \mu_{\text{run2}} = \mu_{\text{run3}}$$

H_a : Not all μ are equal or, at least one is different from the others

To determine which groups are statistically different from one another, a Tukey's Honestly Significant Difference (Tukey's HSD) post-hoc test for pairwise comparisons. All statistical tests were considered significant at an alpha = 0.05.

RESULTS

NH₄-N concentration changes

NH₄-N concentrations were measured in the overlying water column over the 7-day period in each of the experimental units (Table 3.2 & Figure 3.6). In all instances, except for the period between day 5 and 7 in the 10 mg L⁻¹ treatment of Run 3, mean NH₄-N concentrations increased between each measurement for each treatment in each experimental run. Greater increases in NH₄-N concentrations were observed in the microcosms with lower initial NH₄-N concentrations. The microcosms with an initial C_A of 0 mg L⁻¹ ended on day 7 at 8.5, 7.8, and 5.1 mg L⁻¹ in runs 1, 2, and 3, respectively. Meanwhile, the microcosms with an initial C_A of 10 mg L⁻¹ ended on day 7 at 14.8, 13.3, and 11.2 mg L⁻¹ in runs 1, 2, and 3, respectively. These results suggested an inverse relationship between initial NH₄-N concentration and the amount of NH₄-N released from the substrate. Furthermore, the mean NH₄-N concentration change decreased over time. Between days 1 and 3, the NH₄-N concentration increased by 1.4 mg L⁻¹, on average across

all runs and treatments. This change dropped to 0.9 mg L⁻¹ between days 3 and 5 and to 0.5 mg L⁻¹ between days 5 and 7 (Table 3.2). Both inverse relationships suggested that not only was the NH₄-N release rate lower when the overlying water column had higher NH₄-N concentration, but that the NH₄-N release rate decreased as NH₄-N concentrations increased within the seven-day period. These relationships were consistent with the hypothesis that NH₄-N mass transfer rates from the substrate porewater (created as a byproduct of respiration processes) to the overlying water column are driven by the magnitude of the concentration difference between two volumes (i.e., diffusion).

Table 3.2: The mean NH₄-N concentrations on each sampling day for each initial NH₄-N concentration in each experimental run. Day 0 represented the NH₄-N concentrations approximately 1 hour after the microcosms were prepared. The high increase in NH₄-N concentrations in this short period was likely due to the mixing associated with creating the wetland microcosms.

Experimental Run	Initial NH ₄ -N concentrations	Time after initial preparation				
		Day 0	Day 1	Day 3	Day 5	Day 7
Run 1	0	3.0	3.4	5.8	7.1	8.5
	5	7.1	7.8	9.7	11.1	11.9
	10	11.3	12	13	13.5	14.8
Run 2	0	1.6	2.9	5.4	7.0	7.8
	5	6.9	7.6	8.7	10.3	10.7
	10	12.1	12.0	12.4	13.0	13.3
Run 3	0	1.5	2.2	3.6	4.5	5.1
	5	5.8	6.9	8.0	8.3	8.3
	10	10.1	10.4	11.7	11.8	11.2

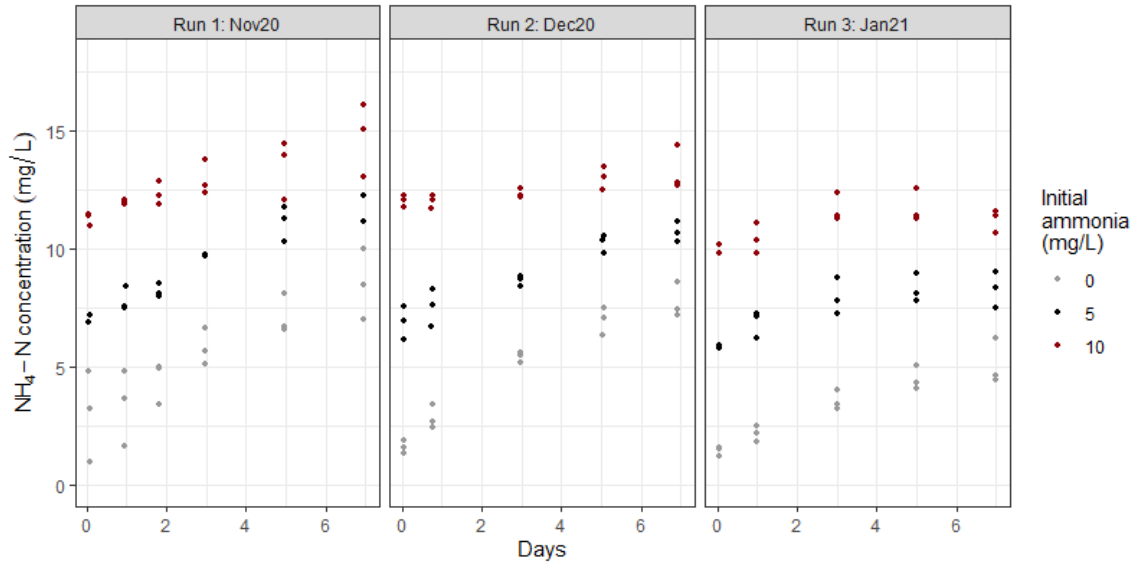


Figure 3.6: The measured $\text{NH}_4\text{-N}$ concentrations over time for each experimental unit. The plots are split by experimental run. The x-axis represented days since the microcosms were started. The y-axis represented the $\text{NH}_4\text{-N}$ concentrations in the overlying water column.

Water quality parameters

Changes in measured water quality parameters are shown in Figure 3.7. The air temperature in the lab was held relatively constant at around 20°C . Therefore, initial mean water temperatures ($21.8 \pm 1.3^\circ\text{C}$) dropped slightly and then were maintained at $20 \pm 0.5^\circ\text{C}$ for each experimental run. Another parameter that was also relatively stable during the study was pH. Initial mean pH values (6.9 ± 0.2) were nearly identical to the end of the study mean pH values (6.9 ± 0.1), although the pH value range declined slightly throughout the experiment. The other two water quality parameters measured (DO and specific conductivity) were not constant over the course of the experiment. Initial mean DO concentrations were near saturation ($75.5 \pm 17\%$) and then dropped to $27.0 \pm 17.3\%$. Alternatively, mean specific conductivity increased from $263 \pm 38.5 \mu\text{S cm}^{-1}$ to $314 \pm 44.9 \mu\text{S cm}^{-1}$.

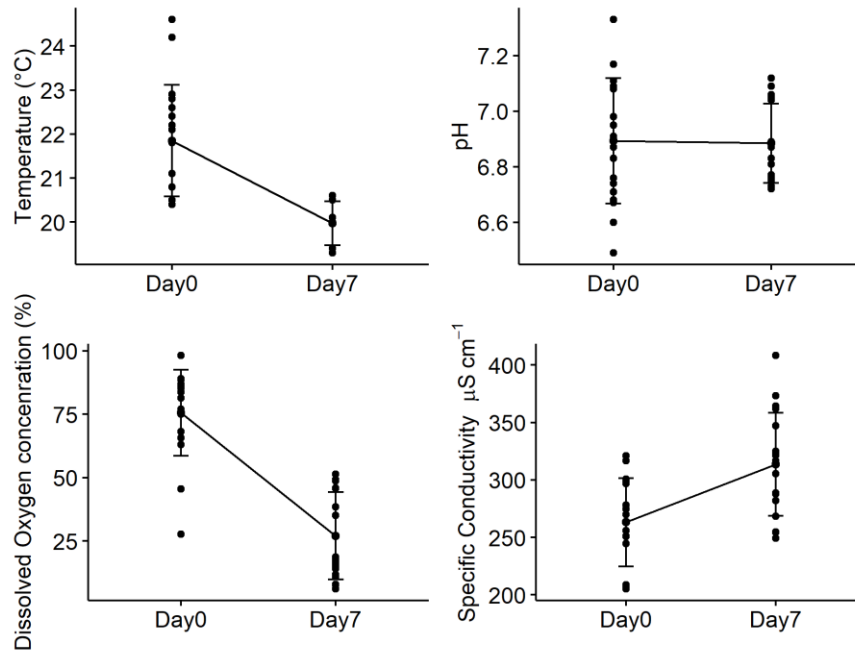


Figure 3.7: Changes in water quality parameters (Temperature, pH, DO (%), and Specific Conductivity) over the study period. Units are different for each parameter and noted on the y-axis label.

The increase in specific conductivity in the overlying water column was the expected product of ammonium ions, and other electrolytes, diffusing from the substrate porewater to the water column. The decrease in dissolved oxygen was also expected because the detritus was still biologically active. Within the biologically active detritus, decomposition and other microbial processes continued to consume dissolved oxygen over the seven-day period. Reaeration was also limited during the study period (the overlying water column was relatively stagnant, and the microcosms were covered when not being sampled), compounding the DO decrease caused by oxygen consumption.

Model calibration

For each of the three runs, the ammonium upward flux in each of the 9 microcosms were calibrated to the model represented in equation 3.3 using measured $\text{NH}_4\text{-N}$ concentrations in the water column (Appendix D). For each experimental unit ($n = 27$), a pair of parameters were

calibrated; the effective porewater concentration C_{pw} and the upward velocity flux or rate constant (k_u). The calibrated C_{pw} values ranged from 4.7 to 21.6 mg-N L⁻¹, with an average of 11.2 mg-N L⁻¹ and a median value of 11.8 mg-N L⁻¹ (Table 3.3 & Figure 3.8). The calibrated k_u values ranged from 0.004 m d⁻¹ to 3.2 m d⁻¹, with an average of 0.3 m d⁻¹ and a median of 0.04 m d⁻¹ (Table 3.3 & Figure 3.8). Model efficiencies (R^2) ranged from 0.04 to 0.99, with an average of 0.77 and a median of 0.89 (Table 3.3). The high mean and median efficiency values suggested that the upward flux of ammonium from the detritus into the water column was captured using this simple first order model. Our hypothesis that NH₄ mass transfer rates from the substrate porewater (created as a byproduct of respiration processes) to the overlying water column are driven by the magnitude of the concentration difference between two volumes (i.e., diffusion) was again supported by the modeling exercise.

Although the model generally performed well, there were four experimental units that were not well represented by the model. Each of the four had k_u values greater than 0.5 m d⁻¹ (Figure 3.8). The low R^2 values associated with these units ($R^2 < 0.5$) indicated that each was poorly calibrated to the model. In each case, it appeared that this was because of a delay in NH₄-N release that was observed in those experimental units, which resulted in a diffusion response that was not represented by the proposed equation. As a result, these values were omitted from further analysis.

Table 3.3: Two-way ANOVA results. Treatment (initial NH₄ concentration) and block (experimental run) were evaluated for their effect on areal NH₄ release rate (J_{UF}). These rates represent ammonium release over a seven-day.

	k_u (m d ⁻¹)	C_{pw} (mg-N L ⁻¹)	R^2
Min	0.004	4.7	0.04
Median	0.04	11.8	0.89
Mean (± SD)	0.29 (± 0.8)	11.2 (± 4.0)	0.77 (± 0.26)
Max	3.2	21.6	0.99

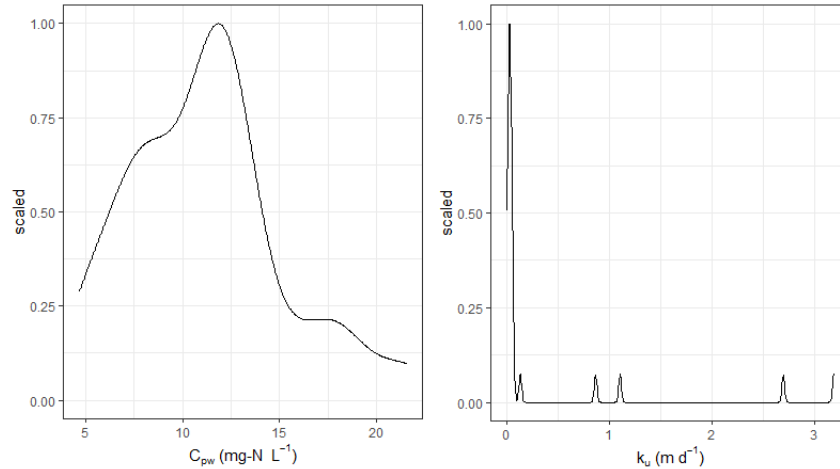


Figure 3.8: Density plots of calibrated parameter values C_{pw} and k_u for every experimental unit ($n = 27$). The plots show the relative distribution of calibrated values. Density estimate was scaled to maximum of 1.

Using the 23 remaining experimental units, the calibrated C_{pw} values had the same range and average values, with only the median value changing to 11.2 mg-N L^{-1} (Table 3.4 & Figure 3.9). Meanwhile, the calibrated k_u values ranged from 0.004 m d^{-1} to 0.13 m d^{-1} , with an average of 0.03 m d^{-1} and a median of 0.03 m d^{-1} (Table 3.4 & Figure 3.9). Average and mean model efficiencies (R^2) increased to 0.85 and a median of 0.92, respectively (Table 3.4).

Table 3.4: Two-way ANOVA results. Treatment (initial NH_4 concentration) and block (experimental run) were evaluated for their effect on areal NH_4 release rate (J_{UF}). These rates represent ammonium release over a seven-day

	k_u (m d^{-1})	C_{pw} (mg-N L^{-1})	R^2
Min	0.004	4.7	0.47
Median	0.03	11.1	0.92
Mean (\pm SD)	0.03 (\pm 0.03)	11.2 (\pm 4.2)	0.85 (\pm 0.15)
Max	0.13	21.5	0.99

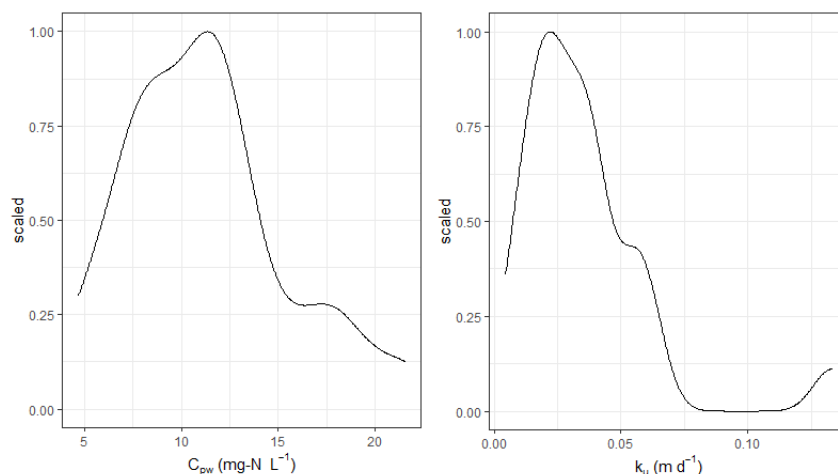


Figure 3.9: Density plots of calibrated parameter values C_{pw} and k_u for the remaining experimental units ($n = 24$). The plots show the relative distribution of calibrated values. Density estimate was scaled to maximum of 1.

Statistical analysis

Porewater concentration (C_{pw})

A statistically significant difference was found in the calibrated C_{pw} values between experimental runs (F-value = 23.5, $p < 0.012$) (Table 3.5). A Tukey post-hoc test revealed that the detritus in Run 3 resulted in a lower C_{pw} value on average (8.6 mg L^{-1}) than the detritus in Run 1 (14.5 mg L^{-1}) ($p < 0.01$) (Figure 3.10). The mean C_{pw} value for Run 2 (11.4 mg L^{-1}) was not significantly different than the mean in Run 1 or Run 3. These results indicated that there was a difference in the potential maximum $\text{NH}_4\text{-N}$ concentrations between Run 1 and Run 3.

Table 3.5: One-way ANOVA results. Experimental runs (Run) were evaluated for their effect on the calibrated C_{pw} values.

	df	Sum Sq	Mean Sq	F-value	P-value
Run	2	136.3	68.1	23.5	0.012
Residuals	18	52.1	2.9		

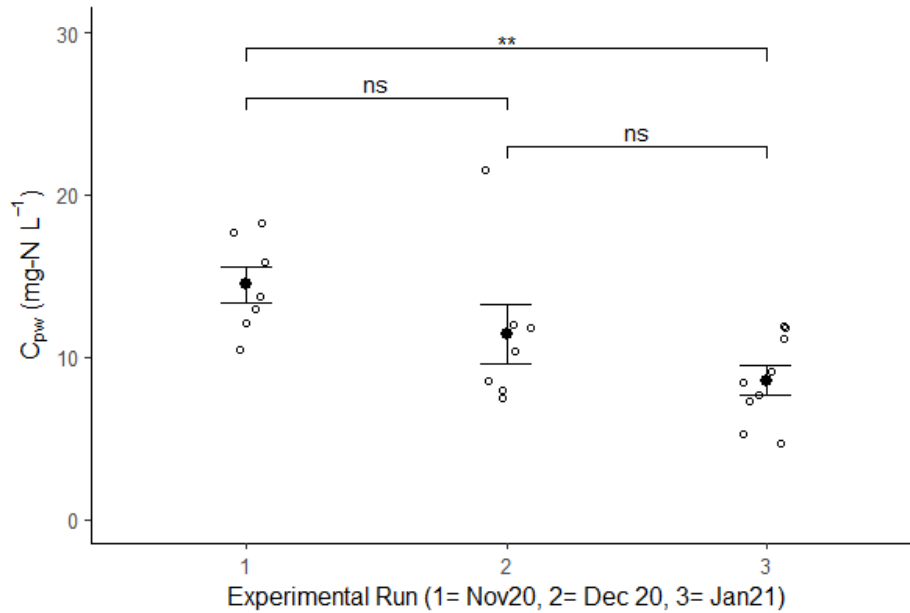


Figure 3.10: Calibrated C_{pw} values (in, mg-N L⁻¹) for each experimental run ($n = 23$). Solid dots represent the mean for each run and error bars represent the standard error. Each run was compared using post-hoc Tukey's HSD. *ns* indicated no significant difference. ** indicated a p-value < 0.01.

Rate constant (k_u)

A statistically significant difference was found in the calibrated k_u values between experimental runs (F-value = 3.97, $p < 0.035$) (Table 3.6). A Tukey post-hoc test revealed that the detritus in Run 3 resulted in a greater k_u value on average (0.051 m d⁻¹) than the detritus in Run 1 (0.018 m d⁻¹) ($p < 0.05$) (Figure 3.11). The mean k_u value for Run 2 (0.031 m d⁻¹) was not significantly different than the mean in Run 1 or Run 3. These results indicated that there was a slight, but statistically significant, difference in the rate of NH₄-N release, with Run 3 having the greatest release rate constant.

Table 3.6: One-way ANOVA results. Experimental runs (Run) were evaluated for their effect on the calibrated k_u values.

	df	Sum Sq	Mean Sq	F-value	P-value
Run	2	0.0044	0.0022	3.97	0.035
Residuals	18	0.0111	0.0005		

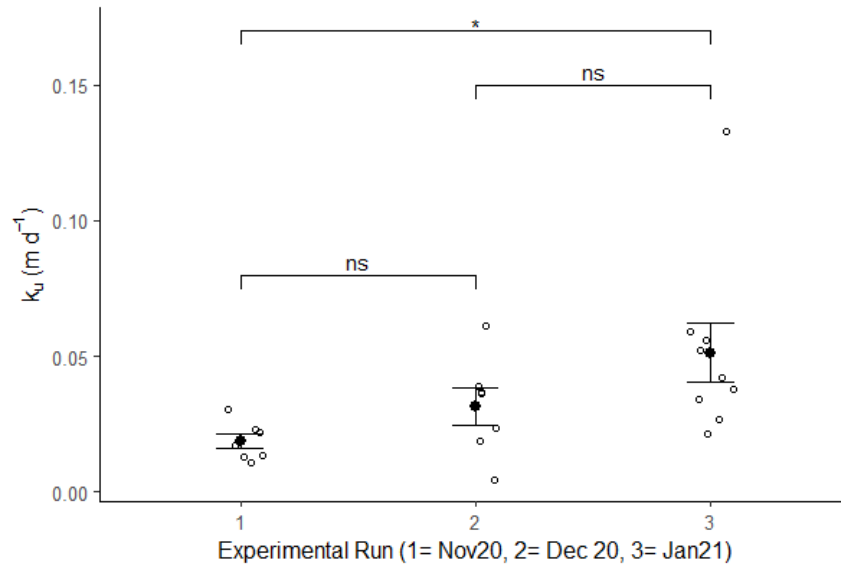


Figure 3.11: Calibrated k_u values (in, m d^{-1}) for each remaining experimental run ($n=23$). Solid dots represent the mean value for each run and error bars represent the standard error. Each run was compared using post-hoc Tukey's HSD. *ns* indicated no significant difference. * indicated a p -value < 0.05 .

One potential cause for the differences in parameter values was the greater detritus nitrogen content in Run 1 (3.6 g-N, or 7270 mg kg^{-1} -DW) relative to Run 3 (1.9 g-N, or 3824 mg kg^{-1} -DW), which indicated that there were differences in detritus composition. These differences likely reflected the heterogeneity of the detritus within the wetland, regardless of the sampling date. In terms of the model, this greater detritus nitrogen content corresponded with greater C_{pw} values in Run 1 relative to Run 3. The link between greater nitrogen content and greater C_{pw} supported the hypothesis that the difference in effective C_{pw} between Run 1 and Run 3 might have a physical meaning.

Nitrogen release also depends on the effective diffusivity of the substrate, which is linked to the tortuosity of the sediment and its porosity (Ullman and Aller, 1982). Overall, our hypothesis is that nitrogen release rates depend on the concentration gradient (hence, on C_{pw}) and on the upward diffusion velocity constant (k_u), which quantifies the effective diffusivity of the substrate. If the different parameter values were indicative of physical differences in the detritus,

then the lower vs. higher effective k_u for Run 1 vs. 3 would also suggest that detritus from Run 1 was less prone to release ammonium upward compared to that of Run 3 (i.e., the Run 1 detritus may have been more compacted with lower porosity, potentially due to an older age). This could explain why $\text{NH}_4\text{-N}$ would tend to accumulate in the detritus and why the N composition and C_{pw} were higher for detritus in Run 1. However, the parameters varied in an opposite manor between runs, which could also occur during model calibration with lower C_{pw} values compensating for greater k_u values or vice versa.

Modeled internal nitrogen release at the Walnut Cove WWTP

Influent $\text{NH}_4\text{-N}$ concentrations at the Walnut Cove WWTP ranged from 0.9 to 12.8 mg L^{-1} , approximately equal to the 1 to 10 mg-N L^{-1} range of $\text{NH}_4\text{-N}$ concentrations in the effluent of WWTPs described in an conventional activated sludge process (Carey & Migliaccio, 2009). Here, all calibrated models ($n=23$) were used to calculate a range of upward fluxes expected at the Walnut Cove WWTP (Influent $\text{NH}_4\text{-N}$ concentrations (C_A) of 2, 4, 6, 8, and 10 mg-N L^{-1}) (Table 3.7).

Each of the calculated J_{UF} values were plotted based on water column $\text{NH}_4\text{-N}$ concentration (C_A) and run (Figure 3.12). Figure 3.12, together with Table 3.7, indicated that the J_{UF} values were similar for each run despite the different detritus. So, although the parameter values were significantly different between Run 1 and Run 3, the expected internal $\text{NH}_4\text{-N}$ release was relatively constant for each sample of detritus. This finding supported the use of this model to represent $\text{NH}_4\text{-N}$ release across the entirety of the wetland cell.

Table 3.7: Upward flux (J_{UF}) ranges expected in the wetland using modeling results from the microcosm experiments. The values are reported in $\text{g-N m}^{-2} \text{d}^{-1}$ and the interval corresponded to the expected range of influent $\text{NH}_4\text{-N}$ concentrations to the Walnut Cove wetland cells.

Experimental Run	Statistical parameter	Water column $\text{NH}_4\text{-N}$ concentration (C_A)				
		2 mg L^{-1}	4 mg L^{-1}	6 mg L^{-1}	8 mg L^{-1}	10 mg L^{-1}
Run1	Mean	0.22	0.18	0.14	0.11	0.07
	Min, Max	0.14, 0.27	0.12, 0.23	0.09, 0.20	0.06, 0.16	0.01, 0.13
Run2	Mean	0.24	0.18	0.12	0.05	0.00
	Min, Max	0.10, 0.51	0.09, 0.39	0.05, 0.27	-0.02, 0.15	-0.09, 0.06
Run3	Mean	0.35	0.24	0.15	0.04	-0.06
	Min, Max	0.09, 0.76	0.02, 0.49	-0.04, 0.35	-0.11, 0.23	-0.31, 0.11
Overall	Mean	0.28	0.21	0.14	0.06	0.00

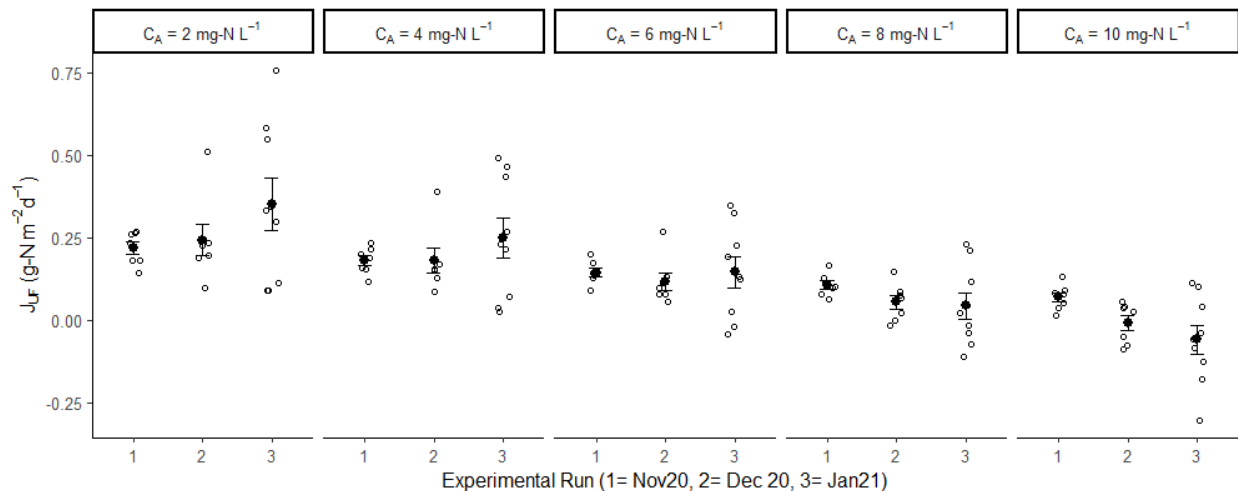


Figure 3.12: Calculated upward flux (J_{UF}) values for each run (1, 2, and 3) and each water column $\text{NH}_4\text{-N}$ concentration (2, 4, 6, 8, and 10 mg L^{-1}) ($n = 23$). The black dot represented the mean J_{UF} value, and the error bars represented the standard error.

In terms of magnitude, this study showed that when influent $\text{NH}_4\text{-N}$ concentrations are between 2 and 10 mg-N L^{-1} , this aged detritus substrate will likely release between 0.28 and $0.00 \text{ g-N m}^{-2} \text{d}^{-1}$ (100 and $0 \text{ g-N m}^{-2} \text{yr}^{-1}$), respectively (Table 3.7). To put these values in the

perspective of the study site, which has a 7200 m² wetland cell surface area and an average inlet NH₄ concentration between 4 and 6 mg L⁻¹, the internal NH₄-N load for each wetland cell would likely range from 370 to 550 kg yr⁻¹. This internal NH₄-N load would be between 30% and 45% of the ~1200 kg-N yr⁻¹ influent nitrogen load to each wetland cell at the study site (Chapter 4).

DISCUSSION

The potential for an accumulated detritus substrate to be an internal nitrogen source in constructed wetlands

The influence of an internal nitrogen source from an aged detritus substrate on FWS CW treatment performance is likely to be a function of both influent nitrogen loading and influent NH₄-N concentrations. Treatment wetlands built to remove nitrogen can be classified as lightly or heavily loaded systems using the influent TKN loading rate (Kadlec & Wallace, 2009). If the influent TKN loading rate is less than 120 g-N m⁻² yr⁻¹, the system can be considered lightly loaded and vice versa. If the aged detritus substrate at this site is a reasonable representation of the detritus substrate at other sites, then lightly loaded systems will be the ones most heavily impacted by the NH₄ release from an aged detritus substrate. Results of this study (J_{UF} ranging from 0 to 100 g-N m⁻² yr⁻¹) suggested that the nitrogen removal ability of lightly loaded FWS CWs will markedly decrease over time as an aged detritus substrate builds and begins to release ammonium into the overlying water.

It should be noted that as the detritus begins to fill the basin, the effective surface area of the FWS CW will decrease due to preferential flow paths (Chapters 2 & 4). With this decrease in the effective surface area, J_{UF} will act over a smaller area. So, while J_{UF} will likely increase over time (as the detritus substrate builds), the lower effective surface area may mitigate a portion of its impact. For example, the Walnut Cove wetland cells were designed to have a surface area of

7200 m². This resulted in an estimated internal NH₄-N load of 370 to 550 kg yr⁻¹ or 30 to 45% of the influent nitrogen load. However, the effective surface area of the cell was estimated to be only 3800 m² (Chapter 4). At this effective area, the internal NH₄-N load for C_A values of 4 and 6 mg-N L⁻¹ would be a smaller 190 to 290 kg yr⁻¹, respectively, or 16 to 24% of the influent nitrogen load. While still a large percentage of the influent nitrogen load, the lower effective surface area markedly reduced the internal NH₄-N load.

For heavily loaded FWS CWs, the influence of internal NH₄ release from an aged detritus substrate will likely have a lesser effect on treatment performance. In these systems, the internal NH₄ release will either be limited by high NH₄ concentrations (> 10 mg-N L⁻¹), which will slow diffusion, or in the case of low NH₄ concentrations at high hydraulic loading rates, even a relatively high internal NH₄ release (i.e., 50 g-N m⁻² yr⁻¹) could be overshadowed by the high influent nitrogen load (>> 120 g-N m⁻² yr⁻¹). Instead, in these heavily loaded FWS CWs, the hydraulic inefficiencies, such as preferential flow paths, produced by the accumulated detritus substrate perhaps will be a greater negative influence on wetland treatment performance by reducing residence time within the wetland cells (Martinez & Wise, 2003; Wang et al., 2006).

Nitrogen dynamics model validation

Despite the lack of direct model validation, checks were performed to ensure that the calibrated parameter values were reasonable. The k_u values were compared to the rate constants for NH₄-N removal. Because both processes occur within the treatment wetland systems and use the water column NH₄-N concentration, the calibrated k_u values should be within an order of magnitude of the NH₄-N removal rate constant. In Kadlec and Wallace (2009), the median NH₄-N removal rate constant was 0.04 m d⁻¹ (14.7 m yr⁻¹), which was nearly identical to the mean k_u value of 0.03 m d⁻¹ (11 m yr⁻¹). For C_{pw}, the calibrated values (11.2 ± 4.0 mg L⁻¹) matched the

porewater $\text{NH}_4\text{-N}$ concentrations observed during porewater sampling at the site (Figure 3.2) and the porewater $\text{NH}_4\text{-N}$ concentrations observed in porewater samplers placed in the organic substrate of an agricultural canal in North Carolina (Birgand, 2000).

To use this method, the other confounding $\text{NH}_4\text{-N}$ processes (see Eq 3.1) were assumed to be negligible within the wetland microcosms in the first seven days of each experimental run. Plant uptake or microbial assimilation (J_{AU}) was likely negligible because there were no plants in the microcosms, and the microcosms were covered by a black plastic. Ammonification (J_{A}) of water column ON was likely negligible since they were loaded with tap water, which had negligible ON concentrations. Nitrification was likely, however, as DO was consumed over the course of each experimental run, and $\text{NH}_4\text{-N}$ and $\text{NO}_3\text{-N}$ concentrations were reduced and increased, respectively after 7 days (Figure 3.5 & Appendix D).

Although nitrification was possible in the microcosms, the nitrification rate was likely negligible in the first seven days of each experimental run because DO consumption over the first seven days did not correspond to observed $\text{NO}_3\text{-N}$ production in the first seven days (Appendix D). This DO consumption paired with a lack of $\text{NO}_3\text{-N}$ production suggested that either the nitrification rate was negligible (the DO consumption was caused by other oxygen consuming biological activity) or that nitrification did occur, but that the denitrification rate within the microcosms was greater than or equal to the nitrification rate during this period. The subsequent presence of both $\text{NO}_3\text{-N}$ and low DO concentrations after seven days indicated that denitrification was likely limited within the microcosms and therefore, nitrification can be assumed to be negligible during the first 7 days of each experimental run. However, the assumption of negligible nitrification cannot be proven by the data gathered in this study and if a

considerable amount of nitrification did occur in the first seven days, then the $\text{NH}_4\text{-N}$ release rates presented herein should be considered conservative.

Another concern was the depth of detritus used in this experiment. Within the microcosms, detritus was added to a depth of 9 cm. While 9 cm was short of the actual detritus substrate depth in the wetland cells (30-45 cm), the vertical profile of porewater $\text{NH}_4\text{-N}$ concentrations (obtained via in-situ porewater sampling, see Figure 3.2) indicated that the depth to maximum porewater concentration was less than 9 cm. This indicated that the concentration gradient being modeled was fully developed within 9 cm of the detritus surface and that the 9 cm depth should have been able to provide an adequate representation of that concentration gradient. Additionally, the detritus in the microcosms was gathered from the entire detritus substrate profile and should be representative of the entire vertical profile of the detritus. In the future, the influence of detritus depth on $\text{NH}_4\text{-N}$ release could be assessed by performing another experiment with varying detritus depths. Furthermore, an additional experiment could be run using both the detritus sampling method used herein and detritus cores that maintain the vertical structure of the detritus. If there is no difference in the parameter values between the two methods, this would indicate that the method used in this experiment adequately represented the field conditions.

Potential application of results

This study was intended to help fill the constructed wetland nitrogen return rate knowledge gap expressed by Kadlec and Wallace (2009). The current method for representing sequential nitrogen dynamics in a treatment wetland are sequential first-order areal conversions (Gerke et al., 2001; Kadlec, 2008; Kadlec & Wallace, 2009). In these conversions, $\text{NH}_4\text{-N}$ production within the wetland is limited to ammonification of organic nitrogen in the water

column (represented using a first-order reaction rate for organic nitrogen removal). This method assumes that the amount of $\text{NH}_4\text{-N}$ added to the overlying water column is equal to the ON removed from the water column and does not consider $\text{NH}_4\text{-N}$ diffusion from the porewater of the aged detritus substrate into the overlying water column. Disregarding this internal $\text{NH}_4\text{-N}$ release produces the potential for suboptimal treatment performance predictions (relative to the initial expected performance) as the system ages. The first-order kinetic model and estimated parameters presented above provide an initial estimate of $\text{NH}_4\text{-N}$ release from an aged detritus substrate. This first-order rate can be implemented into the sequential first-order areal conversion model to improve the ability of that model to represent wetland treatment, especially in wetlands that are over 10 years old.

However, at this point, care should be taken in completely extrapolating this result to other sites. While the goodness of fit is high for the first order model, the results shown here indicated that there is likely variability in the calibrated parameter values. As a result, the calibrated parameter values have the potential to be site specific. Therefore, gathering detritus from only one FWS CW likely limited the applicability of the calibrated parameter values presented herein to an initial estimate for $\text{NH}_4\text{-N}$ release in other FWS CWs.

To develop parameter estimates representative of $\text{NH}_4\text{-N}$ release from an aged detritus substrate for the design of a general treatment wetland, data from other sites and from different times of the year is needed. Therefore, to further our efforts to fill this knowledge gap, the next step would be to gather aged detritus from several different FWS CWs (of various ages, accumulated detritus depths, dominant plant types, etc.) to evaluate if differences in detritus composition influences the ammonium release rates. To further validate the release rates

observed in the laboratory, this study could be scaled up to evaluate ammonium release from detritus filled wetland mesocosms placed outdoors.

While a larger sample size is needed before the results presented herein can be endorsed for widespread use, these results indicated that the model well represents the mechanics of this release and suggested that it has the potential to effectively predict this release. Overall, this study provided a positive first attempt at modeling this release, an estimate of $\text{NH}_4\text{-N}$ release from the accumulated detritus substrate at the site, and a foundation to build upon through the future analysis of various detritus substrates at different locations derived from different dominant vegetation types.

CONCLUSION

Overall, the results showed that diffusion, while not the only mechanism for transfer, can release a substantial amount of $\text{NH}_4\text{-N}$ from accumulated detritus porewater to the overlying water column in an aged FWS CW. Additionally, this study proposed a simple kinetic model to better represent return rates in treatment wetlands, which adequately represented the mechanics of upward $\text{NH}_4\text{-N}$ release from an accumulated detritus substrate to the overlying water column. Parameter values were calibrated for 23 of the 27 wetland microcosms (mean $R^2 = 0.85$). Values ranged from 4.7 to 21.5 mg-N L^{-1} for the porewater $\text{NH}_4\text{-N}$ concentration (C_{pw}) and 0.004 to 0.13 m d^{-1} (1.5 to 47.4 m yr^{-1}) for the rate constant (k_u). Despite this range of values, the range of upward flux (J_{UF}) values was relatively constant for each overlying water column concentration. At the Walnut Cove wetlands, the potential areal ammonium release rates (J_{UF}) from the detritus substrate at an overlying water column concentrations of 4 to 6 mg L^{-1} would be 0.21 and 0.14 $\text{g-N m}^{-2} \text{d}^{-1}$ (70 and 50 $\text{g-N m}^{-2} \text{yr}^{-1}$), respectively. If the accumulated detritus used in this study

was representative of the aged detritus substrate in other FWS CWs, then the $\text{NH}_4\text{-N}$ release from an aged detritus substrate will be detrimental to the nitrogen removal performance of lightly loaded systems ($\text{TKN load} < 120 \text{ g-N m}^{-2} \text{ yr}^{-1}$). The nitrogen release from an aged, accumulated detritus substrate found in this study provides a starting point from which future research can fully quantify the influence of this internal nitrogen source on treatment efficiency and methods to control or prevent it.

REFERENCES

- Birgand, F. (2000). Quantification and Modeling of In-Stream Processes in Agricultural canals of the lower coastal plain [North Carolina State University].
<http://www.lib.ncsu.edu/resolver/1840.16/5233>
- Brix, H. (1997). Do macrophytes play a role in constructed treatment wetlands? *Water Science and Technology*; London, 35(5), 11–17.
- Burchell, M. R., Thompson, T. W., Broome, S. W., Krometis, L. A., & Badgely, B. (2016). Constructed wetlands to polish wastewater in small rural communities—Evaluation of current and potential use to improve water quality trends and protect human health. Final report. (Virginia Tech/ NC State University Regional Collaborative Proposal Planning and Development Grants, p. 29) [Final Report].
- Carey, R. O., & Migliaccio, K. W. (2009). Contribution of Wastewater Treatment Plant Effluents to Nutrient Dynamics in Aquatic Systems: A Review. *Environmental Management*, 44(2), 205–217. <http://dx.doi.org/10.1007/s00267-009-9309-5>
- Gerke, S., Baker, L. A., & Xu, Y. (2001). Nitrogen Transformations in a Wetland Receiving Lagoon Effluent: Sequential Model and Implications for Water Reuse. *Water Research*, 35(16), 3857–3866. [https://doi.org/10.1016/S0043-1354\(01\)00121-X](https://doi.org/10.1016/S0043-1354(01)00121-X)
- Hesslein, R. H. (1976). An in Situ Sampler for Close Interval Pore Water Studies. *Limnology and Oceanography*, 21(6), 912–914.
- Kadlec, R. H. (2008). The effects of wetland vegetation and morphology on nitrogen processing. *Ecological Engineering*, 33(2), 126–141. <https://doi.org/10.1016/j.ecoleng.2008.02.012>
- Kadlec, R. H., Cuvellier, C., & Stober, T. (2010). Performance of the Columbia, Missouri, treatment wetland. *Ecological Engineering*, 36(5), 672–684.
<https://doi.org/10.1016/j.ecoleng.2009.12.009>
- Kadlec, R. H., & Wallace, S. D. (2009). *Treatment Wetlands* (2nd ed.). CRC Press.
- Martinez, C. J., & Wise, W. R. (2003). Hydraulic Analysis of Orlando Easterly Wetland. *Journal of Environmental Engineering*, 129(6), 553–560. [https://doi.org/10.1061/\(ASCE\)0733-9372\(2003\)129:6\(553\)](https://doi.org/10.1061/(ASCE)0733-9372(2003)129:6(553))
- Mitsch, W. J., & Gosselink, J. G. (2015). *Wetlands* (5th ed.). John Wiley & Sons, Inc.
- Mitsch, W. J., Zhang, L., Stefanik, K. C., Nahlik, A. M., Anderson, C. J., Bernal, B., Hernandez, M., & Song, K. (2012). Creating Wetlands: Primary Succession, Water Quality Changes, and Self-Design over 15 Years. *BioScience*, 62(3), 237–250.
<https://doi.org/10.1525/bio.2012.62.3.5>

- Nelder, J. A., & Mead, R. (1965). A Simplex Method for Function Minimization. *The Computer Journal*, 7(4), 308–313. <https://doi.org/10.1093/comjnl/7.4.308>
- Reddy, K. R., Patrick, W. H., & Broadbent, F. E. (1984). Nitrogen transformations and loss in flooded soils and sediments. *C R C Critical Reviews in Environmental Control*, 13(4), 273–309. <https://doi.org/10.1080/10643388409381709>
- RStudio Team. (2021). RStudio: Integrated Development for R. www.rstudio.com
- Sartoris, J. J., Thullen, J. S., Barber, L. B., & Salas, D. E. (1999). Investigation of nitrogen transformations in a southern California constructed wastewater treatment wetland. *Ecological Engineering*, 14(1), 49–65. [https://doi.org/10.1016/S0925-8574\(99\)00019-1](https://doi.org/10.1016/S0925-8574(99)00019-1)
- Thullen, J. S., Sartoris, J. J., & Nelson, S. M. (2005). Managing vegetation in surface-flow wastewater-treatment wetlands for optimal treatment performance. *Ecological Engineering*, 25(5), 583–593. <https://doi.org/10.1016/j.ecoleng.2005.07.013>
- Thullen, J. S., Sartoris, J. J., & Walton, W. E. (2002). Effects of vegetation management in constructed wetland treatment cells on water quality and mosquito production. *Ecological Engineering*, 18(4), 441–457. [https://doi.org/10.1016/S0925-8574\(01\)00105-7](https://doi.org/10.1016/S0925-8574(01)00105-7)
- Ullman, W.J., Aller, R.C., 1982. Diffusion coefficients in nearshore marine sediments1. *Limnol. Oceanogr.* 27, 552–556. <https://doi.org/10.4319/lo.1982.27.3.0552>
- Wang, H., Jawitz, J. W., White, J. R., Martinez, C. J., & Sees, M. D. (2006). Rejuvenating the largest municipal treatment wetland in Florida. *Ecological Engineering*, 26(2), 132–146. <https://doi.org/10.1016/j.ecoleng.2005.07.016>

CHAPTER 4: DETRITUS REMOVAL TO IMPROVE NITROGEN REMOVAL AND EXTEND THE USEFUL LIFE OF A FREE WATER SURFACE CONSTRUCTED WETLAND IN NC

ABSTRACT

This study aimed to both document the process and evaluate the influence of a detritus removal on an aged, poorly performing free water surface (FWS) constructed wetland (CW). A plan for detritus removal and revegetation was developed and implemented in one of the two aged FWS CW cells at the Walnut Cove Wastewater Treatment Plant (WWTP) in April 2019. The detritus removal was completed successfully in less than five working days and at a reasonable cost. Five paired inert tracer tests and a previously initiated inlet/outlet hydrology and water quality monitoring study were conducted over a two-year span to evaluate the changes to internal hydraulics and the nitrogen removal performance when compared to the unimproved wetland cell that served as a control. The results from the tracer tests indicated that the detritus removal doubled both the volumetric efficiency (e), the mean residence time (τ), and hydraulic efficiency index (λ_e) of the rejuvenated wetland relative to the unimproved control cell. Of the nitrogen species analyzed, mean monthly outlet concentrations were significantly different between the two cells for $\text{NH}_4\text{-N}$ ($p = 0.003$), ON ($p < 0.001$), TDN ($p = 0.004$), and TN ($p < 0.001$). Specifically, monthly $\text{NH}_4\text{-N}$ concentrations were approximately 1 mg L^{-1} lower out of cell 1 following detritus removal ($4.5 \pm 2.6 \text{ mg L}^{-1}$) when compared to those out of cell 2 ($5.5 \pm 2.6 \text{ mg L}^{-1}$). Over the two years, the cleaned-out wetland cell 1 removed 610 kg-N (19%), while cell 2 exported 300 kg-N (-9%). Although the internal hydraulics and nitrogen removal performance were better in the rejuvenated cell relative to the aged unimproved cell, both

metrics remained below ideal values expected for a typical FWS CW. Nevertheless, these results provided further evidence that detritus removal can improve wetland hydraulics and treatment efficiency. On this basis, a maintenance plan that includes detritus removal and active vegetation management is paramount to the long-term efficient operation of FWS CWs designed for nutrient removal.

INTRODUCTION

As in natural wetlands, vegetation in free water surface (FWS) constructed wetlands (CWs) will senesce at the end of each growing season, and this decaying biomass (i.e., detritus) falls into a constantly saturated basin. Over time, in a manner similar to bog formation, this detritus begins to accumulate and fill the basin. With average detritus accumulation ranging from 1 to 2 cm yr⁻¹ (Kadlec & Wallace, 2009), the volume of a typical FWS CW basin can be substantially reduced in only 10 to 15 years, a fact noted in several previous FWS CW studies (Kadlec et al., 2010, 2012; Martinez & Wise, 2003; Sartoris et al., 1999; Wang et al., 2006).

Although detritus within FWS CWs provides carbon source and microbial attachment sites, both of which are important in wastewater treatment performance, the accumulation and formation of a thick detritus substrate can also have a negative influence on treatment efficiency. Because of its gradual accumulation, the negative influence of a detritus substrate on treatment efficiency increases with operational age. Physically, an accumulated detritus substrate reduces the volume of the FWS CW basin, which in turn reduces the wetland's hydraulic residence time and produces preferential flow paths and dead zones that reduce the effective wetland surface area (Kadlec & Wallace, 2009; Martinez & Wise, 2003). The hydraulic inefficiencies produced by accumulated detritus were identified as a main contributor to the decline of total phosphorus removal in a large Florida treatment wetland after 13 years of operation (Wang et al., 2006).

While accumulated detritus has been shown to negatively influence phosphorus removal, studies investigating the influence of accumulated detritus on nitrogen removal are limited. However, the inverse correlation between hydraulic loading rate (HLR) and total nitrogen (TN) removal efficiency reported in both Land et al. (2016) & Crumpton et al. (2020) suggests that the reduction in effective wetland surface area caused by accumulated detritus will reduce the nitrogen removal. In addition to the physical influence of an accumulated detritus substrate, Sartoris et al. (1999) noted the potential for an internal nitrogen load from decaying vegetation (i.e., detritus) and suggested that this was a primary cause of low nitrogen removal within a FWS CW in California.

At the Walnut Cove WWTP specifically, 24 years of operation (from 1996 to 2019) had resulted in an accumulated detritus substrate with a depth between 0.3 and 0.45 m in both wetland cells (Figure 4.1). Inert tracer tests conducted in both cells indicated that the detritus layer had caused significant hydraulic inefficiencies that substantially shortened wetland hydraulic residence time and reduced effective wetland surface area (Chapter 2). In addition to reducing physical space available for treatment in the wetland cells, Chapter 3 showed that the accumulated detritus can release a substantial amount of $\text{NH}_4\text{-N}$ and act as an internal nitrogen source. Therefore, the decline in the treatment efficiency of the two FWS CW cells over time was linked to the physical process of detritus (i.e., decaying biomass) accumulation.



Figure 4.1: Left: thickness of accumulated detritus in cell 1. Right: View of wetland cell 1 immediately prior to clean out. Unvegetated short-circuit paths were evident.

Because detritus accumulation associated with age coupled with limited maintenance appeared to be the cause of poor performance, it was hypothesized that the physical removal of the accumulated detritus could rejuvenate this and other aged, poorly performing FWS CWs. A detritus removal should increase the effective wetland surface area and reduce the stored nitrogen pool within the basin, resulting in improved TN removal and reduced internal nitrogen release. Detritus removal has been used successfully to remediate age-related declines in the internal hydraulics and phosphorus removal performance at the large Orlando Easterly Wetland in Florida (Wang et al., 2006). However, this was the only study found by the author that investigated the influence of detritus removal on treatment efficiency, indicating insufficient to support the success of detritus removal in FWS CWs of variable size, location, and pollutant of interest (particularly nitrogen). As noted in Kadlec and Wallace (2009), the lack of information on detritus removal makes it difficult to evaluate the trade-offs between reduced efficiency with age and the cost of renovation.

To test the hypothesis that a detritus removal could improve nitrogen removal in a poorly performing aged FWS CW, detritus was removed from one of the two parallel wetland cells within the Walnut Cove WWTP. This chapter details the technique developed to remove the detritus and the results of a monitoring study aimed at evaluating the effects on hydraulic efficiency and nitrogen removal performance. Because the two wetland cells had the same climatic conditions, influent hydrology, and water quality, the study used the difference between the internal hydraulics and nitrogen removal performance of the two cells as a measure of the influence of the detritus removal on wetland performance. The study objectives were to: (1) develop, implement, and document a process to remove detritus and replant one of the wetland cells; (2) quantify and compare the internal hydraulics and nitrogen removal performance post-wetland rejuvenation (i.e., detritus removal and revegetation) versus a control wetland cell; and (3) evaluate the potential for detritus removal as a widespread maintenance option.

METHODS AND MATERIALS

Methods used in this study were very similar to those used in the previous site assessment study detailed in Chapter 2. An overview of those methods along with the most pertinent details and new methodologies are presented herein.

Site description

This study was performed at the Walnut Cove WWTP located in Walnut Cove, NC (36°17'38.5"N 80°07'57.3"W). Within the WWTP, there were two parallel *Typha*-dominated FWS CW cells that received effluent from a system of upstream lagoons and a *Lemna*-dominated (duckweed) raceway (Figure 4.2). Each wetland cell was designed to have constant pool depth of 0.3 m (1-ft), a bottom width of 19 m (63-ft), 3:1 side slopes, and a length of 350 m (1140-ft), which resulted in a nominal surface area of 7200 m² (0.7 ha), a nominal volume of 2130 m³, and

an aspect ratio of 17:1. To evaluate the influence of the detritus removal, cell 1 was selected for detritus removal, while cell 2 was left in its existing condition to serve as a reference (Figure 4.2).



Figure 4.2: Aerial photograph of the two wetland cells (Image modified from Google Maps). The arrows indicate flow direction. Sampling stations are shown with red circles and the weather station is shown with a blue star.

Detritus Removal

Drying of wetland cell 1 was initiated in late March 2019. Inflow to cell 1 was halted by removing the weir plate and replacing it with a solid metal sheet and all influent wastewater was diverted into cell 2. The wetland cell was drained over the next four weeks. Dredging was initiated in cell 1 on April 22, 2019, using an excavator with an 18-m long boom to collect and remove detritus from the basin (Figure 4.3). Excavated detritus was placed either on the wetland cell side slopes, or between the two wetland cells, which allowed runoff from additional dewatering to be captured in the wetland or held in swales on-site. During detritus removal, clumps containing living cattails (*Typha spp.*) were placed back into the wetland cell on 1.5-m centers to speed vegetation reestablishment (Figure 4.3 & 4.4).



Figure 4.3: Left: the excavator removing detritus from the first half of cell 1. Right: An areal view of both wetland cells during the detritus removal of cell 1. Cell 1 is the top cell in this picture.



Figure 4.4: View of the cell 1, taken from the inlet, shows the removed detritus placed on the cell side slopes and the replanted cattail clumps within the FWS CW basin.

Dredging was completed after five working days on April 29, 2019. On May 10, 2019, the previous inlet weir plate was reinstalled and cell 1 was brought back online to receive wastewater. A temporary outlet weir plate with a lower crest elevation was installed to keep the water depth in cell 1 around 0.15 m (0.5 ft) to improve early vegetation reestablishment.

Vegetation appeared well established by July 2019 (Figure 4.5). On August 23, 2019, the normal water depth of 0.3 m was reestablished by re-installing the original outlet weir plate.



Figure 4.5: Left: view of cell 1, taken from just to the right of the cell inlet, soon after the cell was brought back online in mid-May 2019. Right: View of cell 1, taken from the cell inlet, at the start of the July 26th, 2019, tracer tests with vegetation reestablished.

Hydrology

Wastewater entered the wetlands through a splitter box that diverted the flow evenly into wetland cells 1 and 2, while effluent was discharged from each wetland cell through separate outlets. Sharp-crested contracted weirs with a width of 0.45 m (1.5 ft) controlled flow into and out of the wetland cells. Stage above weir crest (head) was measured at 15-minute intervals at the inlet and outlet weirs using ISCO 730 Bubbler modules integrated into the ISCO 6712 automatic samplers. Stage data were downloaded during site visits using an ISCO 581 Rapid Transfer Device (RTD). A Campbell-Scientific weather station was installed to gather climatic data at 15-minute intervals, including the barometric pressure (in mmHg), total precipitation (mm), air temperature ($^{\circ}\text{C}$), relative humidity (%), wind speed (m/s), wind direction (degrees), net solar radiation (W m^{-2}), net latent radiation (W m^{-2}), albedo, net radiation up (W m^{-2}), and net radiation down (W m^{-2}). Weather station data were downloaded each month.

Stage measurements were converted to flow rates using the Francis (1883) equation, as specified for standard fully contracted weirs in the Bureau of Reclamation's Water Measurement Manual (2001).

$$Q = 3.33(L - 0.2H)(H^{3/2}) \quad (\text{Eq. 4.1})$$

where Q was the volumetric flow ($\text{ft}^3 \text{ s}^{-1}$), L was the length of the weir (ft), and H was the head on the weir (ft). This equation is valid when $H/L \leq 0.33$; a condition that was met during normal flow conditions. After estimation, flow rates were converted to SI units. To reduce the influence of error-inducing noise in stage measurements, the 15-minute flow estimates were averaged to daily flow estimates.

Daily evapotranspiration (ET) losses were estimated using the ASCE standardized Reference ET Equation and data from the weather station (Allen et al., 2005) (See Chapter 2 and Appendix B). Both wetland cells were underlain by a clay layer, so infiltration was assumed negligible. The wetland cells were not designed to store water; therefore, storage ($\Delta S/\Delta t$) should be near zero over the monthly or annual periods. Because of the high potential for debris to accumulate on the outlet weirs and bubbler lines between site visits, daily Q_{in} , P , and ET values, daily Q_{out} values were checked for accuracy using the flow estimate methodology described in chapter 2 and, if necessary, filled using a seasonal linear relationship with daily Q_{in} . Using the corrected Q_{out} data, monthly water balances were evaluated for each wetland using cumulative monthly volumes and equation 4.2.

$$Residual = V_{in} + (P * A_d) - V_{out} - ET * A_s \quad (\text{Eq. 4.2})$$

where V_{in} and V_{out} were the cumulative influent and effluent flow for each cell (m^3), respectively, P was cumulative precipitation (m), A_d was the cell nominal surface area plus the drainage area that contributes surface runoff to each cell (m^2), ET was cumulative evapotranspiration (m), A_s was the nominal cell surface area (m^2), and Residual was the unaccounted-for water volume that would produce water balance closure (m^3).

With infiltration and storage set to zero, any remaining residual water volume was deemed to represent slight measurement or estimate error within the water budget. A positive residual indicated that inputs were greater than outputs. Alternatively, a negative error value indicated that outputs were greater than inputs.

Internal hydraulics

Internal hydraulics were quantified and evaluated using inert tracer testing (Table 4.1). When cell 1 was brought back online in May 2019, water level was held at approximately half its design volume (pool depth of 0.15-m) until August 23rd, 2019, as a precaution to ensure macrophyte reestablishment. During this time, two paired tracer tests were conducted. After August 23, cell 1 was brought back to full volume (pool depth of 0.3-m). Following the adjustment back to full volume, three paired tests were conducted.

Tracer tests were initiated by adding either 150 mL or 200 mL of Rhodamine WT fluorescent dye to each wetland cell's influent stream. Rhodamine WT dye was used as the inert tracer because of its ease of use and visibility. Concern has been raised about the use of Rhodamine WT as a dye to perform wetland hydraulic analysis due to its susceptibility to adsorption on organic material. However, Williams and Nelson (2011) found Rhodamine WT concentrations to be coincident with bromide concentrations in a series of tracer tests conducted

on a 1.2-ha treatment wetland. Additionally, Lin et al. (2003) suggested that Rhodamine WT is a suitable tracer in wetlands with residence times less than one week.

Initial background fluorescence was measured using grab samples collected from each outlet at the start of each test. During the tracer tests, both outlet ISCO automatic samplers collected discrete water samples. In the first four paired tracer tests, sampling was conducted using uniformly spaced 2-hour intervals (Table 4.1). Sampling during the final three paired tests was conducted at variable 1-to-4-hour time intervals to better capture the anticipated breakthrough times. The variable time intervals provided higher frequency sampling near the estimated breakthrough times, while still capturing the desired sampling period. All samples were brought back to the NCSU BAE Ecological Restoration Lab for analysis. Rhodamine WT concentration was measured in each sample using a Cyclops-7 Fluorometer and Databank Handheld Datalogger (Turner Designs, San Jose, CA). Samples were analyzed in accordance with the recommended measurement practices in Appendix B of the Cyclops Submersible Sensors User's Manual (2019). Further description of tracer test data, methodology, analysis, and results can be found in Chapter 2 and Appendix A.

Table 4.1: Overview of tracer experimental setup. Period is broken down into pre-wetland (Pre) and post-wetland rejuvenation (Post). Time interval is the sampling time interval. Sampling start refers to the time at which sampling was initiated after tracer injection (t_0). Note that variable time interval indicates variable sampling frequency used to better capture changes in tracer breakthrough.

Test	Start Date	Wetland cell	Period	Time Interval	Sampling Start	
					Cell 1	Cell 2
1	March 8, 2019	1	Pre	Every 2h	$t_0 + 7h$	
2	March 23, 2019	1 and 2	Pre	Every 2h	$t_0 + 6h$	$t_0 + 22h$
3	July 26, 2019	1 and 2	Post	Every 2h	$t_0 + 30h$	$t_0 + 12h$
4	August 9, 2019	1 and 2	Post	Every 2 h	$t_0 + 22h$	$t_0 + 12h$
5	January 31, 2020	1 and 2	Post	Variable	$t_0 + 12h$	$t_0 + 12h$
6	December 9, 2020	1 and 2	Post	Variable	$t_0 + 9 h$	$t_0 + 9 h$
7	April 23, 2021	1 and 2	Post	Variable	$t_0 + 4 h$	$t_0 + 4 h$

Both the method of moments and the gamma distribution were used to analyze tracer data and develop the residence time distribution (RTD) (Bodin et al., 2012; Kadlec & Wallace, 2009). The mass of tracer recovered (M_{rec}), observed mean residence time (τ) and the spread of the RTD curve (σ^2), and the short-circuiting index (dimensionless time at which 10% of recovered tracer mass has left the basin, t_{10}/t_n) were all estimated using both methods. From the estimates of τ and σ^2 , the number of tanks in series parameter (N), the volumetric efficiency (e), the hydraulic efficiency index (λ_e), and the dimensionless dispersion (σ_ϕ^2) were calculated. A detailed description of the tracer test analysis can be found in chapter 2, along with a further description in Appendix A.

The average values for M_{rec} , τ , N , e , λ_e , t_{10}/t_n , and σ_ϕ^2 were calculated for each wetland cell. These average values were compared to assess the influence of the detritus removal on internal hydraulics. The greater the value of τ , N , and e the better the internal hydraulics. To evaluate the state of the hydraulics in each wetland cell, average values were compared to the performance ranges in Table 4.2.

Table 4.2: Ranges of performance for the three evaluated hydraulic indexes. Ranges modified from thresholds presented in Liu et al. (2020) and Persson et al. (1999). This table refers back to Table 2.1.

Hydraulic Index	Performance Ranges		
	compromised	acceptable	excellent
λ_e	≤ 0.5	$0.5 - 0.75$	> 0.75
σ_{Φ}^2	> 0.2	$0.1 - 0.2$	$0.0 - 0.1$
t_{10}/t_{nom}	$0 - 0.3$	$0.3 - 0.7$	> 0.7

Using the monthly inflows, general hydrologic conditions, including the nominal residence time (t_n) and nominal hydraulic loading rates (HLR_n), were calculated for each month (Equations 4.3 & 4.4).

$$t_n = \frac{V}{Q}$$

(Eq. 4.3)

$$HLR_n = \frac{Q}{A}$$

(Eq. 4.4)

Because inflows and nominal areas were the same for each wetland cell, the t_n and HLR_n were also the same for each wetland cell. In addition to these nominal values, hydraulic data and monthly inflows were used to estimate the effective or mean residence time (τ) and effective hydraulic loading rate (HLR_e) for each month (Eq 4.5). As described in Chapter 2, the term *nominal* will be used to describe values based on the designed size of the wetland cells (i.e., the best estimate of the initial wetland conditions) and the term *effective* will be used to describe values based on the actual wetland conditions (A_e , V_e , HLR_e) estimated from the RTDs.

$$HLR_e = \frac{Q_{in}}{A_e}$$

(Eq 4.5)

where Q_{in} was the median monthly inflow rate ($m^3 d^{-1}$), and A_e was the effective wetland cell surface area (m^2)

A_e was estimated by dividing the effective wetland cell volume ($V_e = V^*e$) by the mean water depth (in the areas where there was flow) during the period (Table 4.3). In cell 1, the mean water depth was estimated to be 0.10 m when the cell was at half volume (June 2019 – August 2019) and 0.20 m when the cell was at full volume (September 2019 – May 2021). In cell 2, the mean water depth was estimated to be 0.15 m for the duration of the monitoring period.

Summary statistics, including the median, mean, and standard deviation (SD) were used to describe the central tendency and range of monthly residence time and HLR values for the study period (June 2019 through May 2021).

Water quality sampling

From May 2019 through May 2021, 500 mL grab samples were obtained at the inlet splitter box and outlet of both cells during weekly site visits. After each grab sample was collected, additional water quality parameters (pH, DO, specific conductivity, and temperature) were measured in the middle of the water column with a YSI Pro field probe (Xylem US, Yellow Springs, OH). The time of measurement ranged from 08:00 and 14:00 depending on weather conditions and necessary site activities (i.e., clearing outlet structures of debris, downloading data, on-site photography, etc.). Grab samples were transported back to the BAE Ecological Restoration Lab on ice and analyzed for NO_3-N (Hach TNT835 vials using EPA Hach Method 10206) and NH_4-N (Hach TNT831 vials using EPA Hach Method 10205) concentrations with a HACH DR3900 spectrophotometer. No site visits were made in April or May 2020 due to

COVID restrictions, so no water quality samples were collected, and no water quality parameters were measured during this period.

In addition to grab sampling, composite weekly water quality sampling was also conducted. Composite samples were collected using a 6712 ISCO automatic sampler set to collect a 300 mL sample two times a day at 12-hour fixed time intervals. The two daily samples were placed into the same 1000 mL ISCO bottle to create a composite daily sample. To preserve the samples in the field, the ISCO bottles were pre-acidified during weekly site visits. Samples were collected weekly, brought back to the BAE Ecological Restoration Lab, and composited into 7-day composite weekly samples for each sample location (inlet, outlet 1, and outlet 2).

Prior to analysis, composite samples were split, and half were filtered through a 0.45 μ m membrane filter. Both filtered and unfiltered samples were submitted to the BAE EAL for analysis. Each composite sample was analyzed for total Kjeldahl nitrogen (TKN), nitrite/nitrate ($\text{NO}_3\text{-N}$), ammonium ($\text{NH}_4\text{-N}$) and chloride (Cl^-) concentrations. From the filtered samples, concurrent dissolved organic nitrogen (DON) concentrations were estimated by subtracting $\text{NH}_4\text{-N}$ from TKN, and total dissolved nitrogen (TDN) concentrations were estimated by adding TKN and $\text{NO}_3\text{-N}$ concentrations. From the unfiltered samples, concurrent total organic nitrogen (ON) concentrations were estimated by subtracting $\text{NH}_4\text{-N}$ from TKN, and total nitrogen (TN) concentrations were estimated by adding TKN and $\text{NO}_3\text{-N}$ concentrations.

The original water quality analysis plan was to rely on samples collected primarily using the continuous automatic composited sampling scheme. This plan was impacted during COVID19 restrictions which limited field visits and more importantly, limited analysis by the BAE EAL. Other periods of continuous automatic sampling were suspended due to site wide floods (in February and November of 2020), tracer tests (January 2020, December 2020, and

April 2021), and nitrate dosing experiments (September 2020, October 2020, and April 2020). Water quality data collection during these periods was continued through grab samples and on-site analysis using the HACH DR3900 spectrophotometer.

Because water quality grab sampling included a greater portion of the study period, this dataset was used to evaluate NO₃-N and NH₄-N concentrations during the monitoring period. However, nitrogen removal cannot be fully assessed without total nitrogen data. Therefore, the more limited composite sampling data were used to evaluate DON, ON, TDN, and TN concentrations.

Nitrogen removal performance

Concentration data

Grab sampling data (NH₄-N and NO₃-N) and weekly composite data (ON, DON, TDN, and TN) were averaged by month to avoid synoptic errors associated with travel time differences within each wetland cell. The central tendency and range of monthly NO₃-N, NH₄-N, DON, ON, TDN, and TN concentrations at each sampling location during the monitoring period were described using summary statistics, including mean, median, and standard deviation. To determine if the two cells had statistically significant differences in nitrogen removal, paired Student's t-tests were used on the average monthly NO₃-N, NH₄-N, ON, DON, TDN, and TN concentrations. Statistical significance was assumed for p-values less than 0.05. The percent concentration changes between inlet and outlet were calculated for each nitrogen species using equation 4.5.

$$\text{Percent (\%) Change} = \left(\frac{C_{in} - C_{out}}{C_{in}} \right) * 100$$

(Eq. 4.5)

where C_{in} was the inlet sample pollutant concentration (mg L^{-1}), and C_{out} was the outlet sample pollutant concentration (mg L^{-1})

Load estimates

Daily influent and effluent loads were estimated for each nitrogen species ($\text{NH}_4\text{-N}$, $\text{NO}_3\text{-N}$, TDN, and TN). For periods without samples (COVID restrictions, site wide floods, nitrate dosing, tracer tests, and equipment malfunction), daily pollutant concentrations were estimated by interpolating between the last known daily concentration and the next known daily concentration (described in Chapter 2 (Moatar & Meybeck, 2005)). Cumulative influent and effluent loads during the study period were estimated by summing the daily loads. The load analysis was conducted in R using method 6 in the RiverLoad package (Nava et al., 2019).

Using the cumulative influent and effluent loads, a load reduction, removal efficiency, and the average daily areal mass removal rate were calculated for each nitrogen species. Pollutant load reductions were calculated by subtracting the effluent load from influent load for each nitrogen species during the 2-year monitoring period. Wetland removal efficiency was calculated by dividing the load reduction by the influent load. The nominal areal mass removal rates (J_{nom} , in $\text{g-N m}^{-2} \text{ day}^{-1}$) for $\text{NO}_3\text{-N}$, $\text{NH}_4\text{-N}$, TDN, and TN were calculated over the entire period using cumulative nitrogen loads, the wetland cell's nominal surface area, and the number of days in the period. Meanwhile, the effective areal mass removal rates (J_{eff} , in $\text{g-N m}^{-2} \text{ day}^{-1}$) for $\text{NO}_3\text{-N}$, $\text{NH}_4\text{-N}$, TDN, and TN were calculated over the entire period using cumulative nitrogen loads, the wetland cell's effective surface area, and the number of days in the period. All analyses were conducted using R software (R Core Team, 2017) and Microsoft Excel.

RESULTS & DISCUSSION

Detritus removal

The techniques used in detritus removal from wetland cell 1 appeared to be successful. The experienced operator positioned the excavator with the 18 m (60 ft) boom on the banks of the wetland cell and worked from downstream to upstream. To help ensure that the proper depth of excavation was maintained, a surveying laser level was set up and elevations were regularly checked. Approximately 10-15 cm (4-6 inches) of detritus was left in place to ensure that the excavator bucket did not penetrate the clay liner and to leave some of the accumulated carbon and microbial community intact. A small buffer of wetland plants (mainly cattail, *Typha spp.*) was left in place at the edges of the wetland cell to help stabilize and filter the dredged material as it was placed on the banks. Other clumps of cattail were excavated and replanted in the wetlands simultaneously as the wetland detritus was removed. Areas near the inlet and outlet of the wetland cell were excavated slightly deeper and not revegetated to help distribute flow evenly across the wetland at the inlet, and to reduce the amount of plant material that may clog the outlet and downstream chlorinator. The entire wetland cell was excavated in five days.

Excavated material dewatered quickly on the banks and the leachate flowed into the wetland. This material also compressed as it dried and vegetated with different types of grasses during the first growing season. Additionally, a metals analysis of this material revealed that zinc, copper, lead, cadmium, and nickel concentrations were all below the pollutant concentration limits for the land application of bulk sewage sludge (US EPA, 1994) (Table 4.3).

Table 4.3: Results from heavy metal analysis of detritus sample. All values are in units of mg/kg DW.

	Cu	Zn	Mn	Cd	Pb	Ni	Cr
Walnut Cove Detritus	39.5	93	184.95	0.85	0.011	1.89	30.5
Ceiling concentration limits¹	4,300	7,500	NA	85	840	420	3000

¹**Ceiling concentration limits for all biosolids applied to land (US EPA, 1994).**

The excavation was completed at a low cost (< 15,000\$ per ha), with a limited amount of equipment and minimal work from Town employees. It was also completed quickly, which allowed the wetland cell to be brought back online in less than two months. The excavation techniques demonstrated at the site were fully embraced by the Town and by the end of the study in May 2021, the Town was considering a plan to clean out wetland cell 2.

Replanting the wetland by utilizing the existing plants and redistributing them evenly across the wetland was also a low cost (no additional plants were purchased) and efficient method. When the large clumps of vegetation were replanted after the excavation, the entire plant and root ball were placed intact within the wetland. This method did not interrupt growth and allowed the wetland plants to quickly recolonize during the first growing season.

Management of the excavated detritus on-site was key to reduce cost. Allowing the excavated material to dewater on the banks prevented runoff from carrying the material offsite and allowed any nutrients to leach back into the wetlands cell for treatment. Based on the analysis of this material, it had the potential to be used as a compost additive for landscaping and should be investigated further.

Hydrology

The median monthly influent flow to both cells ranged from 167 to 672 m³ d⁻¹ with a median value of 379 m³ d⁻¹ (n = 24 months) (Table 4.4). Median monthly outflows were slightly larger in cell 1 relative to cell 2 (403 and 387 m³ d⁻¹, respectively) (Table 4.4). Over the 731-day period, 445 and 451 daily outflow measurements were filled at outlet 1 and outlet 2, respectively. The relatively high percentage of filled data was the result of detritus and muck accumulating on the outlet weirs in between sampling events along with several site wide flooding events. Median monthly ET values were estimated to be slightly greater than precipitation in terms of depth, but monthly precipitation acted over a greater area and was therefore greater in terms of volume (Table 4.4, Figure 4.6). Overall, both wetland cells had relatively well-balanced water budgets with outputs slightly overestimated relative to inputs (-5% and -3% median monthly residuals in cells 1 and 2, respectively). In terms of impact on the water budget, net ET and precipitation were approximately 2% of the surface inflow to each wetland cell and were considered negligible for nutrient budget calculations.

Table 4.4: Summary of median monthly hydrology for both wetland cells at the Walnut Cove WWTP during the monitoring period (June 2019 through May 2021). Inflow, precipitation, and evapotranspiration were assumed to be equal in both cells. Median and mean residuals based on the monthly volumes for each term in the water budget.

	Inlet (m³ d⁻¹)	Outlet 1 (m³ d⁻¹)	Outlet 2 (m³ d⁻¹)	P (mm)	ET (mm)	Cell 1 Residual (% of inflow)	Cell 2 Residual (% of inflow)
Median (IQR)	379 (147)	403 (185)	387 (165)	107 (80)	134 (106)	-5%	-3%
Mean (SD)	403 (119)	423 (146)	414 (147)	116 (62)	134 (53)	-5%	-3%



Figure 4.6: Hydrologic data from the study site during the monitoring period (June 2019 through May 2021). Top: the monthly median inflow and outflow of both cells during the period. Note the inlet flows were the same to both cells. Middle: the monthly precipitation and ET depths (mm) at the site. These were assumed to be the same for both cells. Bottom: Cumulative monthly volumes (m^3) for each term in the water budget.

Because precipitation inputs and ET losses were minor relative to surface inflows and inflows were approximately equal to outflows, concentration changes could be used to quantify nitrogen removal and compare the performance of the two wetland cells. Furthermore, because both cells received the same influent and experienced the same external factors, the influence of the detritus removal on nitrogen removal performance could be tested using paired Student's t-tests between each cell's monthly outlet concentrations.

Internal hydraulics

During tracer tests, the average outflows from each wetland cell ranged from 350 to 470 $\text{m}^3 \text{d}^{-1}$ (0.09 to 0.12 MGD). With median monthly outflows of 403 $\text{m}^3 \text{d}^{-1}$ and 387 $\text{m}^3 \text{d}^{-1}$, the tracer tests were conducted during typical hydrologic conditions, and therefore the results reflected the typical internal hydraulics of the cells. A comparison of RTDs from a paired tracer test in January 2020 is shown in Figure 4.7. Tracer mass recovery, a metric of tracer test validity, was acceptable in both wetland cells with an average of ~80% recovered in cell 1 and ~70% recovered in cell 2 (Table 4.5).

The detritus removal increased both the treatment volume and the effective surface area in cell 1. Even when cell 1 was held at half volume in the 3 months following the detritus removal, its effective volume (V_e) (620 m^3) was still greater than the cell 2 V_e at full volume (580 m^3). At full volume, wetland cell 1 V_e was 1020 m^3 , approximately half of the design or nominal treatment volume (2130 m^3). Using the V_e and estimated depths, the cell 1 effective surface areas were 6180 and 5110 m^2 at half and full volumes, respectively. Note that cell 1 effective surface areas were expected to be greater at full volume; however, there were three site wide floods and a clearing of the berm that held the loose detritus, which likely deposited some of the sediment and detritus back into the cell after it was brought back to full volume. Even with the slightly lower effective surface area at full volume, both cell 1 A_e values were greater than the 3830 m^2 estimated for cell 2 at full volume.

Based on design conditions, the average hydraulic retention time for each wetland cell should have been approximately 5.5 days during the study period (Table 4.5). Mean residence times (τ), derived from hydraulic analysis data, indicated that the actual residence times in cell 1 were approximately half this value at 2.6 days. While lower than expected, this value was still

approximately double the 1.4 day residence time in cell 2. Along with the greater τ , both the number of tanks (N) and the volumetric efficiency (e) were greater in cell 1 (9.5 and 0.48, respectively) relative to cell 2 (4.0 and 0.27). Meanwhile, the median monthly HLR_n was 5.1 cm d^{-1} for both cells and the median HLR_e values were 7.2 and 9.7 in cells 1 and 2, respectively. Both median HLR_e values were slightly greater than the median HLR of 4.3 cm d^{-1} for 116 FWS CWs treating TN reported in Kadlec and Wallace (2009).

When evaluated qualitatively, cell 1 at full volume was hydraulically acceptable for the short-circuiting index (t_{10}/t_n) and the mixing index (σ_{ϕ}^2) and was still considered hydraulically compromised for the overall hydraulic efficiency index (λ_e). However, cell 2 was hydraulically compromised for all three indices.

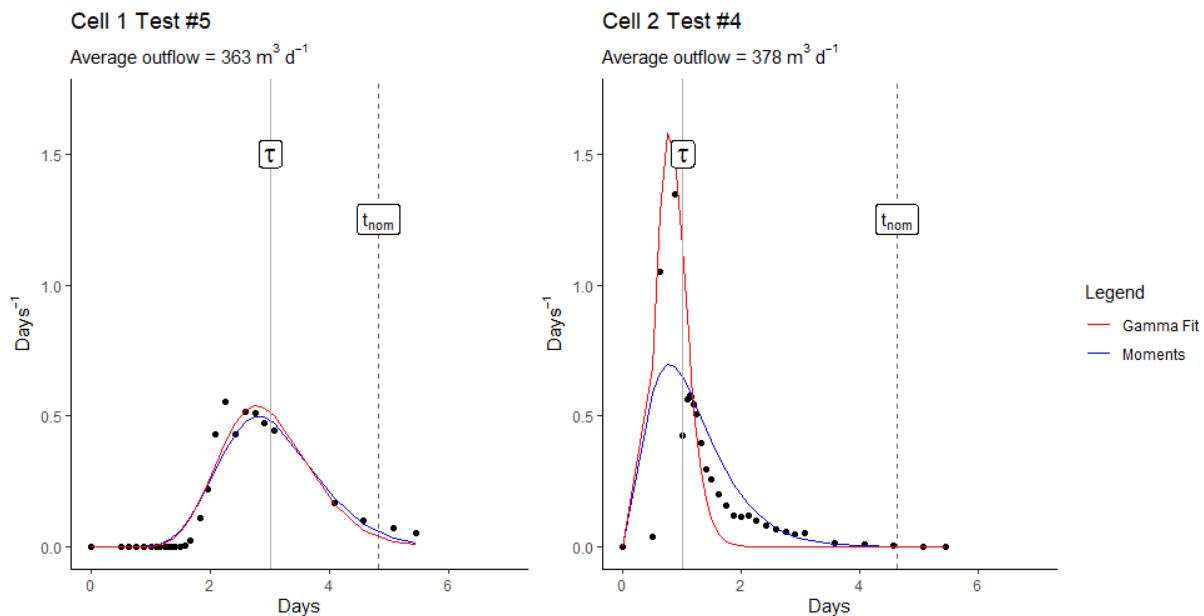


Figure 4.7: Results from the experiment initiated on January 31st, 2020. Vertical lines represent mean actual residence time (τ) and nominal residence time (t_n). The blue line represents the method of moments RTD, while the red line represents the gamma distribution RTD.

Table 4.5: Results from tracer test RTD analysis. Values represent averages by cell, period, and capacity. Cells were maintained at a nominal pool depth of 0.3 m for the duration of the study, except Cell 1, which was held at half-capacity (HC) until August 2019 after detritus removal. Values from both RTD analysis methods were included in the averages.

	Nominal depth (m)	Estimated depth (m)	Tests	Mass Recovery (%)	N	T (d)	t_n (d)	e	V_e (m ³)	A_e (m ²)
Cell 1	0.15	0.1	2	83.6	5.2	1.5	2.4	0.62	620	6180
	0.3	0.2	3	80.6	9.5	2.6	5.5	0.48	1020	5110
Cell 2	0.3	0.15	5	67.3	4.0	1.4	5.3	0.27	580	3830

Table 4.6: Average hydraulic indices for both wetland cells over the study period. The three dimensionless parameters (λ_e , t_{10} , σ_ϕ^2) were averaged over both the moment and gamma fit analysis.

Wetland cell	Tests	Nominal Depth, m	λ_e	t_{10}/t_{nom}	σ_ϕ^2
Cell 1	2	0.15 (6")	0.59	0.21	0.20
	3	0.3 (12")	0.40	0.30	0.13
Cell 2	5	0.3 (12")	0.18	0.13	0.33

Overall, the detritus removal improved the internal hydraulics of cell 1 relative to the values observed earlier in the study and described in Chapter 2. Actual residence time increased from less than 1 day to just over 2.5 days. Not only did the actual residence time increase, but every metric evaluated in this study also indicated improved hydraulic performance in cell 1 after detritus removal: hydraulic efficiency increased, the dimensionless variance decreased, and the hydraulic efficiency index increased (Table 4.6). This consistent improvement in hydraulic performance in wetland cell 1 can be attributed exclusively to the detritus removal because wetland cell 2 (which did not undergo detritus removal) did not exhibit a similar level of improvement.

Although the detritus removal improved hydraulics in cell 1, the improvement was slightly less than what was expected. Persson et al. (1999) stated that a hydraulic efficiency index value (λ) greater than 0.7 indicates a wetland cell with good hydraulic efficiency while λ

between 0.5 and 0.75 is satisfactory and λ is less than 0.5 indicates poor hydraulic efficiency.. The hydraulic efficiency index value for cell 1 after detritus removal increased from 0.1 to 0.4 and was much improved but still short of satisfactory by this metric.

Several factors likely combined to limit maximum impact detritus removal had on internal hydraulics of wetland cell 1; excavated detritus was placed on the side slopes of the cell, large vegetation clumps were replaced within the cell, and a 0.1 to 0.15 m layer of detritus was left in the cell to maintain a carbon pool and microbial community. All these factors were strategic decisions made to reduce costs and maintain conditions important to wetland treatment function. While these methods achieved those goals, the resultant cell volume remained less than the initial design volume after excavation and replanting. Additionally, revegetation of the cell was dramatic, with a nearly 100% macrophyte cover by August 2019. The high density of vegetation paired with several observed muskrat lodges likely led to minor preferential flow paths that led to the lowered the volumetric efficiencies in cell 1 in December 2020 and April 2021 (Appendix A). These preferential flow paths and channelization associated with dense vegetation could be mitigated by improved vegetation management, as suggested by Thullen et al. (2005).

Water quality parameters

The mean monthly water temperatures in the influent ranged from 6.0 to 28.1°C, with an average of 17.3°C (Table 4.7). Because the average monthly water temperatures were greater than 5 °C, wetland water temperatures were generally favorable for biological nitrogen processing during the study period (Vymazal, 2007). Through cell 1, temperatures generally decreased; monthly outlet temperatures ranged from 4.2 to 24.1°C and averaged 14.4°C.

Through cell 2, temperatures often increased; monthly outlet temperatures ranged from 4.8 to 31.8°C and averaged 17.5°C.

The mean monthly dissolved oxygen (DO) concentrations in the influent ranged from 0.2 to 14.9 mg L⁻¹, with an average of 3.8 mg L⁻¹ (Table 4.7). Based on the median flow (379 m³ d⁻¹) and effective areas of 5110 and 3830 m² in cells 1 and 2, respectively, the average monthly inlet DO concentration suggested that there was enough oxygen to support the conversion of 0.05 and 0.06 g-N m⁻² d⁻¹ of NH₄-N to NO₃-N through nitrification in cells 1 and 2, respectively. This estimate did not account for consumption competition or re-aeration with the basin and can be interpreted as an indication that nitrification was likely near or below 0.1 g-N m⁻² d⁻¹ in both cells during the monitoring period. Through cell 1, DO generally decreased and monthly outlet concentrations ranged from 0.1 to 5.9 mg L⁻¹ and averaged 1.7 mg L⁻¹. Through cell 2, this trend was reversed as monthly outlet concentrations ranged from 0.4 to 13.5 mg L⁻¹ and averaged 4.3 mg L⁻¹.

The mean monthly pH in the influent ranged from 6.9 to 8.1, with an average of 7.3 (Table 4.7). Through cell 1, pH generally decreased and monthly outlet values ranged from 6.6 to 7.5 and averaged of 6.9. This trend held in cell 2 as monthly outlet values ranged from 6.8 to 7.6 and averaged 7.1. With monthly average pH values between 6 and 8, both wetland cells were typically within optimal ranges for nitrification and denitrification (Vymazal, 2007).

The mean monthly specific conductivity in the influent ranged from 182 to 475 μS cm⁻¹, with an average of 369 μS cm⁻¹ (Table 4.7). Through cell 1, specific conductivity slightly decreased and monthly outlet values ranged from 161 to 470 μS cm⁻¹ and averaged 363 μS cm⁻¹. In cell 2 with monthly outlet values ranged from 158 to 474 μS cm⁻¹ and averaged of 370 μS cm⁻¹. Notably, low specific conductivity values were used to identify when Town Fork Creek

flooded the site (in February and November 2020) and the subsequent length of time that riverine water diluted the wastewater (March and December 2020) (Figure 4.8). These floods also removed the floating vegetation that provided shade both in the upstream treatment train and within the wetlands, which resulted in an increase in algal photosynthesis and an increase in DO and pH during these periods.

Of the water quality parameters analyzed, mean monthly outlet concentrations were significantly different between the two cells for temperature ($p < 0.001$), DO concentration ($p < 0.001$), and pH ($p < 0.001$) (Figure 4.8). For all three parameters, values at the outlet of wetland cell 2 were greater than wetland cell 1 outlet values. There was no significant difference between the monthly specific conductivity values at each outlet.

The differences in water quality parameter dynamics through the two cells were likely the result of the different vegetation patterns and residence times in the two cells. Starting in June 2019, cell 1 had over 50% vegetation cover (mainly duckweed and cattails) for all periods except for the winter and immediately following site floods. Meanwhile, cell 2 had less than 50% cover for the entire period with the first half of the cell dominated by open shallow water. The shading in cell 1 likely decreased temperature, DO, and pH through the cell by restricting sunlight, atmospheric contact, and algal activity. Additionally, the longer retention times in cell 1 meant that the moderating effect of shading had more time to influence the wastewater.

Table 4.7: Central tendencies and ranges of mean monthly temperature, dissolved oxygen, pH, and specific conductivity during the study period. Values calculated from measurements taken during site visits.

<i>Location</i>	<i>Temperature (°C)</i>			<i>DO (mg L⁻¹)</i>			<i>pH</i>			<i>Specific Conductivity (μS cm⁻¹)</i>		
	<i>Inlet</i>	<i>Out1</i>	<i>Out2</i>	<i>Inlet</i>	<i>Out1</i>	<i>Out2</i>	<i>Inlet</i>	<i>Out1</i>	<i>Out2</i>	<i>Inlet</i>	<i>Out1</i>	<i>Out2</i>
<i>Mean</i>	17.3	14.4	17.5	3.8	1.7	4.3	7.3	6.9	7.1	369	363	370
<i>Median</i>	16.0	13.7	16.4	1.8	0.7	3.8	7.3	6.8	7.0	391	395	398
<i>Min</i>	6.0	4.2	4.8	0.2	0.1	0.4	6.9	6.6	6.8	182	161	158
<i>Max</i>	28.1	24.1	31.8	14.9	5.9	13.5	8.1	7.5	7.6	475	470	474
<i>SD</i>	7.9	7.3	8.7	4.3	2.0	3.7	0.4	0.3	0.2	84	91	91

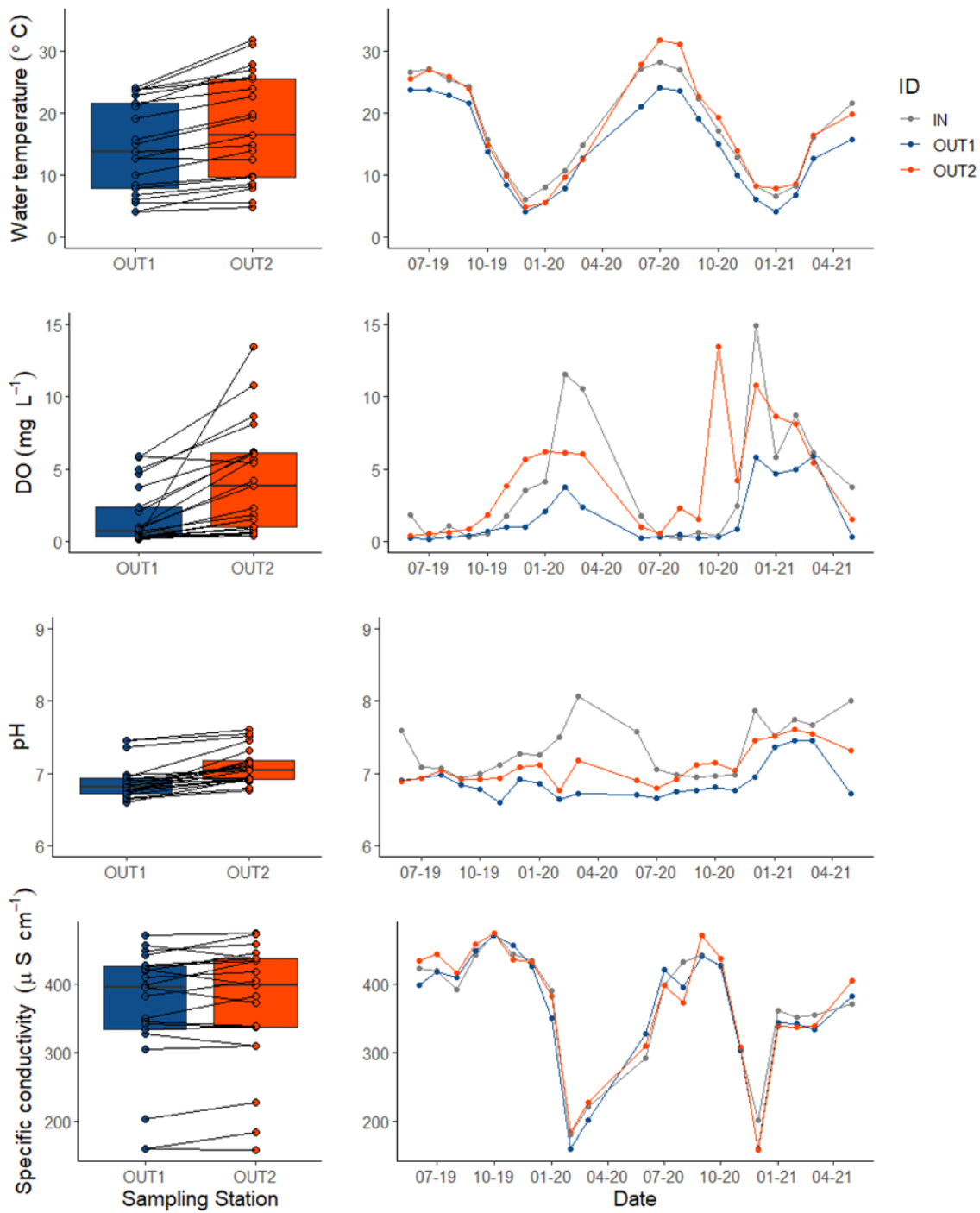


Figure 4.8: Mean monthly water quality parameter measurements (temperature, dissolved oxygen (DO), pH, and specific conductivity) during the monitoring period. IN, OUT1, and OUT2 refer to measurements taken at the inlet splitter box, the cell 1 outlet, and the cell 2 outlet, respectively.

Nitrogen concentrations

Mean monthly $\text{NH}_4\text{-N}$ concentrations were 5.4, 4.5, and 5.5 mg L^{-1} at the inlets, outlet 1, and outlet 2, respectively (Table 4.8). $\text{NH}_4\text{-N}$ concentration dynamics in the two cells had opposing trends. $\text{NH}_4\text{-N}$ concentrations were reduced by 0.9 mg L^{-1} (17%) in cell 1 but slightly increased by 0.1 mg L^{-1} (-2%) in cell 2. Mean $\text{NO}_3\text{-N}$ concentrations were 0.4, 0.6, and 0.3 mg L^{-1} at the inlets, outlet 1, and outlet 2, respectively. Again, concentration dynamics in the two cells had opposing trends; $\text{NO}_3\text{-N}$ concentrations were increased by 0.2 mg L^{-1} (-50%) in cell 1 but slightly decreased by 0.1 mg L^{-1} (25%) in cell 2. The greater $\text{NO}_3\text{-N}$ concentrations observed relative to chapter 2 values were at least partially explained by the analytical methods used for water quality analysis. The minimum detection limit (MDL) for the Hach TNT835 vials was 0.2 mg L^{-1} . The lower $\text{NO}_3\text{-N}$ concentrations reported in chapter 2 would have produced a similar result, if run using the Hach vials. Because these concentrations were so low, $\text{NO}_3\text{-N}$ removal did not have a large bearing on the evaluation of wetland performance. Mean DON concentrations were 1.5, 1.2, and 1.3 mg L^{-1} at the inlets, outlet 1, and outlet 2, respectively. In both cells, DON concentrations decreased. Mean ON concentrations were 3.3, 2.2, and 3.7 mg L^{-1} at the inlets, outlet 1, and outlet 2, respectively. ON concentration dynamics reflected the same trends observed for $\text{NH}_4\text{-N}$, with a decrease through cell 1 (1.1 mg L^{-1} , 33%) and an increase through cell 2 (-0.4 mg L^{-1} , -12%). Mean TDN concentrations were 7.8, 6.6, and 7.5 mg-N L^{-1} at the inlet, outlet 1, and outlet 2, respectively, while mean TN concentrations were 10.1, 7.8, and 10.3 mg-N L^{-1} at the inlet, outlet 1, and outlet 2, respectively. TDN and TN concentrations at all locations were likely skewed upward due to a lack of samples from the 2020 growing season, when inlet and outlet nitrogen concentrations for all species would have been lower, as seen in

the NH₄-N concentration dynamics (Figure 4.9). Nevertheless, when viewed collectively, nitrogen concentrations decreased through cell 1 and increased through cell 2.

Table 4.8: Mean (SD) of monthly nitrogen concentrations from June 2019 through May 2021. Percent reduction derived from median values reported here. Continuous data was not collected from March 2020 through August 2020. Site wide floods removed February, November, and December 2020 from analysis. Nitrate dosing study in April 2021 was removed from analysis. All concentrations in mg-N L⁻¹.

		NH ₄ -N	NO ₃ -N	DON	ON	TDN	TN
Cell 1	IN	5.4 (3.2)	0.4 (0.4)	1.5 (0.8)	3.3 (2.0)	7.8 (3.5)	10.1 (3.8)
	OUT	4.5 (2.6)	0.6 (0.7)	1.2 (0.6)	2.2 (1.4)	6.6 (2.9)	7.8 (3.0)
	% Reduction	17%	-50%	20%	33%	15%	23%
	n	21	21	18	17	18	17
Cell 2	IN	5.4 (3.2)	0.4 (0.4)	1.5 (0.8)	3.3 (2.0)	7.8 (3.5)	10.1 (3.8)
	OUT	5.5 (2.6)	0.3 (0.2)	1.3 (0.6)	3.7 (2.5)	7.5 (2.7)	10.3 (4.0)
	% Reduction	-2%	25%	13%	-12%	4%	-2%
	n	21	21	18	17	18	17

Nitrogen treatment

Of the nitrogen species analyzed, mean monthly outlet concentrations were significantly different between the two cells for NH₄-N ($p = 0.003$), ON ($p < 0.001$), TDN ($p = 0.004$), and TN ($p < 0.001$) (Figure 4.9, 4.10, & 4.11). For NH₄-N, the mean monthly outlet concentrations from cell 1 (detritus removal treatment) and cell 2 (unimproved reference) were 4.5 ± 2.6 and 5.5 ± 2.6 mg L⁻¹, respectively ($n = 21$) (Table 4.8). Mean monthly NO₃-N outlet concentrations from cell 1 and cell 2 were 0.6 ± 0.7 and 0.3 ± 0.2 mg L⁻¹, respectively, with no significant difference ($p = 0.06$) ($n = 21$). The mean monthly DON outlet concentrations from cell 1 and cell 2 were 1.2 ± 0.6 and 1.3 ± 0.6 mg L⁻¹, respectively, with no significant difference ($p = 0.46$) ($n = 18$).

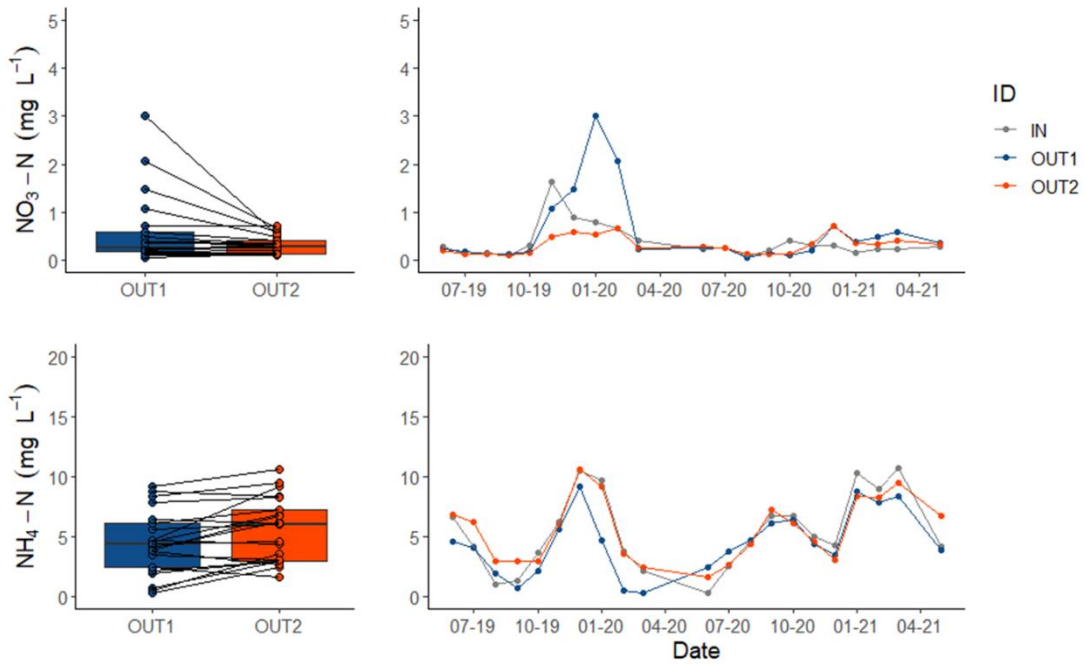


Figure 4.9: Mean monthly concentrations of $\text{NO}_3\text{-N}$ and $\text{NH}_4\text{-N}$ in grab samples collected at OUT1 (cell 1 outlet or detritus removal treatment) and OUT2 (cell 2 outlet or control) during weekly site visits. Within the boxplots, the lines connected mean monthly outlet concentrations for each month.

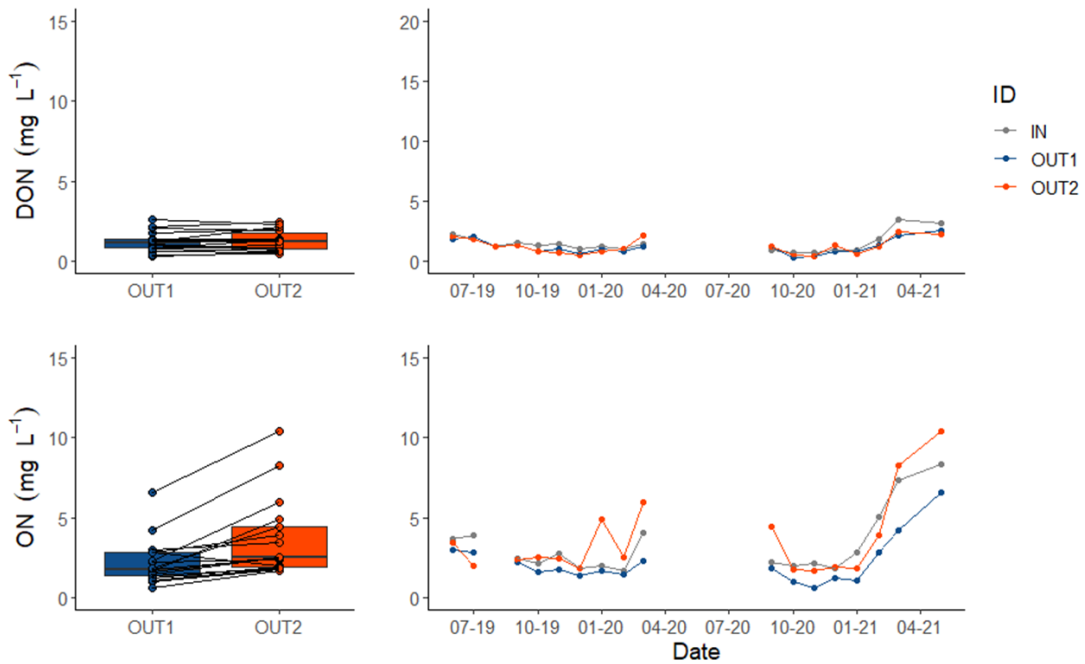


Figure 4.10: Mean monthly concentrations of DON and ON from weekly composite samples collected at OUT1 (cell 1 outlet or detritus removal treatment) and OUT2 (cell 2 outlet or control). Within the boxplots, the lines connected mean monthly outlet concentrations for each month.

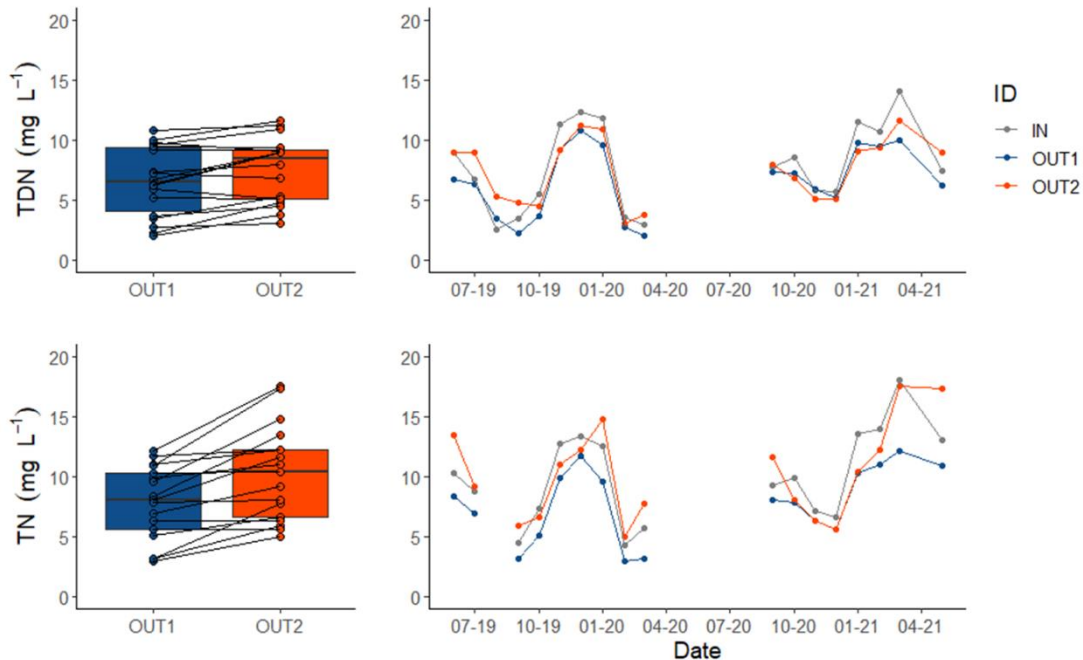


Figure 4.11: Mean monthly concentrations of TDN and TN in weekly composite samples collected at OUT1 (cell 1 outlet or detritus removal treatment) and OUT2 (cell 2 outlet or control). Within the boxplots, the lines connected mean monthly outlet concentrations for each month.

The results from concentration analysis indicated that the detritus removal had a significant influence on nitrogen removal within the Walnut Cove wetlands. Notably, the detritus removal in cell 1 resulted in significantly improved $\text{NH}_4\text{-N}$ removal in cell 1 relative to the unimproved cell 2, which led to the outlet $\text{NH}_4\text{-N}$ concentration in cell 1 being, on average, 1 mg L^{-1} lower than that of cell 2. The improved $\text{NH}_4\text{-N}$ removal resulting from the detritus removal was of particular importance for the Town of Walnut Cove because the site's NPDES permit has $\text{NH}_4\text{-N}$ discharge limit of 10 mg L^{-1} from April through October each year. Potential mechanisms for the improved $\text{NH}_4\text{-N}$ removal in cell 1 included improved assimilation due to the increase in vegetation; improved transfer of nitrogen in the water column to the subsurface (i.e., a hotspot for microbial activity and nitrogen transformation) through increased transpiration; improved nitrification through increased submerged surface area, increased

dissolved oxygen transfer, and increased residence times; and reduced internal nitrogen release through the removal of most of the detritus (i.e., the internal $\text{NH}_4\text{-N}$ source – see Chapter 3). The increase in $\text{NO}_3\text{-N}$ concentrations through cell 1, paired with the decrease in $\text{NO}_3\text{-N}$ concentrations through cell 2 suggested that improved nitrification may also have occurred as a result of the detritus removal and revegetation. However, concentration change data alone does not provide enough evidence to rule out other explanations. For example, cell 2 may have had the same amount of nitrification but more denitrification, or the detritus placed on the side slopes may have leached $\text{NO}_3\text{-N}$ back into wetland cell 1 as it desiccated.

In addition to the improved processing of $\text{NH}_4\text{-N}$, another notable improvement caused by the detritus removal was the higher reduction in ON through cell 1 relative to cell 2. Because both wetland cells had nearly identical DON removal, the increased ON reduction in cell 1 suggested that the detritus removal improved particulate ON (PON) removal. It was likely that removing the detritus from cell 1 reduced the potential for resuspension, which continued to occur in cell 2. It was also likely that the revegetation of cell 1 also improved its ability to intercept and retain suspended particulate matter as wastewater passed over an increased effective surface area. The improved $\text{NH}_4\text{-N}$ and ON removal in cell 1 resulted in an improved nitrogen removal in that cell relative to the reference cell 2. While the detritus removal and revegetation clearly improved nitrogen processing in cell 1 relative to cell 2, the load reduction and mass removal rates were needed to quantify the magnitude of removal at the site and contextualize the nitrogen removal at Walnut Cove relative to other FWS CWs treating nitrogen pollution.

Load removal

The load analysis spanned from June 2019 through May 2021 (excluding April 2021) for a total of 701 days. April 2021 was excluded because that period included the in-situ $\text{NO}_3\text{-N}$ dosing period, which was explored in-depth in Chapter 5. In a similar trend to the concentration analysis, $\text{NH}_4\text{-N}$ was removed through cell 1 (220 kg, 13%) and exported through cell 2 (-90 kg, -5%) (Table 4.9). Following the same trend as $\text{NH}_4\text{-N}$, 400 kg of ON (36%) were removed or retained within cell 1, while cell 2 exported 290 kg (-26%). Notably, ON was the nitrogen species with the largest removal in cell 1, while ON export was the largest export of any nitrogen species in cell 2. When compared to DON removal in both cells (80 kg in cell 1 and 20 kg in cell 2), the ON results suggest that the detritus removal greatly improved PON removal or retention within the cell. The improved particulate nitrogen retention in cell 1 was likely due to the removal of a main particulate source (the accumulated detritus) and the increased vegetation, which likely reduced the resuspension of ON and improved particulate interception and settling. The trend of removal in cell 1 and export in cell 2 was reversed for $\text{NO}_3\text{-N}$ loads since cell 1 exported 80 kg-N (-57%) and cell 2 retained 23 kg-N (23%). However, influent $\text{NO}_3\text{-N}$ loading was an order of magnitude lower than $\text{NH}_4\text{-N}$ loading and accounted for only 5% of the total nitrogen loading. So, while $\text{NO}_3\text{-N}$ removal efficiency appeared poor in the rejuvenated cell, the export from this cell was relatively small and had little bearing on overall nitrogen removal. For TDN, removal was approximately 5 times greater in cell 1 (260 kg-N, 10%) than in cell 2 (30 kg-N, 1%). Total nitrogen removal was even greater in cell 1 with a 610 kg-N (19%) removal, while there was an overall export of nitrogen (-300 kg-N or -9%) in cell 2. In short, more nitrogen was removed in cell 1 following the detritus removal, while cell 2 exported nitrogen over the same

two-year study period. These results provide strong evidence that the detritus removal had a positive influence on nitrogen removal.

Table 4.9: Cumulative loading from June 2019 through May 2021, excluding April 2021. April 2021 was excluded because that was the $\text{NO}_3\text{-N}$ dosing period, which was explored in-depth in chapter 5. Data were filled using linear interpolation for March 2020 through August 2020 for TDN and TN. All loads are in kg (kg d^{-1}).

		NH₄-N	NO₃-N	DON	ON	TDN	TN
Cell 1	IN	1760 (2.5)	140 (0.2)	460 (0.7)	1110 (1.6)	2500 (3.6)	3220 (4.6)
	OUT	1540 (2.2)	230 (0.3)	380 (0.5)	710 (1.0)	2250 (3.2)	2600 (3.7)
	Load Removal	13%	-57%	18%	36%	10%	19%
Cell 2	IN	1760 (2.5)	140 (0.2)	460 (0.7)	1110 (1.6)	2500 (3.6)	3220 (4.6)
	OUT	1850 (2.6)	120 (0.2)	440 (0.6)	1400 (2.0)	2470 (3.5)	3520 (5.0)
	Load Removal	-5%	23%	4%	-26%	1%	-9%

Mass removal rates

Because mass removal rates were used to compare removal in these cells to other values commonly found in literature, $\text{NH}_4\text{-N}$ and TN were the focus of this analysis. $\text{NO}_3\text{-N}$ removal was omitted from this analysis due to the very low influent concentrations and loadings. Over the two-year period, the average daily $\text{NH}_4\text{-N}$ J_{nom} values (which assumes the entire design area was available for treatment) were 0.04 and -0.02 $\text{g-N m}^{-2} \text{d}^{-1}$, in cells 1 and 2, respectively (Table 4.10). When evaluated for total nitrogen, the average daily J_{nom} values were 0.13 and -0.05 $\text{g-N m}^{-2} \text{d}^{-1}$, in cells 1 and 2, respectively. When computed using the effective areas (J_{eff}), average daily $\text{NH}_4\text{-N}$ areal mass removal rates increased to 0.06 and -0.04 $\text{g-N m}^{-2} \text{d}^{-1}$ and TN values increased to 0.19 and -0.10 $\text{g-N m}^{-2} \text{d}^{-1}$ in cells 1 and 2, respectively.

Table 4.10: The average daily nominal and effective areal mass removal rates (J_{nom} and J_{eff} , respectively) for each nitrogen species within each wetland from June 2019 through May 2021, excluding April 2021. A positive mass removal rate indicated a retention, and a negative mass removal rate indicated an internal release.

		NH₄-N	TN
Cell 1	J_{nom}	0.04	0.12
	J_{eff}	0.06	0.17
Cell 2	J_{nom}	-0.02	-0.06
	J_{eff}	-0.04	-0.11

When viewed relative to other FWS CWs, both the NH₄-N and TN areal mass removal rates were well below the 0.3 g-N m⁻² d⁻¹ median annual NH₄-N and TN estimated from 116 FWS wetlands by Kadlec and Wallace (2009). So, while nitrogen removal was improved in cell 1 relative to cell 2, neither cell had adequate nitrogen removal performance during the period. Of particular interest, the TN J_{nom} the cell 1 after the detritus removal was similar to the TN J_{nom} observed in both cells prior to the detritus removal (Chapter 2). While this may suggest that the detritus removal did not improve nitrogen removal, the TN J_{nom} value was still well above the post-cleanout value for cell 2. Instead, it was more likely that pre-cleanout performance was slightly overestimated during the relatively short initial monitoring period.

Influence of seasonality

Because the Walnut Cove WWTP is a biological treatment system, influent concentrations and removal performance will vary seasonally (Metcalf & Eddy, 2003). While not the focus of this study, seasonality is an important component of treatment wetlands. To evaluate this seasonality, the monthly NH₄-N and NO₃-N concentrations were used to find the seasonal means at each sampling station (Figure 4.12). Again, the use of concentrations to evaluate removal was acceptable because both wetland cells were surface flow driven, with only minor

contributions from precipitation or ET. The influence of seasonality was limited to $\text{NH}_4\text{-N}$ and $\text{NO}_3\text{-N}$ because grab sampling included more of the sampling period.

The most notable observation from Figure 4.12 was the varying influent $\text{NH}_4\text{-N}$ concentrations and their influence on removal. Because the FWS CWs rely on biological processes for nitrogen removal, one would have expected more nitrogen removal during the warmer seasons (i.e., spring and summer) (see Figure 4.8) when biological activity would have been greater. However, the exact opposite trend was observed in both cells with $\text{NH}_4\text{-N}$ concentration increases during the spring and summer months through both cells and concentration reductions during the fall and winter months. This trend backed up the claim that the short-term monitoring in Chapter 2 (October through March) likely overestimated annual performance.

There are several potential reasons for the concentration reductions observed during the fall and winter months. First, the lack of nitrogen concentrations reductions in the spring and summer suggested that assimilation did not occur at substantial rates during this period in either cell, or that it occurred at a rapid rate that was not captured using monthly means (i.e., a majority of plant growth over a 2-3 week period). Another potential reason is increased nitrification during the winter months (especially in cell 1). During the spring, summer, and fall months, vegetation (emergent macrophytes and floating vegetation) in cell 1 covered nearly all the wetland surface area, likely limiting wind driven re-aeration and restricting the transfer of oxygen between the surface and the water column. However, when vegetation senescence took place in the late fall months, the water surface became more open to the atmosphere, likely resulting in an increase in submerged biofilm growth and greater DO concentrations (see Figure 4.8). The potential for increased nitrification during the winter months was partially backed by

the $\text{NO}_3\text{-N}$ concentration increase observed through cell 1 during the winter months. When internal release (instead of removal) was considered, the lower influent $\text{NH}_4\text{-N}$ concentrations during the spring and summer months likely led to increased internal $\text{NH}_4\text{-N}$ release from the detritus substrate (especially in wetland cell 2) as the concentration gradient between the porewater concentration and overlying surface water concentration increased (see Chapter 3). It should also be noted that in the spring and summer, both wetland cells had lower outlet $\text{NH}_4\text{-N}$ concentrations than in the fall and winter. These two factors suggested that $\text{NH}_4\text{-N}$ removal did occur during these periods, but that the greater potential internal release during the spring and summer negated that removal.

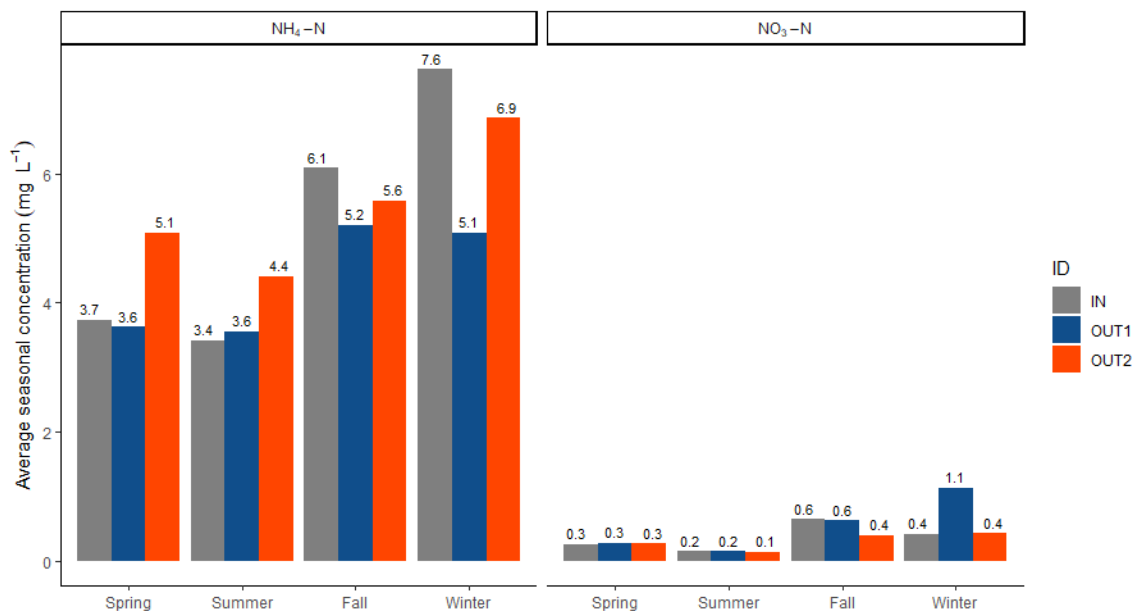


Figure 4.12: Average $\text{NH}_4\text{-N}$ and $\text{NO}_3\text{-N}$ concentrations over the 24-month study period. Spring data were limited by the lack of grab sampling in April and May 2020 due to the COVID 19 pandemic and the removal of April 2021 data which included the nitrate dosing study discussed in chapter 5. Here spring is April-June, summer was July-September, fall was October-December, and winter was January-March.

Future for detritus removal to improve nitrogen removal

Overall, this study showed that detritus removal can improve $\text{NH}_4\text{-N}$, ON , and TN removal in an aging FWS CW receiving $\text{NH}_4\text{-N}$ dominated lagoon effluent. Because $\text{NH}_4\text{-N}$ was the most important nitrogen species to the operators of the Walnut Cove WWTP, cleaning out wetland cell 2 to improve its performance is recommended. If site conditions remain the same (i.e., the influent waste stream continues to be $\text{NH}_4\text{-N}$ dominated), then a more aggressive detritus removal will be necessary in wetland cell 2. Leaving a detritus substrate would likely help to maintain higher denitrification rates (by providing an organic carbon source), but with no influent $\text{NO}_3\text{-N}$ and a discharge limit on $\text{NH}_4\text{-N}$, the focus at this and other similar sites should be on nitrification. Additionally, segments of the wetland cell should alternate between dense revegetation and open water (perpendicular to the flow direction) as suggested by (Keefe et al., 2010; Persson, 2000; Thullen et al., 2002, 2005), instead of the complete revegetation conducted in cell 1. This could provide better oxygen transfer, which will be needed to facilitate the necessary nitrification process, and it will likely improve internal hydraulics by allowing the water to spread back across the full wetland width in the open segments. Broad recommendations to optimize the detritus removal process for nitrogen removal at other sites must wait until after the influence of the detritus removal on $\text{NO}_3\text{-N}$ removal performance has also been evaluated.

While improvement in $\text{NH}_4\text{-N}$ removal was the most important outcome for the Walnut Cove WWTP, FWS CWs are often designed to remove the $\text{NO}_3\text{-N}$. Thus, the $\text{NO}_3\text{-N}$ removal results were expected to be the most pertinent for future detritus removal projects across North America. However, conclusions about $\text{NO}_3\text{-N}$ removal within the wetlands were difficult to develop due to very low $\text{NO}_3\text{-N}$ concentrations in the wastewater entering the wetland cells

(often $<0.5 \text{ mg L}^{-1}$). Both cells showed conditions favorable for denitrification (e.g., low DO, high carbon), but it remains unclear why cell 2 appeared to outperform the newly rejuvenated cell 1 at these low $\text{NO}_3\text{-N}$ concentrations. It was hypothesized that the increased residence time and vegetation density provided by the detritus removal were the source of increased nitrification in wetland cell 1. This increased nitrification created more $\text{NO}_3\text{-N}$ internally, which resulted in more $\text{NO}_3\text{-N}$ export. While this hypothesis fit with what was observed, other potential causes for the $\text{NO}_3\text{-N}$ export could not be ruled out. These included the leaching of $\text{NO}_3\text{-N}$ from the detritus stored on the banks and small flow measurement errors that were magnified when applied to the small $\text{NO}_3\text{-N}$ concentration measurements. These observations were additional motivation to perform the nitrate dosing experiments described in Chapter 5.

Study limitations

While this was a successful endeavor and study, there were two main limitations. The first and most influential limitation was the stoppage of site activities due to COVID restrictions. This stoppage limited the amount of water quality samples that were collected, and no maintenance was conducted on site equipment during most of the spring and summer of 2020. The lack of data during this period required fill data to be used to evaluate total nitrogen dynamics during the first full growing season post-detritus removal, when biological activity at the site would be at its highest. The second limitation was three site-wide floods that occurred at the site, when the adjacent Town Fork Creek overtopped its banks. These floodwaters caused multiple issues: they damaged the on-site equipment, which requires weeks to repair, and they diluted the entire system with riverine water, which influenced water chemistry. In addition to the dilution by riverine water, the floods also influenced water chemistry by removing all the duckweed from the treatment train – a main source of shading in the treatment train. Without

shading, the nutrient-enriched wastewater was fully exposed to sunlight, which created favorable conditions for algal blooms throughout the upstream treatment train. During these algal blooms, influent ammonium concentrations dropped well below the average value ($\sim 2 \text{ mg L}^{-1}$) and influent DO concentrations had major diurnal fluctuations. Overall, these floods impaired our ability to assess true nitrogen removal performance for several weeks after the flood occurred.

It should be noted that sitewide flooding was not expected during this study. When the project was initiated in fall 2018, on-site personnel informed us that site-wide floods only occurred about once every 10 years. USGS stage data collected approximately 10 miles downstream at the Dan River stream gage (ID: 02071000) backed up this claim. The data showed that the average daily stages during the floods of 2/7/2020, 11/13/2020, and 5/22/2020, were the first, second, and third highest stages recorded at the stream gage since 2000.

Taken together, the COVID shutdown and site wide floods severely restricted 2020 data collection efforts. While the impact of the detritus removal on nitrogen removal performance was able to be evaluated with a combination of measured and filled data, filled data was required for total nitrogen concentrations from March 2020 through August 2020 and over 50% of the daily outflow measurements during the monitoring period. While insights and inferences drawn from the data that were available are valid, the lack of 2020 growing season data meant that the concentration reductions, removal efficiencies, and areal mass removal rates should be considered very good estimates but contain some uncertainty.

CONCLUSION

As FWS CWs age across North America, it will become increasingly necessary to develop techniques to remediate the detritus accumulation and decline in treatment efficiency associated with operational age. One such method is detritus removal, and in this study, detritus

was removed from one of the two 20+ year old parallel FWS CWs within the Walnut Cove WWTP. The impact of the detritus removal was evaluated by comparing the internal hydraulics and nitrogen removal of the rejuvenated wetland (cell 1) to the unimproved wetland (cell 2). The process of detritus removal was successful, rapid, and cost effective. Paired tracer tests conducted in both cells revealed that the hydraulic performance of the rejuvenated wetland cell was substantially improved. Although substantially improved, the cell was not brought completely back to its initial hydraulic condition due to conservative strategies that left some detritus in place during the removal process. A comparison of outlet concentrations showed that the rejuvenated wetland (cell 1) removed significantly more $\text{NH}_4\text{-N}$, ON , and TN than the reference (cell 2). Although the results indicated that the detritus removal improved nitrogen removal performance, the overall nitrogen removal performance in the rejuvenated cell 1 was still poor relative to other FWS CWs. This poor performance was likely due to the inlet nitrogen speciation (primarily $\text{NH}_4\text{-N}$), flooding events, and the precautions taken during the detritus removal. Overall, the project results have convinced the Town to make plans to complete a detritus removal in the second wetland. This work will also provide operational and maintenance guidance to other towns across the country with aging wetland systems.

REFERENCES

- Allen, R. G., Walter, I. A., Elliott, R. L., Howell, T. A., Itenfisu, D., Jensen, M. E., & Snyder, R. L. (2005). The ASCE Standardized Reference Evapotranspiration Equation. American Society of Civil Engineers.
- Bodin, H., Mietto, A., Ehde, P. M., Persson, J., & Weisner, S. E. B. (2012). Tracer behaviour and analysis of hydraulics in experimental free water surface wetlands. *Ecological Engineering*, 49, 201–211. <https://doi.org/10.1016/j.ecoleng.2012.07.009>
- Crumpton, W. G., Stenback, G. A., Fisher, S. W., Stenback, J. Z., & Green, D. I. S. (2020). Water quality performance of wetlands receiving nonpoint-source nitrogen loads: Nitrate and total nitrogen removal efficiency and controlling factors. *Journal of Environmental Quality*, 49(3), 735–744. <https://doi.org/10.1002/jeq2.20061>
- Francis, J. B. (1883). *Lowell Hydraulics Experiments (fourth)*. D. Van Nostrand.
- Kadlec, R. H., Cuvellier, C., & Stober, T. (2010). Performance of the Columbia, Missouri, treatment wetland. *Ecological Engineering*, 36(5), 672–684. <https://doi.org/10.1016/j.ecoleng.2009.12.009>
- Kadlec, R. H., Pries, J., & Lee, K. (2012). The Brighton treatment wetlands. *Ecological Engineering*, 47, 56–70. <https://doi.org/10.1016/j.ecoleng.2012.06.042>
- Kadlec, R. H., & Wallace, S. D. (2009). *Treatment Wetlands (2nd ed.)*. CRC Press.
- Keefe, S. H., Daniels, J. S. (Thullen), Runkel, R. L., Wass, R. D., Stiles, E. A., & Barber, L. B. (2010). Influence of hummocks and emergent vegetation on hydraulic performance in a surface flow wastewater treatment wetland. *Water Resources Research*, 46(11). <https://doi.org/10.1029/2010WR009512>
- Land, M., Graneli, W., Grimvall, A., Hoffmann, C. C., Mitsch, W. J., Tonderski, K. S., & Verhoeven, J. T. A. (2016). How effective are created or restored freshwater wetlands for nitrogen and phosphorus removal? A systematic review. *Environmental Evidence*; London, 5. <http://dx.doi.org.prox.lib.ncsu.edu/10.1186/s13750-016-0060-0>
- Lin, A. Y.-C., Debroux, J.-F., Cunningham, J. A., & Reinhard, M. (2003). Comparison of rhodamine WT and bromide in the determination of hydraulic characteristics of constructed wetlands. *Ecological Engineering*, 20(1), 75–88. [https://doi.org/10.1016/S0925-8574\(03\)00005-3](https://doi.org/10.1016/S0925-8574(03)00005-3)
- Liu, J., Dong, B., Zhou, W., & Qian, Z. (2020). Optimal selection of hydraulic indexes with classical test theory to compare hydraulic performance of constructed wetlands. *Ecological Engineering*, 143, 105687. <https://doi.org/10.1016/j.ecoleng.2019.105687>

- Martinez, C. J., & Wise, W. R. (2003). Hydraulic Analysis of Orlando Easterly Wetland. *Journal of Environmental Engineering*, 129(6), 553–560. [https://doi.org/10.1061/\(ASCE\)0733-9372\(2003\)129:6\(553\)](https://doi.org/10.1061/(ASCE)0733-9372(2003)129:6(553))
- Metcalf & Eddy, I. (2003). *Wastewater engineering: Treatment and reuse* (4th ed. / revised by George Tchobanoglous, Franklin L. Burton, H. David Stensel.). Boston : McGraw-Hill, [2003]. <https://catalog.lib.ncsu.edu/catalog/NCSU1557208>
- Moatar, F., & Meybeck, M. (2005). Compared performances of different algorithms for estimating annual nutrient loads discharged by the eutrophic River Loire. *Hydrological Processes*, 19(2), 429–444. <https://doi.org/10.1002/hyp.5541>
- Nava, V., Patelli, M., Rotiroti, M., & Leoni, B. (2019). An R package for estimating river compound load using different methods. *Environmental Modelling and Software*, 117, 100–108.
- Persson, J. (2000). The hydraulic performance of ponds of various layouts. *Urban Water*, 2(3), 243–250. [https://doi.org/10.1016/S1462-0758\(00\)00059-5](https://doi.org/10.1016/S1462-0758(00)00059-5)
- Persson, J., Somes, N. L. G., & Wong, T. H. F. (1999). Hydraulics Efficiency of Constructed Wetlands and Ponds. *Water Science and Technology*; London, 40(3), 291–300.
- R Core Team. (2017). *R: A language and environment for statistical computing*. R Foundation for Statistical Computing. <https://www.R-project.org/>
- Sartoris, J. J., Thullen, J. S., Barber, L. B., & Salas, D. E. (1999). Investigation of nitrogen transformations in a southern California constructed wastewater treatment wetland. *Ecological Engineering*, 14(1), 49–65. [https://doi.org/10.1016/S0925-8574\(99\)00019-1](https://doi.org/10.1016/S0925-8574(99)00019-1)
- Thullen, J. S., Sartoris, J. J., & Nelson, S. M. (2005). Managing vegetation in surface-flow wastewater-treatment wetlands for optimal treatment performance. *Ecological Engineering*, 25(5), 583–593. <https://doi.org/10.1016/j.ecoleng.2005.07.013>
- Thullen, J. S., Sartoris, J. J., & Walton, W. E. (2002). Effects of vegetation management in constructed wetland treatment cells on water quality and mosquito production. *Ecological Engineering*, 18(4), 441–457. [https://doi.org/10.1016/S0925-8574\(01\)00105-7](https://doi.org/10.1016/S0925-8574(01)00105-7)
- Turner Designs. (2019). *Cyclops Submersible Sensors User’s Manual*. Turner Designs. <http://docs.turnerdesigns.com/t2/doc/manuals/998-2100.pdf>
- US Department of the Interior. (2001). *Water Measurement Manual* (3rd ed.). US Department of the Interior, Bureau of Reclamation.
- US EPA. (1994). *A Plain English Guide to the EPA Part 503 Biosolids Rule* (Government EPA/832/R-93/003; p. 180). USEPA.
- Vymazal, J. (2007). Removal of nutrients in various types of constructed wetlands. *Science of The Total Environment*, 380(1–3), 48–65. <https://doi.org/10.1016/j.scitotenv.2006.09.014>

Wang, H., Jawitz, J. W., White, J. R., Martinez, C. J., & Sees, M. D. (2006). Rejuvenating the largest municipal treatment wetland in Florida. *Ecological Engineering*, 26(2), 132–146. <https://doi.org/10.1016/j.ecoleng.2005.07.016>

Williams, C. F., & Nelson, S. D. (2011). Comparison of Rhodamine-WT and bromide as a tracer for elucidating internal wetland flow dynamics. *Ecological Engineering*, 37(10), 1492–1498. <https://doi.org/10.1016/j.ecoleng.2011.05.003>

CHAPTER 5: IN-SITU NITRATE DOSING TO EVALUATE THE INFLUENCE OF PRETREATMENT AND AGE ON NITROGEN REMOVAL IN TREATMENT WETLANDS

ABSTRACT

This study focused on two aspects of free water surface (FWS) constructed wetland (CW) operation and maintenance – nitrogen pretreatment and age. It was conducted to evaluate how improved pretreatment could improve overall nitrogen removal in FWS CWs that receive non-nitrified lagoon effluent within municipal wastewater treatment plants (WWTPs). To simulate the effect of improved pretreatment (i.e., increased upstream nitrification), the previously non-nitrified influent to two parallel FWS CW wetland cells within the Walnut Cove WWTP was continuously dosed with nitrate-enriched water for 31 days (~1 month) in spring 2021. Due to a previously completed wetland rejuvenation in one of the cells, site conditions during the NO₃-N dosing provided an opportunity to assess the influence of age (i.e., accumulated detritus) on NO₃-N removal through a side-by-side comparison of the two cells. Through dosing, the average influent NO₃-N concentration was raised from less than 0.5 mg-N L⁻¹ to 4.4 mg-N L⁻¹. The previously rejuvenated wetland cell (cell 1) removed 82% of the influent NO₃-N, while the unimproved cell (cell 2) removed 77% of the influent NO₃-N. On a nominal area basis, the NO₃-N mass removal rates in both cells were approximately 0.2 g-N m⁻² d⁻¹. These relatively high removal rates demonstrated how having substantial influent NO₃-N can improve nitrogen removal relative to systems that have ammonia-dominated influent. Furthermore, the substantial NO₃-N removal in both the rejuvenated, hydraulically adequate wetland and the aged, detritus filled wetland suggested that operational age may not have a substantial influence on NO₃-N

removal. However, greater TDN removal in the rejuvenated cell indicated that operational age still negatively influenced the removal of other nitrogen species (particularly $\text{NH}_4\text{-N}$) and suggested that wetland maintenance (in this case, detritus removal) is necessary to improve nitrogen removal.

INTRODUCTION

Free water surface (FWS) constructed wetlands (CWs) have been shown to effectively remove nitrogen, especially $\text{NO}_3\text{-N}$, from wastewater (Crumpton et al., 2006, 2020; Drake et al., 2018; García-Lledó et al., 2011; Gerke et al., 2001; Gersberg et al., 1986; Ingersoll & Baker, 1998; Kadlec, 2012; Kovacic et al., 2000; Land et al., 2016; Messer et al., 2017). The organic and anaerobic sediments of these FWS CWs create an environment favorable for $\text{NO}_3\text{-N}$ removal via denitrification (Bachand & Horne, 1999; Ingersoll & Baker, 1998). Although favorable for denitrification, several site-specific factors can influence actual nitrogen removal within these systems.

Because removal rates are often limited by the magnitude of the source, $\text{NO}_3\text{-N}$ must be available within the system to maximize the key removal process of denitrification (Vymazal, 2007). $\text{NO}_3\text{-N}$ availability is of critical importance for FWS CWs receiving non-nitrified wastewater (such as, lagoon effluent) because in these systems, available $\text{NO}_3\text{-N}$ is restricted to the amount of internal $\text{NO}_3\text{-N}$ produced via nitrification; a process that is often limited by the lack of dissolved oxygen (DO) in the anaerobic FWS CW environment. Without either influent $\text{NO}_3\text{-N}$ or internal $\text{NO}_3\text{-N}$ production, denitrification and, subsequently, complete nitrogen removal are also restricted. Improved pretreatment (i.e., increased upstream nitrification) has been identified as a potential method to increase $\text{NO}_3\text{-N}$ availability in these systems and thereby improve nitrogen removal and reduce the amount of nitrogen released to downstream

waterbodies. For example, a modeling study by Gerke et al. (2001) indicated that improved pretreatment was predicted to increase TN removal efficiencies in a FWS CW receiving non-nitrified lagoon effluent by 44% in the winter and 22% in the summer.

Another potential, but not well studied, factor that can affect nitrogen treatment is wetland age, and more specifically the accumulated detritus that builds as wetland age increases (Kadlec & Wallace, 2009; Wang et al., 2006). Previous monitoring studies within this research project indicated that nitrogen removal in two aging FWS CWs was poor due in part to a substantial accumulated detritus substrate that had formed over time and that physically removing the detritus increased both $\text{NH}_4\text{-N}$ and TN removal (Chapters 2 & 4). However, these studies only provided insights into the influence of age on $\text{NH}_4\text{-N}$ removal, not $\text{NO}_3\text{-N}$ removal, because the two wetland cells received non-nitrified influent (i.e., influent $\text{NO}_3\text{-N}$ concentrations were below 0.5 mg L^{-1}) during both study periods.

The current literature on the influence of age on $\text{NO}_3\text{-N}$ is limited and conflicting. Results from macrocosm study of $\text{NO}_3\text{-N}$ removal in a FWS CWs in California suggested that as young FWS CWs age, $\text{NO}_3\text{-N}$ removal rates will improve (Bachand, 1996). The reasoning is that as the wetland ages, the accumulation of biomass will increase organic carbon supply within the basin, and this additional fuel for denitrification will increase denitrification rates. However, this potential for improved performance over time is at odds with other studies, which have suggested that nutrient removal efficiency has the potential to decline as operational age increases (Kadlec et al., 2010; Kadlec & Wallace, 2009; Wang et al., 2006). As with the Bachand (1996) study, these studies also link performance changes to the accumulation of detritus. However, these studies focused on older FWS CWs (> 10 years old), where the accumulation of detritus has resulted in a thick substrate that creates preferential flow paths and dead zones, and

negatively influences wetland hydraulics (Martinez & Wise, 2003). While this process was identified as a main contributor to the decline of total phosphorus removal in the Orlando Easterly Wetland (Martinez & Wise, 2003; Wang et al., 2006; White et al., 2008), studies have not been conducted to see how the long-term accumulation of detritus (i.e., operational age) influences nitrogen removal. Due to the limited studies on the subject and the potential for contradictory influences, the actual influence of age on nitrogen removal, especially $\text{NO}_3\text{-N}$ removal, has not been adequately evaluated. As the hundreds of FWS CWs built to improve water quality through nitrogen removal continue to age, understanding the influence of age will become increasingly critical.

To investigate both the influence of pretreatment and age on nitrogen removal, a nitrate dosing study was initiated at the Walnut Cove WWTP in NC. The nitrate dosing was conducted to simulate the effect of improved pretreatment (i.e., increased lagoon aeration). Because one wetland cell had been previously rejuvenated through detritus removal while the other remained unimproved (see Chapter 4), the nitrate dosing provided an opportunity to not only assess the influence of improved pretreatment on nitrogen removal, but it also allowed for an assessment of the influence of an accumulated detritus substrate on $\text{NO}_3\text{-N}$ removal. Because the accumulation of detritus is the physical embodiment of increasing age in FWS CWs, the influence of the accumulated detritus substrate was inferred in this study to represent the main influence of operational age.

The study objectives were to: (1) quantify the nitrogen removal performance of both wetland cells when they receive substantial loads of $\text{NO}_3\text{-N}$ using removal efficiencies and areal mass removal rates; (2) demonstrate and evaluate the influence of pretreatment that would convert more $\text{NH}_4\text{-N}$ to $\text{NO}_3\text{-N}$ before it enters the wetland cells, through a comparison to

previously quantified nitrogen removal at the site; (3) evaluate the influence of age specifically on $\text{NO}_3\text{-N}$ removal through comparisons between the two wetland cells; and (4) estimate a general $\text{NO}_3\text{-N}$ removal rate constant for future use in wetland design.

MATERIALS AND METHODS

Site monitoring

A full description of the Walnut Cove WWTP and the two FWS CWs, with details about site instrumentation, analytical methodologies, and the detritus removal, can be found in Chapters 2 and 4, but pertinent details for this chapter have been included. The two FWS CWs were designed to each have a surface area of 7200 m^2 , treatment volume of 2130 m^3 , aspect ratio of 17:1, and a pool depth of 0.3m. Sampling stations were located at the inlet splitter box and both wetland outlets (Figure 5.1). Because the inlet weirs were positioned at equal heights, the flow and quality of the wetland influent was assumed to be the same for both cells.



Figure 5.1: Aerial photograph of the two wetland cells (Image modified from Google Maps). The arrows indicate flow direction. Sampling stations are shown with red circles and the weather station is shown with a blue star.

Nitrate Dosing

Prior to the dosing study, the wetland cells received non-nitrified wastewater at an average inlet $\text{NO}_3\text{-N}$ concentration of 0.3 mg-N L^{-1} (Chapter 4). To increase influent $\text{NO}_3\text{-N}$ concentrations, the wetland influent was dosed with calcium nitrate ($\text{Ca}(\text{NO}_3)_2$). Nitrate dosing was conducted in two stages. The first phase consisted of short week-long pilot tests using pulsed $\text{Ca}(\text{NO}_3)_2$ additions to evaluate the feasibility of the study, while the second phase built on the lessons learned from the pilot tests and consisted of a 31-day period of continuous $\text{Ca}(\text{NO}_3)_2$ loading.

In the first stage, two pilot tests were conducted using discrete daily $\text{Ca}(\text{NO}_3)_2$ additions over 5-day periods in the fall 2020 (9/21/2020 - 9/25/2020 and 10/26/2020 – 10/30/2020). A full description of the pilot test methods and analysis can be found in Appendix D, but in brief, a 30 minute pulse of $\text{Ca}(\text{NO}_3)_2$ was added to the influent wastewater each day by dissolving solid pellets of $\text{Ca}(\text{NO}_3)_2$ fertilizer. During the first pilot test, influent $\text{NO}_3\text{-N}$ concentrations were raised to an average of 2.9 mg-N L^{-1} (median of 0.3 mg-N L^{-1}) and the $\text{NO}_3\text{-N}$ removal efficiencies were 87 and 75% in cells 1 and 2, respectively. For the second pilot test, influent NO_3 concentrations were raised to an average of 2.0 mg-N L^{-1} (median of 1.6 mg-N L^{-1}) and the $\text{NO}_3\text{-N}$ removal efficiencies were 85 and 61% in cells 1 and 2, respectively. Based on these results, it was clear that $\text{Ca}(\text{NO}_3)_2$ dosing could be used to increase influent $\text{NO}_3\text{-N}$ loads at the site. However, it was also clear that discrete additions produced high temporal variability in influent $\text{NO}_3\text{-N}$ concentrations and loads and ultimately relatively low mean and median influent $\text{NO}_3\text{-N}$ concentrations.

The second $\text{NO}_3\text{-N}$ dosing used an improved methodology that resulted in a more continuous $\text{NO}_3\text{-N}$ dosing, closer to what would enter the wetland cells if upstream pretreatment

were improved. While the data obtained from the initial dosing experiment was important to evaluate the feasibility of this experiment and refine dosing methodology, data from this second continuous NO₃-N dosing was used for analysis to achieve project objectives. Continuous nitrate dosing was conducted for 31 consecutive days (~1 month) in the spring 2021 (March 21, 2021, to April 20, 2021). Continuous dosing was facilitated using three 1100-L tanks connected in series. The three tanks were connected using a 1” PVC pipe and vertically positioned to ensure gravity would drain the two higher tanks to the lower tank (Figure 5.2). Using this setup, the three tanks acted as a single 3300-L (900-gal) storage tank. The tanks were filled by adding water to tank 3 (see Figure 5.2), which was then gravity fed to the other two tanks. While water was being added, Ca(NO₃)₂ fertilizer was added to tank 3, where it was then mixed until all visible pellets were dissolved. Nitrate-enriched water was pumped out of tank 1 and up to a 19-L (5-gal) distribution container using a Rio® Plus 180 Aqua Pump with a 170 L hr⁻¹ (45 gal hr⁻¹) flow rate (Figure 5.2 & 5.3). The water then discharged from the bottom of the distribution container to the duckweed collector effluent/wetland influent pipe (approximately 25’) through a 0.25” PEX pipe. Meanwhile, the 1” PVC pipe acted as an overflow pipe returning excess water back to tank 1, which provided a constant pressure head of approximately 12 cm within the distribution container for flow through the PEX pipe. This constant pressure head allowed a constant flow rate to be established by adjusting a ball valve placed at the end of the PEX pipe. During the study, the ball valve was adjusted to release 0.5 - 0.7 L min⁻¹ (190 - 270 gal day⁻¹) of nitrate-enriched water into the wastewater just upstream of the influent splitter box.

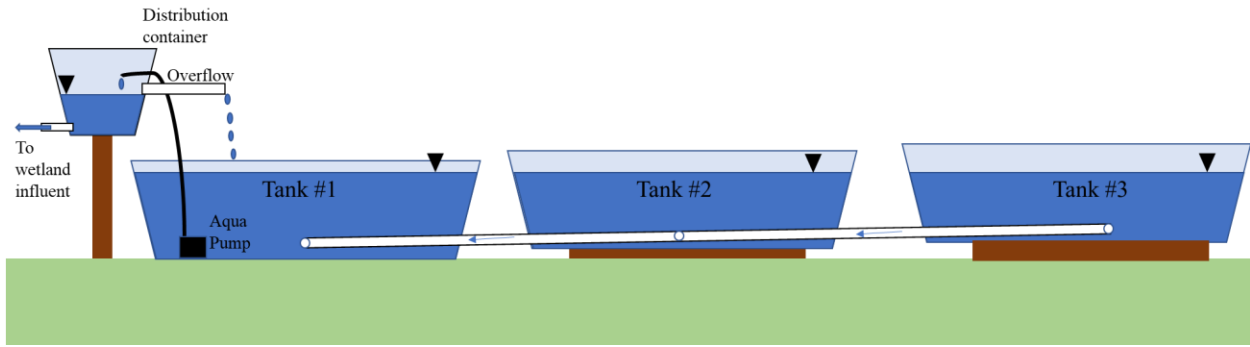


Figure 5.2: A schematic of the continuous dosing setup. Arrows represent the flow direction.



Figure 5.3: Top Left: Filling tank #3 with $\text{Ca}(\text{NO}_3)_2$ fertilizer and source water being added. Top Right: All three tanks connected and tarped with the distribution container visible in the foreground. Bottom Left: The dosing setup with the 0.25" PEX pipe running from the container to wetland influent pipe. Bottom Right: The 0.25" PEX pipe and ball valve used to release the $\text{NO}_3\text{-N}$ enriched water into the wetland influent.

Continuous nitrate dosing was completed using 22.7 kg (50 lb) bags of YaraLiva CALCINIT Greenhouse/Solution Grade 15.5-0-0 dry quick-release $\text{Ca}(\text{NO}_3)_2$ fertilizer (Oslo, Norway). The pelletized fertilizer was added to upper two storage tanks, which were then filled with water from an on-site well and mixed until all visible fertilizer pellets were dissolved. After the fertilizer was added, the tanks were covered by a tarp to minimize the influence of biological growth, evaporation, and precipitation. At the target flow rate, the connected tanks were refilled and were loaded with additional $\text{Ca}(\text{NO}_3)_2$ fertilizer every three days. Over the 31 day monitoring period, 38 bags of $\text{Ca}(\text{NO}_3)_2$ fertilizer were added for a total of 121 kg-N (60.5 kg-N into each wetland).

Data Collection

Water Quality Sampling

Water quality samples were collected at each sampling location (inlet, outlet 1, and outlet 2) using uniform time-based sampling. Daily composite samples were composed of two subsamples collected at 12-h intervals. Sample bottles were pre-acidified using 25% sulfuric acid to preserve the sample at $\text{pH} < 2$ (Burke et al., 2002). All water quality samples were brought back to NC State University and filtered using 0.45 μm filters. Samples were submitted to the North Carolina State University Biological and Agricultural Engineering Environmental Analysis Laboratory (BAE EAL) in Raleigh, NC and analyzed for nitrite-N + nitrate-N ($\text{NO}_3\text{-N}$), Total Kjeldahl Nitrogen (TKN), and ammonium-N ($\text{NH}_4\text{-N}$). Dissolved organic nitrogen (DON) concentrations were calculated by subtracting $\text{NH}_4\text{-N}$ concentrations from TKN concentrations. Total dissolved nitrogen (TDN) concentrations were calculated by adding the $\text{NO}_3\text{-N}$ concentrations to the TKN concentrations.

Water Quality Parameters

Water quality parameters (pH, dissolved oxygen (DO), specific conductivity, and temperature) were measured during each site visit at each sampling location using a YSI Pro field probe (Xylem US, Yellow Springs, OH). Water quality parameter measurements were taken during the daytime between 8:00 and 14:00. Measurements were reported using an average over the period at each location. The water temperature used for modeling purposes in each cell was determined by averaging the inlet and outlet temperatures together.

In addition to discrete measurements, two U26 HOBO Dissolved Oxygen (DO) data loggers (Onset Computer Corporation, Bourne, MA) were installed on March 5th, 2021, to measure water column DO every 30 minutes. One DO data logger was placed in the water column at each wetland outlet. DO data loggers were installed and operated without excessive fouling for the first 11 days of the monitoring period, after which fouling was observed on the sensor tip at each site visit. Therefore, to produce a typical daily DO profile for both locations, average hourly DO concentrations were calculated only for the period from 3/21/2021 to 4/2/2021.

Hydrology and Hydraulics

Stage above weir measurements were made at each sampling location every 15 minutes using the ISCO 6172 automatic samplers integrated with ISCO 730 bubbler modules. Inlet and outlet flows were estimated from stage measurements using the Francis (1883) equation as specified for standard fully contracted weirs in the Bureau of Reclamation's Water Measurement Manual (2001) (Equation 5.1).

$$Q = 3.33(L - 0.2H)(H^{3/2})$$

(Eq 5.1)

where Q = volumetric flow ($\text{ft}^3 \text{ s}^{-1}$), L = length of the weir (ft), and H = head over the weir (ft). Precipitation (P) data were obtained from the on-site weather station. Daily evapotranspiration (ET) losses were estimated using the ASCE standardized Reference ET Equation (Allen et al., 2005) (See Chapter 2 and Appendix B). Because of frequent debris on the outlet weirs, the accuracy of Q_{out} estimates were assessed and, if need be, corrected, using the criteria described in Chapter 2. The cumulative daily Q_{in} , Q_{out} , P, and ET values were used to develop a water balance for each cell during the 31-day period (Equation 5.2).

$$\text{Residual} = V_{\text{in}} + (P * A_d) - V_{\text{out}} - ET * A_s \quad (\text{Eq. 5.2})$$

where, V_{in} and V_{out} were the cumulative influent and effluent daily flow for each cell (m^3), respectively, P was cumulative precipitation (m), A_d was the cell nominal surface area plus the drainage area that contributes surface runoff to each cell (9800 m^2), ET was cumulative evapotranspiration (m), A_s was the nominal cell surface area (7200 m^2), and Residual was the unaccounted-for water volume that would produce water balance closure (m^3). Both wetland cell bottoms were underlain by a clay layer associated with wetland construction, so infiltration was assumed to be negligible. Average daily inflows and outflows were reported, along with the cumulative depth of P and ET, and the residual as a percentage of the inflow.

To estimate actual wetland hydraulics during the study, a paired tracer test initiated on April 23, 2021, using Rhodamine WT dye. The residence time distributions (RTDs) derived from the paired test were used to estimate the number of tanks in series (N) and mean residence time (τ) for in both cells (Appendix A). The number of tanks (N) represented the theoretical number of continuously stirred reactors (CSTRs) or tanks that can be used to characterize non-ideal flow through a FWS CW. The mean residence time was used to calculate the volumetric efficiency (e)

for each cell. Using e , the average daily inflow (Q_{in}), and the nominal treatment volume (V), the mean residence time (τ) for the monitoring period was estimated for each cell. Using e , the effective volume (V_e) of each cell can be estimated (Equation 5.3).

$$V_e = V * e \tag{Eq 5.3}$$

where V is the nominal cell volume (2130 m³) and e is the volumetric efficiency. Using V_e , the effective cell area (A_e) of each cell can be estimated (Equation 5.4).

$$A_e = \frac{V_e}{\bar{h}} \tag{Eq 5.4}$$

where V_e is the effective cell volume and h is the mean water column depth in the areas where water was present (m). The accuracy of the A_e estimate was difficult to ascertain because the depth of the detritus substrate was non-uniform, and mean water column depths had to be approximated using limited observations within the wetland cells. In cell 1, the mean water column depth was estimated to be 0.18 m (8”). In cell 2, the mean water column depth was estimated to be 0.12 m (5”). These approximated values were likely to be within ± 0.025 m (1”) of the actual value. A difference of ± 0.025 m (1”) in water column depth estimates produced an approximate 500 m² difference in the estimated A_e for both cells; therefore, the presented A_e values should be understood to be within ± 500 m² of the actual values.

Wetland studies have been commonly conducted using the designed pool area (i.e., nominal surface area) in their estimates of hydraulics and removal (Crumpton et al., 2020; Drake et al., 2018; Gerke et al., 2001; Kadlec et al., 2012; Kovacic et al., 2000; Sartoris et al., 1999). Therefore, nominal surface areas were also used in this study to calculate the nominal HLR, areal removal rates, and rate constants. However, the non-uniform detritus substrate in both cells

resulted in A_e providing a better estimate of the actual surface area being used for treatment. To estimate performance based on the actual areas used, effective HLR, areal removal rates, and rate constants were also calculated using A_e .

Nitrogen removal performance

Flow weighted average concentrations were calculated for DON, $\text{NH}_4\text{-N}$, $\text{NO}_3\text{-N}$, and TDN at the inlet and outlet of both cells. Percent concentration changes were calculated for each nitrogen species and each cell. A positive value indicated a concentration reduction through the cell, while a negative value indicated a concentration increase.

The daily influent and effluent loads were estimated for DON, $\text{NH}_4\text{-N}$, $\text{NO}_3\text{-N}$, and TDN by multiplying average daily flow rate by the daily pollutant concentration. The cumulative influent and effluent loads during the dosing period were then calculated by summing the daily loads. As an additional check on monitoring accuracy, the cumulative influent nitrate load was compared to the known amount of nitrate added during the dosing process.

Treatment efficiency was evaluated using load reduction, removal efficiency, and areal mass removal rates (or areal mass removal rate) for each nitrogen species in each wetland cell. Load reductions were calculated by subtracting the cumulative outlet loads from cumulative inlet loads. Wetland removal efficiency was calculated by dividing the cumulative load reduction by the cumulative inlet load. Daily load reductions (kg-N d^{-1}) were estimated and converted to areal mass removal rate estimates ($\text{g-N m}^{-2} \text{ day}^{-1}$) by dividing by the area of each cell. Both the nominal and effective areas were used to calculate the nominal (J_{nom}) and effective (J_{eff}) removal rates, respectively (see Chapter 2). All load analyses were conducted using R software (R Core Team, 2017).

NO₃-N removal in CWs were represented by combining first order removal kinetics and a tanks-in-series (TIS) representation of wetland hydraulics (Equation 5.5) (Kadlec & Wallace, 2009).

$$\frac{C_{out}}{C_{in}} = \left(1 + \frac{kA}{NQ_{in}}\right)^{-N}$$

(Eq 5.5)

where A is the wetland surface area (m²), Q_{in} is the average influent flow rate (m³ d⁻¹), C_{in} and C_{out} are the average inlet and outlet pollutant concentration (g-N m³), and N is the number of tanks in series to represent the internal hydraulics. To better represent the actual internal hydraulics of a wetland, the effective wetland area (A_e) can be used (Equation 5.6).

$$\frac{C_{out}}{C_{in}} = \left(1 + \frac{k'A_e}{NQ_{in}}\right)^{-N}$$

(Eq 5.6)

To account for the temperature effects, a modified Arrhenius equation was used to adjust rate constants in equations 5.5 and 5.6 (Equation 5.7)

$$k = k_{20}^{\theta(T-20)}$$

(Eq 5.7)

where k₂₀ is the removal rate coefficient at 20°C, θ is a temperature coefficient, and T is the average water temperature in each wetland cell, calculated by averaging the inlet and outlet temperature measurements. Theta (θ) was assumed to be 1.106, the mean value derived from data on 43 FWS CWs by Kadlec (2012).

RESULTS

Site Conditions

Water quality parameters

Mean water temperatures for the dosing period ranged from 14 to 22 °C (Table 5.1) and were always above the minimum temperature for biological nitrogen processing (5 °C) (Vymazal, 2007). Water temperature increased through cell 2 and decreased through cell 1 (Table 5.1 & Figure 5.4). The increase in temperature through cell 2 and decrease through cell 1 was likely the result of the different vegetation patterns between the two cells (Figure 5.5). Cell 1 had over 50% vegetation cover (mainly duckweed) by April 1st, while in cell 2 the first half was dominated by open shallow water and overall had less than 25% cover for the entire period. The shading in cell 1 likely decreased temperature, DO, and pH through the cell by restricting sunlight and algal activity.

Table 5.1: Mean values for daytime temperature, dissolved oxygen, and pH for the dosing run, which ran from March 21st, 2021 to April 20th, 2021.

Location	Temperature (°C)	DO (mg L ⁻¹)	pH
Inlet	17.4	10.1	8.6
Outlet 1	14.5	3.4	7.2
Outlet 2	21.5	4.6	7.7

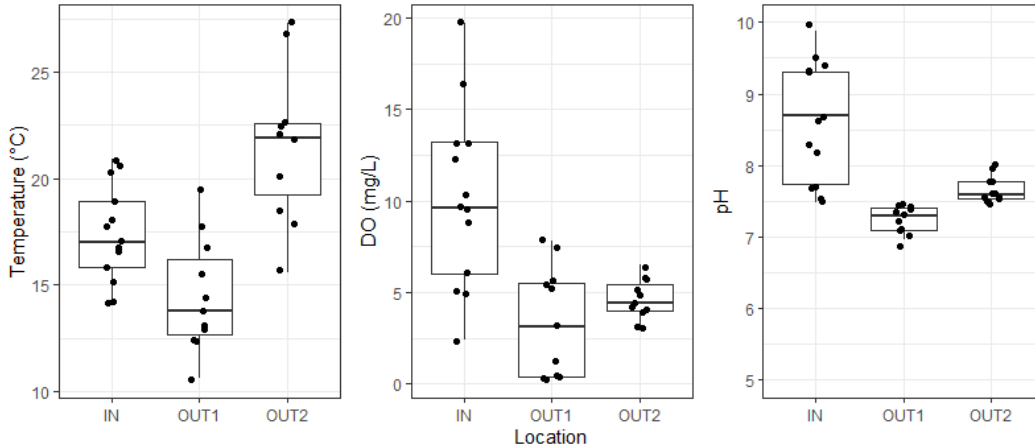


Figure 5.4: Water quality parameter (pH, dissolved oxygen (DO), and temperature) measurements during the dosing period. Measurements were taken at each site visit during daylight hours (between 8:00 and 14:00). IN, OUT1, and OUT2 refer to measurements taken at the inlet splitter box, the cell 1 outlet, and the cell 2 outlet, respectively. Boxplots represent the median and interquartile ranges.



Figure 5.5: Aerial view of wetland cells 1 (left) and 2 (right) taken on April 23rd, 2021, approximately 6 hours after the initiation of the tracer test. Cell 1 was nearly 100% with vegetation (mostly duckweed) made it difficult to visually trace the progression of the tracer from the air. Cell 2 was nearly all open water. Channels through the detritus substrate can be seen in the right half of cell 2.

Mean daytime DO concentrations were above saturation (10.1 mg L^{-1}) at the inlet and decreased to mean outlet concentrations in the $3\text{-}5 \text{ mg L}^{-1}$ range. The elevated values of DO at the inlet were attributed to a seasonal algal bloom in the open water of the upstream duckweed raceway that started in late March 2021 (Figure 5.6). The initial influence of algae within the wetlands were also observed in the 30-min DO measurements at the wetland outlets. Measurements from March 21 to April 3, before either wetland had over 50% vegetation cover, showed that the DO concentrations were highly variable but followed a diurnal pattern. This diurnal pattern suggested that paired photosynthesis and respiration from the algae increased DO during the daylight hours and then consumed DO during the nighttime hours (Figure 5.7 & 5.8). These values suggested that, although DO appeared to be available for nitrification during the daytime hours (Table 5.1), it was near zero most of the time (Figure 5.8). Like DO, pH was evaluated at the inlet with a mean value of 8.6. pH decreased to 7.2 and 7.7 in cells 1 and 2, respectively. pH values within the wetland were within optimal ranges for nitrification and denitrification (Vymazal, 2007). Relative to the open water lagoons upstream of the wetland, the influence of algae within the wetlands was limited by shading. Although algae in the water column certainly had the potential to influence wetland nitrogen processing (especially at the beginning of study), the shading in cell 1 and the short residence times in cell 2 likely limited this influence (Figure 5.5, Figure 5.9 & Table 5.2).



Figure 5.6: Photographs of the duckweed clarifier, just upstream of the inlet splitter box on April 8, 2021. The cloudy green water was indicative of an algal bloom. The photos also show that there was no shading of the nutrient-rich water upstream of the wetland cells during this period.

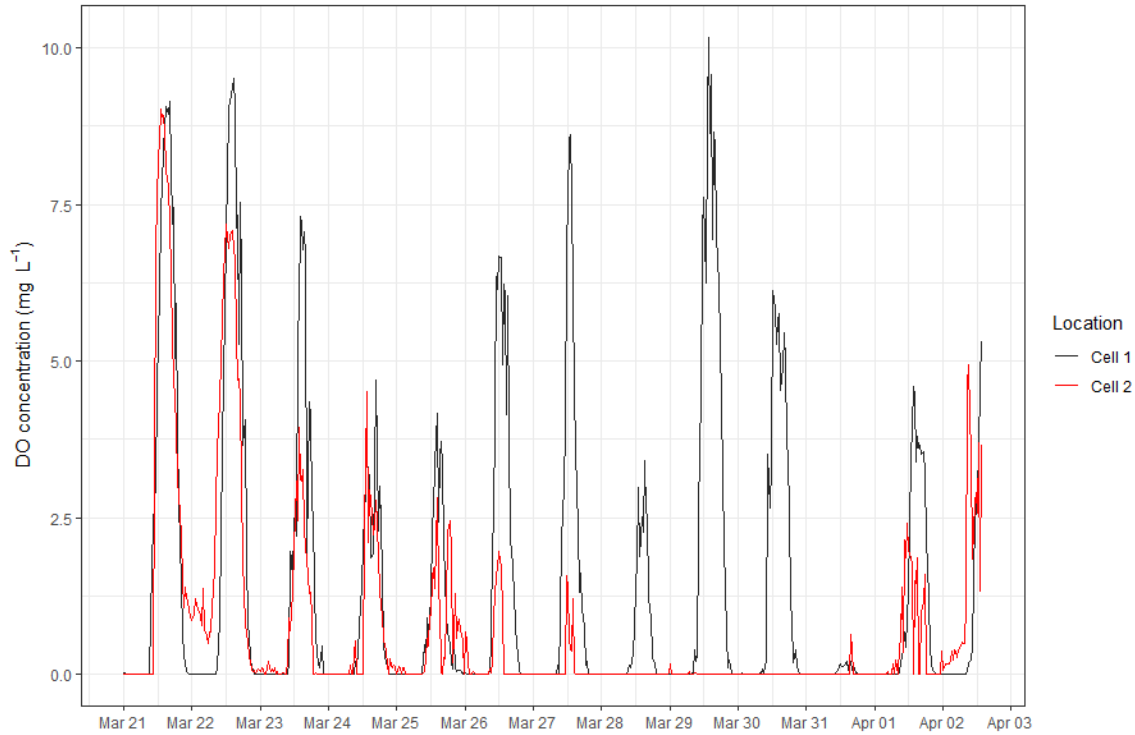


Figure 5.7: Dissolved oxygen (DO) concentrations at the outlet of each FWS CW cell. Concentrations were recorded every 30 minutes by U26 HOBO DO data loggers (Onset Computer Corporation, Bourne, MA).

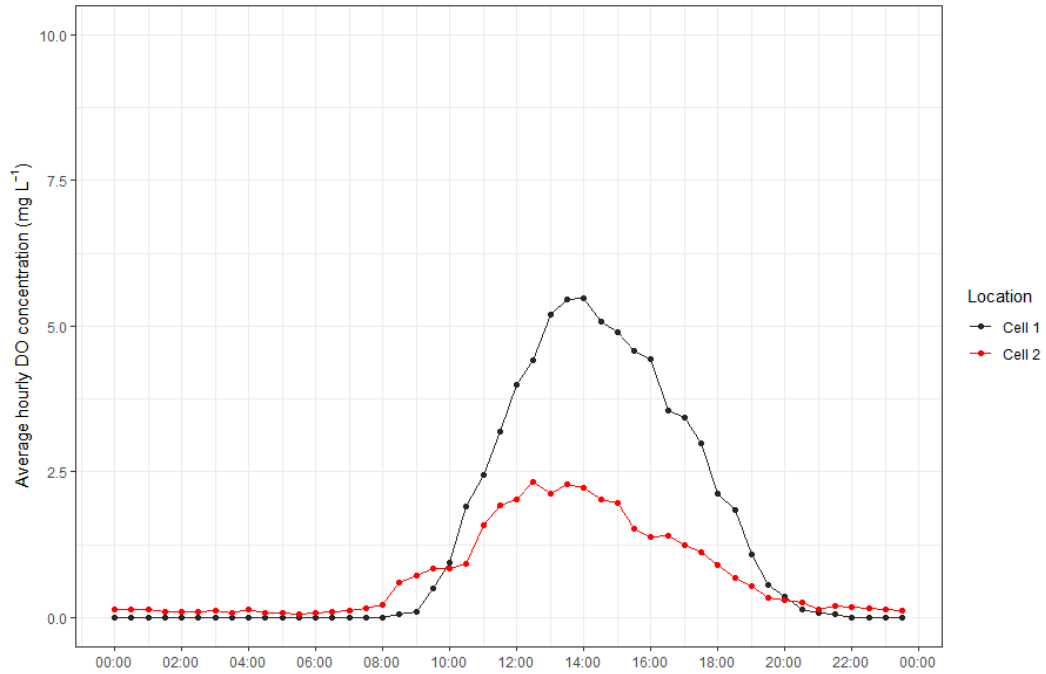


Figure 5.8: Mean hourly DO concentrations (in Eastern Standard Time) at each cell outlet for the period between 3/21/21 and 4/3/21. The diurnal pattern suggested by the data in Figure 5.7 is clearly visible.

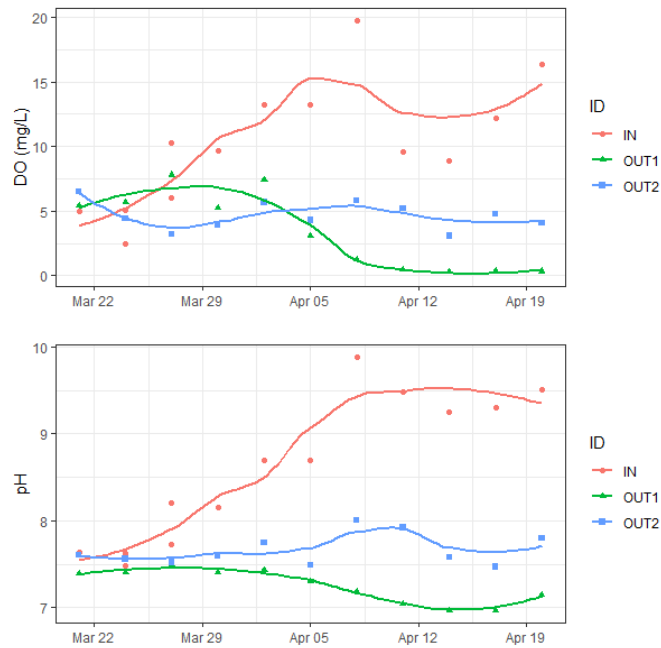


Figure 5.9: DO concentrations and pH during the dosing period at each sampling location. The substantial reduction of DO and pH after April 5th at the cell 1 outlet (OUT1) highlighted the influence of shading on algal activity. Shading did not occur to the same extent in cell 2.

Hydrology and Hydraulics

The mean daily inflow to each cell was $411 \text{ m}^3 \text{ d}^{-1}$ (0.11 MGD). The cumulative inflow volume to each cell was $13,168 \text{ m}^3$. The mean daily outflows were 417 and $441 \text{ m}^3 \text{ d}^{-1}$ for outlets 1 and 2, respectively. Cumulative precipitation was 66 mm, with a cumulative volume of 647 m^3 per cell. Cumulative ET was 190 mm, with a cumulative volume of 1368 m^3 per cell. The much greater influent volume relative to P and ET highlighted the fact that both cells were surface flow driven. Water balance calculations during the period resulted in residuals of -7% and -12% of the influent flow in wetland cell 1 and cell 2, respectively. The negative residuals indicated that there was an overestimation of water outputs, an underestimation of water inputs, or both. There were several potential values that could have produced this slight water balance error, including the flow estimates, the estimated runoff area used to calculate P volumes, the ET estimates, or all three. Overall, the estimation errors were slight, but suggested that load removals calculated with these flows may be conservative.

During the paired tracer test, conducted when the average inflow was $330 \text{ m}^3 \text{ d}^{-1}$, the mean residence times (τ) in cells 1 and 2 were 2.8 and 1.1 d, respectively (Table 5.2). Based on τ , the e values were 0.37 and 0.17 in cells 1 and 2, respectively. Based on these results, at the $411 \text{ m}^3 \text{ d}^{-1}$ mean daily inflow, the mean residence times over the study period were estimated to be 1.9 and 0.9 d, in cells 1 and 2, respectively. Based on these e values and the estimated mean water depths, the effective surface areas were 4380 m^2 and 3020 m^2 in cells 1 and 2, respectively. These effective areas were 61% and 42% of the nominal wetland area (7200 m^2). The number of tanks (N) representing wetland cells 1 and 2 were 8.1 and 2.2, respectively.

Overall, cell 1 was expected to have better internal hydraulics because of the detritus removal in 2019 (Chapter 4). This expected performance difference was confirmed by the tracer

test data which showed that the hydraulic conditions were consistently better in cell 1. The number of tanks (N), the volumetric efficiency (e), the mean residence times (τ) were all greater in cell 1. When compared to the median N value of 4.4 for FWS CWs reported in a meta-analysis conducted by Kadlec (2012), the N value in cell 1 was above average and the N value in cell 2 was below average.

Table 5.2: Hydraulic conditions within the two FWS CW cells at the Walnut Cove WWTP during the nitrate dosing period. The number of tanks (N) and the volumetric efficiency (e) were used as part of equations 5.5 and 5.6 to estimate a nitrate removal rate constant for each wetland cell.

Dosing Run	Wetland	Water column depth, h (m)	Number of tanks, N	Volumetric efficiency, e	Effective surface area, A_e (m ²)	Mean residence time, τ (d)
3/21/21 to 4/20/21	Cell 1	0.18	8.1	0.37	4380	1.9
	Cell 2	0.12	2.2	0.17	3020	0.9

Notably, the e value for cell 1, while greater than cell 2, was still only 0.37, well below the expected 0.70 for a FWS CW treating nitrate reported in Kadlec (2012). While that 0.7 value was likely inflated by the relatively young wetlands reported in the study, the e value of 0.37 was suboptimal and indicated that slightly over one third of cell 1's nominal wetland volume was used for treatment (Persson et al., 1999). The lower than optimal e value was likely the result of the decision to leave both a thin layer of detritus as a carbon source and to replant mounds of *Typha spp.* during the cleanout of wetland cell 1. Because of this decision, cell 1 was not reset to age 0, but likely represented a wetland with an operational age between 5 and 10 years.

Nitrogen removal performance

Concentration changes

Water quality samples were collected for all 31 days at the inlet, outlet 1, and outlet 2 sampling stations. Mean inlet $\text{NO}_3\text{-N}$ were increased from less than 0.5 mg-N L^{-1} (see Chapter 4) to 4.4 mg L^{-1} during continuous dosing of $\text{Ca}(\text{NO}_3)_2$ (Table 5.3). At the start of April, more

Ca(NO₃)₂ fertilizer was added during the refilling process to increase inlet NO₃-N concentrations (Figure 5.10). Along with the greater Ca(NO₃)₂ additions, inflows declined in April resulting in a further increase in NO₃-N concentrations. Mean outlet NO₃-N concentrations were 0.8 and 0.9 mg L⁻¹ at outlet 1 and outlet 2, respectively. NO₃-N was reduced by 3.6 and 3.4 mg L⁻¹ (82 and 77%) on average in cells 1 and 2, respectively (Table 5.4). When viewed collectively, mean TDN concentrations were 15.8, 9.4, and 12.0 mg L⁻¹ at the inlet, outlet 1, and outlet 2, respectively. Both cells had a TDN concentration reduction, with the cell 1 TDN reduction (6.4 mg L⁻¹, 40%) nearly double the reduction in cell 2 (3.8 mg L⁻¹, 24%). The difference in TDN concentration reductions between the two cells was the result of slightly greater DON and NO₃-N reductions in cell 1 paired with NH₄-N concentration increases through cell 2.

Table 5.3: Flow-weighted average concentrations of nitrogen species at each sampling location during the period from 3/21/2021 to 4/21/2021. The inlet sampling station represents influent to both cells.

Sampling Station	Average concentrations (mg-N L ⁻¹)			
	NO ₃ -N	NH ₄ -N	DON	TDN
Inlet	4.4	7.4	4.0	15.8
Outlet 1	0.8	6.3	2.3	9.4
Outlet 2	0.9	8.2	2.8	12.0

Table 5.4: Concentration change through the wetland based on flow weighted mean concentrations during the study period. A positive change indicated a decrease through the wetland and a negative change indicated an increase through the wetland.

Wetland	Concentration changes through cell, in mg-N L ⁻¹ (%)			
	NO ₃ -N	NH ₄ -N	DON	TN
Cell 1	3.7 (83%)	1.1 (15%)	1.6 (41%)	6.4 (40%)
Cell 2	3.5 (79%)	-0.9 (-12%)	1.2 (30%)	3.8 (24%)

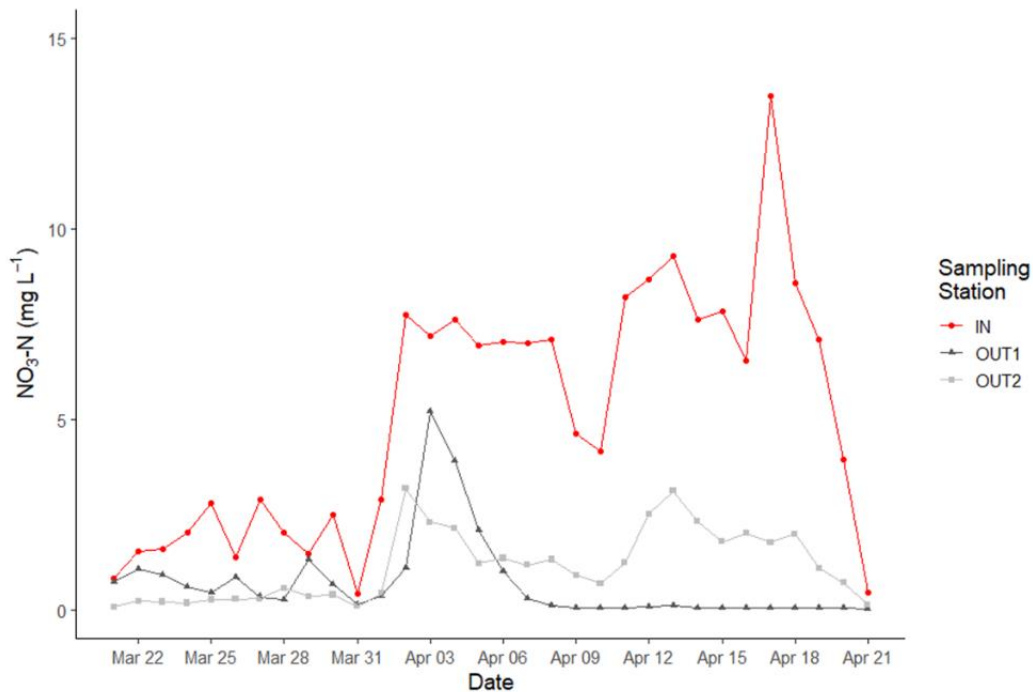


Figure 5.10: NO₃-N concentrations for each daily sample during the monitoring period. Sampling stations are labelled as IN (inlet), OUT1 (outlet 1), and OUT2 (outlet 2).

Mass dynamics

The sampling scheme adequately captured the added NO₃-N load, with the observed cumulative inlet NO₃-N load (58 kg each or 116 kg in total) accounting for over 95% of the known added NO₃-N load (60.5 kg each or 121 kg total) (Table 5.5 & Figure 5.11). Of the 58 kg of NO₃-N added to each cell, 10 and 13 kg of NO₃-N were released from cells 1 and 2, respectively. NO₃-N removal efficiency was 82% and 77% in cells 1 and 2, respectively. The TDN removal efficiencies followed the same trends observed in the concentration analysis but were slightly lower due to the greater outflows relative to inflows during the study period.

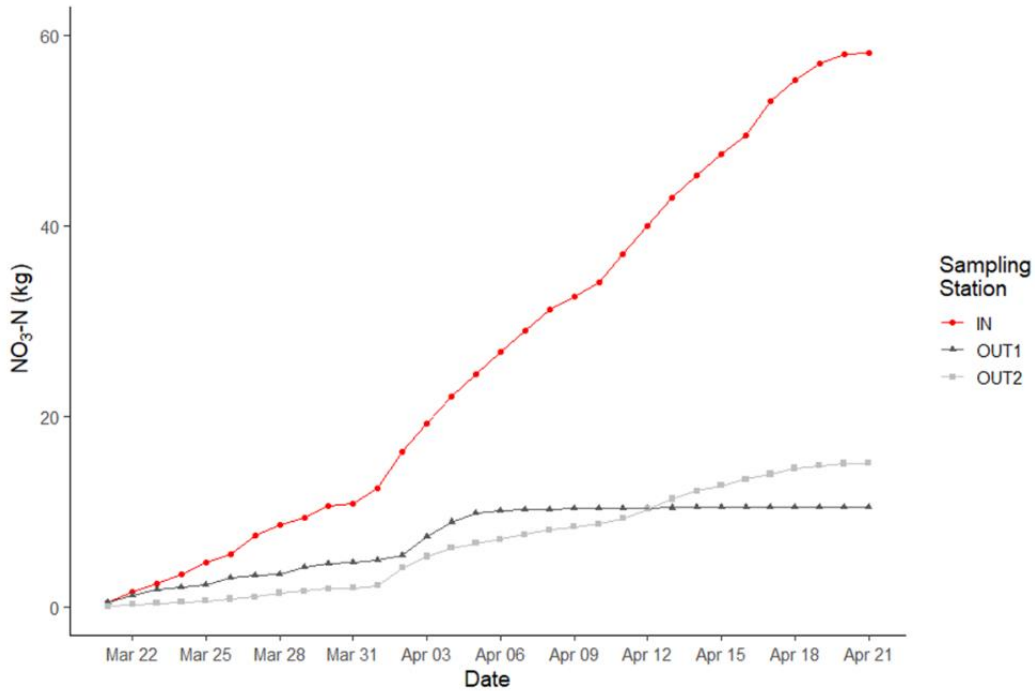


Figure 5.11: Cumulative daily NO₃-N loads (in, kg) during the monitoring period. Sampling stations are labelled as IN (inlet), OUT1 (outlet 1), and OUT2 (outlet 2).

Table 5.5: Influent and effluent loads for each nitrogen species during the dosing run 3/21/2021 to 4/21/2021 (n = 31 days). Loads were presented in kg, with kg d⁻¹ reported in parentheses. The load reduction and removal efficiency were bolded.

Wetland	Sampling Station	Load, in kg (kg d ⁻¹ , or % for removal efficiency)			
		NO ₃ -N	NH ₄ -N	DON	TDN
Cell 1	Inlet	58 (1.9)	97 (3.1)	52 (1.7)	207 (6.7)
	Outlet	10 (0.3)	84 (2.7)	31 (1.0)	125 (4.0)
	Removal	48 (82%)	13 (14%)	21 (40%)	82 (40%)
Cell 2	Inlet	58 (1.9)	97 (3.1)	52 (1.7)	207 (6.7)
	Outlet	13 (0.4)	116 (3.7)	39 (1.4)	169 (5.4)
	Removal	45 (77%)	-19 (-20%)	13 (25%)	38 (19%)

The nominal areal removal rates for NO₃-N ($J_{\text{nom, NO}_3}$) were 0.22 and 0.20 g m⁻² d⁻¹ in cells 1 and 2, respectively (Table 5.6). The effective areal removal rates ($J_{\text{eff, NO}_3}$) for NO₃-N were greater than J_{nom} values at 0.35 and 0.48 g m⁻² d⁻¹ in cells 1 and 2, respectively. Notably, when considered on an effective area basis, cell 2 provided more NO₃-N removal per m² than cell 1. When all nitrogen species were considered, the same trends from the concentration and load analysis were observed. These trends produced $J_{\text{nom, TDN}}$ rates of 0.37 and 0.17 g m⁻² d⁻¹ in cells 1 and 2, respectively, and $J_{\text{eff, TDN}}$ rates of 0.60 and 0.41 g m⁻² d⁻¹ in cells 1 and 2, respectively.

Table 5.6: Areal mass removal rates of nitrogen species within each wetland during the period from 3/21/2021 to 4/21/2021 (n = 31 days). A positive removal rate indicated a retention, and a negative removal rate indicated an internal release. J_{nom} was the nominal areal mass removal rates and J_{eff} was the effective areal mass removal rate.

Wetland	Surface Area (m ²)		Pollutant areal removal rate (g-N m ⁻² d ⁻¹)			
			NO ₃ -N	NH ₄ -N	DON	TDN
Cell 1	7200	J_{nom}	0.22	0.06	0.09	0.37
	4380	J_{eff}	0.35	0.10	0.15	0.60
Cell 2	7200	J_{nom}	0.20	-0.09	0.06	0.17
	3020	J_{eff}	0.48	-0.20	0.14	0.41

TIS model parameter values for NO₃-N removal

The k and k' values were calculated using the mean NO₃-N concentrations from Table 5.3, Q_{in} of 411 m³ d⁻¹, the N and e values from Table 5.2, and the temperature values from Table 5.1. The k_{20} values were 60 and 48 m yr⁻¹ for cells 1 and 2, respectively. k_{20}' values, which used A_e along with N values, were 99 and 115 m yr⁻¹ for cells 1 and 2, respectively. Like the areal NO₃-N removal rates, when the nominal area was used cell 1 had a greater removal rate constant (k_{20}), but when the effective area was considered, then cell 2 had a greater removal rate constant (k_{20}').

DISCUSSION

Improved pretreatment to improve nitrogen removal

During the one-month study, TDN removal efficiencies were 40% and 19% in cells 1 and 2, respectively. In chapter 2, which spanned from November 2019 through March 2019, the TN removal efficiencies were 11% and 8% in cells 1 and 2, respectively. TN and not TDN was used for this period because TKN samples were not filtered prior to analysis. In chapter 4, which spanned from June 2019 through May 2021 (post cell 1 rejuvenation), TDN removal efficiencies were 12% and 2% in cells 1 and 2, respectively. Relative to either previous period, both cells had increased nitrogen removal efficiencies during the dosing experiment, which suggested that increasing the ratio of $\text{NO}_3\text{-N}$ to $\text{NH}_4\text{-N}$ in the influent will likely improve nitrogen removal in FWS CWs. These results indicated that improved pretreatment will likely improve the nitrogen removal performance in FWS CWs receiving non-nitrified wastewater.

To quantify the potential increase in nitrogen removal provided by improved pretreatment at the Walnut Cove WWTP, three scenarios of variable influent nitrogen speciation were evaluated. The scenarios were conducted using data and parameters from cell 1 (i.e., best case scenario). Potential $\text{NO}_3\text{-N}$ removal was predicted using the TIS model with an N value of 8.1 (Table 5.2), a Q_{in} of $411 \text{ m}^3 \text{ d}^{-1}$, a k_{20} value of 60 m d^{-1} , and a water temperature of 20°C . Potential $\text{NH}_4\text{-N}$ removal was predicted by assuming a 10% removal efficiency (Table 5.5). Potential ON removal was predicted by assuming a 30% removal efficiency (Table 5.5). The three scenarios represented the influent nitrogen speciation if (1) no improvement in pretreatment occurred; (2) improved pretreatment converted 25% of the influent $\text{NH}_4\text{-N}$; (3) improved pretreatment converted 75% of the influent $\text{NH}_4\text{-N}$ (Table 5.7). The predictions indicated that a no change scenario would result in an 18% nitrogen removal efficiency, which was

approximately equal to the previously observed TN removal in the improved cell 1 (Chapters 4). However, if pretreatment could convert 25% of the influent $\text{NH}_4\text{-N}$ to $\text{NO}_3\text{-N}$ before entering the wetlands, then the TN removal efficiency increases to 30%. And, if that pretreatment could be enhanced to the extent that 75% of the influent $\text{NH}_4\text{-N}$ was converted to $\text{NO}_3\text{-N}$, then the TN removal efficiency increases to an even greater 55%. These scenarios suggested that nitrogen removal could be substantially increased through improved pretreatment in a cleaned-out wetland cell within the Walnut Cove WWTP, which would greatly reduce the amount of nitrogen entering Town Fork Creek.

Table 5.7: Three scenarios to examine effect of improved pretreatment on nitrogen removal in the Walnut Cove wetlands. The influent nitrogen speciation was based on the general values observed in this chapter, along with chapters 2 and 4. The no change scenario included no improvement in upstream pretreatment. Scenarios 2 & 3 included improved upstream pretreatment, at 25% or 75% of the influent $\text{NH}_4\text{-N}$ was nitrified before entering the two wetland cells.

Nitrogen Species	Influent (mg L^{-1})	Effluent (mg L^{-1})		
		Scenario 1: No change	Scenario 2: 25% influent $\text{NH}_4\text{-N}$ N converted	Scenario 3: 75% influent $\text{NH}_4\text{-N}$ N converted
$\text{NO}_3\text{-N}$	0.1	0.01	0.2	0.4
$\text{NH}_4\text{-N}$	6.0	5.4	4.0	1.3
ON	3.9	2.7	2.7	2.7
TN	10.0	8.1 (18%)	7.0 (30%)	4.4 (55%)

Operational age as an influence on $\text{NO}_3\text{-N}$ removal

Wetland aging has been linked to the formation of a substantial detritus substrate and a decline in the internal hydraulics of a wetland (Kadlec & Wallace, 2009; Martinez & Wise, 2003; Wang et al., 2006). So, while both FWS CW cells in the Walnut Cove WWTP had the same operational age, the previous detritus removal in cell 1 resulted in that cell being representative of a relatively young, hydraulically acceptable FWS CW. Meanwhile, cell 2, which had never been improved, represented an aged, hydraulically compromised FWS CW.

Although differences in accumulated detritus and internal hydraulics between the two cells were large, differences in NO₃-N removal were small. NO₃-N removal efficiencies were 82% and 77% in cells 1 and 2, respectively. Similarly, nominal areal mass removal rates (J_{nom}) were 0.22 and 0.20 g-N m⁻² d⁻¹, respectively, and removal rate constants (k_{20}) of 60 and 48 m yr⁻¹, respectively.

For context, the areal mass removal rates and rate constants were compared to other studies. The 0.2 g m⁻² d⁻¹ removal rates in this study were within the 0.003 to 1.02 g-N m⁻² d⁻¹ range of denitrification rates in FWS CWs reported in Vymazal (2007). When compared to removal rates in another study conducted in North Carolina, the rates were on the upper end of the 0.1 to 0.2 g-N m⁻² d⁻¹ range of NO₃-N removal rates observed in FWS CW mesocosms prepared with an organic substrate and an overlying NO₃-N concentration of 4 mg-N L⁻¹ (Messer et al., 2017). When compared to other field scale studies, the rates were within the 0.04 to 0.48 g-N m⁻² d⁻¹ range of NO₃-N areal mass removal rates observed in six studies of FWS CWs receiving NO₃-N enriched wastewater (Crumpton et al., 2006; Drake et al., 2018; García-Lledó et al., 2011; Hunt et al., 1999; Kovacic et al., 2000; Mitsch et al., 2014). Furthermore, the removal rate constants (k_{20}) of 60 and 48 m yr⁻¹ were greater than the median k_{20} of 25 m yr⁻¹ for FWS CWs observed in Kadlec (2012). Taken together, the fact that both the rejuvenated and unimproved wetland cells provided adequate NO₃-N removal, coupled with the similarity in performance between the two cells, indicated that age may only be a minor influence on NO₃-N removal in FWS CWs.

However, this conclusion was complicated by the NO₃-N removal observed when using the effective cell surface areas. When evaluated on an effective surface area basis, cell 2 provided more NO₃-N removal, with both areal mass removal rates (J_{eff}) and removal rate

constants (k_{20}) greater in cell 2 than cell 1. This indicated that more $\text{NO}_3\text{-N}$ was removed per m^2 in the cell 2 and suggested that the aged, detritus-filled environment in cell 2 was more conducive to denitrification. The finding that the “older” wetland (cell 2) provided greater $\text{NO}_3\text{-N}$ removal per m^2 supported the hypothesis by some that increasing wetland age (especially for relatively young wetlands) will increase denitrification rates presumably due to increased organic carbon to fuel denitrification (Bachand, 1996). Denitrification rates may also be increased by improved transfer to the wetland substrate as water depth decreases due to the accumulation of detritus.

These findings imply that the influence of age on $\text{NO}_3\text{-N}$ removal may not have been minor, but only appeared minor because it is the net product of these two contradictory processes. As a wetland ages, the accumulation of detritus will gradually reduce wetland hydraulic function resulting in a decline in the effective cell surface area and removal efficiency. However, as the wetland ages, that accumulated detritus can also increase the areal denitrification (i.e., $\text{NO}_3\text{-N}$ removal) rate. Of these two contradictory processes, the one with the greater influence on $\text{NO}_3\text{-N}$ removal will likely depend on several site factors (including influent $\text{NO}_3\text{-N}$ loading rate, cell bathymetry, influent nitrogen speciation, vegetation coverage, vegetation species, etc.); thus, the influence of age on $\text{NO}_3\text{-N}$ removal will also likely be site specific. The influence of age may also vary temporally. For example, $\text{NO}_3\text{-N}$ removal efficiency may increase during the first 10 years of operation as increasing denitrification rates outweigh losses in effective surface area, then decrease through the next 10 as substantial declines in effective surface area outweigh increased denitrification rates. Further studies are needed to evaluate which site-specific factors are more important for each process and evaluate the temporal variability of the two influences.

The influence of age on total nitrogen removal

While age appeared to have only a minor influence on $\text{NO}_3\text{-N}$ removal, there was a clear disparity in TDN removal efficiencies between the two cells (40% and 19% in cells 1 and 2, respectively), which indicated that overall nitrogen removal was influenced by age. This disparity was driven by the differences in $\text{NH}_4\text{-N}$ removal efficiencies (14% and -20% in cells 1 and 2, respectively). The disparity in $\text{NH}_4\text{-N}$ removal and similarity in $\text{NO}_3\text{-N}$ removal between the two cells suggested that the influence of age or more specifically, the poor internal hydraulics associated with age, on nitrogen removal in FWS CWs will likely be a function of inlet nitrogen speciation.

For FWS CWS receiving $\text{NO}_3\text{-N}$ dominated influent, such as agricultural drainage (Crumpton et al., 2006; Ikenberry et al., 2014) or package plant effluent (US EPA, 2000; Chapter 6), the results indicated that increasing operational age may not substantially reduce nitrogen removal performance. This does not mean that maintenance can be neglected in these systems, but it does suggest that FWS CWs receiving $\text{NO}_3\text{-N}$ dominated influent may be operated with longer intervals between detritus removals. Additionally, these detritus removals should not remove all the detritus from the basin; instead, some detritus should be left in the cell to sustain higher denitrification rates during the post-rejuvenation start-up period.

Alternatively, for FWS CWs receiving $\text{NH}_4\text{-N}$ dominated influent, the results from this chapter, along with those in Chapters 2 and 4 indicated that increasing operational age has the potential to severely restrict nitrogen removal. Decreasing surface areas can limit re-aeration and subsequently lower DO concentrations within the water column. These lower DO concentrations can then limit the aerobic process of nitrification. Additionally, the reduced residence time, associated with declining volumetric efficiency over time, can reduce the time available for the

paired nitrification/denitrification process. Finally, the preferential flow paths created by the accumulated detritus have the potential to limit contact with nitrification hotspots (i.e., submerged stems and litter), which can lower the nitrification rate and subsequently the denitrification rate. In these systems, maintenance should be undertaken frequently to maintain design residence times and design surface areas. Furthermore, because of this potential for age to negatively influence $\text{NH}_4\text{-N}$ removal, increased pretreatment (i.e., upstream nitrification) can be a practical method to increase the longevity of the system.

CONCLUSION

Based on results from the 31-day dosing period, age of the wetland cell (defined in this study as correlated to the amount of accumulated detritus) did not have a substantial impact on $\text{NO}_3\text{-N}$ removal. Both the rejuvenated and revegetated FWS CW cell (cell 1) and an unmaintained, detritus-filled FWS CW cell (cell 2) had similar $\text{NO}_3\text{-N}$ removal efficiencies with removal rates that fell within the upper portion of the 0.05 and 0.48 $\text{g-N m}^{-2} \text{d}^{-1}$ range of $\text{NO}_3\text{-N}$ removal observed in other FWS CWs studies. Interestingly, when evaluated using effective cell surface areas, cell 2 removed more $\text{NO}_3\text{-N}$ than cell 1 on a per m^2 basis, which suggested that the shallow, detritus-filled environment of cell 2 may have been more conducive to $\text{NO}_3\text{-N}$ removal (i.e., denitrification). But the fact that cell 1 removed more $\text{NO}_3\text{-N}$ on a per kg basis indicated that this increase in removal was restricted by the poor internal hydraulics. Overall, by artificially adding $\text{NO}_3\text{-N}$, we were able to demonstrate that improved upstream nitrification can improve nitrogen removal in FWS CWs receiving $\text{NH}_4\text{-N}$ dominated influent. These findings, along with those from chapters 2 and 4, indicated that the processes of aging had a varying influence the removal of different nitrogen species. This suggested that the inlet nitrogen speciation may be a key factor in predicting the influence of age on nitrogen removal in FWS CWs.

REFERENCES

- Allen, R. G., Walter, I. A., Elliott, R. L., Howell, T. A., Itenfisu, D., Jensen, M. E., & Snyder, R. L. (2005). The ASCE Standardized Reference Evapotranspiration Equation. American Society of Civil Engineers.
- Bachand, P. A. M. (1996). Effects of managing vegetative species, hydraulic residence time, wetland age and water depth on removing nitrate from nitrified wastewater in constructed wetland macrocosms in the Prado Basin, Riverside County, California [Ph.D., University of California, Berkeley].
<https://www.proquest.com/docview/304270571/abstract/71A9A8B5383847E7PQ/1>
- Bachand, P. A. M., & Horne, A. J. (1999). Denitrification in constructed free-water surface wetlands: I. Very high nitrate removal rates in a macrocosm study. *Ecological Engineering*, 14(1–2), 9–15. [https://doi.org/10.1016/S0925-8574\(99\)00016-6](https://doi.org/10.1016/S0925-8574(99)00016-6)
- Burke, P. M., Hill, S., Iricanin, N., Douglas, C., Essex, P., & Tharin, D. (2002). Evaluation of Preservation Methods for Nutrient Species Collected by Automatic Samplers. *Environmental Monitoring and Assessment*, 80(2), 149–173.
<https://doi.org/10.1023/A:1020660124582>
- Crumpton, W. G., Stenback, G. A., Fisher, S. W., Stenback, J. Z., & Green, D. I. S. (2020). Water quality performance of wetlands receiving nonpoint-source nitrogen loads: Nitrate and total nitrogen removal efficiency and controlling factors. *Journal of Environmental Quality*, 49(3), 735–744. <https://doi.org/10.1002/jeq2.20061>
- Crumpton, W. G., Stenback, G., Miller, B., & Helmers, M. (2006). Potential Benefits of Wetland Filters for Tile Drainage Systems: Impact on Nitrate Loads to Mississippi River Subbasins. Agricultural and Biosystems Engineering Technical Reports and White Papers. https://lib.dr.iastate.edu/abe_eng_reports/8
- Drake, C. W., Jones, C. S., Schilling, K. E., Amado, A. A., & Weber, L. J. (2018). Estimating nitrate-nitrogen retention in a large constructed wetland using high-frequency, continuous monitoring and hydrologic modeling. *Ecological Engineering*, 117, 69–83.
<https://doi.org/10.1016/j.ecoleng.2018.03.014>
- García-Lledó, A., Ruiz-Rueda, O., Vilar-Sanz, A., Sala, L., & Bañeras, L. (2011). Nitrogen removal efficiencies in a free water surface constructed wetland in relation to plant coverage. *Ecological Engineering*, 37(5), 678–684.
<https://doi.org/10.1016/j.ecoleng.2010.06.034>
- Gerke, S., Baker, L. A., & Xu, Y. (2001). Nitrogen Transformations in a Wetland Receiving Lagoon Effluent: Sequential Model and Implications for Water Reuse. *Water Research*, 35(16), 3857–3866. [https://doi.org/10.1016/S0043-1354\(01\)00121-X](https://doi.org/10.1016/S0043-1354(01)00121-X)

- Gersberg, R. M., Elkins, B. V., Lyon, S. R., & Goldman, C. R. (1986). Role of aquatic plants in wastewater treatment by artificial wetlands. *Water Research*, 20(3), 363–368. [https://doi.org/10.1016/0043-1354\(86\)90085-0](https://doi.org/10.1016/0043-1354(86)90085-0)
- Hunt, P. G., Stone, K. C., Humenik, F. J., Matheny, T. A., & Johnson, M. H. (1999). In-Stream Wetland Mitigation of Nitrogen Contamination in a USA Coastal Plain Stream. *Journal of Environmental Quality*, 28(1), 249–256. <https://doi.org/10.2134/jeq1999.00472425002800010030x>
- Ikenberry, C. D., Soupir, M. L., Schilling, K. E., Jones, C. S., & Seeman, A. (2014). Nitrate-Nitrogen Export: Magnitude and Patterns from Drainage Districts to Downstream River Basins. *Journal of Environmental Quality*, 43(6), 2024–2033.
- Ingersoll, T. L., & Baker, L. A. (1998). Nitrate removal in wetland microcosms. *Water Research*, 32(3), 677–684. [https://doi.org/10.1016/S0043-1354\(97\)00254-6](https://doi.org/10.1016/S0043-1354(97)00254-6)
- Kadlec, R. H. (2012). Constructed Marshes for Nitrate Removal. *Critical Reviews in Environmental Science and Technology*, 42(9), 934–1005. <https://doi.org/10.1080/10643389.2010.534711>
- Kadlec, R. H., Cuvellier, C., & Stober, T. (2010). Performance of the Columbia, Missouri, treatment wetland. *Ecological Engineering*, 36(5), 672–684. <https://doi.org/10.1016/j.ecoleng.2009.12.009>
- Kadlec, R. H., Pries, J., & Lee, K. (2012). The Brighton treatment wetlands. *Ecological Engineering*, 47, 56–70. <https://doi.org/10.1016/j.ecoleng.2012.06.042>
- Kadlec, R. H., & Wallace, S. D. (2009). *Treatment Wetlands* (2nd ed.). CRC Press.
- Kovacic, D. A., David, M. B., Gentry, L. E., Starks, K. M., & Cooke, R. A. (2000). Effectiveness of Constructed Wetlands in Reducing Nitrogen and Phosphorus Export from Agricultural Tile Drainage. *Journal of Environmental Quality*, 29(4), 1262–1274. <https://doi.org/10.2134/jeq2000.00472425002900040033x>
- Land, M., Graneli, W., Grimvall, A., Hoffmann, C. C., Mitsch, W. J., Tonderski, K. S., & Verhoeven, J. T. A. (2016). How effective are created or restored freshwater wetlands for nitrogen and phosphorus removal? A systematic review. *Environmental Evidence*; London, 5. <http://dx.doi.org.prox.lib.ncsu.edu/10.1186/s13750-016-0060-0>
- Martinez, C. J., & Wise, W. R. (2003). Hydraulic Analysis of Orlando Easterly Wetland. *Journal of Environmental Engineering*, 129(6), 553–560. [https://doi.org/10.1061/\(ASCE\)0733-9372\(2003\)129:6\(553\)](https://doi.org/10.1061/(ASCE)0733-9372(2003)129:6(553))
- Messer, T. L., Burchell, M. R., Birgand, F., Broome, S. W., & Chescheir, G. (2017). Nitrate removal potential of restored wetlands loaded with agricultural drainage water: A mesocosm scale experimental approach. *Ecological Engineering*, 106, 541–554. <https://doi.org/10.1016/j.ecoleng.2017.06.022>

- Mitsch, W. J., Zhang, L., Waletzko, E., & Bernal, B. (2014). Validation of the ecosystem services of created wetlands: Two decades of plant succession, nutrient retention, and carbon sequestration in experimental riverine marshes. *Ecological Engineering*, 72, 11–24. <https://doi.org/10.1016/j.ecoleng.2014.09.108>
- Persson, J., Somes, N. L. G., & Wong, T. H. F. (1999). Hydraulics Efficiency of Constructed Wetlands and Ponds. *Water Science and Technology*; London, 40(3), 291–300.
- Sartoris, J. J., Thullen, J. S., Barber, L. B., & Salas, D. E. (1999). Investigation of nitrogen transformations in a southern California constructed wastewater treatment wetland. *Ecological Engineering*, 14(1), 49–65. [https://doi.org/10.1016/S0925-8574\(99\)00019-1](https://doi.org/10.1016/S0925-8574(99)00019-1)
- US EPA. (2000). Wastewater Technology Fact Sheet Package Plants. United States Environmental Protection Agency, 1–7.
- Vymazal, J. (2007). Removal of nutrients in various types of constructed wetlands. *Science of The Total Environment*, 380(1–3), 48–65. <https://doi.org/10.1016/j.scitotenv.2006.09.014>
- Wang, H., Jawitz, J. W., White, J. R., Martinez, C. J., & Sees, M. D. (2006). Rejuvenating the largest municipal treatment wetland in Florida. *Ecological Engineering*, 26(2), 132–146. <https://doi.org/10.1016/j.ecoleng.2005.07.016>
- White, J. R., Gardner, L. M., Sees, M., & Corstanje, R. (2008). The Short-Term Effects of Prescribed Burning on Biomass Removal and the Release of Nitrogen and Phosphorus in a Treatment Wetland. *Journal of Environmental Quality*, 37(6), 2386–2391. <https://doi.org/10.2134/jeq2008.0019>

CHAPTER 6: ASSESSMENT OF NITROGEN RELEASE FROM A MINOR WWTP AND POTENTIAL FOR FWS CW IMPLEMENTATION TO IMPROVE NITRATE REMOVAL

ABSTRACT

In 2019, there were approximately 400 minor wastewater treatment plants (WWTPs) with individual national pollutant discharge elimination system (NPDES) permits in North Carolina. Of these 400, only 79 had monitoring requirements for nitrogen species other than ammonium ($\text{NH}_4\text{-N}$). Without monitoring requirements for other nitrogen species, the total amount of nitrogen released from these systems is unaccounted for in watershed estimates. To demonstrate the potential magnitude of this unaccounted-for nitrogen, the effluent of the Danbury WWTP, a minor WWTP in NC, was sampled twice a month in 2019. The mean concentrations for $\text{NH}_4\text{-N}$, nitrate ($\text{NO}_3\text{-N}$), and total nitrogen (TN) were 2.1, 13.5, and 15.8 mg L^{-1} , respectively. The estimated TN load discharged from the Danbury WWTP was 5.8 times greater than the $\text{NH}_4\text{-N}$ -only load reported in accordance with the site's NPDES permit. Thus, the current reporting methodology did not account for approximately 755 kg (1664 lbs.) of nitrogen discharged into the Dan River in 2019, the majority of which was $\text{NO}_3\text{-N}$. This potential for substantial (and unaccounted-for) $\text{NO}_3\text{-N}$ effluent loads paired with the widespread distribution of WWTPs within NC indicated that improved nitrogen removal at these WWTPs could help facilitate reduced nitrogen loads to surface waters in North Carolina. An ideal treatment system to provide this improved removal was identified to be the free water surface (FWS) constructed wetland (CW). Using the data gathered in literature (including the previous chapters), an uncertainty analysis was used to predict the wetland area required for both 50% and 90% $\text{NO}_3\text{-N}$ removal

(400 and 700 kg yr⁻¹, respectively) at the site. The results indicated that a 0.2 ha (0.5 acre) wetland could provide 50% NO₃-N removal efficiency, while a larger 0.6 ha (1.5 acre) wetland could provide 90% removal efficiency at the Danbury WWTP. The estimated removal rates and costs for either wetland implementation scenario suggested that relatively small FWS CWs attached to minor WWTPs would be a cost-appropriate method to reduce nitrogen loadings to surface waters in many locations across NC.

INTRODUCTION

Excess nutrient loading to downstream water bodies results in accelerated eutrophication (Anderson et al., 2002; Howarth et al., 2011; Smith et al., 1999). One known nutrient source is the discharge from municipal or domestic wastewater treatment plants (WWTPs) (Carey & Migliaccio, 2009). As a point source, effluent concentrations discharged from WWTPs must be below limits set in each WWTP's individual national pollutant discharge elimination system (NPDES) permit. This permit also sets the water quality monitoring requirements (e.g., locations, frequency, and water quality parameters). These NPDES permits are critical to protect downstream water quality and provide some information on the magnitude of pollutants that are discharged into watersheds.

In North Carolina (NC), regulations for nitrogen release from minor WWTPs focus on the ammonium form of nitrogen (NH₄-N). Here, minor WWTPs are defined as publicly owned treatment works (POTWs), private sewerage systems (SIC code: 4952), elementary and secondary schools (SIC Code: 8211), correctional institutions (SIC Code: 9223), and operators of residential mobile home sites (SIC Code: 6515) with permitted flows below 1 MGD and an active individual NPDES in 2019. The governmental enforcement and compliance history online (ECHO) database showed that 267 of the 394 minor WWTPs within NC had discharge limits for

effluent $\text{NH}_4\text{-N}$ concentrations, and all the 394 minor WWTPs were required to at least monitor effluent $\text{NH}_4\text{-N}$ concentrations (US EPA, 2020). These regulations focus on $\text{NH}_4\text{-N}$ because elevated $\text{NH}_4\text{-N}$ concentrations are acutely toxic to aquatic life and have the potential to cause a depletion of dissolved oxygen levels within the receiving water (NC DEQ, 2021; US EPA, 1999). Because nitrate ($\text{NO}_3\text{-N}$) and total nitrogen (TN) concentrations have not been found to be acutely toxic, a similar focus has not been placed on these nitrogen species in many locations. The ECHO database indicated that 79 of the 394 minor WWTP outfalls were monitored for TN concentrations and only 2 of those 79 had discharge limits. For $\text{NO}_3\text{-N}$ concentrations, only 58 had monitoring requirements and no minor WWTP had discharge limits. Within the ECHO database, $\text{NO}_3\text{-N}$ is monitored and reported under the umbrella term “inorganic nitrogen” (US EPA, 2020).

To reduce $\text{NH}_4\text{-N}$ concentrations, minor WWTPs use aerated systems (e.g., activated sludge, extended aeration) to facilitate the aerobic nitrification process and reduce $\text{NH}_4\text{-N}$ concentrations to low levels (Carey & Migliaccio, 2009). This focus on nitrification was noted by the US EPA in their fact sheet on package plants – a common type of pre-fabricated modular minor WWTP that uses activated sludge with or without with extended aeration (USEPA, 2000). Nitrification-only treatment results in the transformation of influent $\text{NH}_4\text{-N}$ to effluent $\text{NO}_3\text{-N}$, which does not remove nitrogen from the wastewater. Based on values from Tchobanoglous et al. (2003) and reported in Carey & Migliaccio (2009), this process can be expected to release effluent with $\text{NO}_3\text{-N}$ concentrations between 10 and 30 mg L^{-1} . At effluent flow rates ranging from 38 and 3800 $\text{m}^3 \text{d}^{-1}$ (0.01 and 1 MGD) and $\text{NO}_3\text{-N}$ concentrations ranging from 10 to 30 mg L^{-1} , the unaccounted discharge of $\text{NO}_3\text{-N}$ from each minor WWTPs to streams and rivers could range from 138 at the lowest flow and $\text{NO}_3\text{-N}$ concentration to 41,450 kg yr^{-1} at the highest flow

and NO₃-N concentration. However, without monitoring or reporting requirements, the NO₃-N concentrations in the effluent of minor WWTPs in NC is typically unknown.

This potential for substantial, and unaccounted-for, NO₃-N in minor WWTP effluent paired with the widespread distribution of minor WWTPs within NC suggested that improved nitrogen removal at these facilities could help reduce nitrogen loads to surface waters across NC. One potential treatment system that could be paired with these systems is the free water surface (FWS) constructed wetland (CW), which has been proven to be particularly efficient at NO₃-N removal through denitrification (Bachand & Horne, 1999; Crumpton et al., 2020; Drake et al., 2018; Ingersoll & Baker, 1998; Kadlec, 2012; Messer et al., 2017). The strategic implementation of constructed wetlands to capture and treat the effluent from package plants could be a simple, low-cost approach to further reduce N loads to surface waters.

As an initial step to evaluate the expansion of FWS CWs for improved nitrogen removal in NC, the effluent from a minor WWTP in NC without NO₃-N monitoring requirements was sampled during 2019. Using this minor WWTP as a case study, the study objectives were to: (1) quantify the effluent loads for all nitrogen species; (2) estimate the FWS CW area needed to provide varying NO₃-N removal efficiencies at the site; and (3) provide an initial estimate of the nitrogen removed, land required, and capital cost for widespread implementation.

METHODS AND MATERIALS

Site Description

The Danbury WWTP (NPDES ID: NC0082384) is a minor WWTP located in Stokes County, NC. The WWTP is a package plant that receives and treats the municipal wastewater for the 250 persons using both primary and secondary treatment (Figure 6.1). In the Danbury WWTP, influent wastewater first passes through a bar screen and into an equalization chamber.

Then, the wastewater is then split into two parallel aeration basins, each with three 15 HP blowers, where it is treated using activated sludge. Finally, this mixed liquor moves into a clarifier before it passes through a UV disinfection unit and is discharged from the system. Treated wastewater is discharged into the Dan River, which is part of the Roanoke River Basin (Reach Code: 03010103000496).



Figure 6.1: A photograph of the Danbury WWTP. The flow direction is away from the photographer.

The maximum effluent flow from the Danbury WWTP was set at 0.1 MGD in the site's NPDES permit. In 2019, the average monthly effluent flow was $160 \text{ m}^3 \text{ d}^{-1}$ (0.04 MGD) with a range from $110 \text{ m}^3 \text{ d}^{-1}$ (0.03 MGD) in March to $240 \text{ m}^3 \text{ d}^{-1}$ (0.06 MGD) in September. When compared to median flow rate of 0.01 MGD for all 394 minor WWTPs in NC, the Danbury WWTP was slightly larger than the typical plant (US EPA, 2020). However, of the 394 minor WWTPs, the 195 WWTPs with an average flow greater than 0.01 MGD accounted for 27.6 MGD of the cumulative 28.2 MGD of effluent released in 2019. Within these 195 WWTPs, the

median effluent flow rate was 0.08 MGD and a mean effluent flow rate of 0.14 MGD in 2019.

Within this population, the Danbury WWTP was slightly smaller than most.

The plant's NPDES permit set discharge limits for BOD₅, fecal coliforms, pH, and TSS. For BOD₅ and TSS, the average monthly concentrations were required to be at or below 30 mg L⁻¹. For pH, the monthly minimum value was 6 and the monthly maximum value was 9. For fecal coliforms, the average monthly value had to be below 200 counts per 100 mL. No discharge limits were required for any nitrogen species. The NPDES permit required NH₄-N concentrations to be monitored, but only the maximum monthly NH₄-N concentration had to be reported.

Data Collection

Water quality samples were collected approximately twice a month in 2019 (n = 23). Samples were collected by submerging a 500mL HDPE container to the middle of the effluent water column at a location immediately following the UV disinfection unit. All samples were transported back to the NCSU BAE Ecological Restoration Laboratory immediately after collection. Samples were acidified using sufficient 25% sulfuric acid to preserve the sample at pH less than 2 and stored at or below 4°C prior to analysis. Samples were filtered through a 0.45µm membrane filter. The samples were analyzed by the NCSU BAE Environmental Analysis Laboratory (EAL). The EAL analyzed all samples for total Kjeldahl nitrogen (TKN), NH₄-N, and NO₃-N using standard EPA protocols. Total dissolved nitrogen (TDN) concentrations were estimated by adding TKN and NO₃-N concentrations.

In accordance with the site's NPDES permit, effluent flow rates and water temperature were continuously monitored by the Town. The site operator collected weekly water quality samples. Average monthly flows, average monthly water temperature, and maximum monthly

NH₄-N concentrations were reported and can be found in the ECHO database (US EPA, 2020). Data from 2016 through 2020 reported by the Town were collected from this database and used in this study.

Data Analysis

Effluent nitrogen loading

Both NPDES and grab sample datasets for 2019 are shown in the Appendix E. Using the NPDES dataset, the 2019 NH₄-N load was calculated and reported in the discharge monitoring report (DMR). For the DMR Pollutant Loading report, the annual mass discharged was calculated using the maximum NH₄-N concentration for each month, since this was the only NPDES data available. While not ideal, the use of monthly maximum NH₄-N concentrations provided a worst-case scenario of annual NH₄-N effluent load. Using the NCSU bi-monthly grab sampling data, mean monthly NH₄-N, NO₃-N, and TDN concentrations were calculated. Mean monthly concentrations were used to estimate the annual NH₄-N, NO₃-N, and TDN loads in 2019 (Equation 6.1).

$$M = \frac{\sum_{i=1}^{12} Q_i n_i C_i}{10^3}$$

(Eq 6.1)

where, M was the annual mass released (kg), Q_i was the site's reported mean flow for each month (m³ d⁻¹), n_i is the number of days in the month, and C_i is the effluent constituent concentration (g m⁻³).

Constructed wetland design

FWS CWs intended to reduce nitrogen loads from minor WWTP will be designed for NO₃-N removal, due to the elevated NO₃-N concentrations expected in the minor WWTP effluent, especially those like package plants with aerated basins for conventional activated

sludge treatment (US EPA, 2000). For this study, constructed wetland NO₃-N removal was represented by combining first order removal kinetics and a tanks-in-series (TIS) representation of wetland hydraulics (Equation 6.2) (Kadlec & Wallace, 2009).

$$\frac{C_{out}}{C_{in}} = \left(1 + \frac{kA}{NQ_{in}}\right)^{-N}$$

(Eq 6.2)

where k is the removal rate constant (m d⁻¹), A is the wetland surface area (m²), Q_{in} is the average influent flow rate (m³ d⁻¹), C_{in} and C_{out} are the average inlet and outlet pollutant concentration (g m⁻³), and N is the number of tanks-in-series (TIS) used to represent the internal hydraulics. To account for the temperature effects, a modified Arrhenius equation was used to adjust the rate constant (k₂₀) (Equation 6.3)

$$k = k_{20}^{\theta(T-20)}$$

(Eq 6.3)

where k₂₀ is the removal rate coefficient at 20°C, θ is a temperature coefficient, and T is the average water temperature in each wetland cell, calculated by averaging the inlet and outlet temperature measurements. Theta (θ) was assumed to be 1.106, the mean value derived from data on 43 FWS CWs by Kadlec (2012).

A typical constraint on CW implementation is the area required to build them (Jasper et al., 2014; Kadlec, 2009). Therefore, the wetland area required for a certain level of treatment can be used as a metric of feasibility. In this study and for these sized WWTPs, adequate treatment was defined as a 50% NO₃-N removal and excellent treatment was defined as a 90% NO₃-N removal. The required wetland area per MGD of flow was predicted for both adequate (A₅₀¹) and excellent treatment (A₉₀¹) options using the methodology presented in Jasper et al. (2014).

A Monte Carlo simulation was then used to capture the influence of N, k, and water temperature on the required area. For the A_{50}^1 analysis, C_{out}/C_{in} was set to 0.5 (i.e., 50% removal efficiency assuming the influent flow is equivalent to the effluent flow). For the A_{90}^1 analysis, C_{out}/C_{in} was set to 0.1 (i.e., 90% removal efficiency assuming the influent flow is equivalent to the effluent flow). The rate constant (k_{20}) was estimated to range uniformly from 0.068 $m\ d^{-1}$ (25 $m\ yr^{-1}$) to 0.16 $m\ d^{-1}$ (60 $m\ yr^{-1}$). This range was selected because it spanned from the median annual average k_{20} value of 0.068 $m\ d^{-1}$ reported in Kadlec (2012) to the regional k_{20} value of 0.16 $m\ d^{-1}$ observed in cell 1 during the spring 2021 nitrate dosing study (Chapter 5). Because these values are greater than the median k_{20} value reported in Kadlec(2012), this distribution assumes above average NO_3-N removal. The N value was estimated to range uniformly from 1 to 10 in accordance with values reported in Kadlec (2012) and results from the tracer tests conducted at the Walnut Cove WWTP (Appendix A). These N and k values should be representative of a FWS CW in NC receiving NO_3-N enriched effluent with an operational age ranging from 0 to 25 years. To solve equation 6.3 in each iteration, water temperature was randomly selected from a uniform distribution of temperatures ranging from 0 to 30°C. For either A_{50}^1 or A_{90}^1 ($ha\ MGD^{-1}$), equation 6.2 was rearranged to equation 6.4 or 6.5, respectively, and solved.

$$A_{50}^1 = 0.3785 \left(0.5^{-\frac{1}{N}} - 1 \right) N/k$$

(Eq 6.4)

$$A_{90}^1 = 0.3785 \left(0.1^{-\frac{1}{N}} - 1 \right) N/k$$

(Eq 6.5)

Simple linear regressions were used to develop a relationship between $\ln(A_{50}^1)$ and water temperature ($^{\circ}\text{C}$) as well as $\ln(A_{90}^1)$ and water temperature ($^{\circ}\text{C}$). Using these relationships, the A_{50}^1 or A_{90}^1 was predicted for each month using monthly effluent water temperatures from the Danbury WWTP over the period from 2016 to 2020. Water temperature at the Danbury WWTP was likely to be representative monthly water temperatures of other minor WWTPs in NC (especially in the piedmont region). Therefore, the monthly A_{50}^1 and A_{90}^1 values can be used to approximate the required wetland areas at other minor WWTPs in the state. These results were plotted on an annual time scale and a trend line was fitted through the data using local polynomial regression fitting (LOESS). To estimate the necessary wetland area needed for 50 or 90% $\text{NO}_3\text{-N}$ removal (A_{50} or A_{90} , in ha) at the Danbury WWTP specifically, the monthly A_{50}^1 or A_{90}^1 values were multiplied by corresponding monthly average effluent flow (MGD) from the Danbury WWTP. All analyses were conducted using R software (R Core Team, 2017).

RESULTS

Danbury WWTP Effluent

NDPES sampling

In 2019, monthly maximum $\text{NH}_4\text{-N}$ effluent concentrations reported by the Town ranged from 0.33 mg L^{-1} to 14.4 mg L^{-1} (Figure 6.2). The mean monthly maximum $\text{NH}_4\text{-N}$ concentration was 3.50 mg L^{-1} , and the median value was 1.35 mg L^{-1} . Notably, the maximum $\text{NH}_4\text{-N}$ concentration was observed in March, when the plant aerators malfunctioned for several days (personal communication with site operator). The annual $\text{NH}_4\text{-N}$ load released from the Danbury WWTP, according to this dataset, was 157 kg (347 lbs.). The magnitude of this $\text{NH}_4\text{-N}$ load discharged fell in the range of reported $\text{NH}_4\text{-N}$ loads discharged in the previous three years

(2016, 2017, and 2018), which suggested that this was a typical year for nitrogen treatment in the Danbury WWTP (Table 6.1).

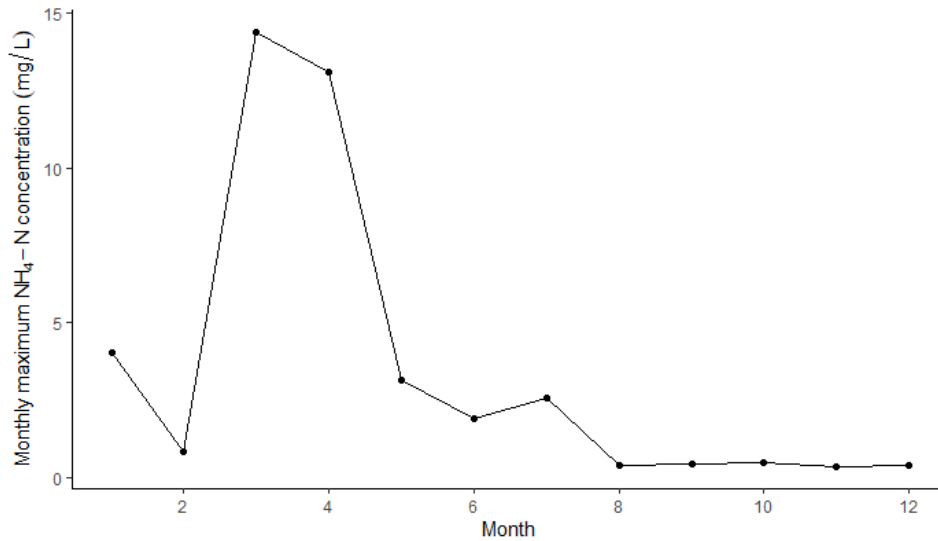


Figure 6.2: Monthly maximum NH₄-N concentrations in Danbury WWTP effluent in 2019 based on reported NPDES data obtained from the ECHO database.

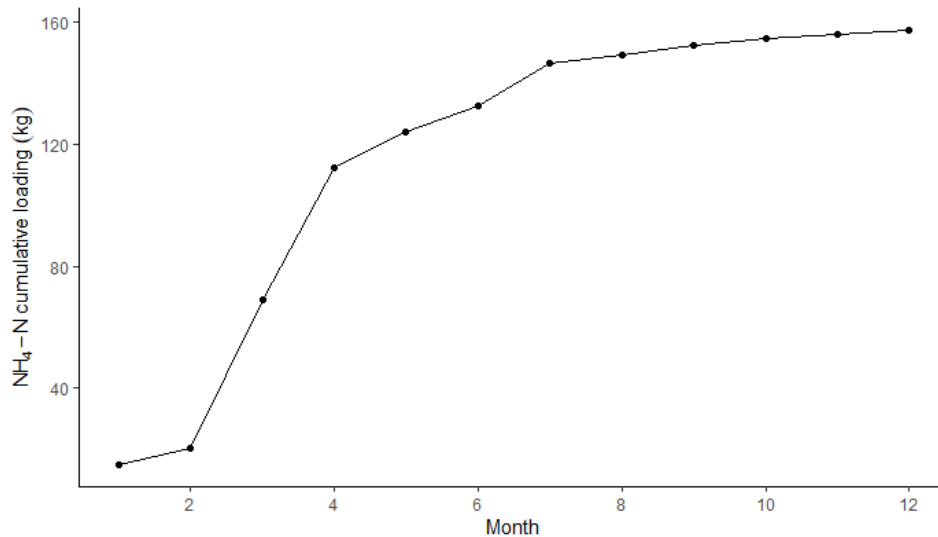


Figure 6.3: Cumulative NH₄-N effluent load from Danbury WWTP in 2019 based on reported NPDES data obtained from the ECHO database.

Table 6.1: Annual effluent NH₄-N loads (in kg and lbs.) from the Danbury WWTP for 2016-2019 as reported in the ECHO database.

Year	2016	2017	2018	2019
NH₄-N load	163 kg (360 lbs.)	93 kg (205 lbs.)	200 kg (442 lbs.)	157 kg (347 lbs.)

NCSU Sampling

The monthly NH₄-N concentrations ranged from 0.1 to 8.4 mg L⁻¹, with an average of 2.1 mg L⁻¹ (Figure 6.4 & Table 6.2). The monthly mean NH₄-N concentrations followed a similar pattern to the NPDES data (Figure 6.5). This similarity was evident in the March and April data, when mean NH₄-N concentrations increased due to aerator malfunction. In addition to the similar pattern, the similar values in the second half of 2019 showed that effluent NH₄-N concentrations varied only slightly during this period, and differences in concentrations were likely a function of sample timing between NCSU and the site operators. Monthly NO₃-N ranged from 6.0 to 19.8 mg L⁻¹, with an average of 13.5 mg L⁻¹. Monthly TDN concentrations ranged from 10.5 to 20.7 mg L⁻¹, with an average of 16.0 mg L⁻¹. Annual effluent loads for NH₄-N, NO₃-N, and TN were estimated to be 95 kg (209 lbs.), 797 kg (1758 lbs.), and 913 kg (2012 lbs.), respectively (Figure 6.6). The NH₄-N load calculated when using the monthly mean NH₄-N concentrations was 62 kg less than the load calculated using the NPDES data. The lower NH₄-N load value was expected because the NPDES data used only monthly maximum NH₄-N concentrations. Overall, when samples were analyzed for all nitrogen species, it was found that an additional 755 kg of unaccounted-for nitrogen were released by the site, mostly in the form of NO₃-N.

Table 6.2: Statistical summary of monthly effluent nitrogen data from grab samples in 2019 (n = 12). Concentrations are shown in units of mg L^{-1} .

Nitrogen Species	$\text{NH}_4\text{-N}$	$\text{NO}_3\text{-N}$	TKN	TDN
Mean	2.1	13.5	2.4	16.0
Median	0.6	12.7	1.1	16.0
Min	0.1	6.0	0.1	10.5
Max	8.4	19.8	10.1	20.7

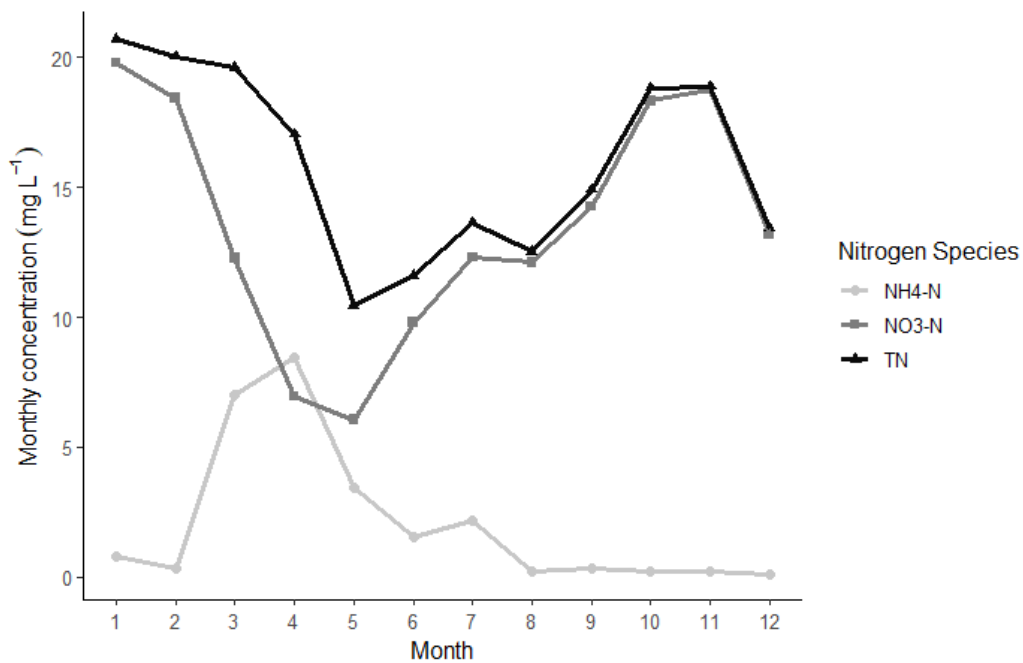


Figure 6.4: Mean monthly $\text{NH}_4\text{-N}$, $\text{NO}_3\text{-N}$, and TN concentrations in 2019 for the NCSU grab sampling data. Note the increase in $\text{NH}_4\text{-N}$ in the 3rd and 4th months (March and April), which shows when the aerators malfunctioned and how long it took the system to bring working properly again.

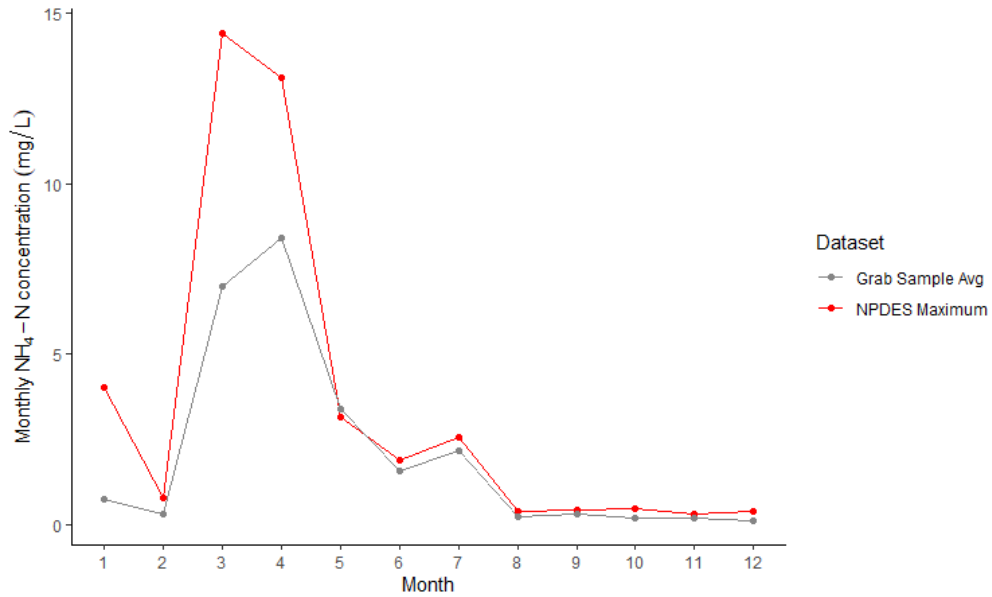


Figure 6.5: Comparison of monthly mean $\text{NH}_4\text{-N}$ concentrations estimated from grab sampling program with monthly maximum $\text{NH}_4\text{-N}$ concentrations estimated from samples collected by site operator.

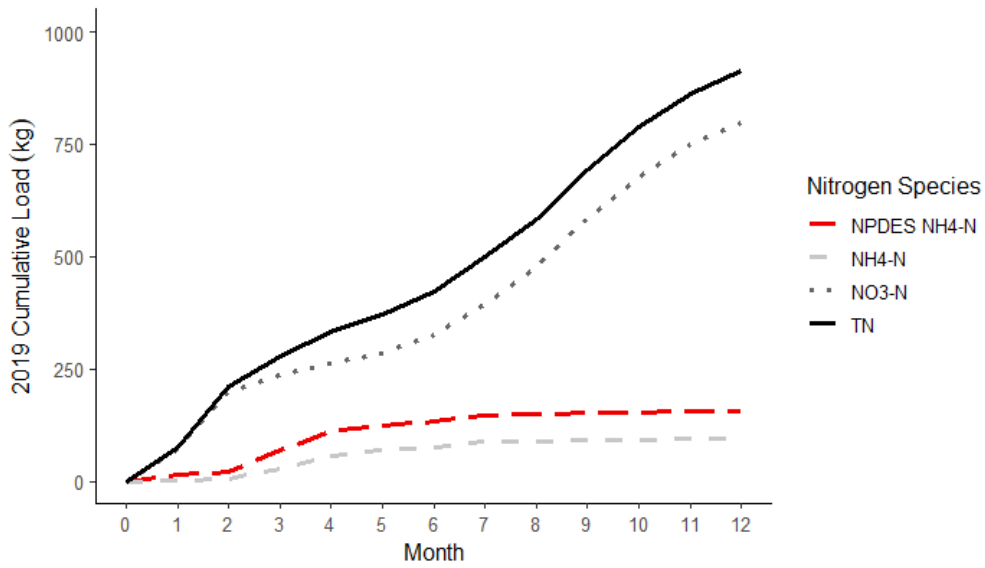


Figure 6.6: Cumulative loads for $\text{NH}_4\text{-N}$ based on monthly maximum concentrations in the ECHO database (NPDES $\text{NH}_4\text{-N}$) and $\text{NH}_4\text{-N}$, $\text{NO}_3\text{-N}$, and TN based on the grab sampling program.

Wetland Design

Monte Carlo Uncertainty Analysis

Five thousand iterations of the Monte Carlo uncertainty analysis were run to determine the wetland area required to treat NO₃-N from this package plant. For the A₅₀¹ analysis (area for 50% NO₃-N reduction per MGD), the linear regression of ln(A₅₀¹) vs temperature had an R² = 0.92. The linear relationship was $\ln(A_{50}^1) = -0.10 * \text{temperature} + 3.0$ (Figure 6.7). For the A₉₀¹ analysis (area for 90% NO₃-N reduction per MGD), the simple linear regression of ln(A₉₀¹) vs temperature had an R² = 0.86. The linear relationship was $\ln(A_{90}^1) = -0.10 * \text{temperature} + 4.4$ (Figure 6.8). For both analyses, temperature values in the uncertainty analysis spanned from 2.8 to 29.9°C; therefore, the relationship was assumed to hold between these values.

Predicted A₅₀¹ values for FWS CWs receiving minor WWTP effluent in NC ranged from 1 to 8 ha MGD⁻¹, with a mean of 3 ha MGD⁻¹ (n = 52) (Figure 6.9). Predicted A₉₀¹ values were greater than A₅₀¹ values with a range from 6 to 34 ha MGD⁻¹ and mean of 14 ha MGD⁻¹ (n = 52). Using average monthly effluent flows from 2016 through 2020, the wetland area needed for both 50% and 90% NO₃-N removal from the Danbury WWTP effluent were predicted for each month (Figure 6.10). Figure 6.10 suggested that a wetland area of 0.2 ha (0.5 acres) could provide 50% NO₃-N removal for every month, while a 0.6 ha (1.5 acre) wetland could provide 90% NO₃-N removal for every month but December and January. Notably, a wetland area of 0.4 ha (1 acre) could provide at least 50% NO₃-N removal in all months and 90% NO₃-N during the growing season (April – October).

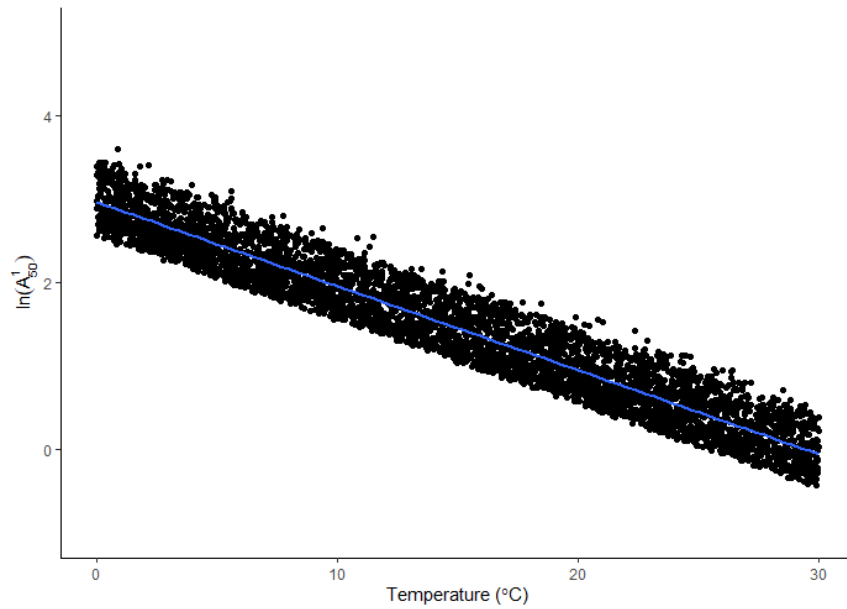


Figure 6.7: Relationship between $\ln(A_{50}^1)$ and temperature (in °C) for the 5000 iterations of the Monte Carlo uncertainty analysis. The regression was represented using the blue line. This relationship was used to predict monthly A_{50}^1 values at the Danbury WWTP.

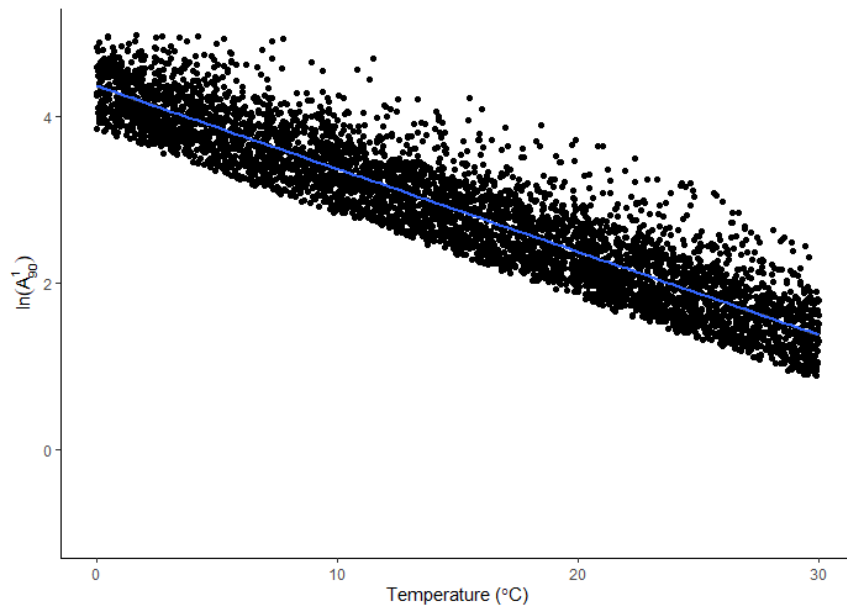


Figure 6.8: Relationship between $\ln(A_{90}^1)$ and temperature (in °C) for the 5000 iterations of the Monte Carlo uncertainty analysis. The regression was represented using the blue line. This relationship was used to predict monthly A_{90}^1 values at the Danbury WWTP.

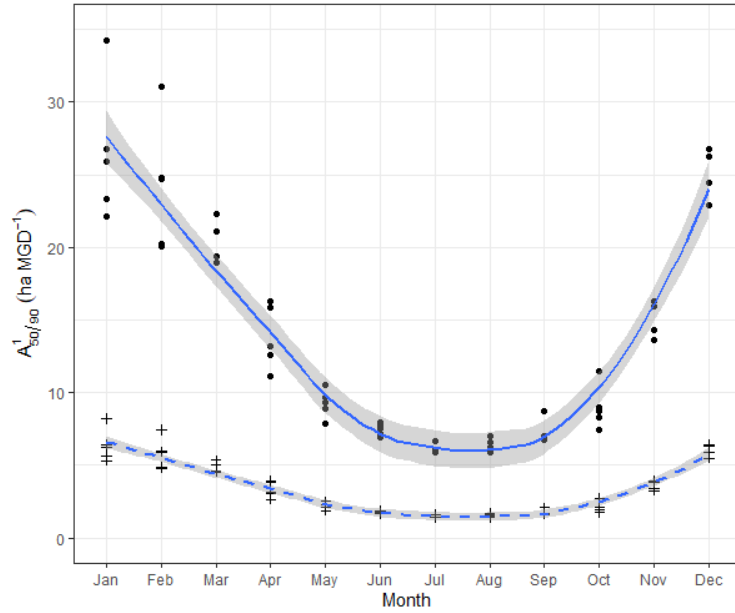


Figure 6.9: Initial estimate of the required wetland area (in ha MGD^{-1}) necessary for 50% and 90% $\text{NO}_3\text{-N}$ removal from minor WWTPs in NC. The solid blue line represents a LOESS regression through area required for 90% $\text{NO}_3\text{-N}$ removal (A_{90}^1). The dashed black line represents a LOESS regression through area required for 50% $\text{NO}_3\text{-N}$ removal (A_{50}^1). For both regressions, the shaded area represents the 95% standard error.

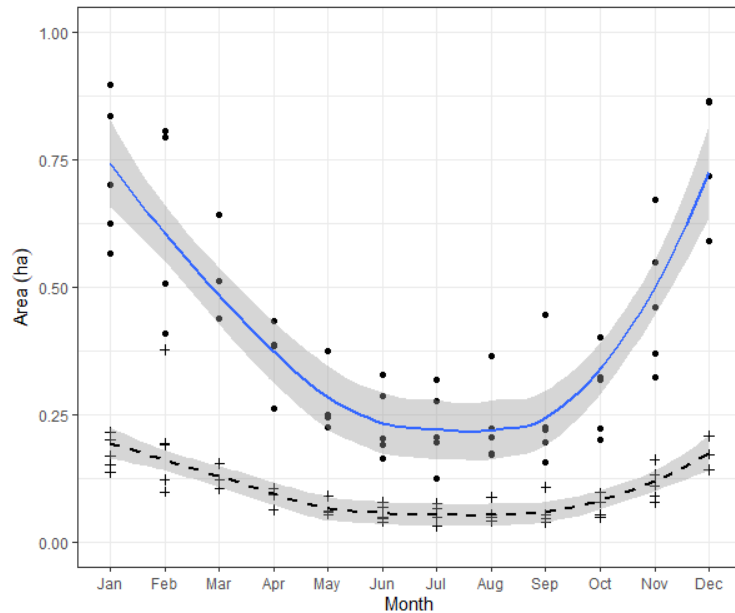


Figure 6.10: Required wetland area (in ha) necessary for 50% and 90% $\text{NO}_3\text{-N}$ removal from the Danbury WWTP effluent based on monthly data from 2016-2020 ($n = 52$). The solid blue line represents a LOESS regression through area required for 90% $\text{NO}_3\text{-N}$ removal (A_{90}). The dashed black line represents a LOESS regression through area required for 50% $\text{NO}_3\text{-N}$ removal (A_{50}). For both regressions, the shaded area represents the 95% standard error.

DISCUSSION

Unaccounted-for nitrogen load from a minor WWTP

The results confirmed that minor WWTPs with secondary treatment (typically activated sludge) release a $\text{NO}_3\text{-N}$ enriched effluent. The average effluent $\text{NO}_3\text{-N}$ concentration of 13.3 mg L^{-1} at this site was within the 10 to 30 mg L^{-1} range provided by Tchobanoglous et al. (2003), and likely would have been slightly higher if not for the aerator failure in March. When this $\text{NO}_3\text{-N}$ is accounted for, the actual total amount of nitrogen discharged to surface waters is much higher. In the case of the Danbury WWTP, an additional 755 kg nitrogen (1664 lbs.) were discharged from this minor WWTP into the Dan River in 2019 (Figure 6.6). This amount of nitrogen was 5.8 times greater than the effluent loads calculated and reported using only NPDES data. When compared to agricultural runoff, this minor WWTP, with an average flow rate of 0.04 MGD , exported approximately 1000 kg of TN in 2019, mostly in the form of $\text{NO}_3\text{-N}$; which equates to the nitrogen export expected from 25 ha (62-acres) of tile-drained cropland in the Midwest USA - based on an estimated nitrogen export of $40 \text{ kg ha}^{-1} \text{ yr}^{-1}$ from Ikenberry et al. (2014).

Overall, the comprehensive nitrogen data collected at the Danbury WWTP adds quantitative evidence to support the hypothesis that minor WWTPs without nitrate monitoring or discharge limits release more nitrogen in the form of $\text{NO}_3\text{-N}$ than is accounted for under the current permitting system. While speculative, if each of the 195 largest minor WWTP in NC released an effluent with a similar $\text{NO}_3\text{-N}$ concentration (13 mg L^{-1}), they would have cumulatively discharged approximately $496,000 \text{ kg yr}^{-1}$ ($1,094,000 \text{ lbs. yr}^{-1}$) of unaccounted-for nitrogen in the form of $\text{NO}_3\text{-N}$ to NC surface waters. Discharge of this unaccounted-for $\text{NO}_3\text{-N}$

load will only continue to increase the risk of eutrophication in the water bodies of NC and should be mitigated.

Potential Danbury WWTP wetland

The results suggested that a 0.2 ha could be added to the treatment train of the Danbury WWTP to remove 50% of the currently exported $\text{NO}_3\text{-N}$. If more removal is desired, then a 0.6 ha (1.5 acre) wetland could be added to remove 90% of the currently exported $\text{NO}_3\text{-N}$ for most of the year. Using the flow and water quality in 2019, a 50% reduction effluent $\text{NO}_3\text{-N}$ would remove 400 kg yr^{-1} , while a 90% reduction would remove 720 kg yr^{-1} . For either wetland design, this annual removal is equivalent to a wetland areal removal rate between 0.3 and $0.5 \text{ g m}^{-2} \text{ d}^{-1}$ (110 and $180 \text{ g m}^{-2} \text{ yr}^{-1}$).

Urban stormwater wetlands are quite common across NC and are great measures to mitigate stormwater flow and are lauded for nutrient removal ability. However, they receive runoff only during rainfall events, and that runoff is typically low in nutrients, so nitrogen removal rates are limited. For example, the total nitrogen removal rate in a CW receiving urban stormwater runoff in Florida was $0.03 \text{ g-N m}^{-2} \text{ d}^{-1}$ ($12 \text{ g-N m}^{-2} \text{ yr}^{-1}$) (Griffiths & Mitsch, 2020). In a FWS CW system receiving urban and golf course runoff in Indiana, nitrogen removal was estimated to be $0.04 \text{ g-N m}^{-2} \text{ d}^{-1}$ ($15 \text{ g m}^{-2} \text{ yr}^{-1}$) during storm events and $0.003 \text{ g-N m}^{-2} \text{ d}^{-1}$ ($1 \text{ g m}^{-2} \text{ yr}^{-1}$) during baseflow (Kohler et al., 2004). In North Carolina, two FWS CWs receiving urban stormwater runoff had removal rates near $0.001 \text{ g-N m}^{-2} \text{ d}^{-1}$ ($0.5 \text{ g m}^{-2} \text{ yr}^{-1}$) (Mazer, 2018; Merriman & Hunt, 2014). Instead, a FWS CW installed to receive the Danbury WWTP effluent would be closer to the 0.1 to $0.5 \text{ g-N m}^{-2} \text{ d}^{-1}$ (37 to $180 \text{ g m}^{-2} \text{ yr}^{-1}$) range of nitrogen removal observed in FWS CWs receiving $\text{NO}_3\text{-N}$ enriched agricultural runoff (Drake et al., 2018; Hunt et al., 1999; Kovacic et al., 2006). Since the potential $\text{NO}_3\text{-N}$ removal rate in constructed wetlands

placed downstream of wastewater package plants would be well above those observed in urban stormwater wetlands, it makes sense that these systems should be at least equally considered and more widely accepted as BMPs to help protect watershed health.

Estimated cost of implementation

An initial estimate of capital costs for a FWS CW indicated that the 0.2 ha FWS CW option would cost between \$40,000 and \$86,000, while the 0.6 ha FWS CW option would cost between \$120,000 and \$180,000 in 2021 US dollars (Table 6.3). At these prices, 10 years of nitrogen removal (4,000 kg-N at 50% removal or 7,200 kg-N at 90% removal) from this minor WWTP would cost between \$10 and \$25 kg⁻¹; well below the \$3000 per kg of nitrogen removal provided by a gravel CW treating urban stormwater, as reported in Houle et al. (2013). This cost per kg-N was approximately equal to the value that the State of North Carolina has placed on nitrogen credits in nutrient sensitive waters within the state (NC DEQ, 2019). This equivalence suggested that the building of FWS CWs to remove nitrogen from minor WWTPs would be a cost appropriate solution to nitrogen pollution and, for FWS CWs built in basins with NSW, that the return on investment may be approximately 5 - 10 years.

Table 6.3: Comparison of the nitrogen removal (in kg yr⁻¹), capital costs, and potential nitrogen credits for both the 50% and the 90% removal options.

	50% removal (0.2 ha design)	90% removal (0.6 ha design)
NO₃-N removal	400 kg yr ⁻¹	720 kg yr ⁻¹
Estimated capital cost*	\$40,000 to \$86,000	\$120,000 to \$180,000
Nitrogen credit⁺	\$8,700 to \$21,800 yr ⁻¹	\$15,600 to \$39,300 yr ⁻¹

* Lower value based on 200,000\$ ha⁻¹ average cost of six FWS CWs built in Iowa (Drake, 2018). The upper value was based on equation 23.1 in Kadlec and Wallace (2009).

+ Values based on the Nutrient Offset Rates Per Credit reported on the NC DEQ website. The lower value was based on the 9.83\$ per lbs.-N in the Tar-Pamlico basin. The upper value was based on the 24.77\$ per lbs.-N in the Neuse river basin outside of the Falls Lake Watershed. Note: most minor WWTPs are not located within basins with nutrient credits, but if the program was expanded, these are good estimates of the potential rates.

Widespread implementation of FWS CWs for tertiary treatment at minor WWTPs enhances NO₃-N removal.

Overall, if the goal of FWS CW implementation is to remove nitrogen, as is the case with the FWS CWs built to treat agricultural runoff, then the projected areal NO₃-N removal rates for a FWS CW at the Danbury WWTP indicated that adding FWS CWs to minor WWTP will be a highly efficient method to achieve this goal. Additionally, the relatively low cost and small areas needed to build these systems increases the feasibility of widespread implementation.

Furthermore, the results of chapter 5 indicated that these systems, when built to remove NO₃-N and operated with regular maintenance, should provide 20 years or more of adequate NO₃-N removal. In addition to nitrogen removal, a new unit-process focused FWS CW design may provide additional removal of an even wider range of emerging contaminants that have been documented in wastewater (Jasper et al., 2013).

Based on the considerations described above, what would widespread implementation require in terms of overall nitrogen removal, capital cost, and area needed. Using the speculative NO₃-N release estimate from a previous section, the annual NO₃-N load discharged from minor WWTPs in NC would be approximately 500,000 kg-N. FWS CWs built to remove 50% of this NO₃-N load would provide an additional nitrogen removal of 250,000 kg-N yr⁻¹. From figure 6.8, an A₅₀¹ of approximately 5 ha MGD⁻¹ would provide 50% or greater NO₃-N removal over the entire year. At this value, 50% NO₃-N removal would require the building a cumulative 140 ha (340 acres) of FWS CW at a total cost of \$28,000,000 (based on the estimated \$200,000 ha⁻¹). When distributed over a 10-year period, this would cost approximately \$11 per kg-N removed.

Future Work

This study was conducted as a demonstration of the unaccounted-for nitrogen released by a minor WWTP in NC and an initial assessment of the wetland size needed to provide

substantial $\text{NO}_3\text{-N}$ removal at these facilities. A more comprehensive estimate of unaccounted-for nitrogen in the form of $\text{NO}_3\text{-N}$ released from minor WWTPs (i.e., sampling at more than one site) is needed to provide a better estimate of both the amount of total nitrogen released from these facilities and the amount of nitrogen that could be removed through the widespread implementation of FWS CWs. Additionally, this study did not provide a detailed economic analysis of the cost to build a FWS CW in NC. A regional cost estimate that includes potential operation and maintenance costs is needed to provide a better estimate of the total cost required for widespread implementation. With more detailed estimates of both cost and potential nitrogen removal, a cost-benefit analysis could be conducted to compare the effectiveness of this strategy relative to other potential methods to improve nitrogen removal in NC (e.g., precision agriculture, agricultural BMPs, improved livestock waste management, etc.).

CONCLUSION

Monitoring requirements and discharge limits for minor WWTPs in NC often focus solely on the $\text{NH}_4\text{-N}$ form of nitrogen and, as a result, these systems have the potential to release a substantial amount of unaccounted for nitrogen in the form of $\text{NO}_3\text{-N}$. In the case study presented, the facility met the water quality limits of their permit and operated their facility within the designated guidelines. They also significantly reduced $\text{NH}_4\text{-N}$ concentrations even though it was not technically required in their permit and reported effluent concentrations and loads. However, when all species of nitrogen were monitored, the results indicated that this minor WWTP released 755 kg more nitrogen, mostly in the form of $\text{NO}_3\text{-N}$, than was reported in 2019 as part of their NPDES permit. Here I argue that targeted use of relatively small FWS CWs for tertiary treatment at these WWTPs could provide an opportunity for improved nitrogen removal in NC. For example, a small 0.2 ha (0.5 acre) FWS CW could remove 50% of the $\text{NO}_3\text{-}$

N in the Danbury WWTP effluent ($\sim 400 \text{ kg yr}^{-1}$), while a 0.6 ha (1.5 acre) FWS CW could remove 90% ($\sim 700 \text{ kg yr}^{-1}$) of the effluent $\text{NO}_3\text{-N}$ load. On a larger scale, if FWS CWs could be implemented into the treatment train of the largest 200 minor WWTP in NC, they have the potential to removal an additional 250,000 kg-N per year.

REFERENCES

- Anderson, D. M., Glibert, P. M., & Burkholder, J. M. (2002). Harmful algal blooms and eutrophication: Nutrient sources, composition, and consequences. *Estuaries*, 25(4 B), 704–726. <https://doi.org/10.1007/BF02804901>
- Bachand, P. A. M., & Horne, A. J. (1999). Denitrification in constructed free-water surface wetlands: I. Very high nitrate removal rates in a macrocosm study. *Ecological Engineering*, 14(1–2), 9–15. [https://doi.org/10.1016/S0925-8574\(99\)00016-6](https://doi.org/10.1016/S0925-8574(99)00016-6)
- Carey, R. O., & Migliaccio, K. W. (2009). Contribution of Wastewater Treatment Plant Effluents to Nutrient Dynamics in Aquatic Systems: A Review. *Environmental Management*, 44(2), 205–217. <http://dx.doi.org/10.1007/s00267-009-9309-5>
- Crumpton, W. G., Stenback, G. A., Fisher, S. W., Stenback, J. Z., & Green, D. I. S. (2020). Water quality performance of wetlands receiving nonpoint-source nitrogen loads: Nitrate and total nitrogen removal efficiency and controlling factors. *Journal of Environmental Quality*, 49(3), 735–744. <https://doi.org/10.1002/jeq2.20061>
- Drake, C. W. (2018). A study of nitrogen fate and transport in agricultural landscapes at the field, wetland, and watershed scales. University of Iowa.
- Drake, C. W., Jones, C. S., Schilling, K. E., Amado, A. A., & Weber, L. J. (2018). Estimating nitrate-nitrogen retention in a large constructed wetland using high-frequency, continuous monitoring and hydrologic modeling. *Ecological Engineering*, 117, 69–83. <https://doi.org/10.1016/j.ecoleng.2018.03.014>
- Griffiths, L. N., & Mitsch, W. J. (2020). Nutrient retention via sedimentation in a created urban stormwater treatment wetland. *Science of The Total Environment*, 727, 138337. <https://doi.org/10.1016/j.scitotenv.2020.138337>
- Houle, J. J., Roseen, R. M., Ballestero, T. P., Puls, T. A., & Sherrard, J. (2013). Comparison of Maintenance Cost, Labor Demands, and System Performance for LID and Conventional Stormwater Management. *Journal of Environmental Engineering*, 139(7), 932–938. [https://doi.org/10.1061/\(ASCE\)EE.1943-7870.0000698](https://doi.org/10.1061/(ASCE)EE.1943-7870.0000698)
- Howarth, R., Chan, F., Conley, D. J., Garnier, J., Doney, S. C., Marino, R., & Billen, G. (2011). Coupled biogeochemical cycles: Eutrophication and hypoxia in temperate estuaries and coastal marine ecosystems. *Frontiers in Ecology and the Environment*, 9(1), 18–26. <https://doi.org/10.1890/100008>
- Hunt, P. G., Stone, K. C., Humenik, F. J., Matheny, T. A., & Johnson, M. H. (1999). In-Stream Wetland Mitigation of Nitrogen Contamination in a USA Coastal Plain Stream. *Journal of Environmental Quality*, 28(1), 249–256. <https://doi.org/10.2134/jeq1999.00472425002800010030x>

- Ikenberry, C. D., Soupir, M. L., Schilling, K. E., Jones, C. S., & Seeman, A. (2014). Nitrate-Nitrogen Export: Magnitude and Patterns from Drainage Districts to Downstream River Basins. *Journal of Environmental Quality*, 43(6), 2024–2033.
- Ingersoll, T. L., & Baker, L. A. (1998). Nitrate removal in wetland microcosms. *Water Research*, 32(3), 677–684. [https://doi.org/10.1016/S0043-1354\(97\)00254-6](https://doi.org/10.1016/S0043-1354(97)00254-6)
- Jasper, J. T., Jones, Z. L., Sharp, J. O., & Sedlak, D. L. (2014). Nitrate Removal in Shallow, Open-Water Treatment Wetlands. *Environmental Science & Technology*, 48(19), 11512–11520. <https://doi.org/10.1021/es502785t>
- Jasper, J. T., Nguyen, M. T., Jones, Z. L., Ismail, N. S., Sedlak, D. L., Sharp, J. O., Luthy, R. G., Horne, A. J., & Nelson, K. L. (2013). Unit Process Wetlands for Removal of Trace Organic Contaminants and Pathogens from Municipal Wastewater Effluents. *Environmental Engineering Science*, 30(8), 421–436. <https://doi.org/10.1089/ees.2012.0239>
- Kadlec, R. H. (2009). Comparison of free water and horizontal subsurface treatment wetlands. *Ecological Engineering*, 35(2), 159–174. <https://doi.org/10.1016/j.ecoleng.2008.04.008>
- Kadlec, R. H. (2012). Constructed Marshes for Nitrate Removal. *Critical Reviews in Environmental Science and Technology*, 42(9), 934–1005. <https://doi.org/10.1080/10643389.2010.534711>
- Kadlec, R. H., & Wallace, S. D. (2009). *Treatment Wetlands* (2nd ed.). CRC Press.
- Kohler, E. A., Poole, V. L., Reicher, Z. J., & Turco, R. F. (2004). Nutrient, metal, and pesticide removal during storm and nonstorm events by a constructed wetland on an urban golf course. *Ecological Engineering*, 23(4), 285–298. <https://doi.org/10.1016/j.ecoleng.2004.11.002>
- Kovacic, D. A., Twait, R. M., Wallace, M. P., & Bowling, J. M. (2006). Use of created wetlands to improve water quality in the Midwest—Lake Bloomington case study. *Ecological Engineering*, 28(3), 258–270. <https://doi.org/10.1016/j.ecoleng.2006.08.002>
- Mazer, K. E. (2018). *Converting Dry Ponds to Constructed Stormwater Wetlands to Enhance Water Quality Treatment* [Master's Thesis, North Carolina State University]. <http://www.lib.ncsu.edu/resolver/1840.20/35788>
- Merriman, L. S., & Hunt, W. F. (2014). Maintenance versus Maturation: Constructed Storm-Water Wetland's Fifth-Year Water Quality and Hydrologic Assessment. *Journal of Environmental Engineering*, 140(10), 05014003. [https://doi.org/10.1061/\(ASCE\)EE.1943-7870.0000861](https://doi.org/10.1061/(ASCE)EE.1943-7870.0000861)
- Messer, T. L., Burchell, M. R., Birgand, F., Broome, S. W., & Chescheir, G. (2017). Nitrate removal potential of restored wetlands loaded with agricultural drainage water: A

- mesocosm scale experimental approach. *Ecological Engineering*, 106, 541–554.
<https://doi.org/10.1016/j.ecoleng.2017.06.022>
- NC DEQ. (2019). NC DEQ: Current Rate Schedules.
<https://deq.nc.gov/about/divisions/mitigation-services/dms-customers/fee-schedules>
- NC DEQ. (2021). History and Water Quality Overview.
<https://deq.nc.gov/about/divisions/water-resources/water-resources-permit-guidance/npdes-industrial-stormwater/history-water-quality-overview>
- Smith, V. H., Tilman, G. D., & Nekola, J. C. (1999). Eutrophication: Impacts of excess nutrient inputs on freshwater, marine, and terrestrial ecosystems. *Environmental Pollution*, 100, 179–196. [https://doi.org/10.1016/S0269-7491\(99\)00091-3](https://doi.org/10.1016/S0269-7491(99)00091-3)
- Tchobanoglous, G., Burton, F. L., & Stensel, D. (2003). *Wastewater engineering: Treatment and reuse* (4th ed.). McGraw-Hill. <https://catalog.lib.ncsu.edu/catalog/NCSU1557208>
- US EPA. (1999). 1999 Update of Ambient Water Quality Criteria for Ammonia (Government EPA-822-R-99-014; p. 153). U.S. Environmental Protection Agency.
- US EPA. (2000). *Wastewater Technology Fact Sheet Package Plants*. United States Environmental Protection Agency, 1–7.
- US EPA. (2020). Enforcement and Compliance History Online [Database]. ECHO.
<https://echo.epa.gov/>

CHAPTER 7: SUMMARY AND CONCLUSIONS

SUMMARY

The core of this dissertation was focused on 35 months of field-scale monitoring at the two 20+ year-old parallel free water surface (FWS) constructed wetlands (CWs) within the Walnut Cove wastewater treatment plant (WWTP) (one of three WWTPs with currently operational treatment wetlands in North Carolina). This field data provided a rare look at the performance of a FWS CWs treating municipal wastewater in North Carolina (NC) and helped to address the knowledge gap in long-term or late-stage nitrogen removal performance in FWS CWs. Nitrogen removal within the FWS CWs was notably poor due to an accumulated detritus substrate and a lack of available nitrate ($\text{NO}_3\text{-N}$). Along with poor internal hydraulics, a laboratory study showed that the aged detritus substrate within the FWS CWs released a considerable amount of ammonium ($\text{NH}_4\text{-N}$), which indicated that the detritus substrate was an internal nitrogen source that further reduced treatment efficiency. To address the poor performance, detritus was removed from one of the cells and subsequent monitoring demonstrated that maintenance techniques can improve nitrogen removal in aging FWS CWs. Finally, to investigate the $\text{NO}_3\text{-N}$ removal performance in the wetland cells, an in-situ $\text{NO}_3\text{-N}$ dosing study was conducted, and the results indicated that both wetland cells were highly efficient at removing $\text{NO}_3\text{-N}$. When the results of the dosing study were paired with a 12-month monitoring study focused on quantifying the effluent nitrogen load from the Danbury WWTP (a package plant), together they provided an estimate of both the unaccounted-for nitrogen release from minor WWTPs in NC and the potential $\text{NO}_3\text{-N}$ removal that could be attained by implementing FWS CWs at these facilities. This research demonstrated that widespread implementation of FWS CWs could be used to help meet water quality goals and reduce nitrogen

loadings in NC. Outside of the direct objectives, this research should provide a resource for future WWTP operators seeking to improve nitrogen removal through a rejuvenation of their aged wetlands or the building of new wetlands.

MAJOR CONCLUSIONS

The eight major conclusions derived from this dissertation are summarized below:

1. Expect a decline in nitrogen removal performance in FWS CW cells receiving $\text{NH}_4\text{-N}$ dominated lagoon effluent as operational age increases (i.e., as the amount of accumulated detritus increases). In the first six months of the study, TN removal efficiencies were 11% and 8%, in cells 1 and 2, respectively and the removal rate was $0.1 \text{ g-N m}^{-2} \text{ d}^{-1}$ in each cell (based on nominal cell volumes), well below what has been observed at other FWS CWs treating nitrogen-enriched wastewater. In the next 24 months, nitrogen removal was worse in the unimproved wetland cell 2, with a TN removal efficiency of -9%.
2. The substantial accumulated detritus substrate was a primary cause for the lack of nitrogen removal in both 20+ year-old wetland cells. The accumulated detritus substrate resulted in poor hydraulic efficiency and produced an internal nitrogen source. Because annual litterfall and the accumulation of detritus are part of the natural wetland aging, the negative influence of a detritus substrate will likely build as operational age increases.
3. Accumulated detritus can transfer a substantial amount of $\text{NH}_4\text{-N}$ from porewater to the overlying water column in an aged FWS CW. This release was well represented using a simple first-order kinetics model. In a laboratory study, the potential areal ammonium release rates (J_{UF}) from the detritus substrate at overlying water column

concentrations of 4 and 6 mg L⁻¹ were 0.21 and 0.14 g-N m⁻² d⁻¹ (70 and 50 g-N m⁻² yr⁻¹), respectively. If this study was representative of the aged detritus substrate in other FWS CWs, then the NH₄-N release will be detrimental to the nitrogen removal performance of lightly loaded systems (TKN load < 120 g-N m⁻² yr⁻¹).

4. Detritus removal and revegetation can be used to improve nitrogen removal in FWS CWs that have been negatively influenced by years of accumulated detritus due to lack of maintenance. The rejuvenated wetland cell (cell 1) had substantially improved internal hydraulics and removed significantly more NH₄-N, ON, and TN than the reference (cell 2) over the 24-month period that followed the detritus removal.
5. Adequate upstream pretreatment is critical for optimizing nitrogen removal in FWS CWs treating WWTP effluent. During the dosing studies, TDN removal efficiencies were 40% and 19% in cells 1 and 2, respectively. These nitrogen removal efficiencies were greater than those of either previous monitoring period and suggested that increasing the ratio of NO₃-N to NH₄-N in the influent will likely improve nitrogen removal in FWS CWs.
6. Influent nitrogen speciation will determine the influence of wetland age and lack of maintenance on nitrogen removal. During the in-situ dosing study, both the rejuvenated and non-rejuvenated wetland cells had NO₃-N removal rates (0.2 – 0.5 g-N m⁻² d⁻¹) in the upper portion of the range of expected NO₃-N removal rates. However, greater TDN removal in the rejuvenated cell indicated that operational age still negatively influenced the removal of other nitrogen species (particularly, NH₄-N).

7. Minor WWTPs in NC can release a substantial amount of unaccounted-for nitrogen, especially in the form of $\text{NO}_3\text{-N}$, to downstream water bodies. A relatively small minor WWTP with an average effluent flow of $180 \text{ m}^3 \text{ d}^{-1}$ (0.04 MGD) was found to release approximately 800 kg-N of unaccounted-for $\text{NO}_3\text{-N}$ in 2019. In 2019, there were approximately 200 such minor WWTPs across NC with effluent flow rates great enough to contribute greater than or equal to 800 kg-N of unaccounted-for nitrogen.
8. Widespread implementation of FWS CWs into the treatment train of minor WWTPs has the potential to substantially reduce nitrogen release to downstream water bodies in NC. Using the effluent $\text{NO}_3\text{-N}$ concentrations from the monitored WWTP and estimates of wetland removal rates, FWS CWs built to remove 50% of this $\text{NO}_3\text{-N}$ load from minor WWTPs in NC could provide an additional nitrogen removal of $250,000 \text{ kg-N yr}^{-1}$.

AREAS OF FUTURE WORK

The effectiveness and frequency of maintenance methods (Maintain to sustain)

FWS CWs are often considered low maintenance practices, which often results in less active management than is required. However, without active management, the aging process (i.e., the accumulation of a detritus substrate) will likely result in a decline in performance until the point at which they are deemed a failure and a system upgrade is recommended. For FWS CWs as part of tertiary treatment in WWTPs, failure will result in effluent pollutant concentrations that are greater than the discharge limits in the site's individual NPDES permit. Changing this viewpoint and improving management has the potential to mitigate declining treatment performance and extend the design life of treatment wetlands well past 15 to 20 years. As the results in this dissertation made clear, the design life of a FWS CW does not have to end.

Instead, maintenance techniques, such as the detritus removal described herein, can be used to rejuvenate aging FWS CWs and restart their life cycle (Figure 7.1).

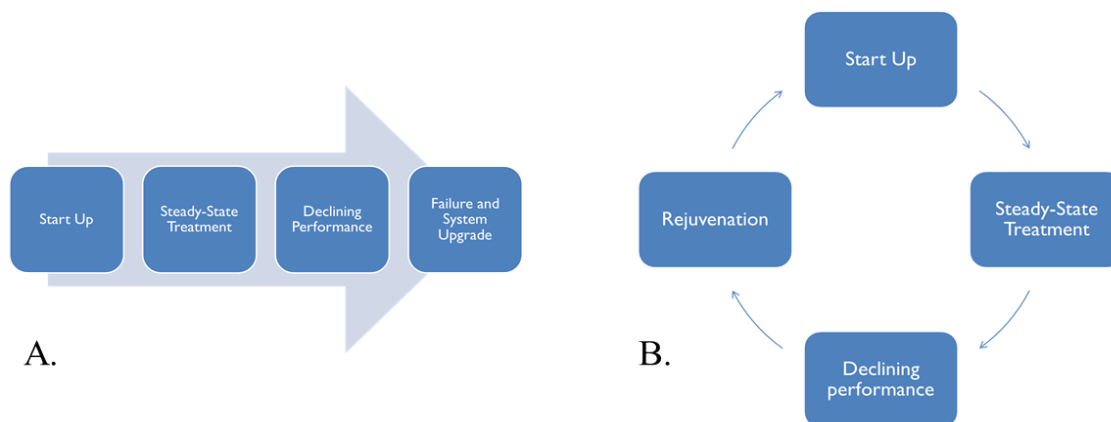


Figure 7.1: Two potential life cycles for treatment wetlands. A. The life cycle of an unmaintained wetland, where the system eventually begins to fail and must be replaced. B. The treatment wetland life cycle when a wetland rejuvenation is performed. If active management is employed, the operational age at which declining performance becomes a problem will be increased.

The studies included herein identified that an accumulated detritus substrate can have a negative influence on nitrogen treatment and demonstrated that detritus removal can improve $\text{NH}_4\text{-N}$ and ON removal (Chapter 4) and $\text{NO}_3\text{-N}$ removal (Chapter 5). However, wetland maintenance is a relatively unexplored topic. Further work is needed to answer the questions of when, where, and how much detritus removal should occur.

In terms of timing, the work herein indicated that 20+ years is too long to wait before removing detritus. Wetland cell 2 (the non-rejuvenated cell) performed poorly for the duration of the study and it was likely that both cells had been performing poorly for several years prior to the start of monitoring. What then should the frequency of detritus removal be? In one of the only other studies on detritus removal, Wang et al. (2006) noted that a detritus removal was required at the Orlando Easterly Wetland after only 13 years of operation. Additionally, detritus accumulation rates of $1\text{-}2\text{ cm yr}^{-1}$ suggest that a typical 30 cm deep basin could be filled in as

little 15 years. If the basin can be filled in 15 years, then it is likely that the detritus substrate will impact treatment in less than 15 years. This indicates that detritus removal should be conducted at least every 10-15 years. Future work will need to be conducted to pinpoint when the benefits of accumulated detritus (an organic carbon source for denitrification and microbial attachment sites) are outweighed by the negatives (a channelized flow that reduces surface area, residence time, and contact with microbial attachment sites). An exploration into the length of operation at which performance decline would be helpful for wetland operators. With this information, they could estimate a timeline of expected performance decline, which would allow for the scheduling and budgeting of wetland rejuvenation procedures.

For the question of how much detritus can be removed, it will be difficult to bring any wetland cell back to the 100% of the design or nominal treatment volume (i.e., remove all of the detritus) because of the need to maintain the structure and integrity of the wetland basin. How much detritus should then be left in the wetland cell? At the Walnut Cove WWTP, most of the detritus was removed from the entire length of the wetland cell, but a layer of detritus was left in the basin to maintain a carbon source and microbial communities. Leaving this detritus layer resulted in only a partial recovery of the internal hydraulics within the rejuvenated cell (Chapter 4). This suggested that more detritus should have been removed. However, removing all the detritus would have removed the organic carbon source needed for denitrification. Thus, future work should investigate the trade-off between the amount of detritus left in the basin and further improving internal hydraulics. Furthermore, other maintenance techniques, such as vegetation harvesting, may reduce the need for detritus removal to occur in the first place. But further work is needed to determine if harvesting is cheaper, quicker, or better for treatment efficiency than periodic detritus removal and revegetation.

Finally, the work within this dissertation was regional, with a focus on FWS CWs treating WWTP effluent within NC. Due to the natural processes of senescence and litterfall, detritus will accumulate in all FWS CWs, but future work should be undertaken to demonstrate the validity of the results and assertions found herein at other treatment wetlands of varying size, location, and dominant vegetation. Overall, active maintenance methods of FWS CWs (and other best management practices) need to be studied because these methods are necessary for sustaining or improving the expected treatment efficiencies of these systems; treatment efficiencies necessary to adequately reduce the pollutant loads discharging into our waterbodies.

Detailed estimate of nitrogen release from minor WWTPs and cost to implement FWS CWs across NC

This dissertation monitored nitrogen release from two of the approximately 200 minor WWTPs with the potential to release considerable nitrogen loads: the package plant Danbury WWTP and the lagoon-based Walnut Cove WWTP. To ensure the validity of the assertion in Chapter 6 that the nitrogen release from the Danbury WWTP was representative of other minor WWTPs, a broader sampling initiative should be undertaken with a goal to determine the annual effluent load of each nitrogen species at 10 to 20 different minor WWTPs. The 10 to 20 sites should have the area and funds available for the addition of a FWS CW, which would allow them to be initial case studies for widespread FWS CW implementation. Additionally, this work provided an initial estimate into the amount of wetland area and the capital costs for building such systems, but future work is needed to further assess the total costs associated with such a project and better estimate the wetland areas needed for specific locations.

Treatment Wetland Database

There is a distinct need for a new, updated treatment wetland database. A large wetland performance database would allow new analysis techniques, such as machine learning, to provide new insights into the factors that influence treatment performance. Because many treatment wetlands were built in the 1990s and 2000s, this new database would allow for a better understanding of late-stage performance. If this database included maintenance techniques, then the influence of these techniques on treatment efficiency could be evaluated. Furthermore, if some of the systems in the new database had also been previously included in the old database, this would allow for a performance comparison to identify when treatment performance may begin to decline. As part of this research, a standard operating procedure for treatment wetland monitoring could be developed to provide a consistent database structure to inform and encourage standardized data collection in studies seeking to evaluate treatment performance.

OVERALL CONCLUSION

Constructed wetlands have the potential to be an invaluable tool to reduce nitrogen loads across NC. However, for this tool to be effective, it must be maintained. Monitoring at the two FWS CWs within the Walnut Cove WWTP showed how poor treatment efficiency can be if limited maintenance is performed and detritus substrate is allowed to build up over 20+ years of operation. This dissertation showed that detritus removal and revegetation, a novel approach to nitrogen removal improvement, can rejuvenate a poorly performing wetland cell. Of course, for a tool to be most effective, it must also be used. Within NC, minor WWTPs provide a unique opportunity to expand the use of FWS CWs and deliver targeted nitrogen removal. By expanding the use of FWS CWs, we can help to meet NC's nutrient reduction goals and continue to reduce nitrogen loadings to NC's streams, rivers, lakes, estuaries, and sounds.

REFERENCES

- Wang, H., Jawitz, J. W., White, J. R., Martinez, C. J., & Sees, M. D. (2006). Rejuvenating the largest municipal treatment wetland in Florida. *Ecological Engineering*, 26(2), 132–146. <https://doi.org/10.1016/j.ecoleng.2005.07.016>

APPENDICES

APPENDIX A: HYDRAULIC ANALYSIS

Rhodamine WT concentration was measured in each sample using a Cyclops-7 Fluorometer and Databank Handheld Datalogger (Turner Designs, San Jose, CA). Samples were run in accordance with the recommended measurement practices in Appendix B of the Cyclops Submersible Sensors User's Manual (2019).

Average daily outflows were assigned to all samples taken during that day. To alleviate concerns of premature truncation due to limited sampling times for all test prior to the 12/9/2021 tests (when sampling time was expanded), the tails of all tests were extended past the last sample to approximately $2t_n$ using an exponential decay curve fit to the recession limb. The average outflows from each cell ranged from 283 to 517 m^3d^{-1} .

Table A.1: Details of conditions during tracer tests.

<i>Date</i>	<i>Period</i>	<i>Cell</i>	<i>Test</i>	<i>Water column depth, m</i>	<i>Nominal basin volume, m³</i>	<i>Avg outflow, m³d⁻¹ (gpm)</i>	<i>Nominal residence time, days</i>
3/8/2019	pre	1	1	0.3 (12")	2130	463 (85)	4.6
3/23/2019	pre	1	2	0.3 (12")	2130	354 (65)	6.0
7/26/2019	post	1	3	0.15 (6")	1030	471 (86)	2.2
8/9/2019	post	1	4	0.15 (6")	1030	387 (71)	2.7
1/31/2020	post	1	5	0.3 (12")	2130	362 (66)	5.9
12/9/2020	post	1	6	0.3 (12")	2130	517 (95)	4.1
4/23/2021	post	1	7	0.3 (12")	2130	283 (52)	7.5
3/23/2019	pre	2	1	0.3 (12")	2130	364 (67)	5.9
7/26/2019	post	2	2	0.3 (12")	2130	444 (81)	4.8
8/9/2019	post	2	3	0.3 (12")	2130	361 (66)	5.9
1/31/2020	post	2	4	0.3 (12")	2130	377 (69)	5.6
12/9/2020	post	2	5	0.3 (12")	2130	494 (91)	4.3
4/23/2021	post	2	6	0.3 (12")	2130	340 (62)	6.3

RTD Plots

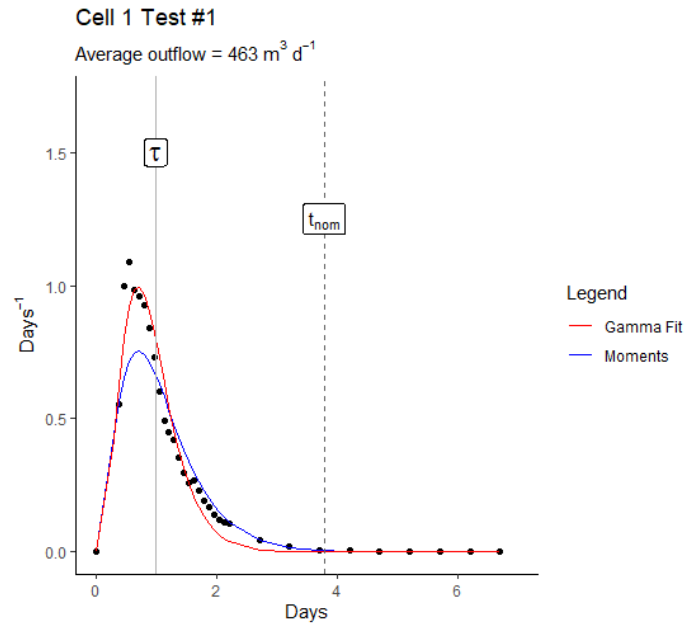


Figure A.1: Results and analysis of the experiment initiated on March 8th, 2019. This experiment was a pilot test for site and only cell 1 was investigated. Vertical lines represent mean actual residence time (τ) and nominal residence time based on plug-flow characteristics (t_{nom}). The blue line represents the RTD built from the method of moments. The red line represents the RTD built from fitting a gamma distribution.

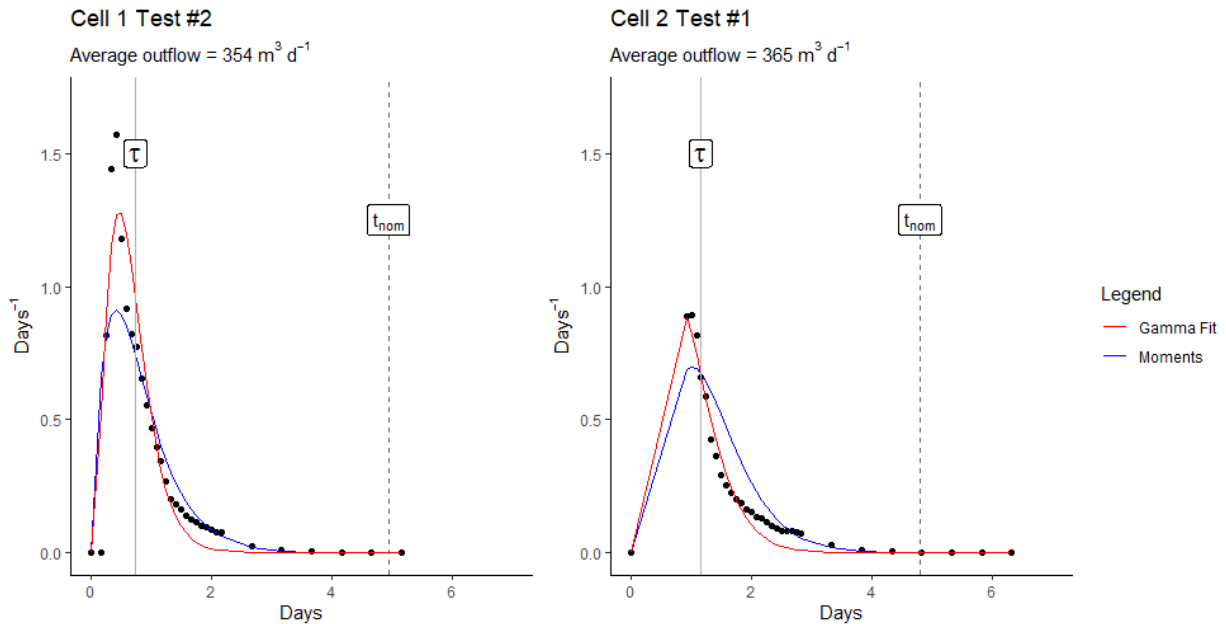


Figure A.2: Results and analysis of the experiment initiated on March 23rd, 2019. Vertical lines represent mean actual residence time (τ) and nominal residence time based on plug-flow characteristics (t_{nom}). The blue line represents the RTD built from the method of moments. The red line represents the RTD built from fitting a gamma distribution.

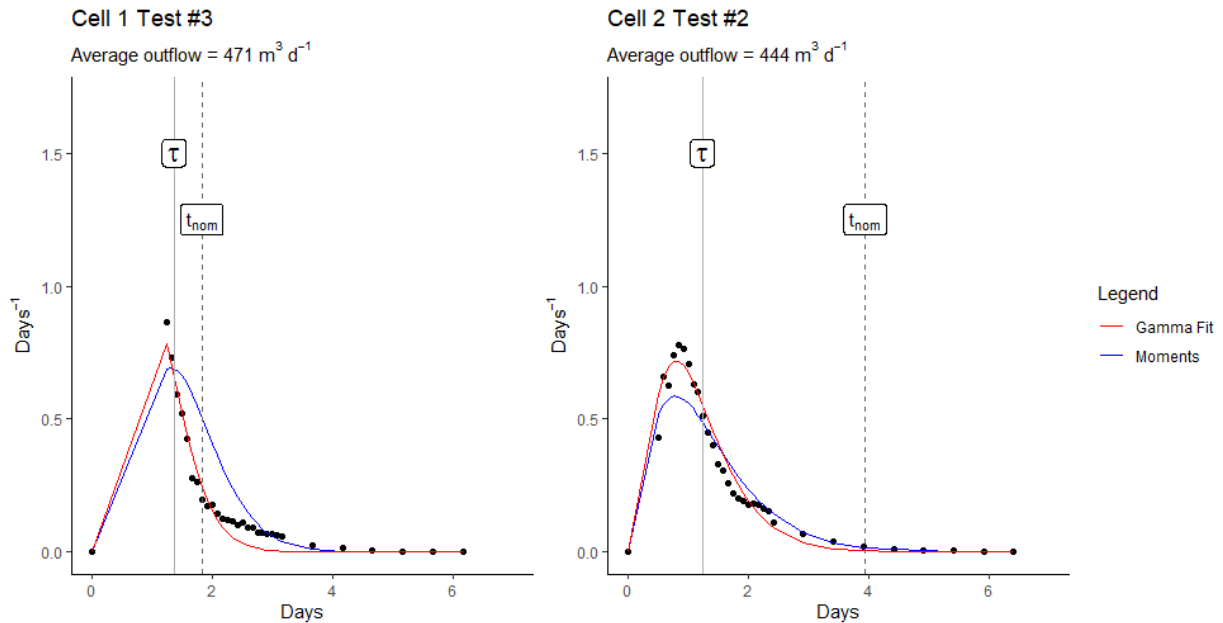


Figure A.3: Results and analysis of the experiment initiated on July 26th, 2019. The first experiment conducted after cell 1 detritus removal. Vertical lines represent mean actual residence time (τ) and nominal residence time based on plug-flow characteristics (t_{nom}). The blue line represents RTD built from the method of moments. The red line represents RTD built from fitting a gamma distribution.

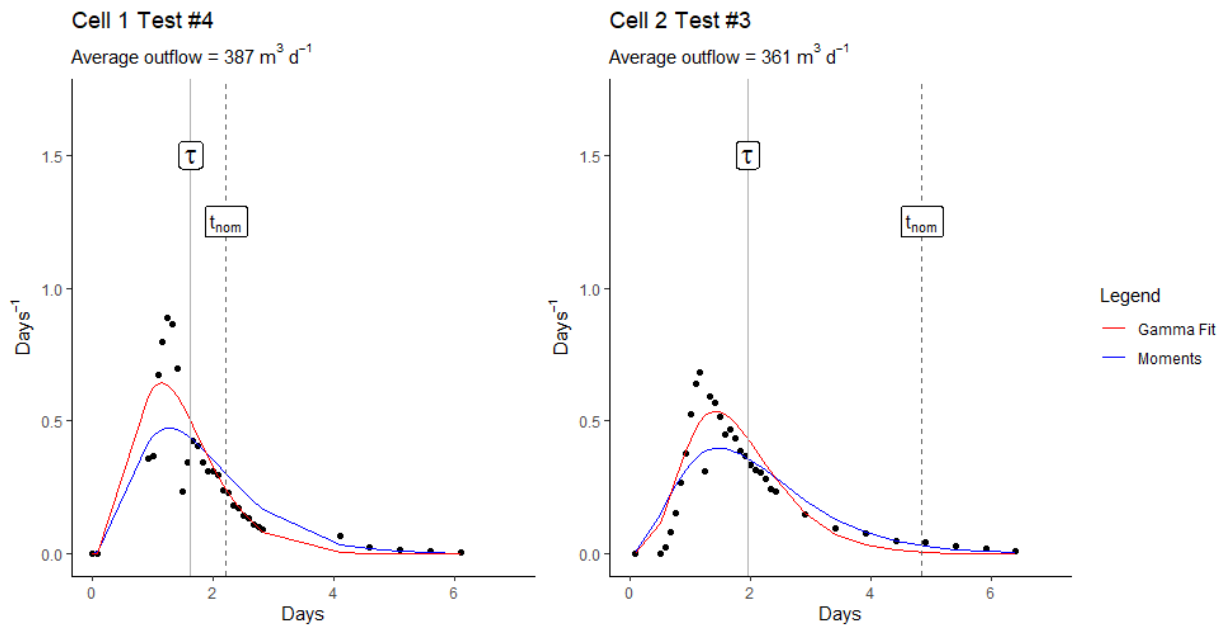


Figure A.4: Results and analysis of the experiment initiated on August 9th, 2019. Vertical lines represent mean actual residence time (τ) and nominal residence time based on plug-flow characteristics (t_{nom}). The blue line represents RTD built from the method of moments. The red line represents RTD built from fitting a gamma distribution.

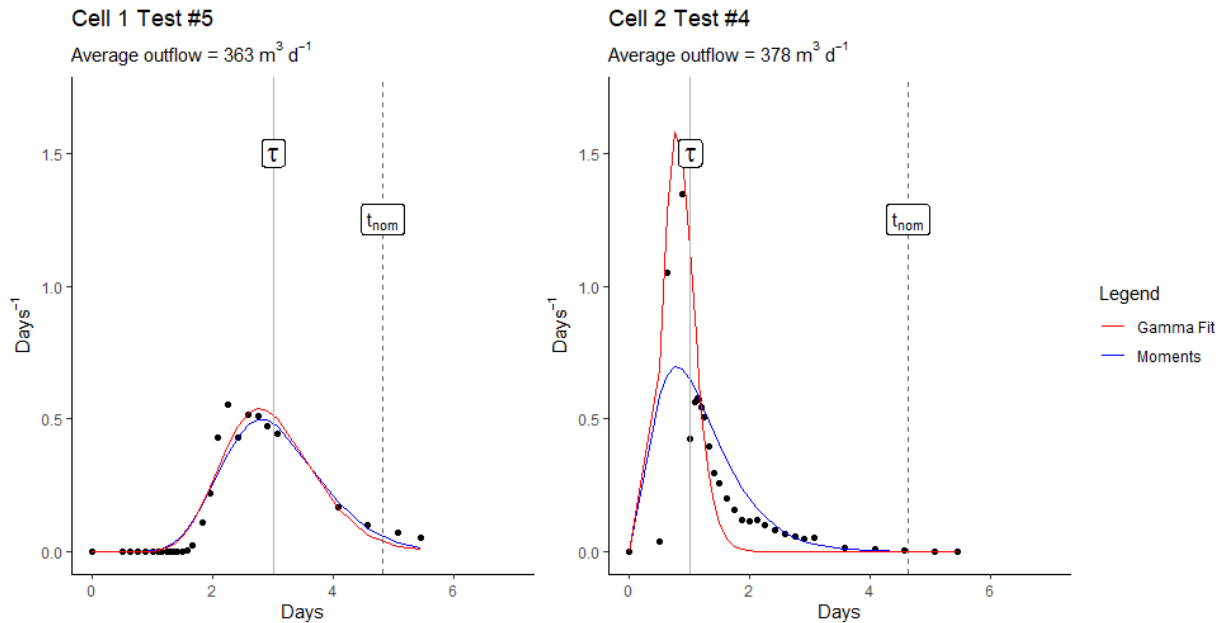


Figure A.5: Results and analysis of the experiment initiated on January 31st, 2020. The first experiment run with cell 1 back to full capacity (basin depth of 12"). Vertical lines represent mean actual residence time (τ) and nominal residence time based on plug-flow characteristics (t_{nom}). The blue line represents RTD built from the method of moments. The red line represents RTD built from fitting a gamma distribution.

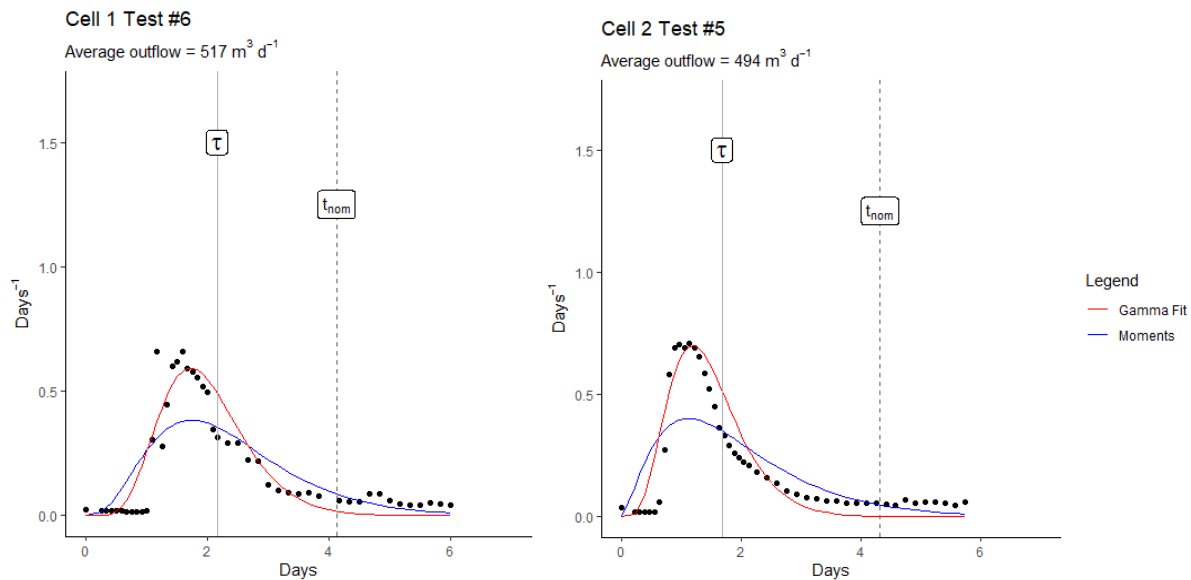


Figure A.6: Results and analysis of the experiment initiated on December 9th, 2020. Both cells were operated at full capacity (basin depth of 12"). Vertical lines represent mean actual residence time (τ) and nominal residence time based on plug-flow characteristics (t_{nom}). The blue line represents RTD built from the method of moments. The red line represents RTD built from fitting a gamma distribution.

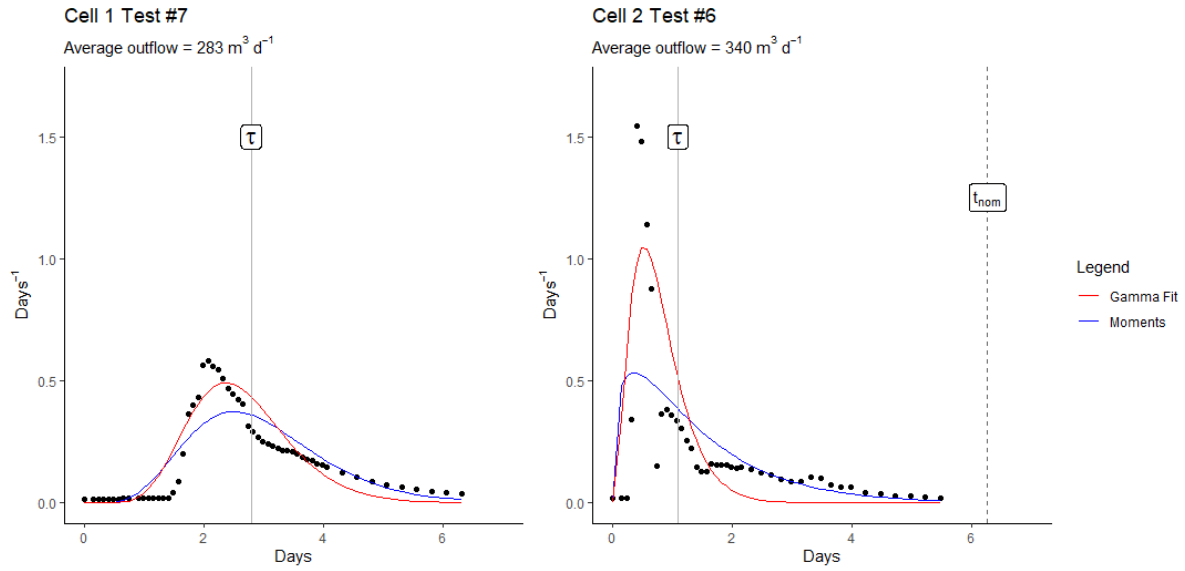


Figure A.7: Results and analysis of the experiment initiated on April 23rd, 2021. Both cells were operated at full capacity (basin depth of 12"). Vertical lines represent mean actual residence time (τ) and nominal residence time based on plug-flow characteristics (t_{nom}). The blue line represents RTD built from the method of moments. The red line represents RTD built from fitting a gamma distribution.

Table A.2: Results from tracer test RTD analysis.

Date	Cell	Mass recovered	Method of Moments						Gamma fit method					
			Hydraulic efficiency	# of tank	Mean residence time	Hydraulic efficiency Index	Time to 10%	Dimensionless variance	Hydraulic efficiency	# of tank	Mean residence time	Hydraulic efficiency Index	Time to 10%	Dimensionless variance
		%	e_v	N	τ (days)	λ_e	t_{10}	σ_0^2	e_v	N	τ (days)	λ_e	t_{10}	σ_0^2
3/8/2019	1	63.67	0.23	3	1.1	0.2	0.10	0.35	0.20	4	0.9	0.15	0.10	0.24
3/23/2019	1	64.15	0.13	2	0.8	0.1	0.05	0.49	0.11	3	0.7	0.08	0.05	0.30
7/26/2019	1	64.01	0.72	6	1.6	0.6	0.11	0.15	0.53	6	1.2	0.45	0.11	0.16
8/9/2019	1	103.24	0.67	3	1.8	0.5	0.24	0.29	0.55	5	1.5	0.43	0.24	0.22
1/31/2020	1	108.95	0.52	14	3.0	0.5	0.36	0.07	0.51	15	3.0	0.47	0.36	0.07
12/9/2020	1	83.48	0.56	4	2.3	0.4	0.30	0.25	0.48	8	2.0	0.42	0.30	0.13
4/23/2021	1	49.50	0.39	7	2.9	0.3	0.24	0.15	0.35	10	2.6	0.31	0.24	0.10
3/23/2019	2	51.51	0.22	4	1.3	0.2	0.04	0.23	0.17	4	1.0	0.13	0.04	0.23
7/26/2019	2	38.18	0.27	2	1.3	0.2	0.10	0.40	0.24	3	1.2	0.16	0.10	0.31
8/9/2019	2	38.18	0.36	3	2.1	0.3	0.17	0.30	0.30	5	1.8	0.24	0.17	0.21
1/31/2020	2	97.84	0.21	3	1.2	0.1	0.11	0.33	0.15	11	0.9	0.14	0.11	0.09
12/9/2020	2	77.37	0.44	2	1.9	0.3	0.20	0.42	0.33	5	1.4	0.27	0.20	0.18
4/23/2021	2	84.88	0.22	1	1.4	0.1	0.06	0.75	0.12	3	0.8	0.08	0.06	0.33

Exponential decay functions and R Code

Exponential decay plots for each test

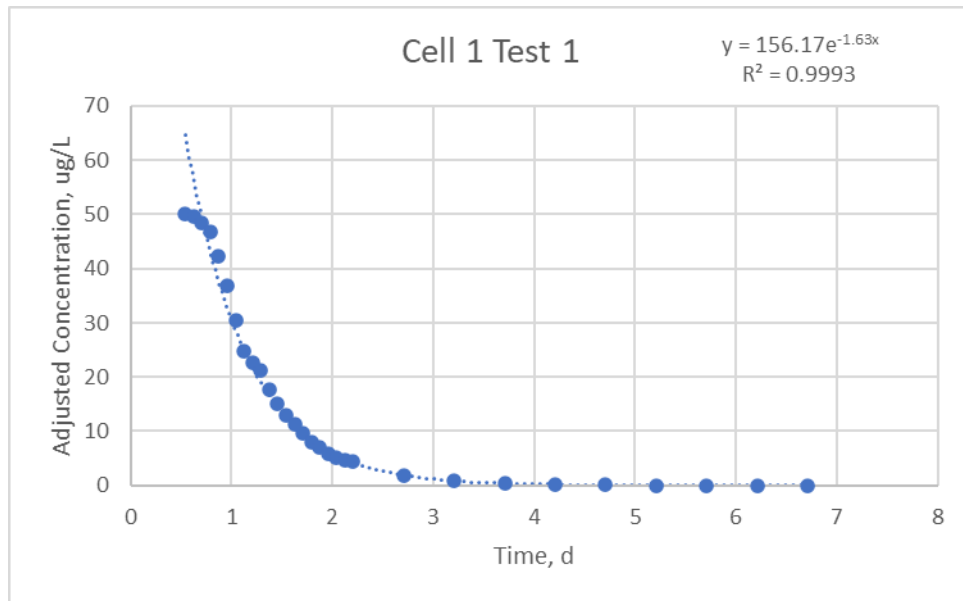


Figure A.8: The exponential decay function used to extend cell 1 test 1 data past the sampling truncation point. The exponential decay formula and R^2 value are in the top right of the figure.

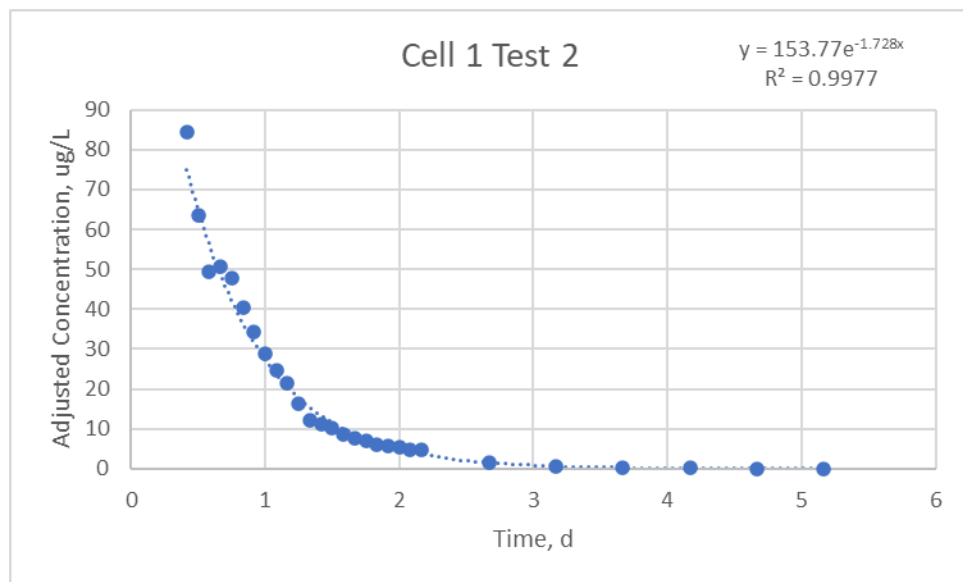


Figure A.9: The exponential decay function used to extend cell 1 test 2 data past the sampling truncation point. The exponential decay formula and R^2 value are in the top right of the figure.

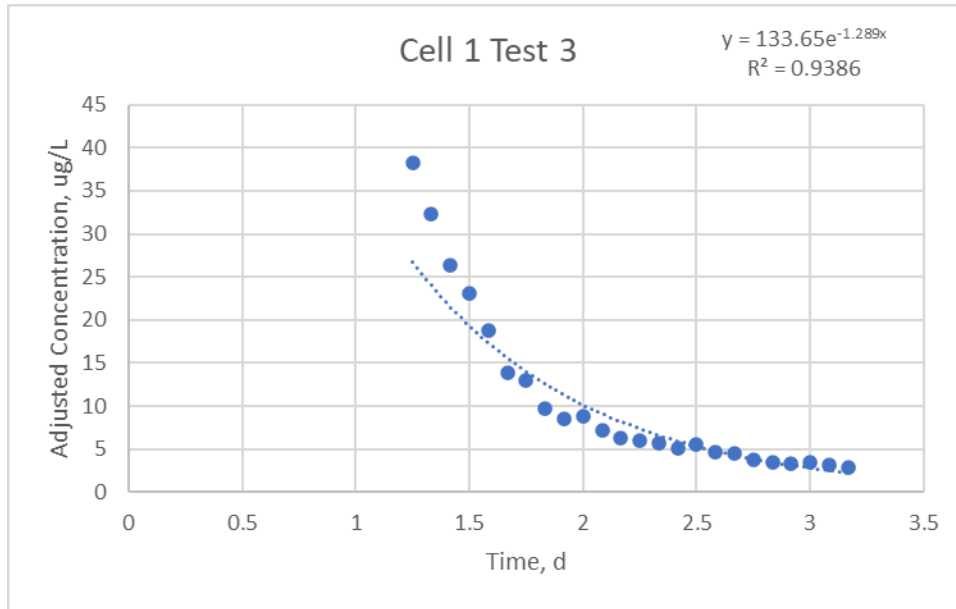


Figure A.10: The exponential decay function used to extend cell 1 test 3 data past the sampling truncation point. The exponential decay formula and R^2 value are in the top right of the figure.

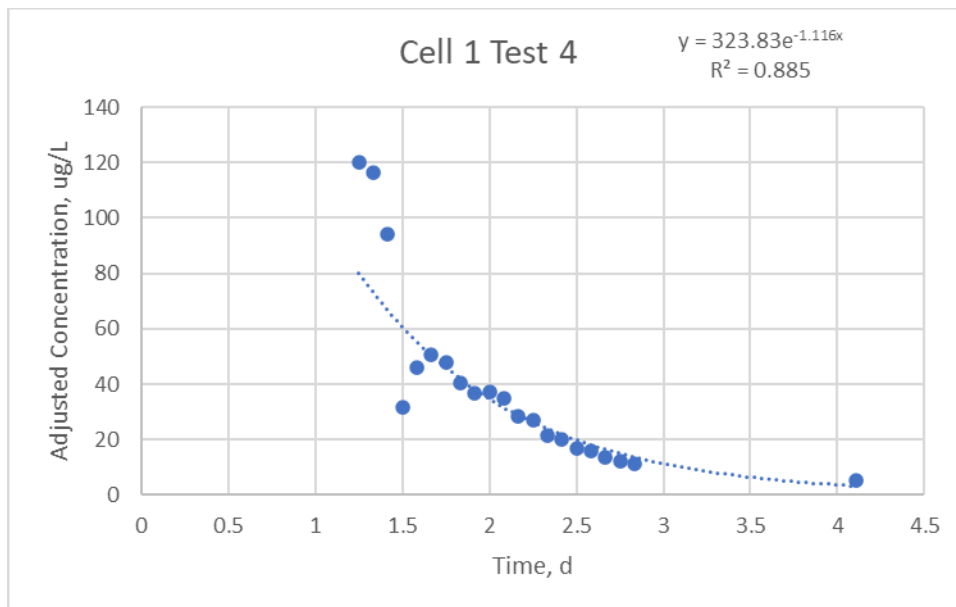


Figure A.11: The exponential decay function used to extend cell 1 test 4 data past the sampling truncation point. The exponential decay formula and R^2 value are in the top right of the figure.

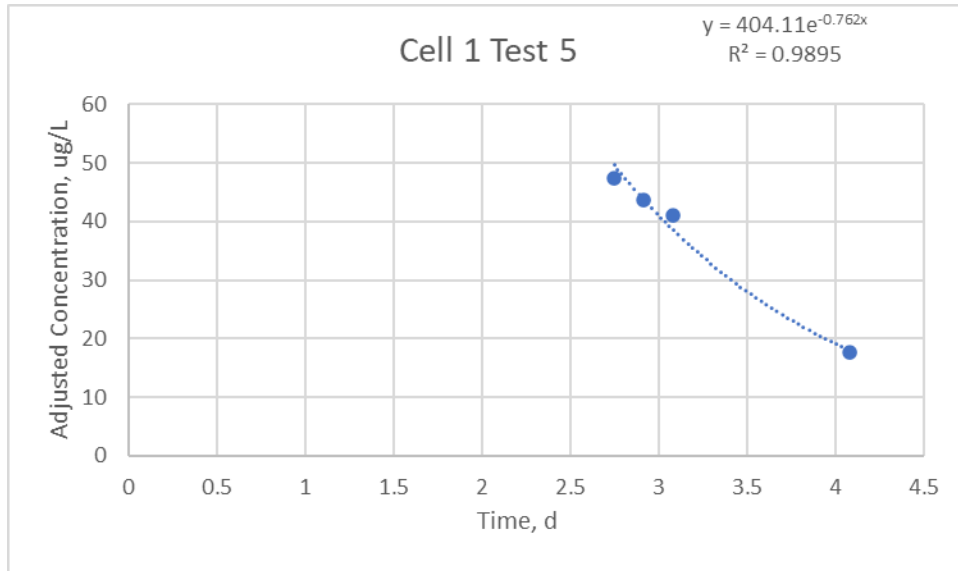


Figure A.12: The exponential decay function used to extend cell 1 test 5 data past the sampling truncation point. The exponential decay formula and R^2 value are in the top right of the figure.

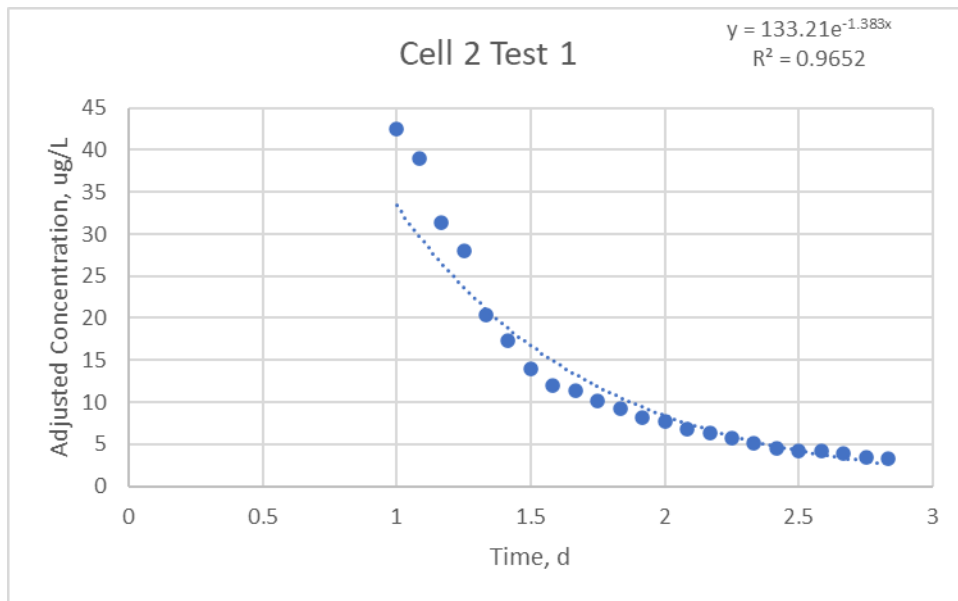


Figure A.13: The exponential decay function used to extend cell 2 test 1 data past the sampling truncation point. The exponential decay formula and R^2 value are in the top right of the figure.

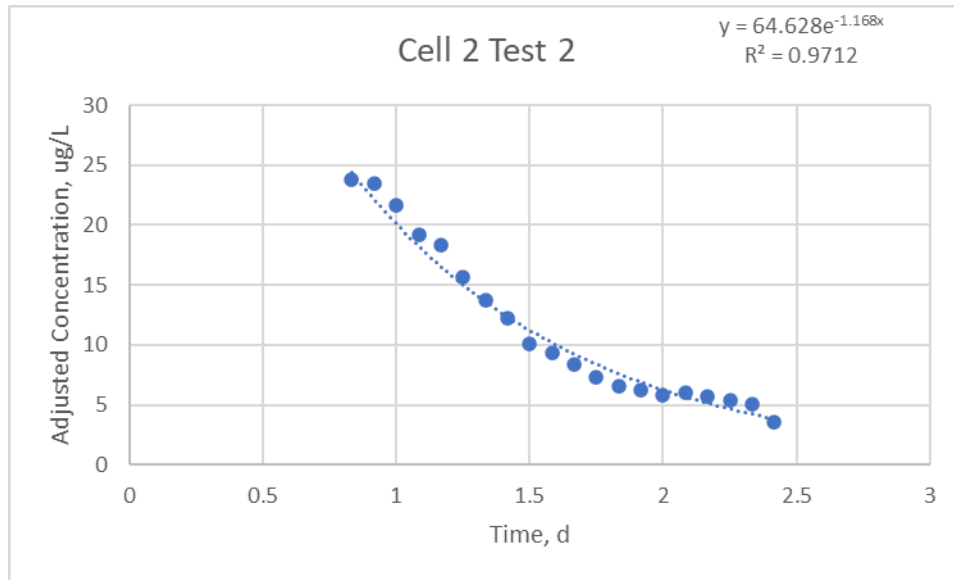


Figure A.14: The exponential decay function used to extend cell 2 test 2 data past the sampling truncation point. The exponential decay formula and R^2 value are in the top right of the figure.

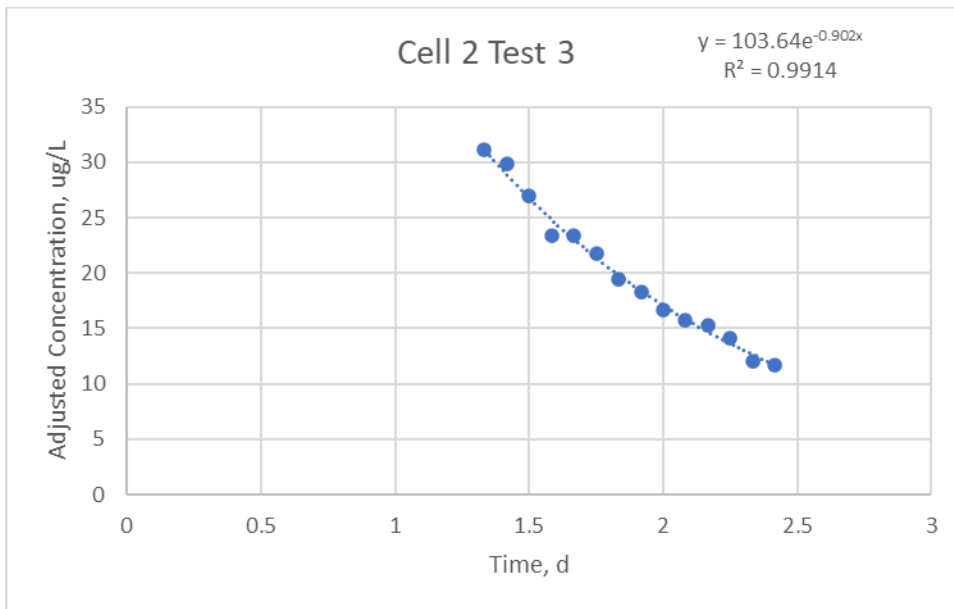


Figure A.15: The exponential decay function used to extend cell 2 test 3 data past the sampling truncation point. The exponential decay formula and R^2 value are in the top right of the figure.

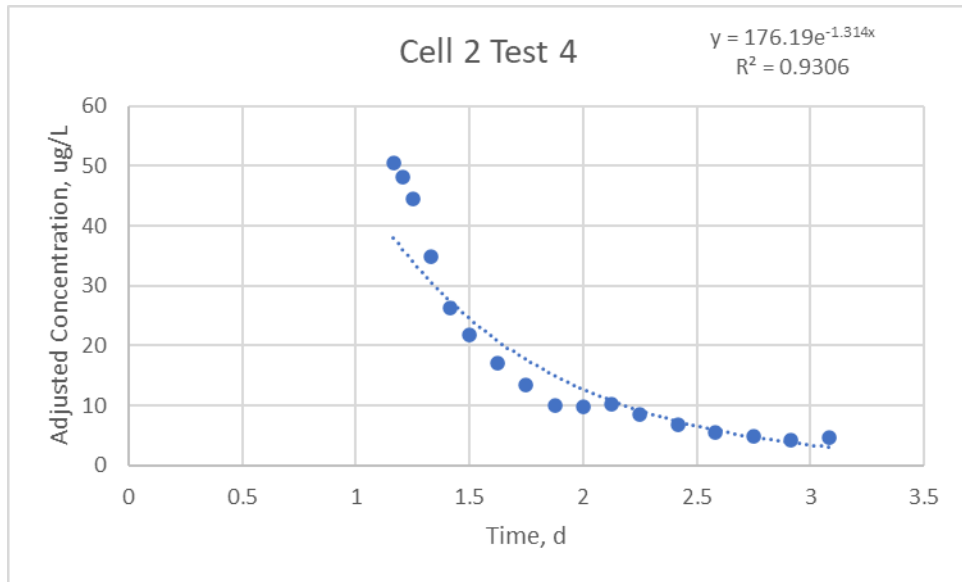


Figure A.16: The exponential decay function used to extend cell 2 test 4 data past the sampling truncation point. The exponential decay formula and R^2 value are in the top right of the figure.

R code example for hydraulic analysis

```
#Author: Brock Kamrath
#Date Created: 3/26/2020

#Objective: Hydraulic analysis of common dataset format for tracer tests at walnut Cove
load packages
rm(list=ls(all=TRUE))
library(tidyverse)
library(lubridate)
library(plyr)
library(dplyr)
library(readxl)
library(formattable)

# C value needed for plotting RTDs
c <- 1

# list of file names in the hydraulic_analysis folder and with the tt_o2 start of name
filenames <- list.files(path = "hydraulic_analysis/",
                        pattern = "tt_o1",
                        full.names = TRUE)
# limits list to the first four filenames, which is equal to the four test files
filenames <- filenames[1:4]
for (f in filenames) {

data <- read_excel(f, sheet = "main_ext")

#site sheet has the weir plate and tracer volume
site <- read_excel(f, sheet = "site")
head(data)

# Wetland Description
# plate # at outlet weir
weir_num <- site$weir[1]

# Volume of tracer used (L)
trace_vol <- site$trace_vol[1]

if(weir_num == 4){
  #nominal wetland volume (L)
  V <- 2130560
} else {
  #nominal wetland volume (L)
  V <- 1030000
}

#Mass of tracer added (ug)
mass_added <- 238000000*trace_vol

#find the time weighted average flow during the tracer test
# Time weighted average flow (Lpd)
Q_avg <- sum(data$Q_Lpd*data$deltat_d)/sum(data$deltat_d)
# Time weighted average flow (gpm)
Q_avg_gpm <- Q_avg/(3.785*24*60)

#Nominal retention time (days)
t_nom <- V/Q_avg

#Calculate the theta value
data <- data%>%
  mutate(time_prev = lag(time_d),
         Q_Lpd_prev = lag(Q_Lpd),
         C_uGL_prev = lag(C_uGL))
```

```

#set a vector for M0 to NA values
data$M0 <- as.numeric(rep(NA,nrow(data)))

#set a vector for e(t) to NA values
data$e_t <- as.numeric(rep(NA,nrow(data)))

#set a vector for e(t) to NA values
data$e_t_deltat_d <- as.numeric(rep(NA,nrow(data)))

#set a vector for f(t) to NA values
data$f_t <- as.numeric(rep(NA,nrow(data)))

#set a vector for M1 to NA values
data$M1 <- as.numeric(rep(NA,nrow(data)))

#set a vector for M2 to NA values
data$M2 <- as.numeric(rep(NA,nrow(data)))

# set the first M0 value to 0
data$M0[1] <- 0

# set the first M1 value to 0
data$M1[1] <- 0

# set the first M2 value to 0
data$M2[1] <- 0

# set the first e_t_deltat_d value to 0
data$e_t_deltat_d[1] <- 0

# set the first e_t_deltat_d value to 0
data$f_t[1] <- 0

#for loop to solve for M0
for(i in 2:nrow(data)){
  data$M0[i] <- (((data$Q_Lpd[i-1]*data$C_ugL[i-1])+(data$Q_Lpd[i]*data$C_ugL[i]))/2)*(data$time_d[i]-
data$time_d[i-1])
}

# sum of mass recovered in ug
M0_sum <- sum(data$M0)

#for loop to solve for e_t
for(i in 1:nrow(data)){
  data$e_t[i] <- (data$Q_Lpd[i]*data$C_ugL[i])/M0_sum
}

#for loop to solve for e_tavgdeltat and f_t
for(i in 2:nrow(data)){
  data$e_t_deltat_d[i] <- ((data$e_t[i]+data$e_t[i-1])/2)*(data$time_d[i]-data$time_d[i-1])
  data$f_t[i] <- data$e_t_deltat_d[i]+data$f_t[i-1]
}

#check for unity
unity <- sum(data$e_t_deltat_d)

# for loop to solve for M1 and M2
for(i in 2:nrow(data)){
  data$M1[i] <- (((data$time_d[i-1]*data$Q_Lpd[i-1]*data$C_ugL[i-
1])+(data$time_d[i]*data$Q_Lpd[i]*data$C_ugL[i]))/2)*(data$time_d[i]-data$time_d[i-1])
  data$M2[i] <- (((data$time_d[i-1]^2)*data$Q_Lpd[i-1]*data$C_ugL[i-
1])+(data$time_d[i]^2)*data$Q_Lpd[i]*data$C_ugL[i]))/2*(data$time_d[i]-data$time_d[i-1])
}

#mass recovered (%)
mass_rec <- (M0_sum/mass_added)*100

```

```

# 10% of mass recovered through the system
m10 <- 0.1*M0_sum

# Actual retention time, First normalized moment (d)
tau <- sum(data$M1)/M0_sum

# Effective volume as decimal
e <- tau/t_nom

# The normalized second moment of the RTD, variance (d^2)
sigma2 <- (sum(data$M2)/M0_sum)-(tau^2)

#N value for method of moments
N <- (tau^2)/sigma2

# I_e is similar to I_m due to the numerically equal value between I_m and e,
# but is an improvement on I_m. I_e reflects the RTD shape due to addition of N in
# the formula
lamda_e <- e*(1-(1/N))

#sigma theta is a dimensionless measure of dispersive processes
sigma_theta2 <- sigma2/(tau^2)

# Calculate the when 10% of the mass added reaches the outlet relative to t_nom
mass_cum <- cumsum(data$M0)
time_d <- data$time_d

t10 <- 0
for(i in 1:length(mass_cum)){
  if(m10 > mass_cum[i]){
    t10 <- ((m10-mass_cum[i])/(mass_cum[i+1]-mass_cum[i]))*(time_d[i+1]-time_d[i])+time_d[i]
  }
}

#normalize t10
t10n <- t10/t_nom

obs <- data.frame(data$time_d, data$e_t)
colnames(obs)

obs1 <- obs %>%
  setNames(c('date', 'E_t'))

ggplot(data)+
  geom_point(aes(x=time_d,y=e_t))+
  geom_line(aes(x=time_d,y = f_t),color="blue")+
  geom_vline(aes(xintercept=tau))

#Moment analysis using Gamma distribution
gamma <- function(data,N,tau){
  dat <- data%>%
  mutate(e_t = dgamma(time_d, shape = N, scale=tau/N),
         f_t = pgamma(time_d, shape = N, scale=tau/N))

  outputs <- data.frame(date=dat$time_d,e_t=dat$e_t,f_t=dat$f_t)
  return(outputs)
}

#1.par: Define initial values - N, tau----
#use nominal values provided
initial_values <- c(N,tau)

#2.fn: function that returns the SSE ----
#for model, which will be minimized

```

```

error <- function(parameters,observed_reponses,explanatory_variables){
  #Assign initial values to parameters
  #N value from data
  N <- parameters[1]
  #tau
  tau <- parameters[2]

  #Run model
  simulated_responses <- gamma(explanatory_variables,N,tau)

  #Merge with observations
  sim_obs <- inner_join(observed_reponses,simulated_responses,by="date")

  #Calculate SSE
  sse <- sum((sim_obs$E_t-sim_obs$e_t)^2)

  #Return
  return(sse)
}

#read in weather file
dat <- data
observations <- obs1

# Calibrate
cal <- optim(par=initial_values,
            fn=error,
            gr=NULL,
            observed_reponses=observations,
            explanatory_variables=dat,
            method="Nelder-Mead")

cal

#apply calibrated maize model
simulation <- gamma(data,N=N,tau=tau)
simulation_calibrated <- gamma(data,N=cal$par[1],tau=cal$par[2])

#####
# check for unity in gamma fit
#set a vector for M0 to NA values
simulation_calibrated$e_t_deltat_d <- as.numeric(rep(NA,nrow(data)))

# set first value to zero
simulation_calibrated$e_t_deltat_d[1] <- 0

#for loop
for(i in 2:nrow(simulation_calibrated)){
  simulation_calibrated$e_t_deltat_d[i] <- ((simulation_calibrated$e_t[i]+simulation_calibrated$e_t[i-1])/2)*(simulation_calibrated$date[i]-simulation_calibrated$date[i-1])
}

# Check on values for unity, should be 1
unity_gam <- sum(simulation_calibrated$e_t_deltat_d)
#####

e_gamma <- cal$par[2]/t_nom
lamda_e_gamma <- (cal$par[2]/t_nom)*(1-(1/cal$par[1]))
sigma_theta2_gamma <- 1/cal$par[1]

for(i in 1:nrow(simulation_calibrated)){
  if(simulation_calibrated$f_t[i] < 0.10){
    t10_gam <- (((0.10-simulation_calibrated$f_t[i])/(simulation_calibrated$p_t[i+1]-simulation_calibrated$f_t[i]))*(simulation_calibrated$date[i+1]-simulation_calibrated$date[i]))+simulation_calibrated$date[i])
    t10_gam <- t10/t_nom
  }}

```

```

results <-
c(mass_rec,Q_avg,t_nom,e,N,tau,lamda_e,t10n,sigma_theta2,e_gamma,cal$par[1],cal$par[2],lamda_e_gamma,t10_g
am,sigma_theta2_gamma,unity,unity_gam)
results <- formattable(results, digits = 2, format = "f")
print(results)
#####
Q_m3d <- round(Q_avg/1000) # Convert
average Q from Lpd to m3d
tau_avg <- (tau+cal$par[2])/2
mytitle <- substitute(paste("Cell 1 Test #",c,), list(c=c)) # Plot
title with c variable for test
mysubtitle <- substitute(paste("Average outflow = ",Q_m3d,~"m^3~"d^-1),list(Q_m3d=Q_m3d)) # Subtitle
states average outflow for test
colors <- c("Moments" = "blue","Gamma Fit" = "red") # Color values for
legend

# Create plots for each tracer test with both methods displayed
p <- ggplot()+
  geom_point(data=data,aes(time_d,e_t),color="black")+
  geom_line(data=simulation,aes(date,e_t,color="Moments"))+
  geom_line(data=simulation_calibrated,aes(date,e_t, color="Gamma Fit"))+
  geom_vline(aes(xintercept=tau_avg),color="gray70")+
  geom_vline(aes(xintercept=t_nom),linetype = 2, color="gray40")+
  geom_label(aes(x=tau_avg,y=1.5),label=expression(paste(tau)),size = 6)+
  geom_label(aes(x=t_nom,y=1.25),label= expression(paste("t["nom])),size=4)+
  labs(x="Days",y=expression(paste("Days"^-1)),color = "Legend", title = mytitle, subtitle = mysubtitle)+
  lims(x=c(0,7), y=c(0,1.7))+
  scale_color_manual(values = colors)+
  theme_classic()

# Print plots
print(p)

# Add 1 to the C variable that states the test number for the plot title
c <- c+1
}

```

APPENDIX B: EVAPOTRANSPIRATION CALCULATION

Evapotranspiration was estimated using meteorological data from the on-site weather station. The weather station collected 15-min data of atmospheric pressure p (mmHg), precipitation (mm), air temperature T ($^{\circ}\text{C}$), relative humidity RH (%), and wind velocity at 2 m height U_2 (m s^{-1}), net short-wave solar radiation R_{ns} (W m^{-2}), and net outgoing long-wave radiation R_{nl} (W m^{-2}). From this 15 min data, mean daily values were calculated for p , U_2 , R_{ns} , and R_{nl} . Radiation measurements were converted from $\text{W m}^{-2} \text{d}^{-1}$ to $\text{MJ m}^{-2} \text{d}^{-1}$ by multiplying by 0.0864. Min and max values were calculated for T and RH . Reference evapotranspiration was estimated for daily time steps using the standardized ASCE Penman-Monteith equation (Equation B.1).

$$ET_{REF} = \frac{0.408\Delta(R_n - G) + \gamma \frac{C_N}{T + 273} U_2 (e_s - e_a)}{\Delta + \gamma(1 + C_d U_2)}$$

(Eq. B.1)

where

ET_{REF} = standardized reference crop evapotranspiration for tall surfaces (0.5 m, alfalfa) (mm d^{-1}),

Δ = slope of the saturation vapor pressure-temperature curve ($\text{kPa } ^{\circ}\text{C}^{-1}$), as calculated in Equation B.2

R_n = measured net radiation at the crop surface ($\text{MJ m}^{-2} \text{d}^{-1}$), calculated by

G = soil head flux density at the soil surface ($\text{MJ m}^{-2} \text{d}^{-1}$), set to zero

γ = psychrometric constant ($\text{kPa } ^{\circ}\text{C}^{-1}$), as calculated by $\gamma = 0.000665 * P$, where P is the mean atmospheric pressure (kPa)

C_N = numerator constant ($\text{K mm s}^3 \text{Mg}^{-1} \text{d}^{-1}$), set to 1600

e_s = saturation vapor pressure at 1.5 to 2.5 m height (kPa), as calculated in equation B.4

e_a = mean actual vapor pressure at 1.5 to 2.5 m height (kPa), as calculated in equation B.5

C_d = denominator constant ($K \text{ mm s}^3 \text{ Mg}^{-1} \text{ d}^{-1}$), set to 0.38

The slope of the saturation equation

$$\Delta = 2503 \frac{(0.6108 e^{\left(\frac{17.27 T_{mean}}{T_{mean} + 237.3}\right)})}{(T_{mean} + 237.3)^2}$$

(Eq. B.2)

where

T_{mean} = mean daily air temperature ($^{\circ}\text{C}$), as calculated by $((T_{max} + T_{min})/2)$

Saturation vapor pressure equation

$$e_s = \frac{e^{\circ}(T_{max}) + e^{\circ}(T_{min})}{2} \quad (\text{Eq. B.3})$$

where

$E^{\circ}(T)$ = saturation vapor pressure function (kPa)

$$e^{\circ}(T) = (0.6108 e^{\left(\frac{17.27 T}{T + 237.3}\right)}) \quad (\text{Eq. B.4})$$

Actual vapor pressure equation

$$e_a = \frac{e^{\circ}(T_{min}) \frac{RH_{max}}{100} + e^{\circ}(T_{max}) \frac{RH_{min}}{100}}{2} \quad (\text{Eq. B.5})$$

where

RH_{max} = daily maximum relative humidity (%)

RH_{min} = daily minimum relative humidity (%)

R code example for weather data

```
## -----
##
## Script name: daily_weather
##
## Purpose of script: return average daily values of weather parameters important for water balance
##
## Author: Brock Kamrath
##
## Date Created: 2020-06-25
## Email: bjkamrat@ncsu.edu
##
## -----
## Notes:
##
## -----
options(scipen = 6, digits = 4) # I prefer to view outputs in non-scientific notation
## -----

#convert BP to kPa
daily_weather <- function(weather)
{
  weather$bp_kpa <- weather$bp_mmhg/7.501

  mdw <- weather%>%
    group_by(date)%>%
    summarise(bp_kpa = mean(bp_kpa),
              precip_mm = sum(rain_mm),
              Tmin = min(atep_C),
              Tmax = max(atep_C),
              Tmean = (Tmin+Tmax)/2,
              RH = mean(rh_per),
              RHmax = max(rh_per),
              RHmin = min(rh_per),
              u2_ms = mean(ws_ms),
              Rns_Wm2 = mean(Rns_Wm2),
              Rnl_Wm2 = mean(Rnl_Wm2))%>%
    mutate(y = (0.000665*bp_kpa), # psychrometric constant
           Rns_MJm2 = Rns_Wm2*0.0864,
           Rnl_MJm2 = Rnl_Wm2*0.0864,
           Rn = Rns_MJm2 - Rnl_MJm2,
           delta = 2503*(0.6108*exp((17.27*Tmean)/(Tmean+237.3)))/((Tmean + 237.3)^2), # slope of the
           vapor pressure curve
           eTmax = 0.6108*exp((17.27*Tmax)/(Tmax+237.3)),
           eTmin = 0.6108*exp((17.27*Tmin)/(Tmin+237.3)),
           es = (eTmax + eTmin) / 2,
           ea = (eTmin*RHmax/100 + eTmax*RHmin/100)/2)

  #what is being returned
  return(mdw)
}
```

R code for ET calculation

```
## -----  
##  
## Script name: daily_ET  
##  
## Purpose of script: estimate daily ET values  
##  
## Author: Brock Kamrath  
##  
## Date Created: 2020-06-26  
## Email: bjkamrat@ncsu.edu  
##  
## -----  
## Notes: The ET  
##  
## -----  
library(zoo)  
library(ggplot2)  
  
daily_et <- function(data){  
  # groundwater is 0  
  G <- 0  
  
  # Parameters for ET calculation  
  Cn <- 1600  
  Cd <- 0.38  
  # Calculation of reference ET using the ASCE standardized Reference ET Equation  
  mdw <- data %>%  
    mutate(ETrs = (0.408*delta*(Rn-G)+(y*(Cn/(Tmean+273))*u2_ms*(es-ea)))/  
             (delta + (y*(1+(Cd*u2_ms)))))  
  
  kco <- 1.0  
  #ET daily  
  mdw$ET <- kco*mdw$ETrs  
  
  #ET rolling mean over 3 days  
  mdw1 <- mdw %>%  
    select(date,srate=ET)%>%  
    mutate(ETc_ma07 = rollmean(srate,k=3,fill=NA))  
  
  ET_plot <- ggplot(mdw1)+  
    geom_line(aes(date,srate))+  
    geom_line(aes(date,ETc_ma07),color="blue")+  
    labs(x = "Date",y = "ET (mm/d)")  
  
  ggsave(filename = paste0("graphs/ET_plot.png"), plot = ET_plot, width = 12, height = 10, dpi = 300, units  
= "cm")  
  # select a group of output  
  output <- data.frame(mdw$date,mdw$precip_mm,mdw$ET)  
  colnames(output)<- c("date","precip_mm","ETc_mm")  
  
  #convert both precip and et to M3  
  output$W_temp <- mdw$water_temp  
  output$A_temp <- mdw$Tmean  
  output$A_temp_max <- mdw$Tmax  
  output$A_temp_min <- mdw$Tmin  
  output$wind <- mdw$u2_ms  
  output$net_rad <- mdw$Rn  
  
  colors <- c("Precip" = "blue", "ET" = "green", "Air Temp" = "orange", "Net Rad" = "red" )  
  
  weather_plot <- ggplot(output, aes(x=date))+  
    geom_line(aes(y = precip_mm, color="Precip"))+  
    geom_line(aes(y = ETc_mm,color="ET"))+  
    geom_line(aes(y = A_temp,color="Air Temp"))+  
  }
```

```
geom_line(aes(y = net_rad ,color="Net Rad"))+
labs(x = "Date",
     y = "multiple values",
     color = "Legend") +
scale_color_manual(values = colors)

ggsave(filename = paste0("graphs/weather_plot.png"), plot = weather_plot, width = 12, height = 10, dpi =
300, units = "cm")

# return dataset of precip and et for each day

return(output)
}
```

**APPENDIX C: LINEAR RELATIONSHIPS BETWEEN Q_{IN} AND Q_{OUT} AT BOTH
OUTLETS**

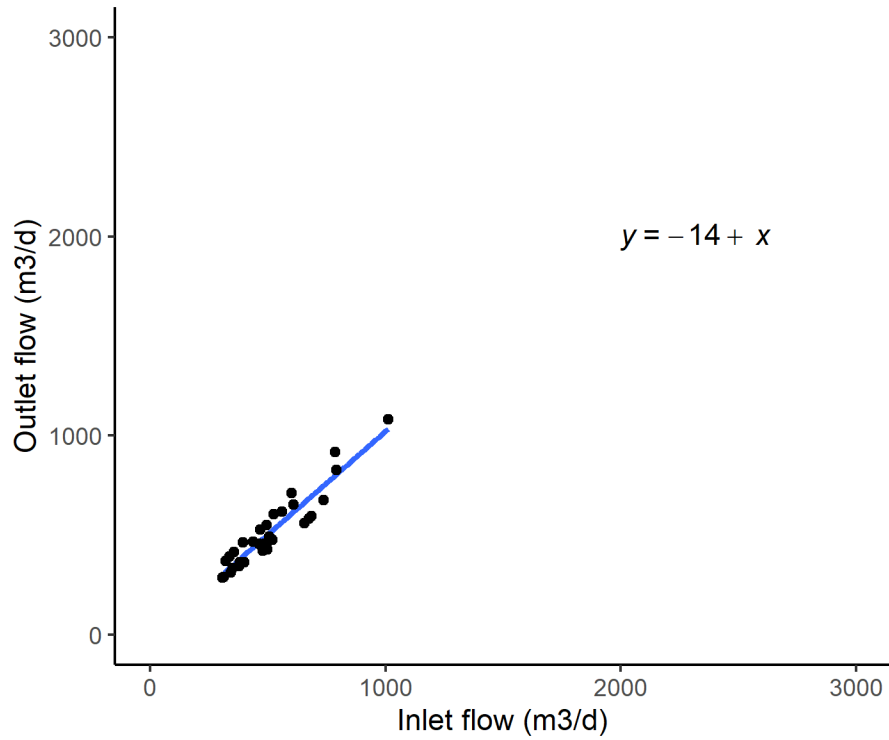


Figure C.1: Q_{out} v. Q_{in} relationship in wetland cell 1 for fall 2018. Erroneous values have been removed.

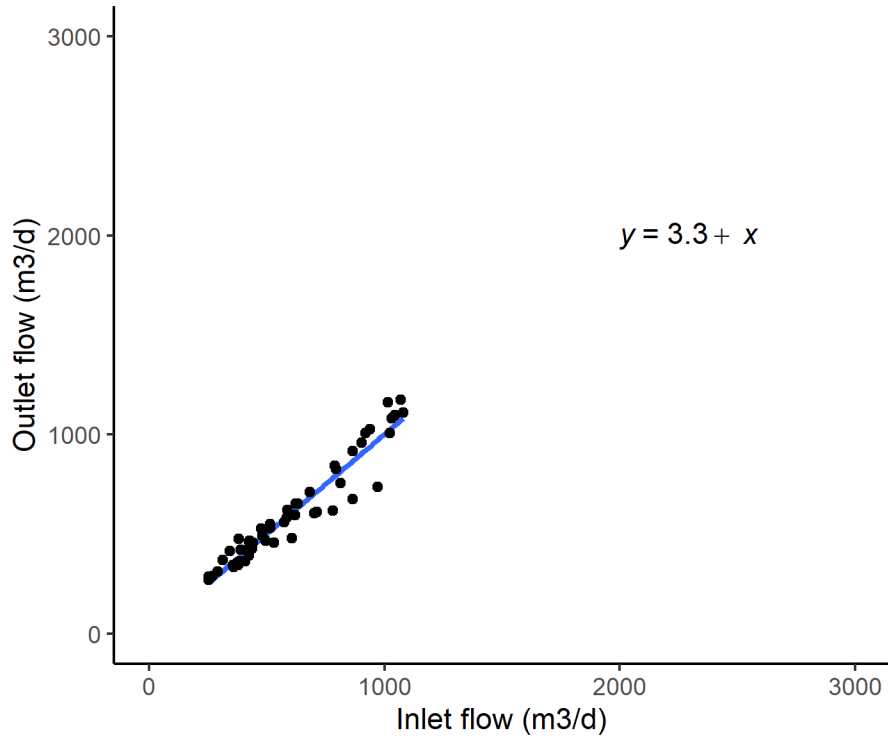


Figure C.2: Q_{out} v. Q_{in} relationship in wetland cell 2 for fall 2018. Erroneous values have been removed.

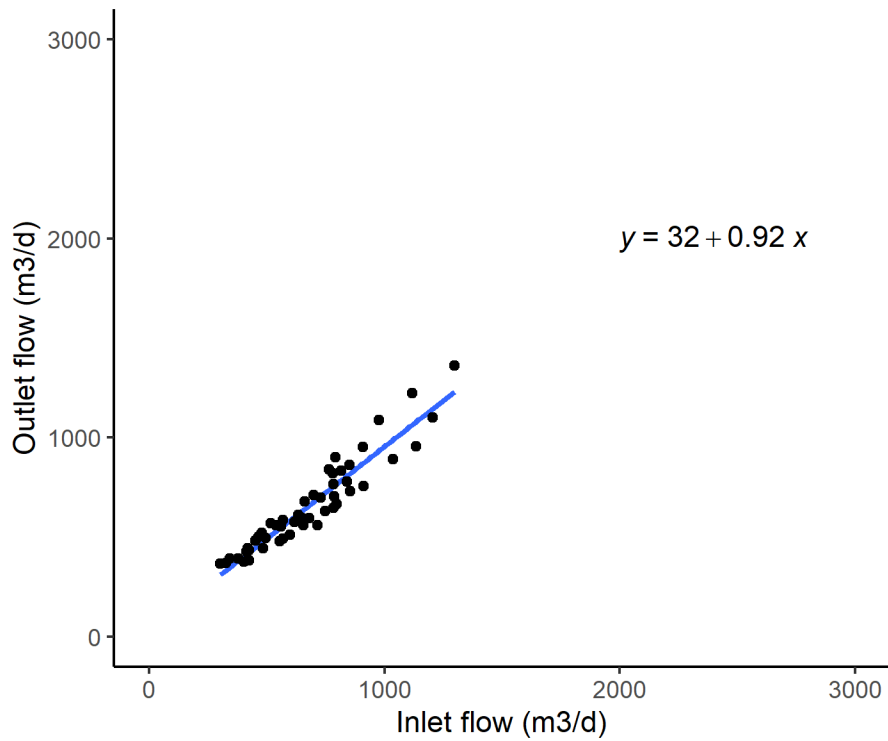


Figure C.3: Q_{out} v. Q_{in} relationship in wetland cell 1 for winter 2019. Erroneous values have been removed.

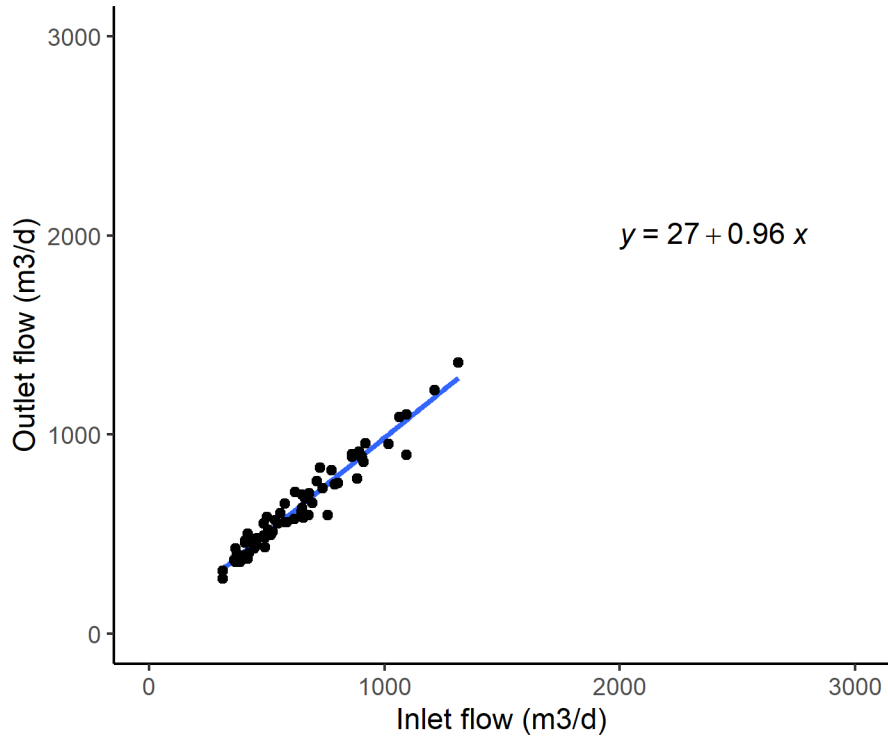


Figure C.4: Q_{out} v. Q_{in} relationship in wetland cell 2 for winter 2019. Erroneous values have been removed.

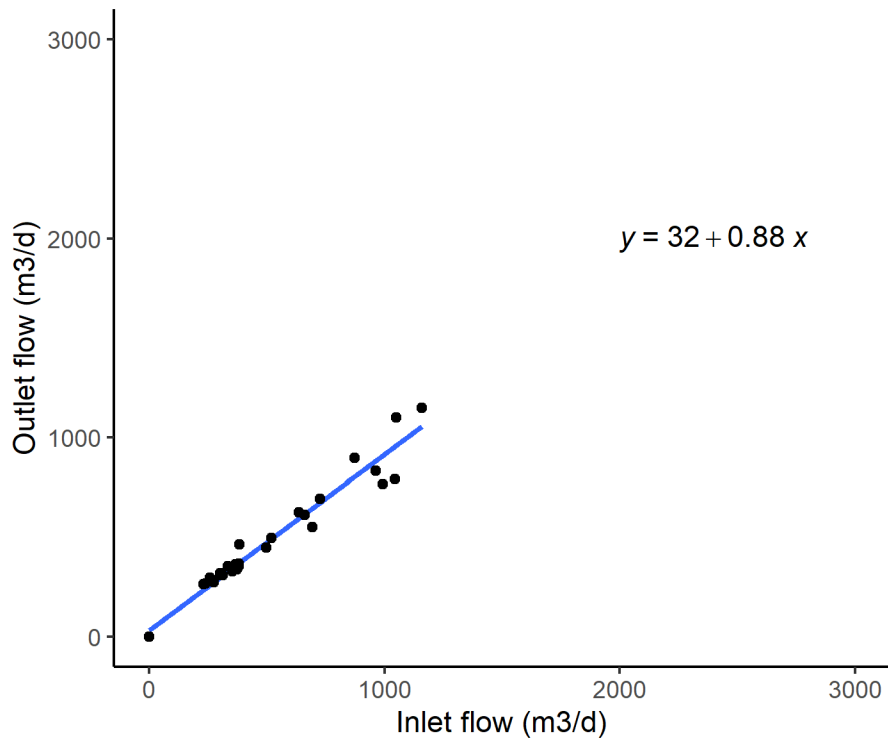


Figure C.5: Q_{out} v. Q_{in} relationship in wetland cell 1 for spring 2019. Erroneous values have been removed.

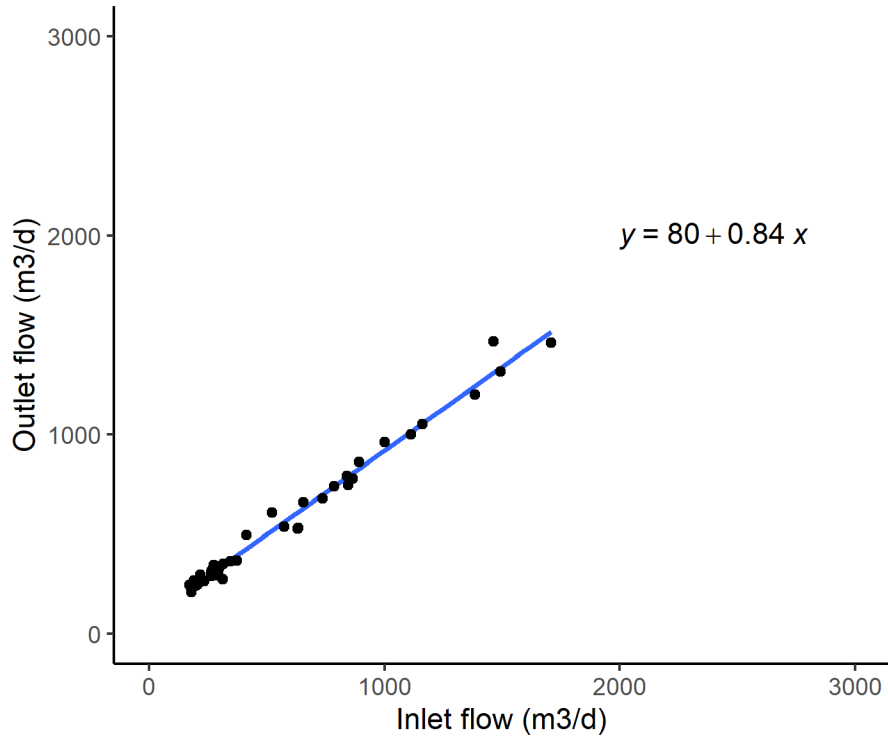


Figure C.6: Q_{out} v. Q_{in} relationship in wetland cell 2 for spring 2019. Erroneous values have been removed.

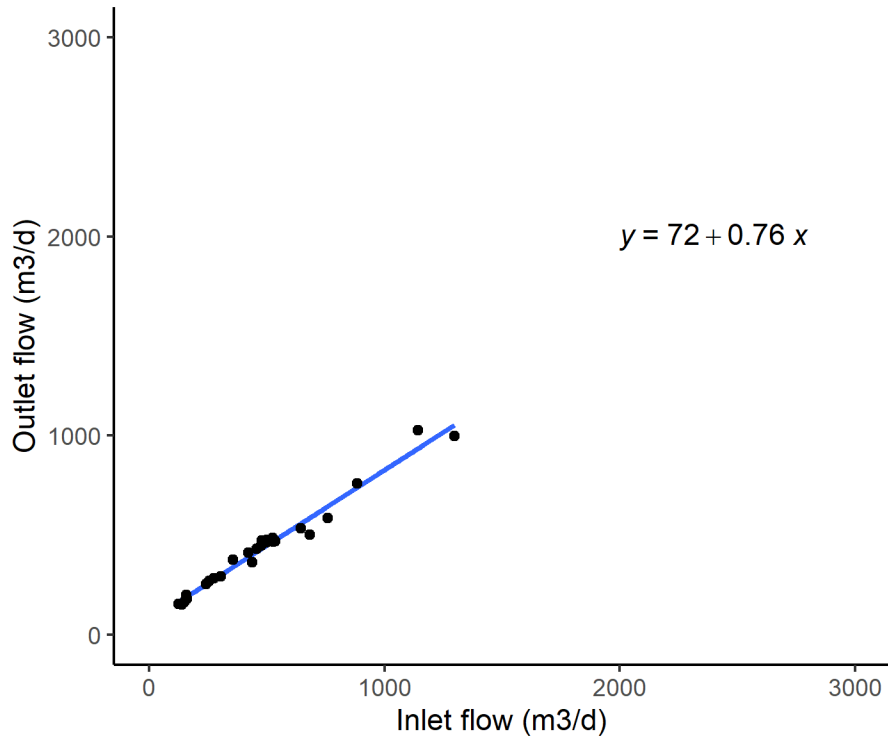


Figure C.7: Q_{out} v. Q_{in} relationship in wetland cell 1 for summer 2019. Erroneous values have been removed.

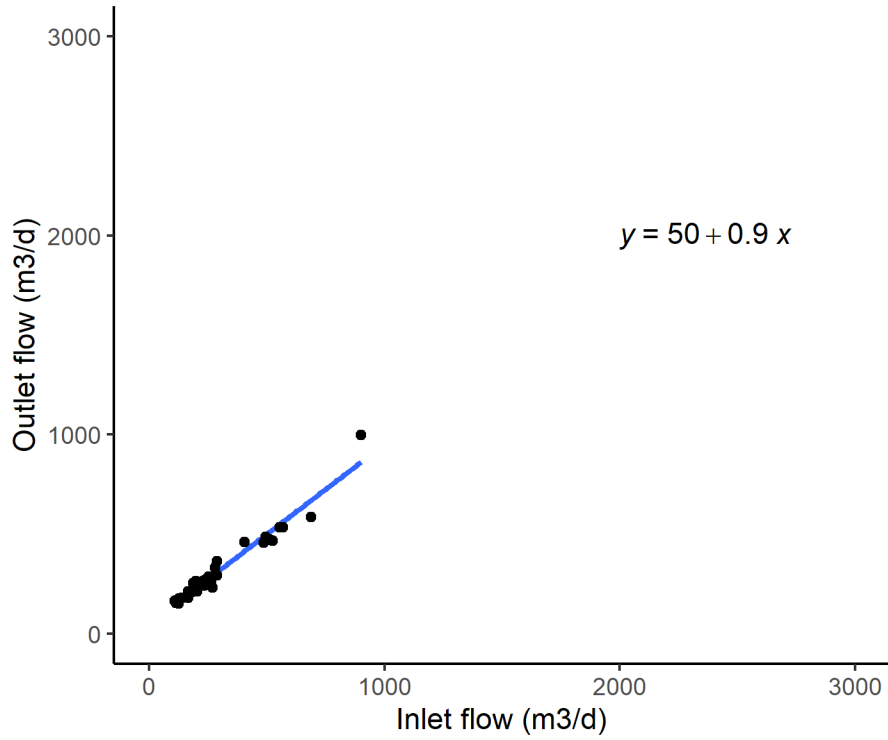


Figure C.8: Q_{out} v. Q_{in} relationship in wetland cell 2 for summer 2019. Erroneous values have been removed.

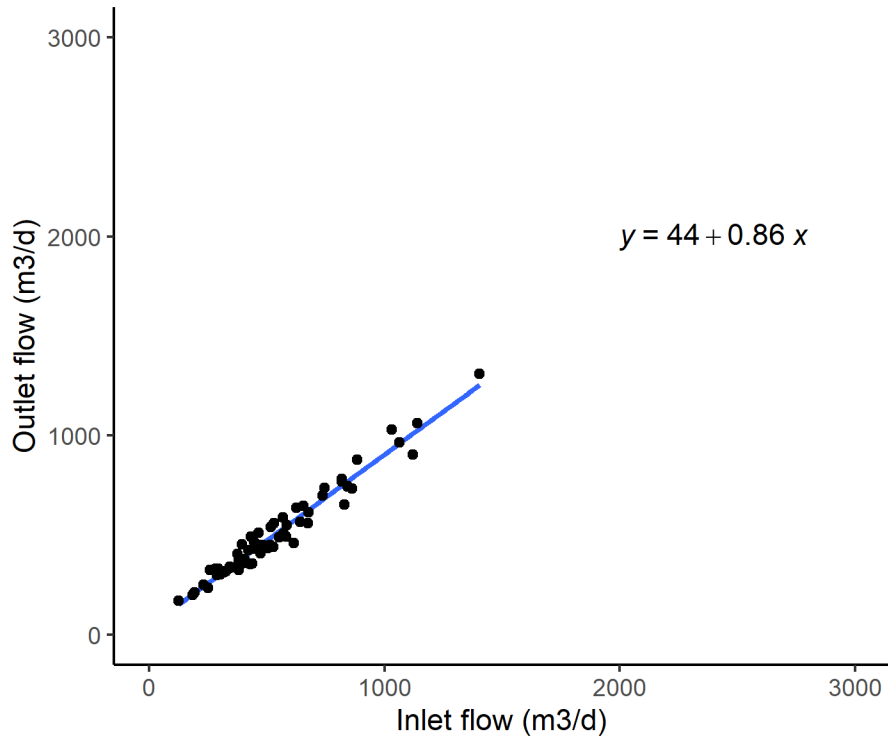


Figure C.9: Q_{out} v. Q_{in} relationship in wetland cell 1 for fall 2019. Erroneous values have been removed.

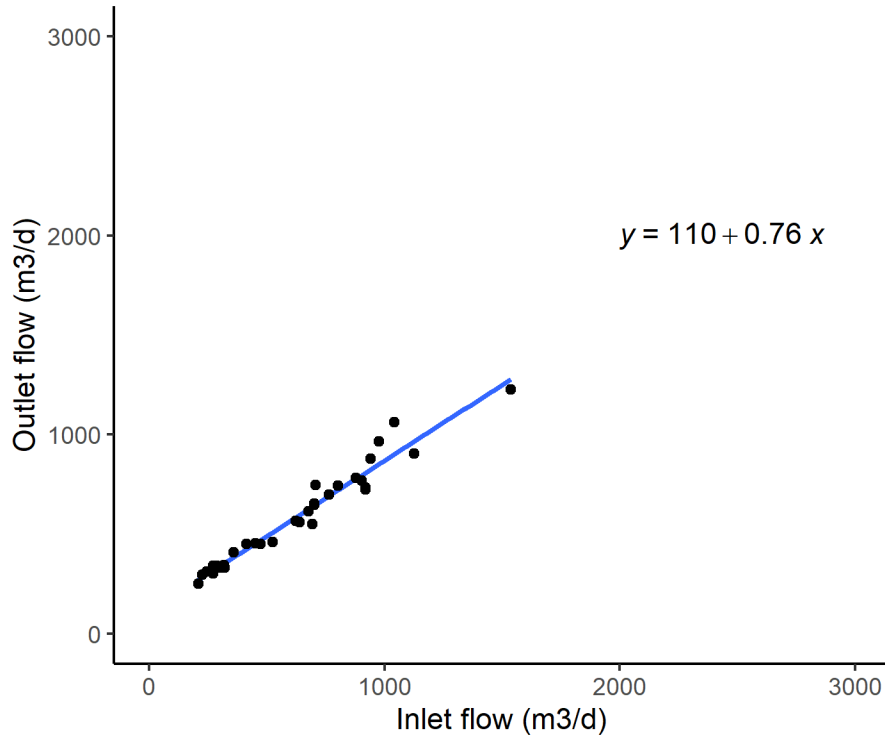


Figure C.10: Q_{out} v. Q_{in} relationship in wetland cell 2 for fall 2019. Erroneous values have been removed.

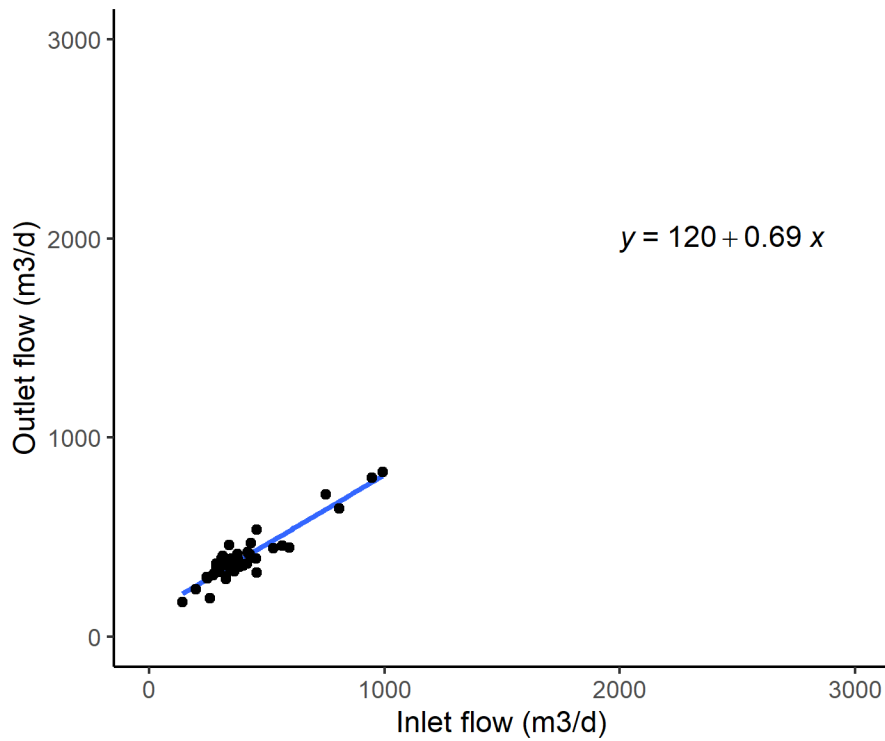


Figure C.11: Q_{out} v. Q_{in} relationship in wetland cell 1 for winter 2020. Erroneous values have been removed.

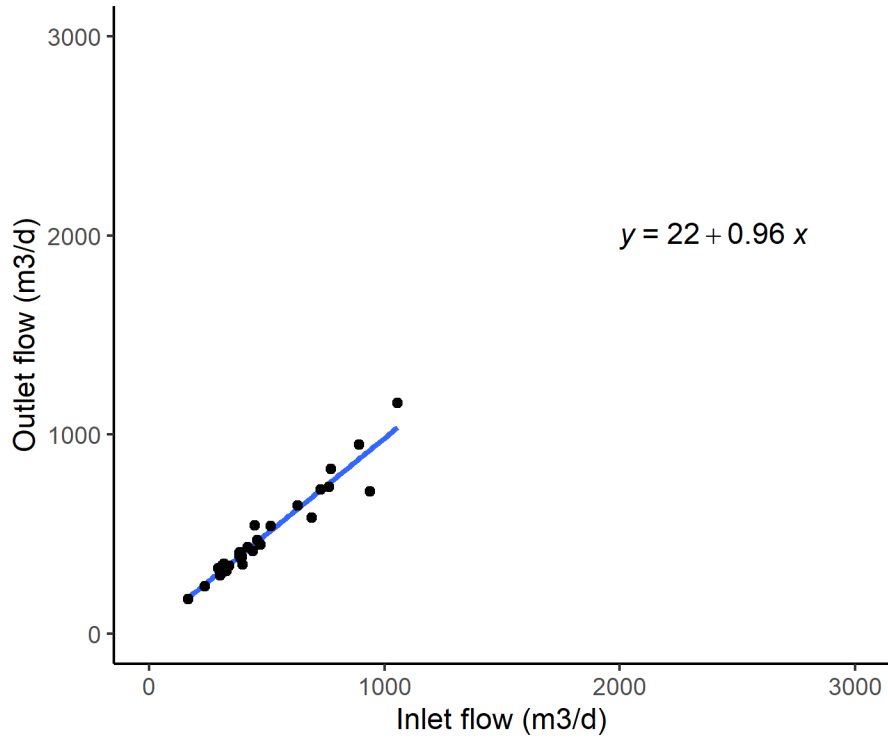


Figure C.12: Q_{out} v. Q_{in} relationship in wetland cell 2 for winter 2020. Erroneous values have been removed.

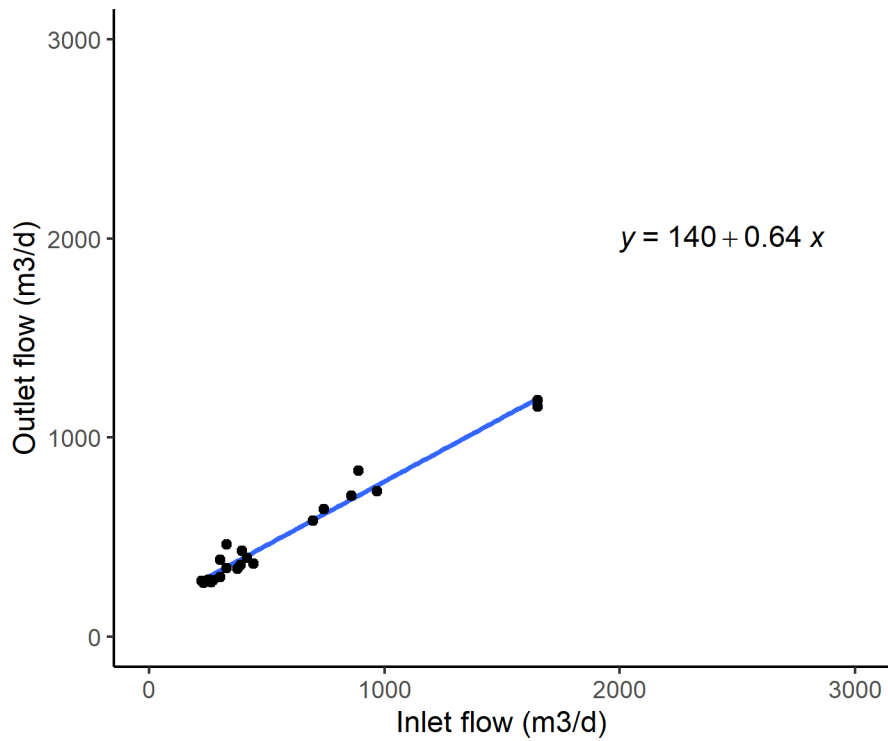


Figure C.13: Q_{out} v. Q_{in} relationship in wetland cell 1 for spring 2020. Erroneous values have been removed.

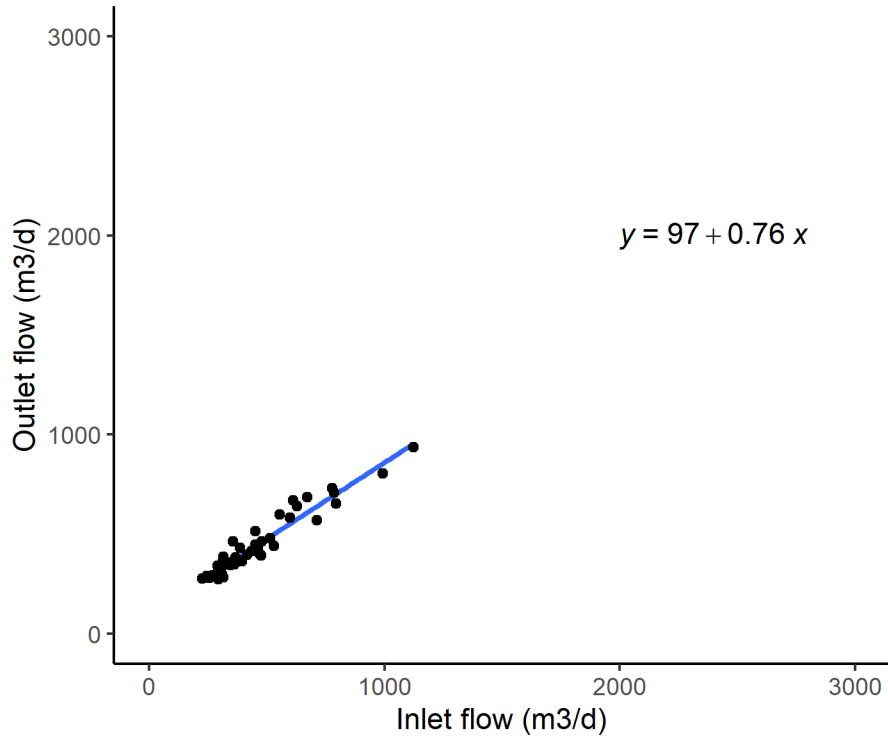


Figure C.14: Q_{out} v. Q_{in} relationship in wetland cell 2 for spring 2020. Erroneous values have been removed.

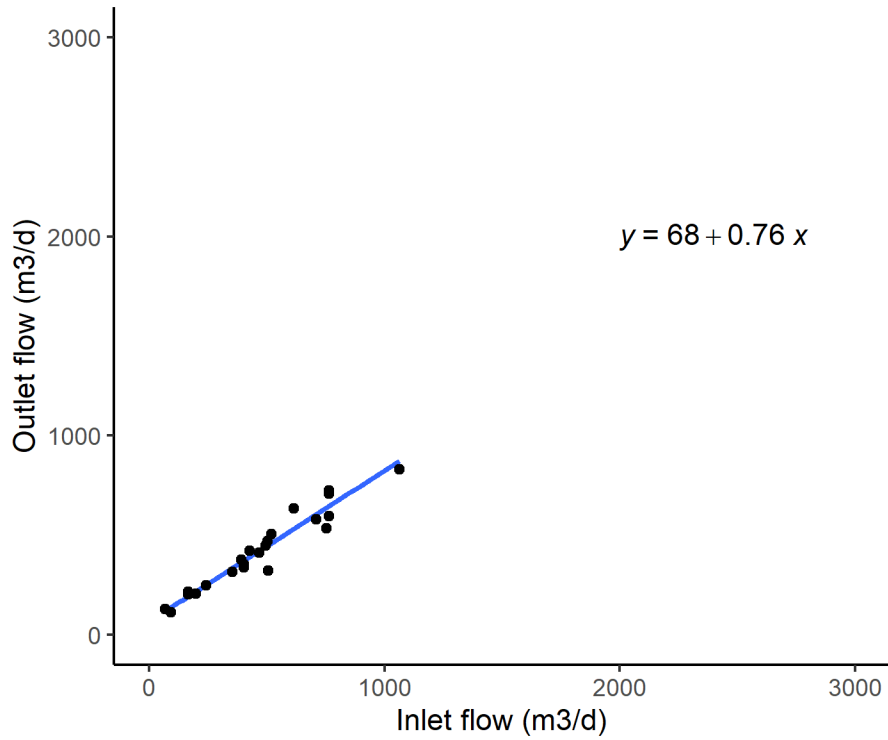


Figure C.15: Q_{out} v. Q_{in} relationship in wetland cell 1 for summer 2020. Erroneous values have been removed.

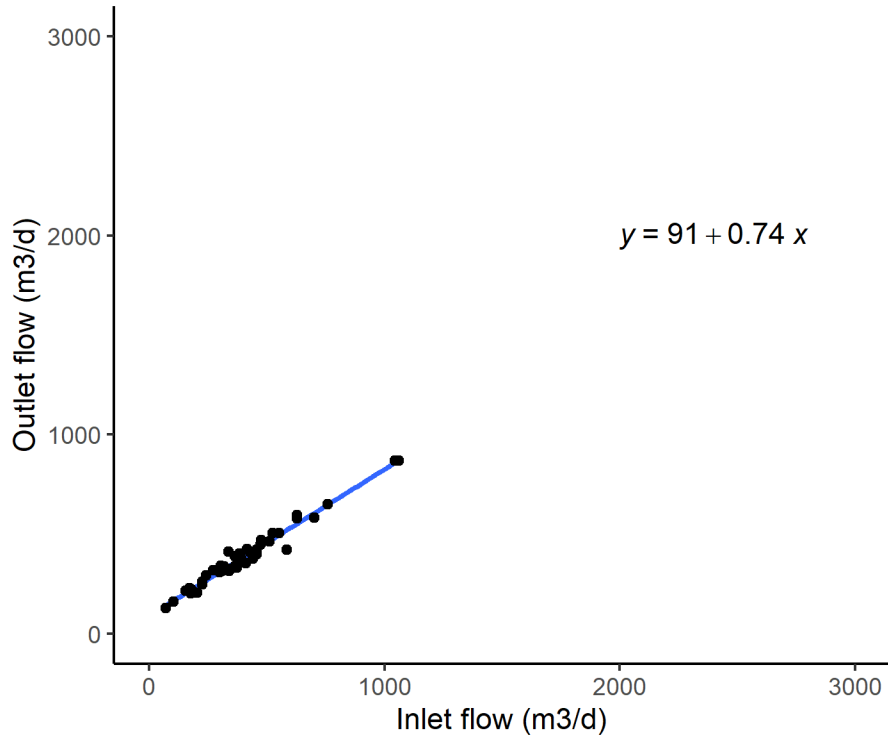


Figure C.16: Q_{out} v. Q_{in} relationship in wetland cell 2 for summer 2020. Erroneous values have been removed.

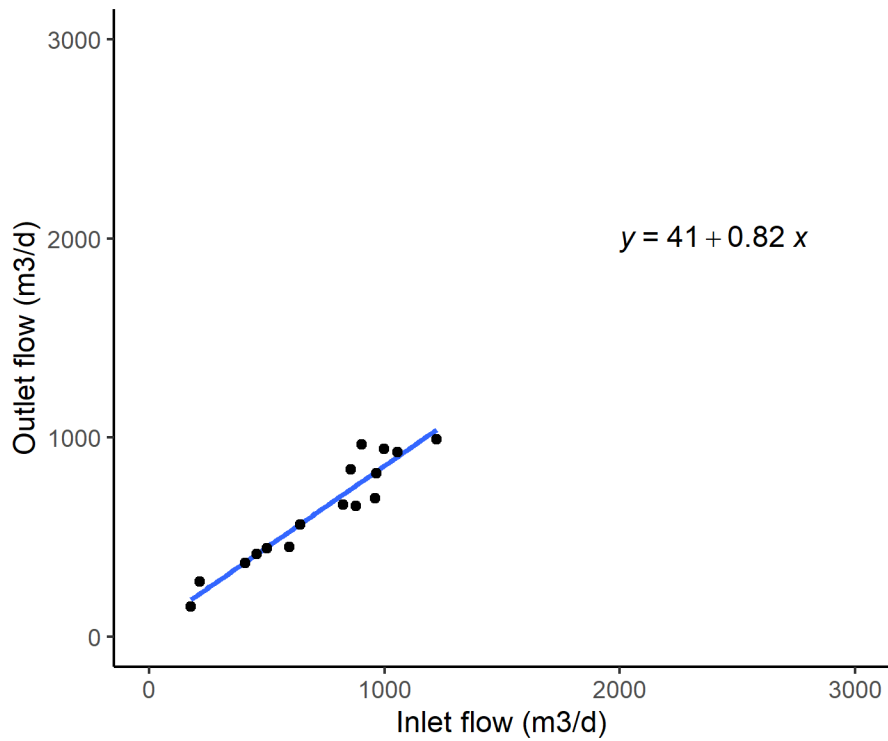


Figure C.17: Q_{out} v. Q_{in} relationship in wetland cell 1 for fall 2020. Erroneous values have been removed.

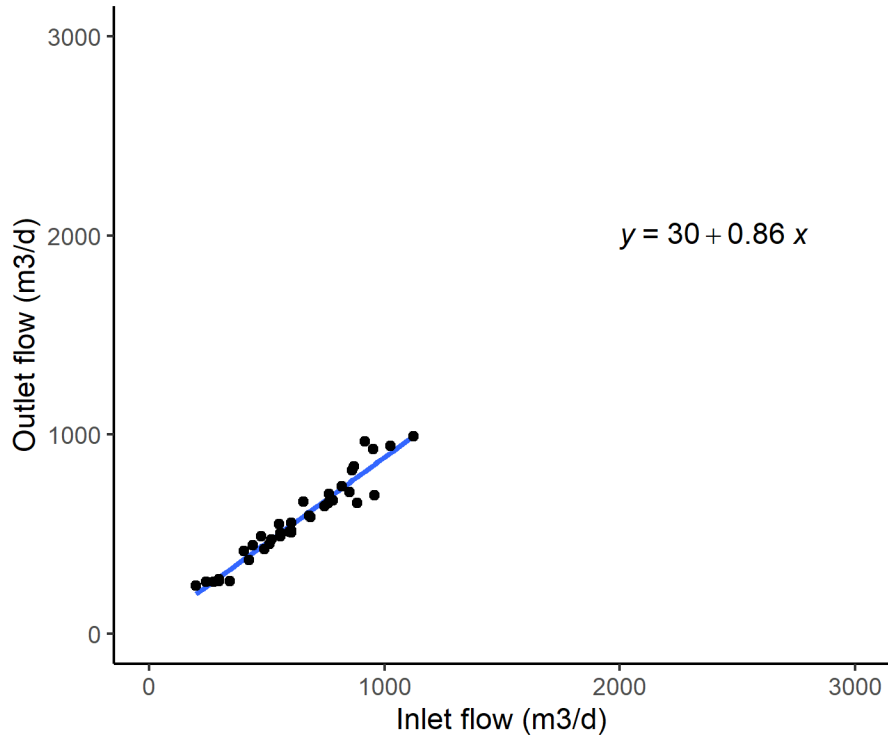


Figure C.18: Q_{out} v. Q_{in} relationship in wetland cell 2 for fall 2020. Erroneous values have been removed.

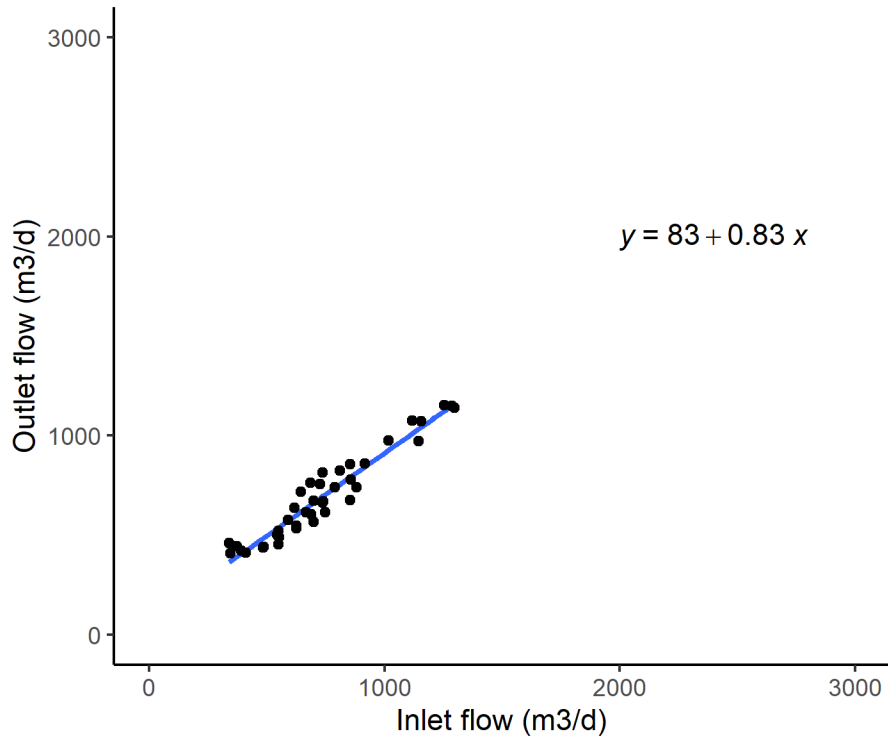


Figure C.19: Q_{out} v. Q_{in} relationship in wetland cell 1 for winter 2021. Erroneous values have been removed.

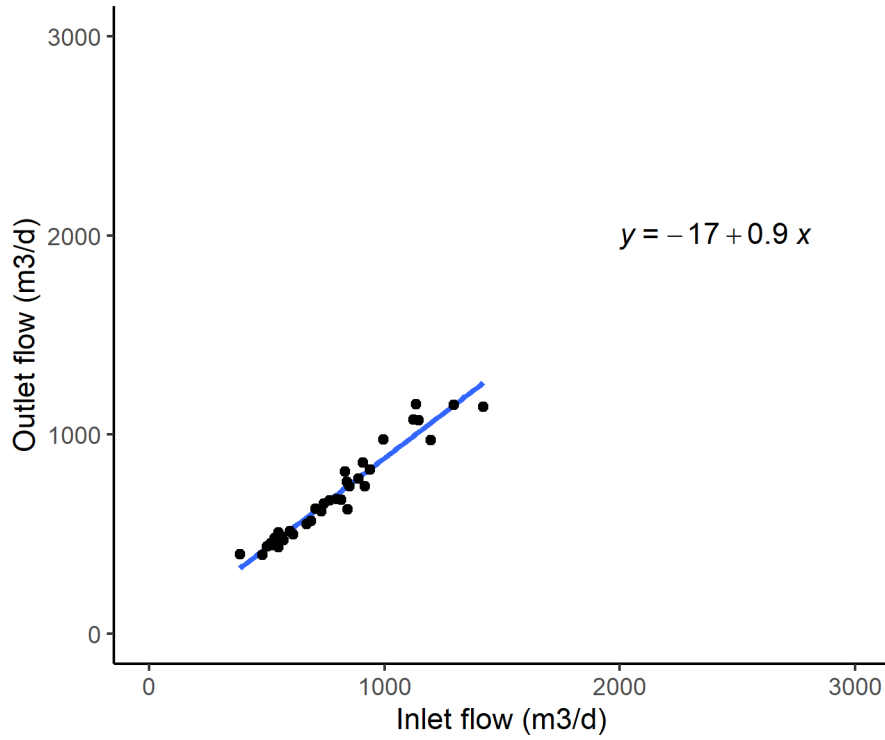


Figure C.20: Q_{out} v. Q_{in} relationship in wetland cell 2 for winter 2021. Erroneous values have been removed.

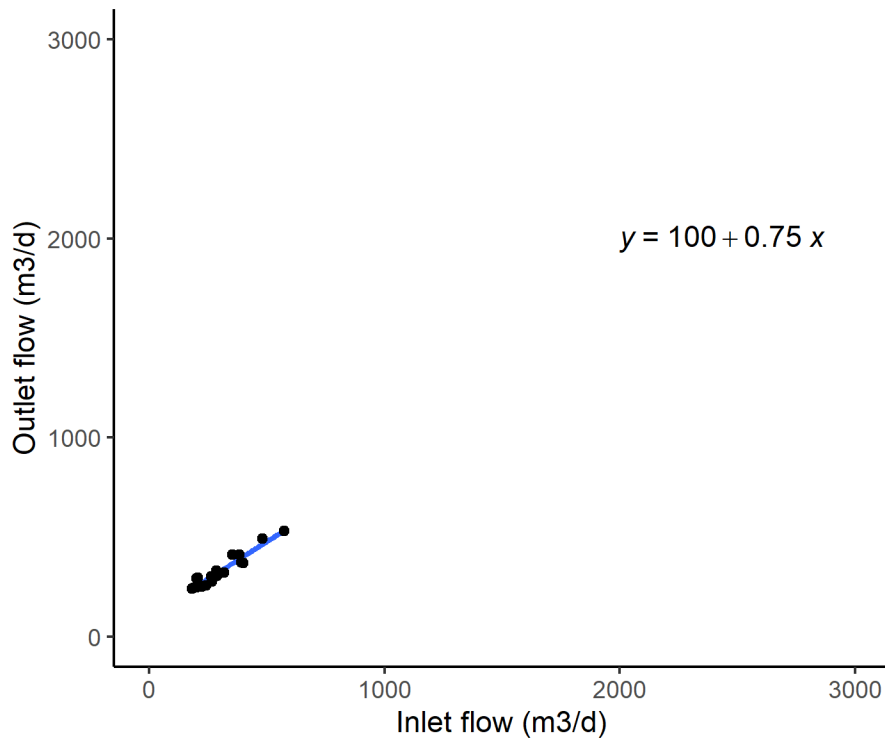


Figure C.21: Q_{out} v. Q_{in} relationship in wetland cell 1 for spring 2021. Erroneous values have been removed.

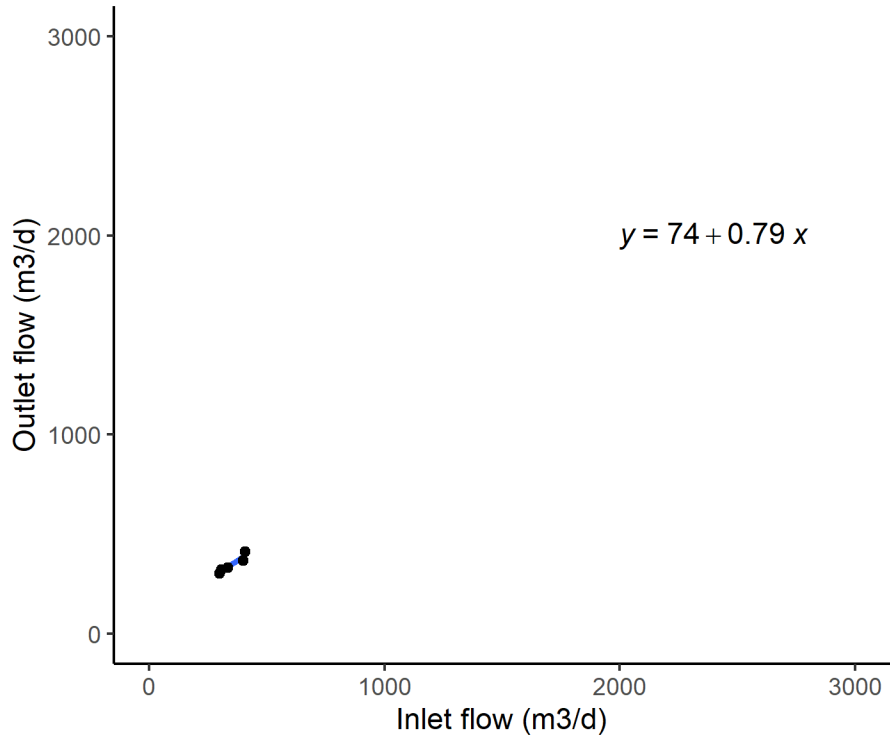


Figure C.22: Q_{out} v. Q_{in} relationship in wetland cell 2 for spring 2021. Erroneous values have been removed.

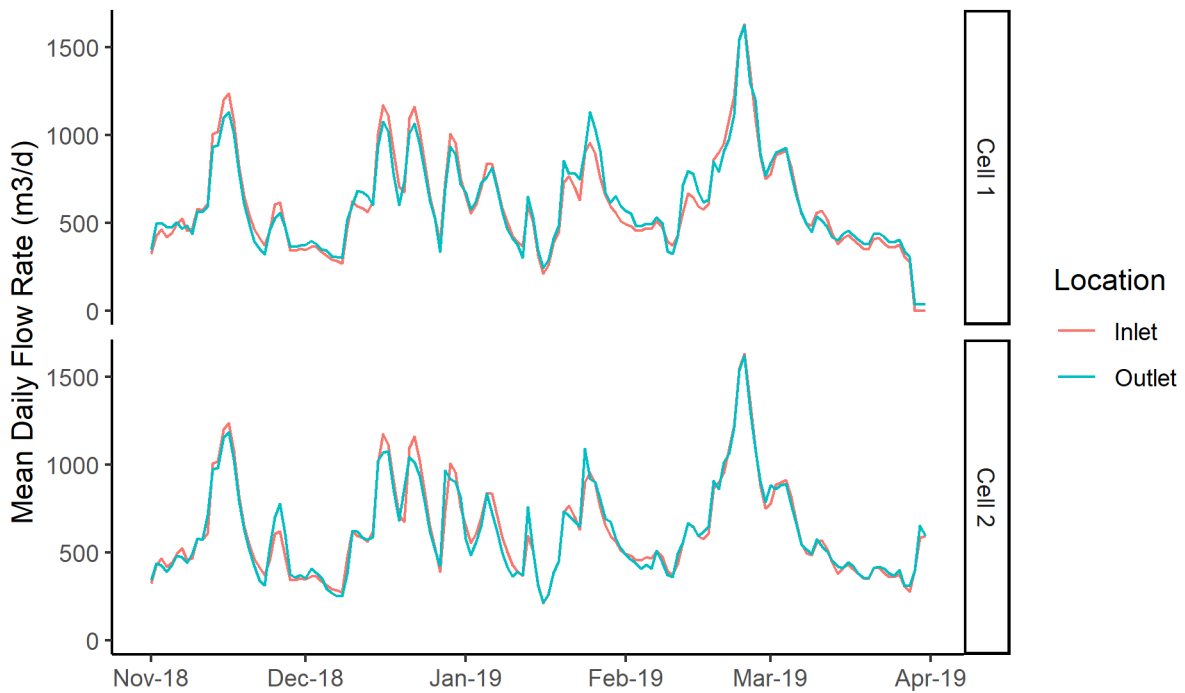


Figure C.23: Filled mean daily flow during the pre-detritus cleanout period (Nov 18 – Apr 19).

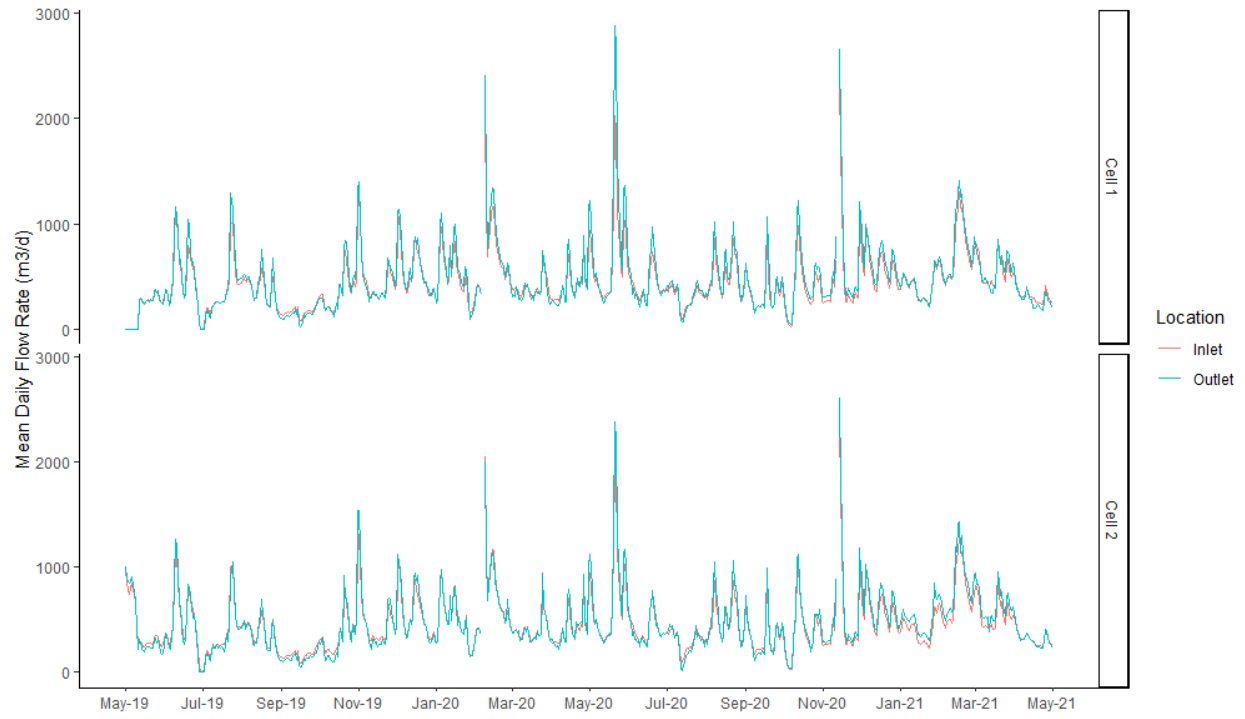


Figure C.24: Filled mean daily flow during the pre-detritus cleanout period (May 19 – May 21).

APPENDIX D: CHAPTER III SUPPLEMENTAL INFORMATION

Porewater sampling

Two porewater experiments were conducted; one in October 2019 and another in January 2020. In the October experiment, two porewater samplers (Figure D.1) were installed into the surface of the accumulated detritus substrate, which was above the water level. The samplers were submerged into the detritus up to the fifth slot in the samplers and left for one week. After one week, the porewater samplers were removed from the detritus. The water was extracted from each slot using a syringe, placed in 15 mL test tubes, and transported back to Weaver Laboratories on ice. Water quality samples were analyzed immediately using a HACH DR3900 Spectrophotometer (HACH, Loveland, CO). Samples were analyzed for ammonium concentrations (mg-N L^{-1} or g-N m^{-3}) using TNTplus 832 vials and the USEPA compliant method 10205. In the second experiment, we aimed to observe a complete porewater profile. Sampler 1 was installed 5 slots deep into the underlying clay layer, while sampler 2 was installed into the muck surface 2 meters away.



Figure D.1: Photograph of both porewater samplers used in the porewater experiments.

Nitrogen content in detritus substrate

The amount of nitrogen within the detritus was estimated using the nitrogen content, substrate bulk density, and the estimated volume of substrate in each microcosm. The detritus substrate was added while still moist to preserve microbial communities within the substrate. Therefore, the weight of the substrate added to the microcosm was a wet weight. To obtain the dry weight of the detritus in the microcosms, the substrate bulk density (0.17 g/cm^3), obtained in a previous sampling muck, was multiplied by the approximate volume of substrate in the microcosm (10 cm x 13 cm x 20 cm). This estimated dry weight of 0.5 kg was then multiplied by the average nitrogen content in the detritus.

Table D.1: Nitrogen content of detritus substrate in microcosms prior to experiment initiation.

Experimental Run	Nitrogen content (mg/kg-DW)	Estimate of N in microcosm substrate (g)
1	7270	3.6
2	5950	3.0
3	3824	1.9

Nitrate concentration dynamics in microcosms

Nitrate concentrations increased in each experimental run after approximately seven days (Table A2, Figure A1). The magnitude of increase changed between runs; the first run (Run 1) had the lowest nitrate increase in the last run (Run 3) had the greatest nitrate increase. The nitrate increase can likely be attributed to nitrification within the wetland microcosms but is unclear why the magnitude of the increase changed. It is suggested by the authors that the extra time between sampling periods in Run 1 likely allowed time for denitrification to remove some of the produced nitrate. Nitrate dynamics were not a focus of the experiment, instead they were a check on potential nitrification within the microcosms.

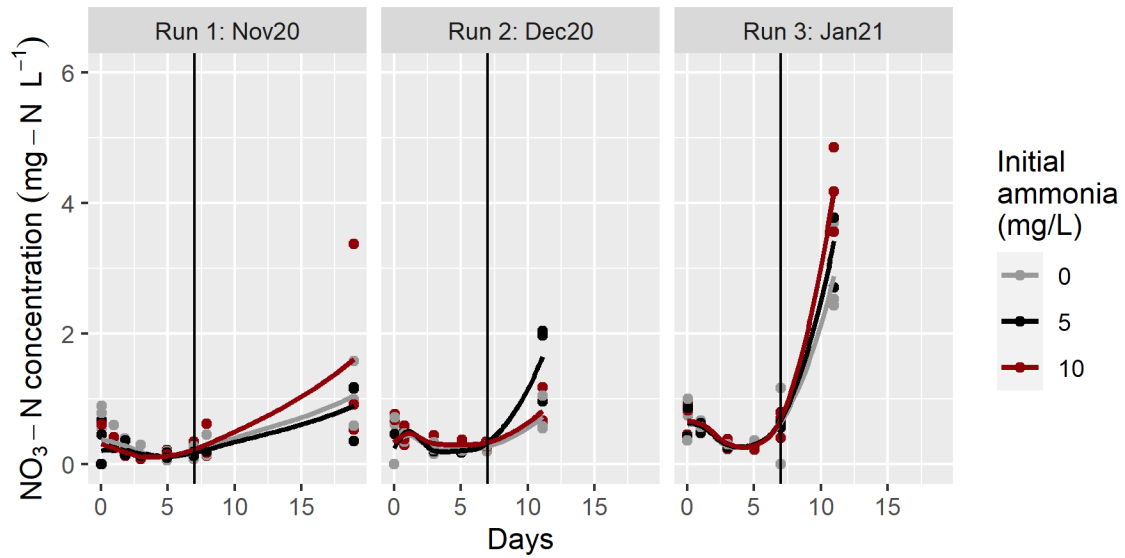


Figure D.2: $\text{NO}_3\text{-N}$ concentrations for each treatment in each run for all sampling dates. The black vertical line represents day 7. The MDL for nitrate was 0.23 mg-N L^{-1} .

Table D.2: Mean nitrate concentrations in the water column in the period from day 0 to day 7 and the mean nitrate concentrations in the period after day 7.

Experimental Run	Day 0-7	Day > 7
1	0.2	0.7
2	0.3	1.1
3	0.5	3.5
Overall	0.3	1.5

First-order kinetic models for each experimental unit

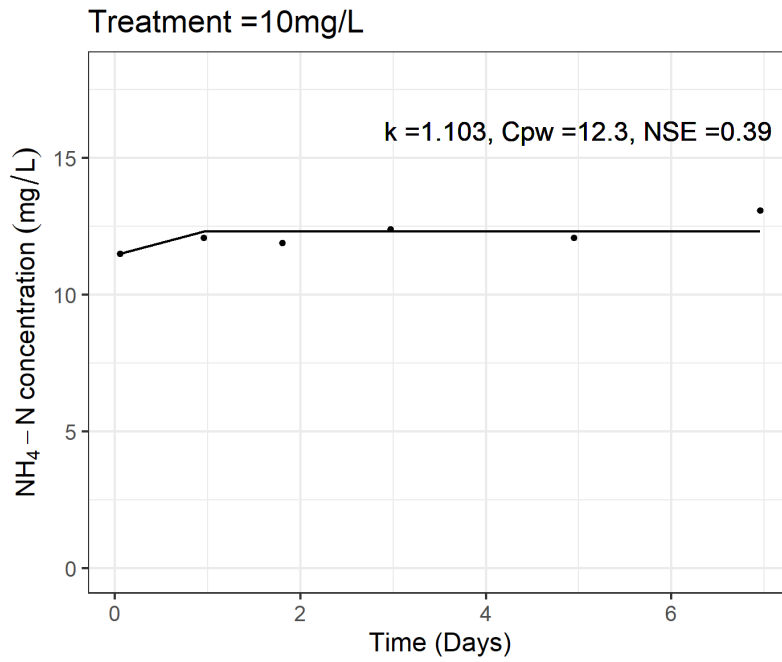


Figure D.3: experimental unit 1 – Run 1.

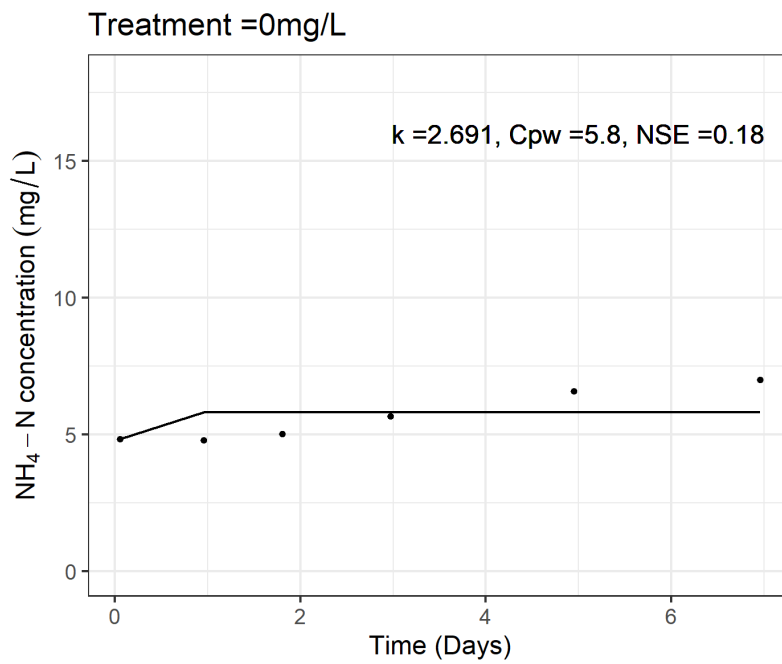


Figure D.4: experimental unit 2 – Run 1.

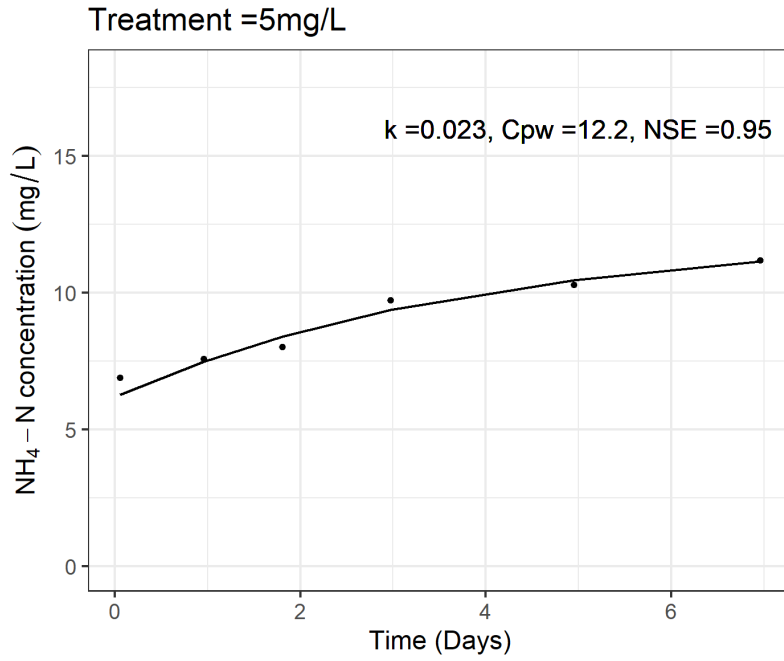


Figure D.5: experimental unit 3 – Run 1.

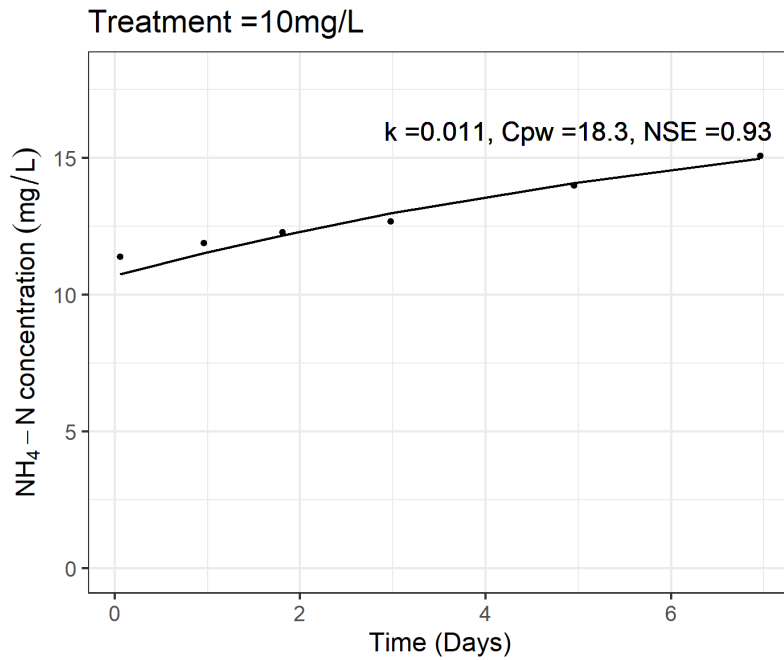


Figure D.6: experimental unit 4 – Run 1.

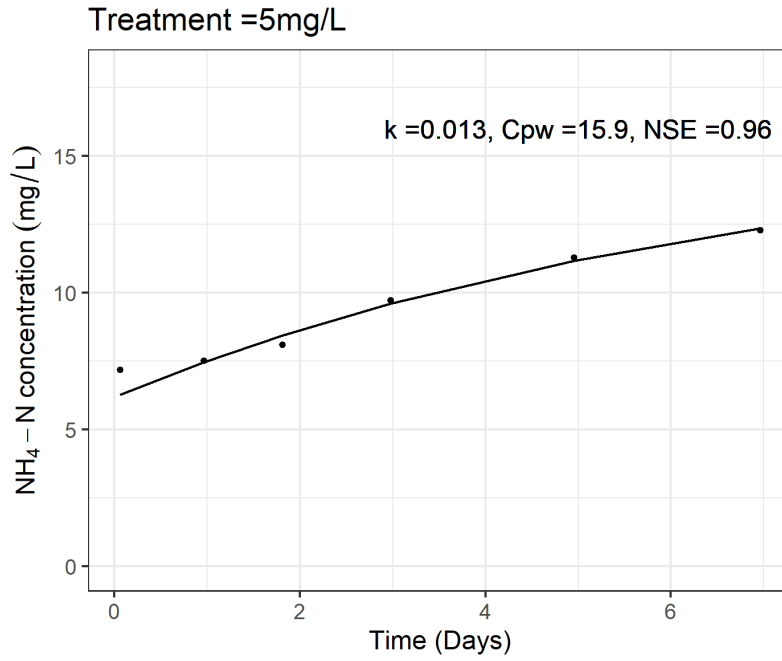


Figure D.7: experimental unit 5 – Run 1.

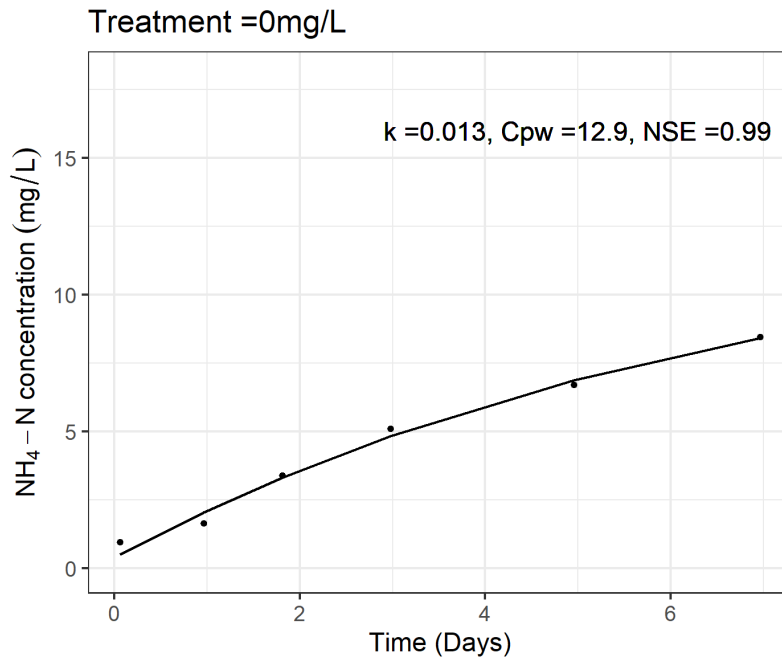


Figure D.8: experimental unit 6 – Run 1.

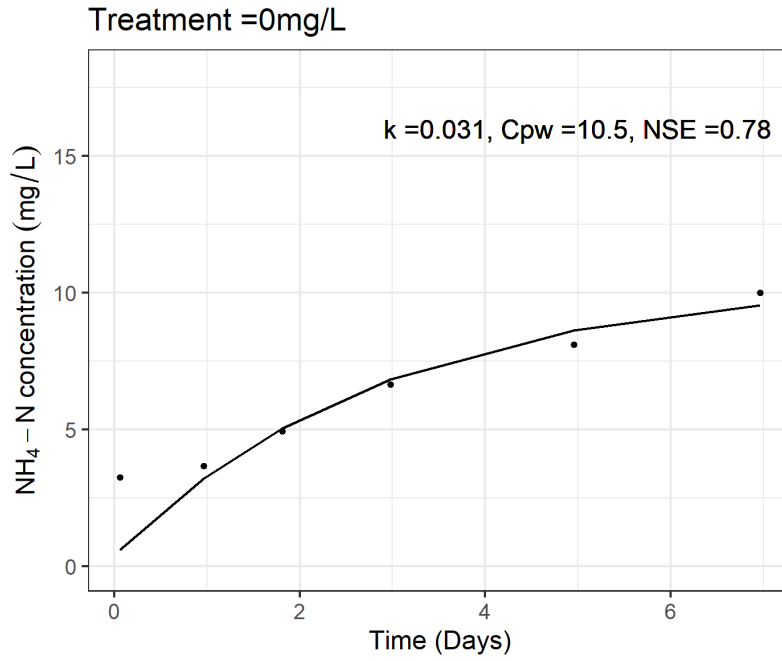


Figure D.9: experimental unit 7 – Run 1.

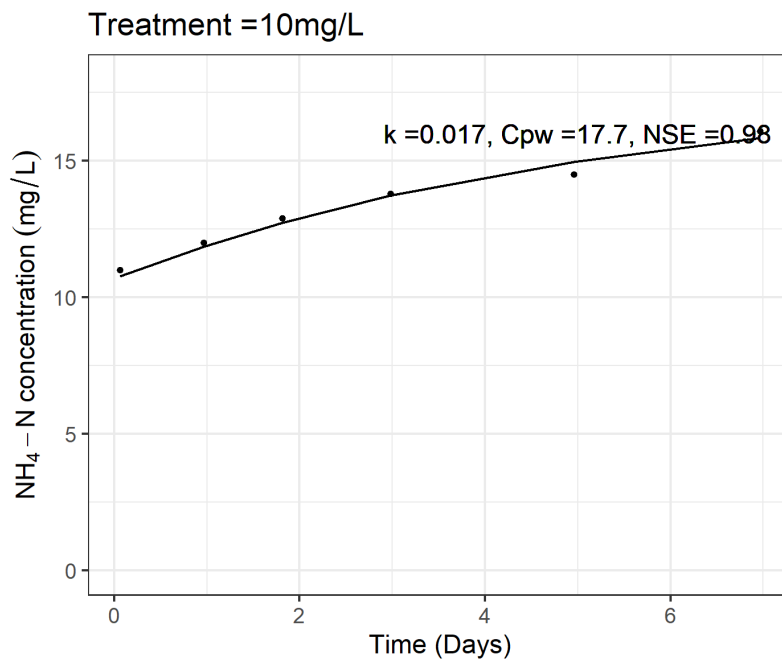


Figure D.10: experimental unit 8 – Run 1.

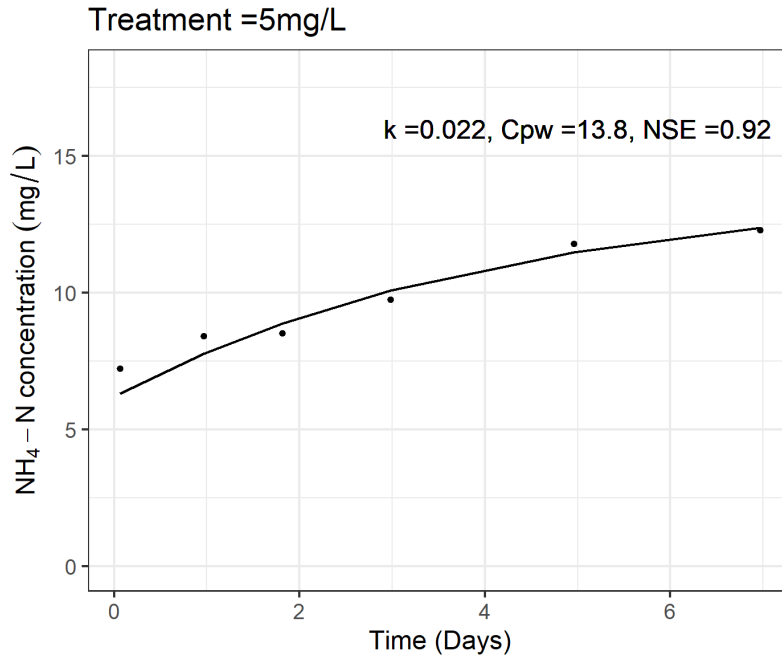


Figure D.11: experimental unit 9 – Run 1.

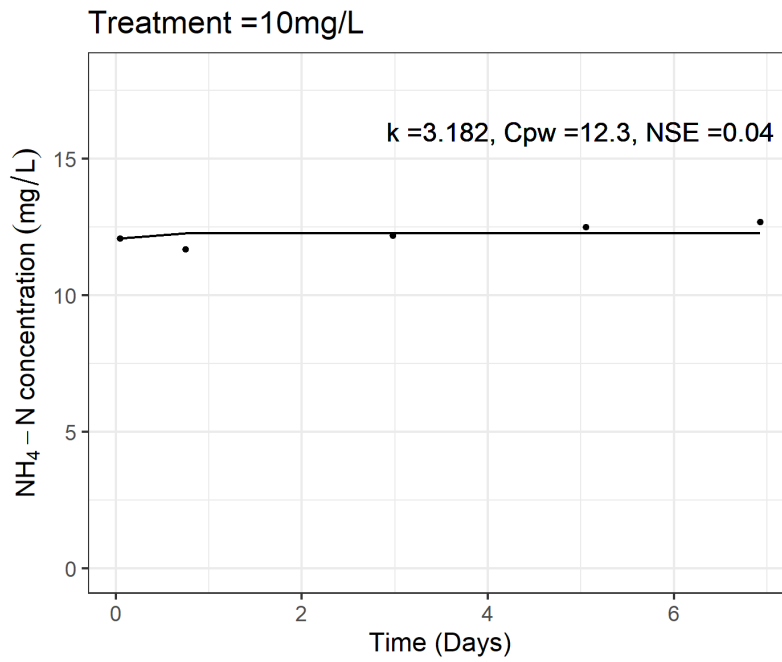


Figure D.12: experimental unit 10 – Run 2.

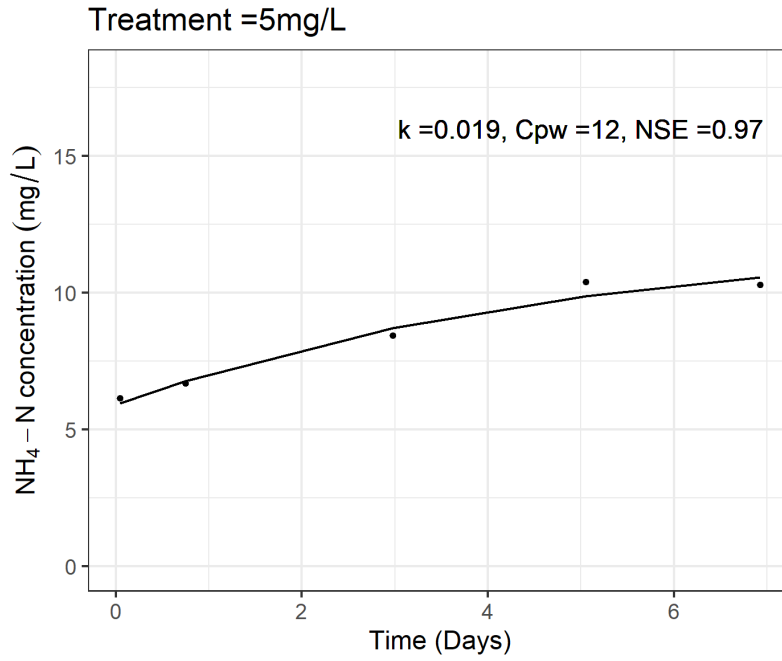


Figure D.13: experimental unit 11 – Run 2.

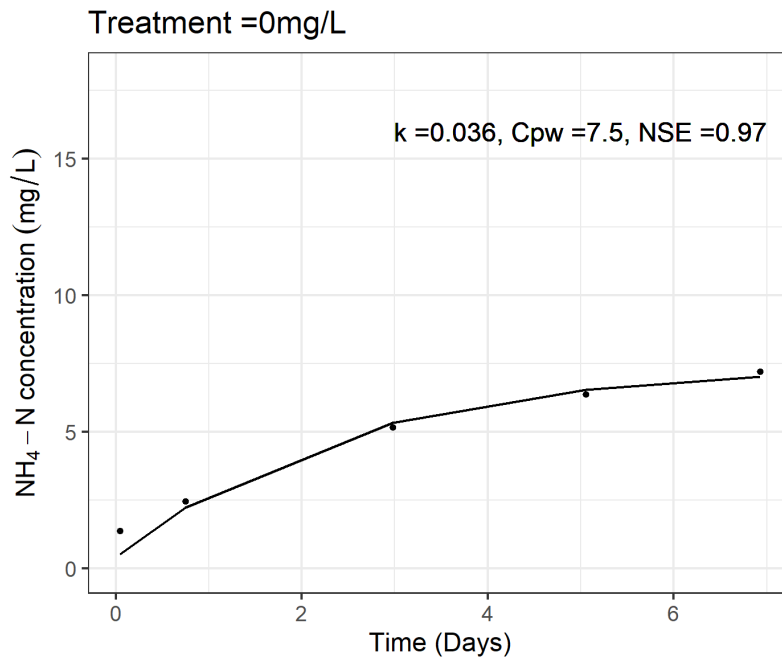


Figure D.14: experimental unit 12 – Run 2.

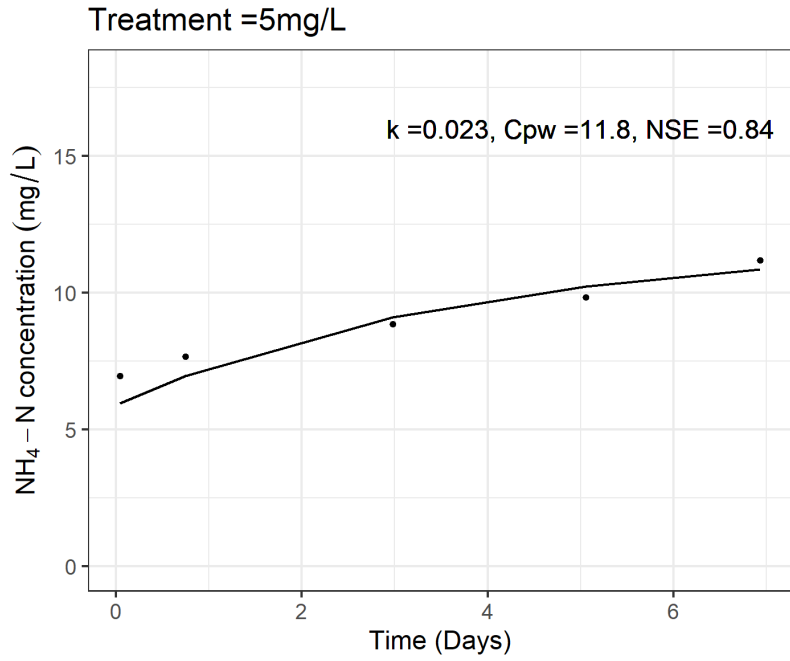


Figure D.15: experimental unit 13 – Run 2.

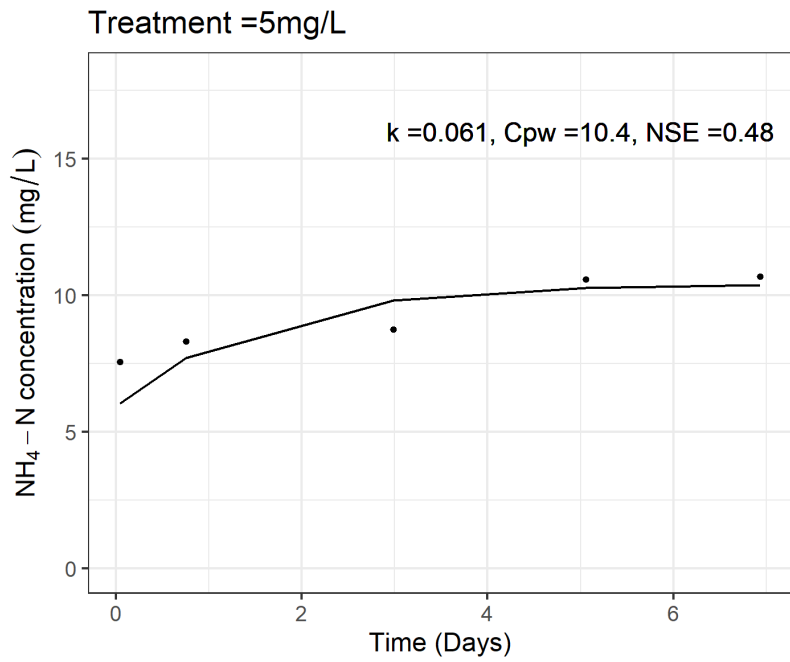


Figure D.16: experimental unit 14 – Run 2.

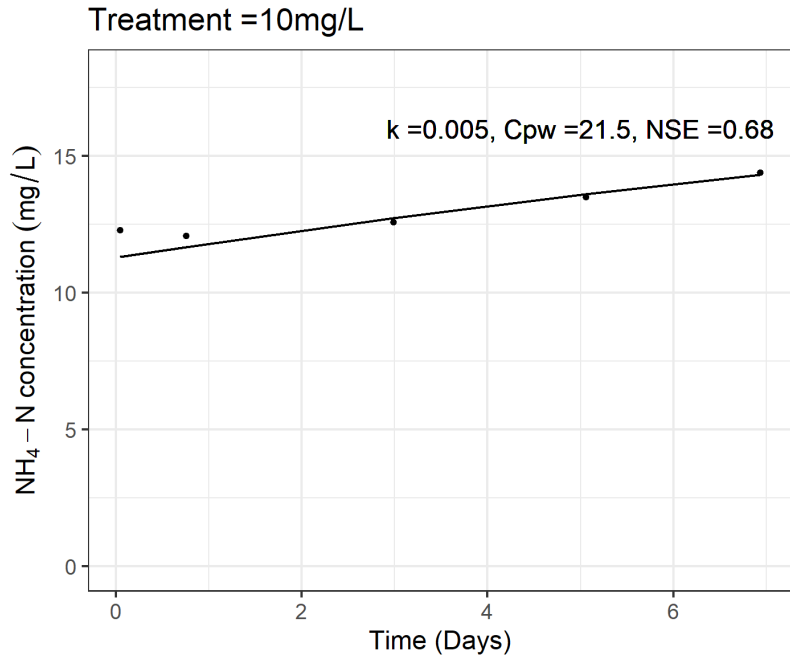


Figure D.17: experimental unit 15 – Run 2.

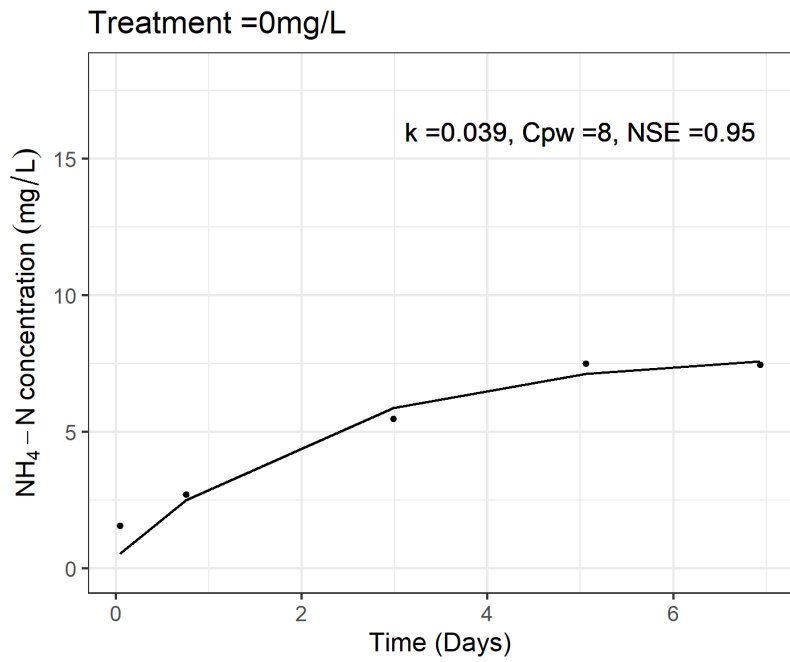


Figure D.18: experimental unit 16 – Run 2.

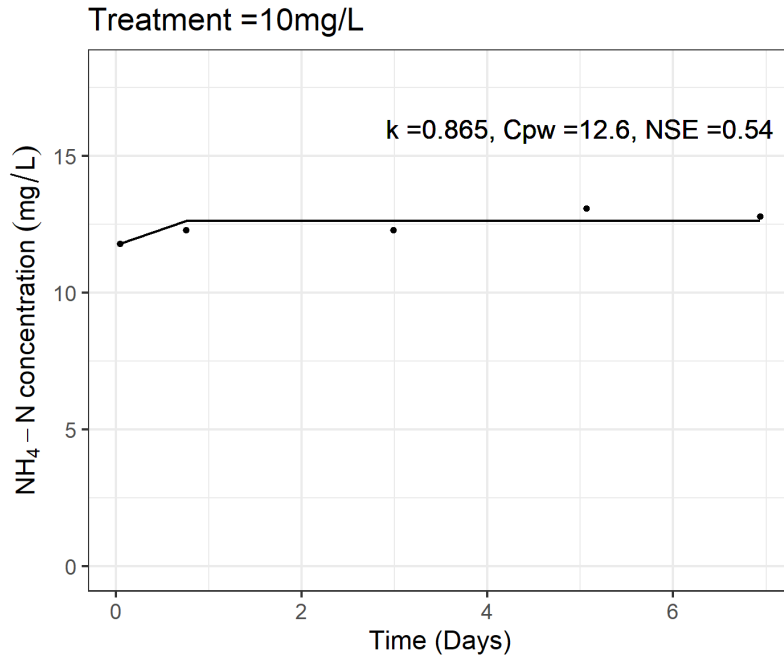


Figure D.19: experimental unit 17 – Run 2.

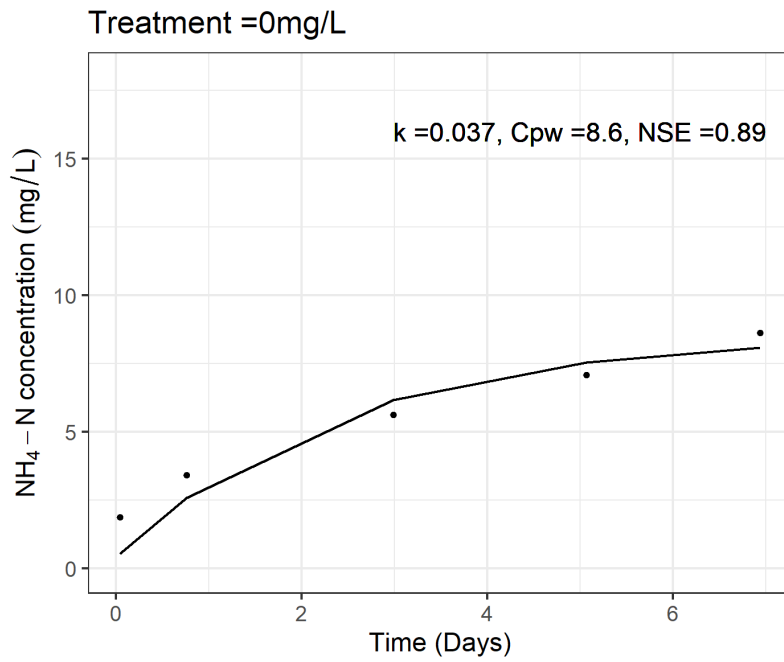


Figure D.20: experimental unit 18 – Run 2.

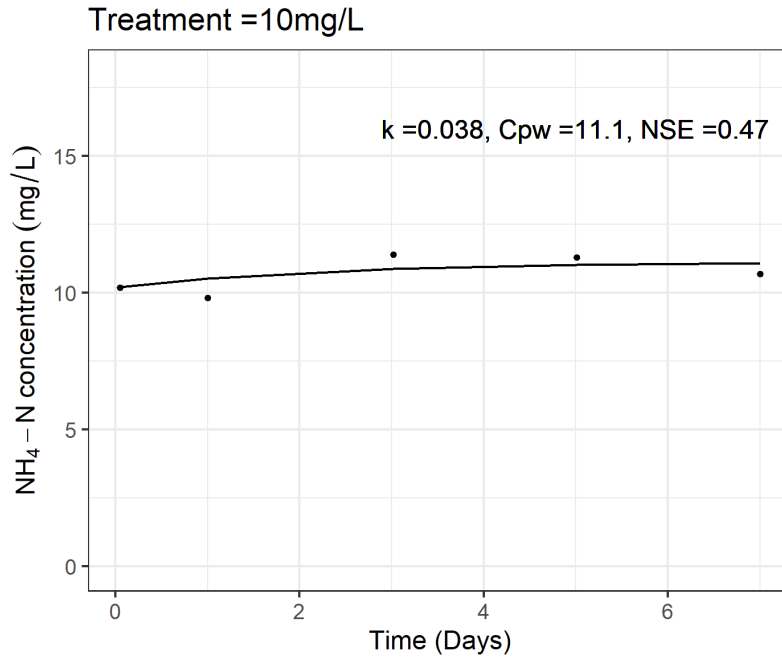


Figure D.21: experimental unit 19 – Run 3.

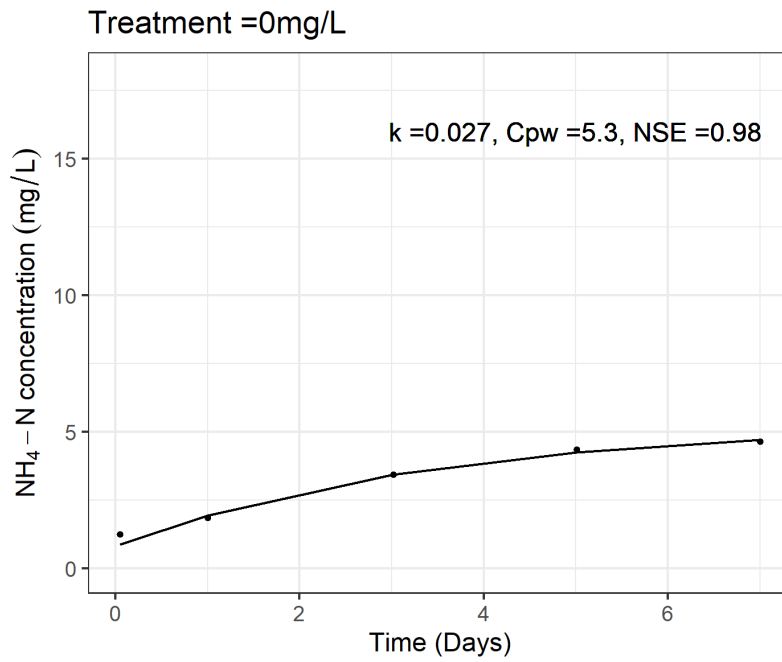


Figure D.22: experimental unit 20 – Run 3.

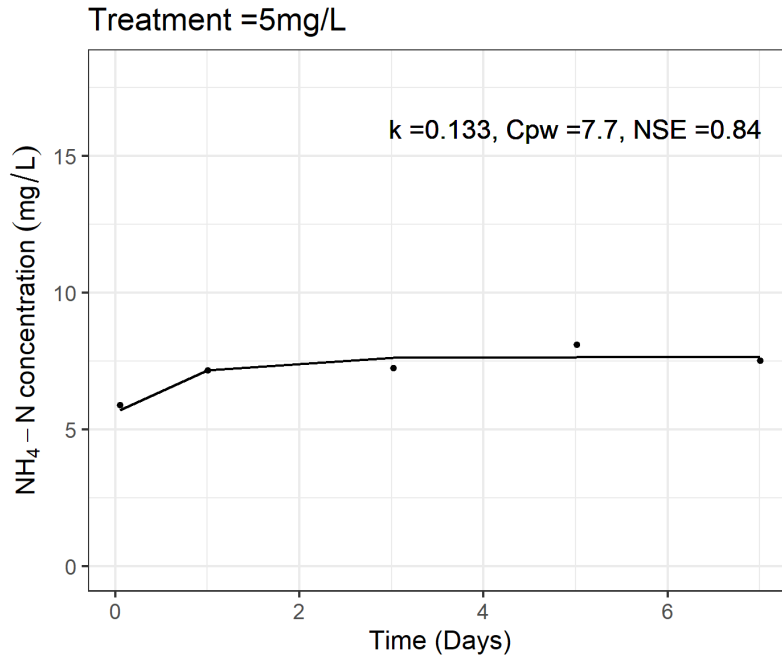


Figure D.23: experimental unit 21 – Run 3.

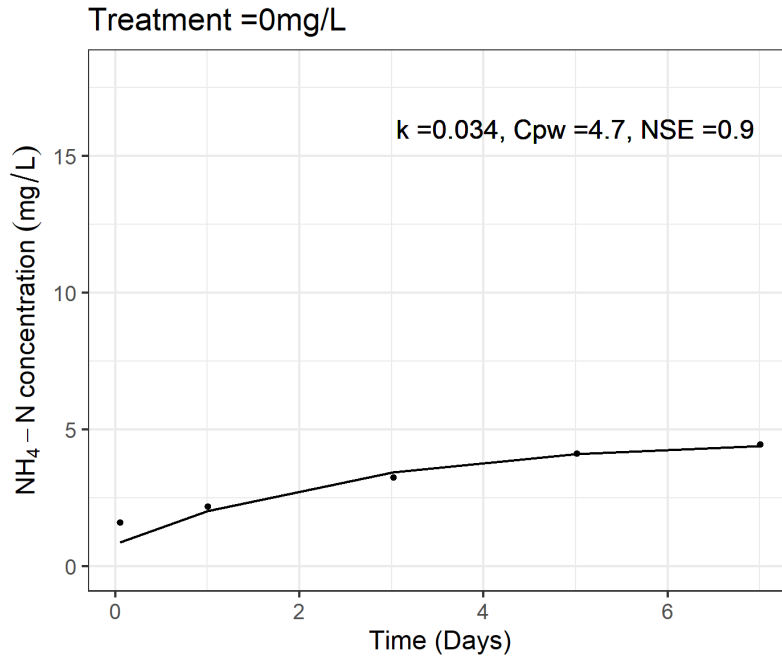


Figure D.24: experimental unit 22 – Run 3.

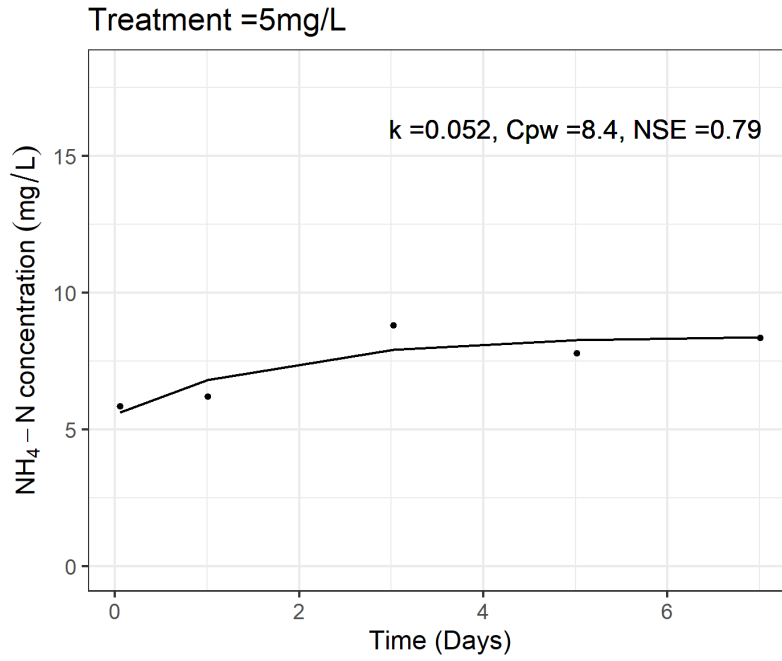


Figure D.25: experimental unit 23 – Run 3.

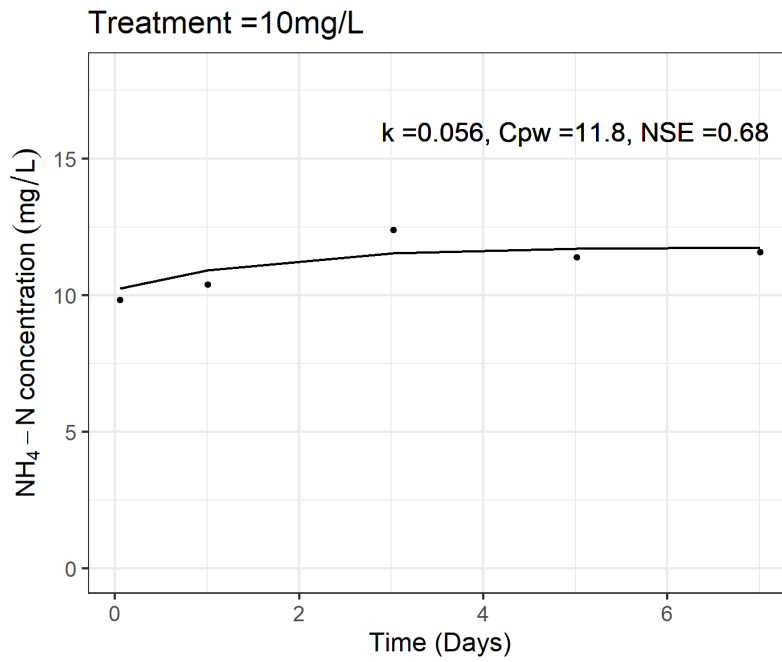


Figure D.26: experimental unit 24 – Run 3.

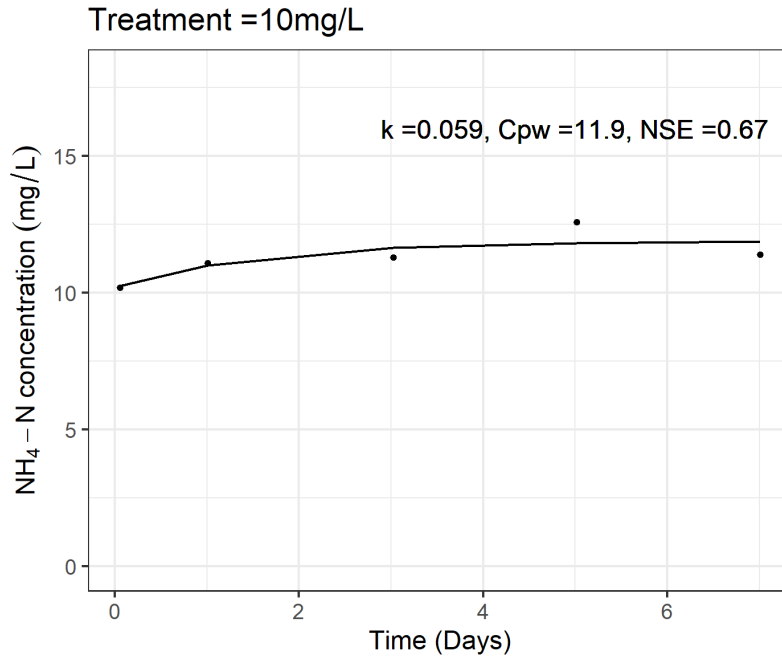


Figure D.27: experimental unit 25 – Run 3.

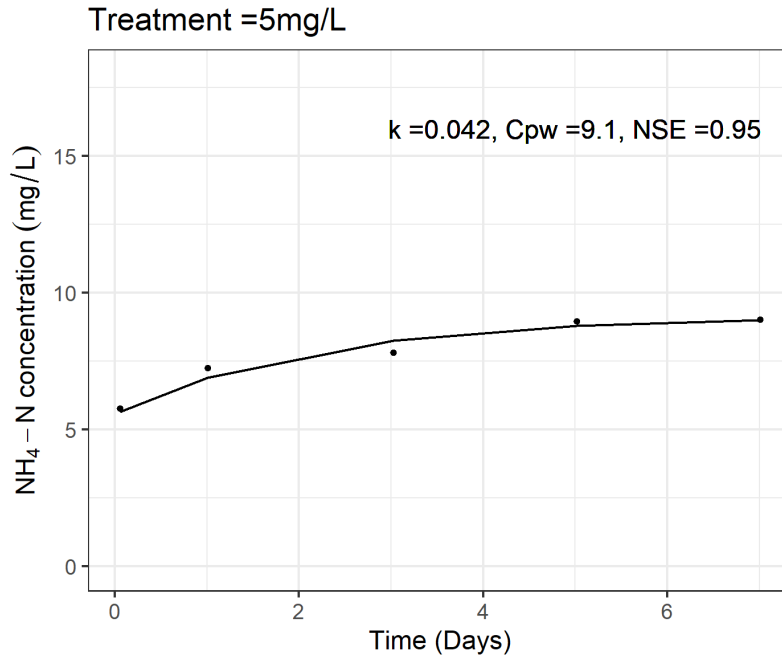


Figure D.28: experimental unit 26 – Run 3.

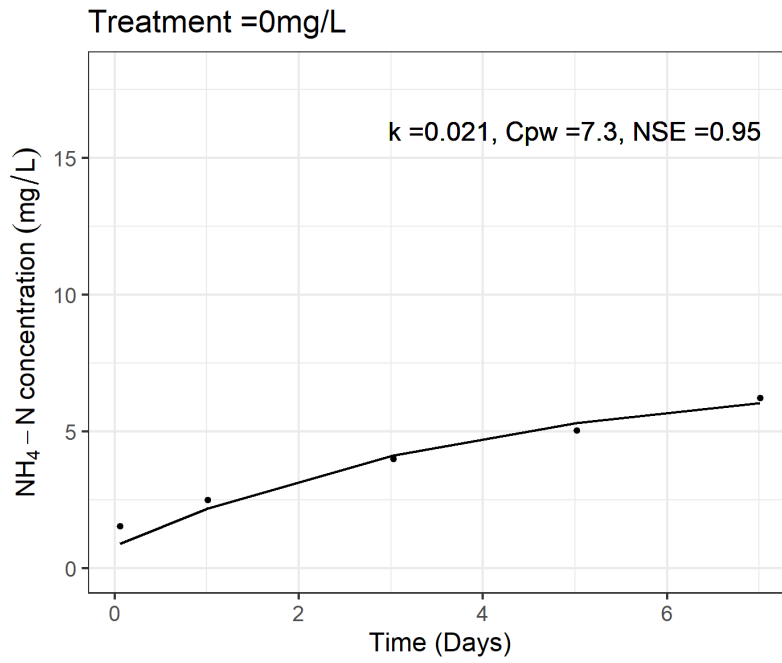


Figure D.29: experimental unit 27 – Run 3.

Table D.3: Table of results (omitted data has been italicized)

Run	Treatment	Eu	k	Cpw	R²
1	<i>10</i>	<i>1</i>	<i>1.103</i>	<i>12.3</i>	<i>0.39</i>
1	<i>0</i>	<i>2</i>	<i>2.691</i>	<i>5.8</i>	<i>0.18</i>
1	5	3	0.023	12.2	0.95
1	10	4	0.011	18.3	0.93
1	5	5	0.013	15.9	0.96
1	0	6	0.013	12.9	0.99
1	0	7	0.031	10.5	0.78
1	10	8	0.017	17.7	0.98
1	5	9	0.022	13.8	0.92
2	<i>10</i>	<i>1</i>	<i>3.182</i>	<i>12.3</i>	<i>0.04</i>
2	5	2	0.019	12.0	0.97
2	0	3	0.036	7.5	0.97
2	5	4	0.023	11.8	0.84
2	5	5	0.061	10.4	0.48
2	10	6	0.005	21.5	0.68
2	0	7	0.039	8.0	0.95
2	<i>10</i>	<i>8</i>	<i>0.865</i>	<i>12.6</i>	<i>0.54</i>
2	0	9	0.037	8.6	0.89
3	10	1	0.038	11.1	0.47
3	0	2	0.027	5.3	0.98
3	5	3	0.133	7.7	0.84
3	0	4	0.034	4.7	0.90
3	5	5	0.052	8.4	0.79
3	10	6	0.056	11.8	0.68
3	10	7	0.059	11.9	0.67
3	5	8	0.042	9.1	0.95
3	0	9	0.021	7.3	0.95

ANOVA Results

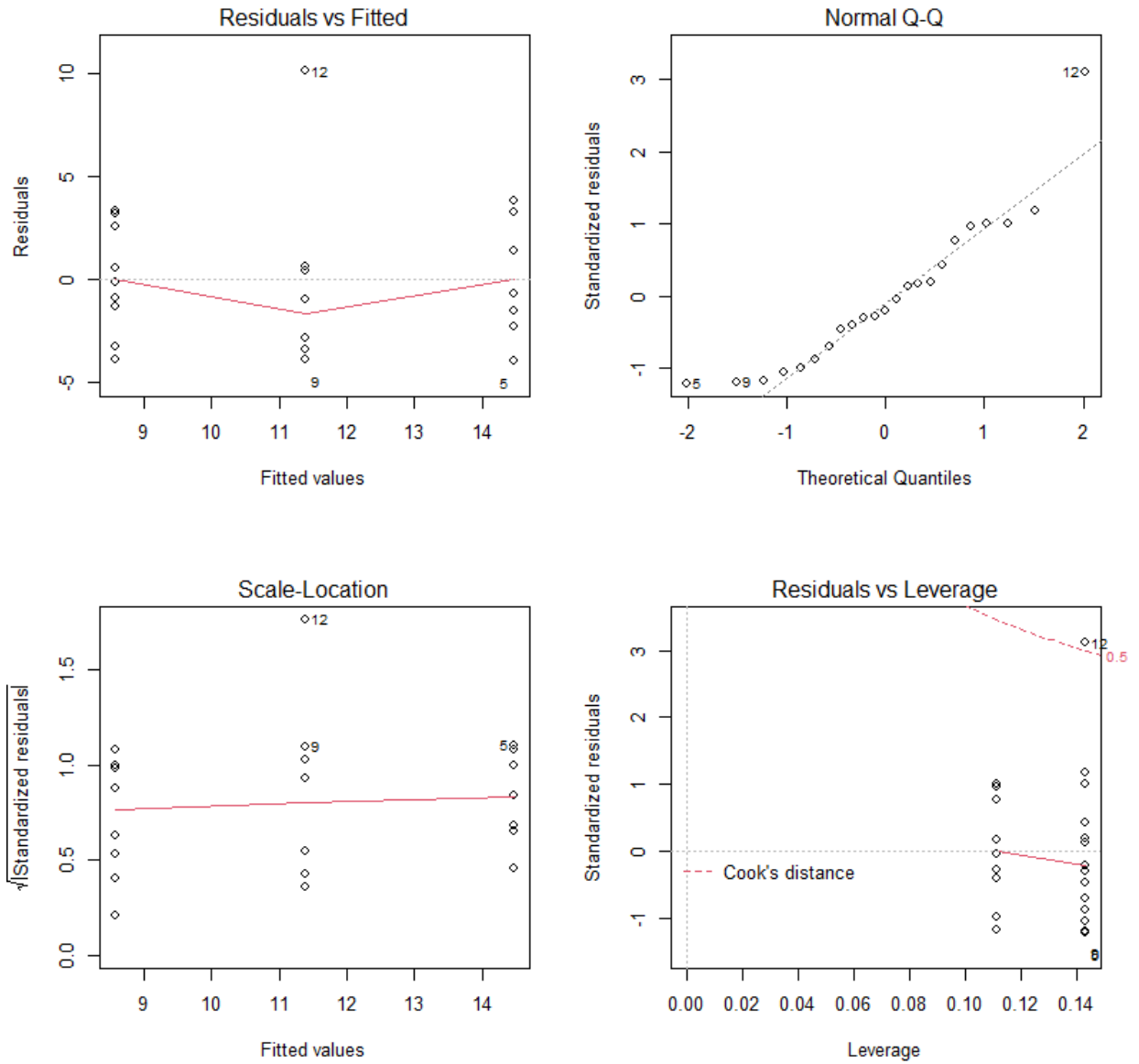


Figure D.30: Plots of ANOVA results for C_{pw} v. Run

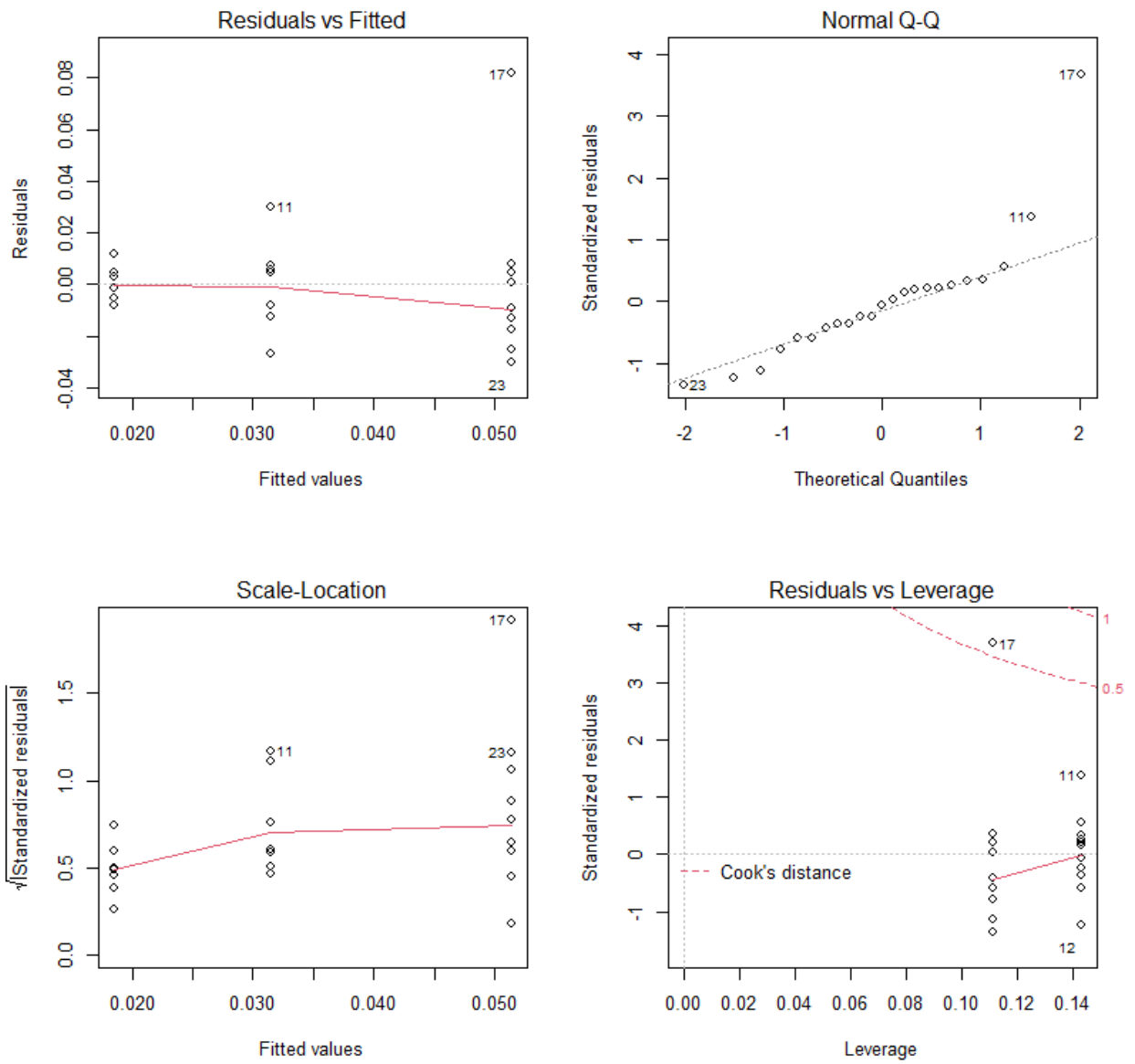


Figure D.31: Plots of ANOVA results for k_u v. Run

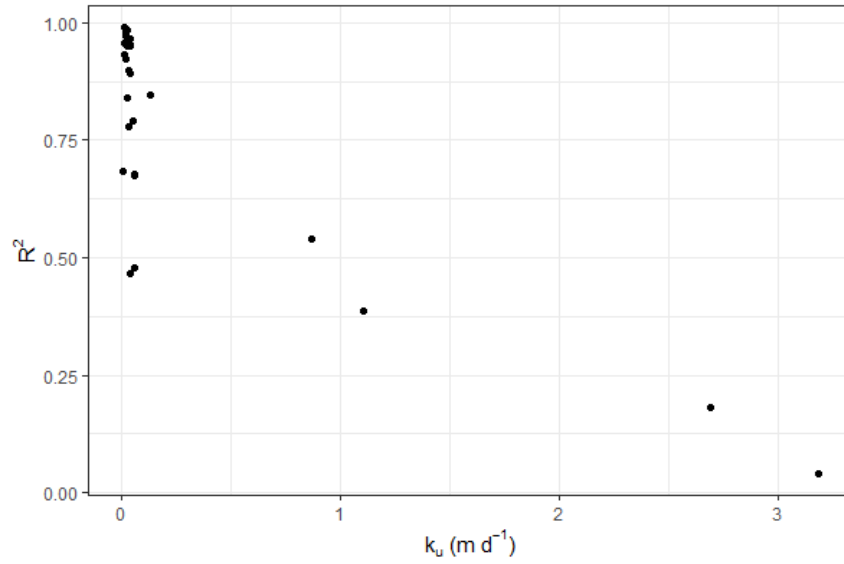


Figure D.32: Plot of model efficiency (R^2) vs. the release rate constant (k_u). The correlation between low (or poor) model efficiency and high k_u values was readily apparent in this plot.

R Code for Chapter III analysis

R script to run model

```
## -----  
##  
## Script name: tracer_to_rtd  
##  
## Purpose of script: Hydraulic analysis of common dataset format for tracer tests at walnut Cove  
##  
## Author: Brock Kamrath  
##  
## Date Created: 2020-07-09  
##  
## Email: bjkamrat@ncsu.edu  
##  
## -----  
## Notes: Use the function tracer_to_  
##  
## -----  
options(scipen = 6, digits = 4) # I prefer to view outputs in non-scientific notation  
## -----  
## load up our functions into memory  
rm(list=ls(all=TRUE))  
source("src/cal_analysis.R")  
## -----  
#load packages  
library(plyr)  
library(dplyr)  
library(tidyverse)  
library(readxl)  
library(lubridate)  
library(readxl)  
library(formattable)  
library(gridExtra)  
library(ggpubr)  
library(ggsignif)  
library(broom)  
library(agricolae)  
library(rstatix)  
  
# list of file names in  
#initialize readin listing  
mysheets_fromexcel <- list()  
  
mysheetlist <- excel_sheets(path="all_split.xlsx")  
  
z <- 1  
#check to make sure its working  
data <- read_excel(path="all_split.xlsx", sheet = mysheetlist[1])  
cal_analysis(data)  
  
results <- cal_analysis(data)  
  
# limits list to the first four filenames, which is equal to the four test files  
for (i in 1:length(mysheetlist)){  
  data <- read_excel(path="all_split.xlsx", sheet = mysheetlist[i])  
  results[i,] <- cal_analysis(data)  
  z <- z+1  
}  
  
results  
results <- results %>%  
  mutate(Run = as.factor(Run),  
         Treatment = as.factor(Treatment))
```

```

write.csv(results,"all_split.csv",row.names=FALSE)

results%>%
  dplyr::summarise(across(where(is.numeric), ~ sd(.x, na.rm = TRUE)))

results%>%
  group_by(Run) %>%
  dplyr::summarise(across(where(is.numeric), ~ max(.x, na.rm = TRUE)))

cpw_plot <- ggplot(results)+
  geom_density(aes(Cpw, ..scaled..))+
  labs(x= expression(paste(C[pw]," (mg-N ",L^-1,"))))+
  theme_bw()

k_plot <- ggplot(results)+
  geom_density(aes(k,..scaled..))+
  labs(x=expression(paste(k[u]," (m ",d^-1,"))))+
  theme_bw()

ef_plot <- ggplot(results)+
  geom_density(aes(EF))+
  facet_wrap(~Run)+
  labs(y="Model Efficiency")

ggplot(results)+
  geom_point(aes(x = Cpw, y = EF))+
  labs(y = expression(paste(R^2)), x = expression(paste(k[u]," (m ",d^-1,"))))+
  theme_bw()

grid.arrange(cpw_plot,k_plot,nrow=1)

# remove outlying k values
noout <- results %>%
  filter(k <= 0.5)

cpw_plot <- ggplot(noout)+
  geom_density(aes(Cpw, ..scaled..))+
  labs(x= expression(paste(C[pw]," (mg-N ",L^-1,"))))+
  theme_bw()

k_plot <- ggplot(noout)+
  geom_density(aes(k, ..scaled..))+
  labs(x=expression(paste(k[u]," (m ",d^-1,"))))+
  theme_bw()

grid.arrange(cpw_plot,k_plot,nrow=1)

cpw_plot <- ggplot(noout)+
  geom_density(aes(Cpw))+
  labs(x= expression(paste(C[pw]," (mg-N ",L^-1,"))))+
  facet_wrap(~Run)+
  theme_bw()

k_plot <- ggplot(noout)+
  geom_density(aes(k))+
  labs(x=expression(paste(k[u]," (m ",d^-1,"))))+
  facet_wrap(~Run)+
  theme_bw()

EF_plot <- ggplot(noout)+
  geom_density(aes(EF))+
  labs(x=expression(paste("Model Efficiency (",R^2,")")))+
  facet_wrap(~Run)+
  theme_bw()

grid.arrange(cpw_plot,k_plot, EF_plot,nrow=3)

```

```

noout%>%
  dplyr::summarise(across(where(is.numeric), ~ sd(.x, na.rm = TRUE)))

#####
# Evaluate data

cpw_mod <- lm(Cpw ~ Run, data = noout)
plot(cpw_mod, which = 3, add.smooth = FALSE)
plot(cpw_mod, which = 2, add.smooth = FALSE)
anova(cpw_mod)

cpw_means <- noout %>%
  group_by(Run) %>%
  dplyr::summarise(Means = mean(Cpw, na.rm=TRUE))

cpw_means

cpw_aov <- aov(cpw_mod)
par(mfrow = c(2,2))
plot(cpw_aov)
par(mfrow=c(1,1))

res<-cpw_aov$residuals
shapiro.test(res)
acf(res)
hist(res,main="Histogram of
residuals",xlab="Residuals")

TukeyHSD(cpw_aov)

cpw.stat.test <- aov(cpw_mod) %>%
  tukey_hsd()

HSD.test(cpw_aov, trt = c("Run"), console = TRUE)

# step 1. calculate means for each treatment combination
cpw_stats <-
  noout %>%
  group_by(Run) %>% # <- remember to group by the two factors
  dplyr::summarise(Means = mean(Cpw), SEs = sd(Cpw)/sqrt(n()))

# step 2: plot

plot <- ggplot(data = noout, aes(x = Run, y = Cpw))+
  geom_point(cex = 1.5, pch = 1.0, position = position_jitter(w = 0.1, h = 0))+
  stat_summary(fun.data = 'mean_se', geom = 'errorbar', width = 0.2) +
  stat_summary(fun.data = 'mean_se', geom = 'pointrange') +
  geom_point(data=cpw_stats, aes(x=Run, y=Means))+
  stat_pvalue_manual(cpw.stat.test, label = "p.adj.signif",
    y.position = c(26, 29, 23))+
  theme_classic2() +
  labs(x = "Experimental Run (1= Nov20, 2= Dec 20, 3= Jan21)",
    y = expression(paste(C[pw]," (mg-N ",L^-1,")))")+
  lims(y = c(0,30))

plot

#####
# Conduct same analysis with rate constant (k)

k_mod <- lm(k ~ Run, data = noout)
plot(k_mod, which = 3, add.smooth = FALSE)
plot(k_mod, which = 2, add.smooth = FALSE)
anova(k_mod)

```

```

k_means <- noout %>%
  group_by(Run) %>%
  dplyr::summarise(Means = mean(k, na.rm=TRUE))

k_means

k_aov <- aov(k_mod)
par(mfrow = c(2,2))
plot(k_aov)
par(mfrow=c(1,1))

res<-k_aov$residuals
shapiro.test(res)
acf(res)
hist(res,main="Histogram of
residuals",xlab="Residuals")

TukeyHSD(k_aov)

k.stat.test <- aov(k_mod) %>%
  tukey_hsd()

HSD.test(k_aov, trt = c("Run"), console = TRUE)

# step 1. calculate means for each treatment combination
k_stats <-
  noout %>%
  group_by(Run) %>% # <- remember to group by the two factors
  dplyr::summarise(Means = mean(k), SEs = sd(k)/sqrt(n()))

# Step 2: plot
plot <- ggplot(data = noout, aes(x = Run, y = k))+
  geom_point(cex = 1.5, pch = 1.0, position = position_jitter(w = 0.1, h = 0))+
  stat_summary(fun.data = 'mean_se', geom = 'errorbar', width = 0.2) +
  stat_summary(fun.data = 'mean_se', geom = 'pointrange') +
  geom_point(data=k_stats, aes(x=Run, y=Means))+
  stat_pvalue_manual(k.stat.test, label = "p.adj.signif",
    y.position = c(0.08, 0.17, 0.15))+
  theme_classic2() +
  labs(x = "Experimental Run (1= Nov20, 2= Dec 20, 3= Jan21)",
    y =expression(paste(k[u], " (m ",d^-1,")")))

plot

#####
# Conduct same analysis with the model efficiency (EF)
ef_mod <- lm(EF ~ Run, data = noout)
plot(ef_mod, which = 3, add.smooth = FALSE)
plot(ef_mod, which = 2, add.smooth = FALSE)
anova(ef_mod)

ef_means <- noout %>%
  group_by(Run) %>%
  dplyr::summarise(Means = mean(EF, na.rm=TRUE))

ef_means

ef_aov <- aov(ef_mod)
res<-ef_aov$residuals
shapiro.test(res)
hist(res,main="Histogram of
residuals",xlab="Residuals")

TukeyHSD(ef_aov)

ef.stat.test <- aov(ef_mod) %>%
  tukey_hsd()

```

```

HSD.test(ef_aov, trt = c("Run", "Treatment"), console = TRUE)
# step 1. calculate means for each treatment combination
ef_stats <-
  noout %>%
  group_by(Run) %>% # <- remember to group by the two factors
  dplyr::summarise(Means = mean(EF), SEs = sd(EF)/sqrt(n()))

# Step 2: plot
plot <- ggplot(data = noout, aes(x = Run, y = EF))+
  geom_point(cex = 1.5, pch = 1.0, position = position_jitter(w = 0.1, h = 0))+
  stat_summary(fun.data = 'mean_se', geom = 'errorbar', width = 0.2) +
  stat_summary(fun.data = 'mean_se', geom = 'pointrange') +
  geom_point(data=ef_stats, aes(x=Run, y=Means))+
  stat_pvalue_manual(ef.stat.test, label = "p.adj.signif",
                    y.position = c(1.08, 1.15, 1.02))+
  theme_classic2() +
  labs(x = "Experimental Run (1= Nov20, 2= Dec 20, 3= Jan21)",
       y = expression(paste("Model Efficiency ( ", R^2, ")))")+
  scale_y_continuous(breaks = c(0.2,0.4,0.6,0.8,1.0))+
  coord_cartesian(ylim=c(0, 1.2))

plot

```

R script of model

```
#Script objective: calibration of model
#Author: Brock Kamrath
#Date: 2/6/2020

#1.clear workspace and load packages ----
library(tidyverse)
library(lubridate)
library(janitor)
library(readxl)
library(hydroGOF)
library(formattable)

citation(package = "stats")

cal_analysis <- function(cal_data){
#user defined-function----
#parameters all intialized to random value, except depth.. depth should be 0.09 m
release_model <- function(data,k = 1,Cpw = 10,d = 0.09){

  #add vector for predicted values
  data$pred_nh4 <- as.numeric(rep(NA,nrow(data))) #use NA so that you know where a mistake may be occuring

  #Calculate predicted value
  for(i in 1:nrow(data)){
    data$pred_nh4[i] <- Cpw - (Cpw-data$nh4_o[i])*exp((-k/d)*data$time_diff[i])
  }
  #create outputs data_frame---- includes run, treatment, time from 0 (time_diff),
  # actual msmt (nh4), and predicted value (pred_nh4)
  outputs <- data.frame(run = data$run, treat = data$treatment,
                        time = data$time_diff, nh4 = data$nh4,
                        pred_nh4 = data$pred_nh4)

  return(outputs)
}

#1.par: Define initial values - k,Cpw----
#use nominal values provided
initial_values <- c(0.1,10)

#2.fn: function that returns the SSE ----
#for model, which will be minimized
release_error <- function(par,observed_responses){
  #Assign initial values to parameters
  # rate constant (ku), (m/d)
  k <- par[1]
  #Ammonium porewater concentration (mg/L)
  Cpw <- par[2]
  #depth (m)
  d <- 0.09

  #Run model
  sim_res <-release_model(observed_responses, k, Cpw, d)

  #Calculate SSE
  sse <- sum((sim_res$nh4-sim_res$pred_nh4)^2)

  #Return
  return(sse)
}

#####
# Calibrate using optim
cal <- optim(par=initial_values,
            fn=release_error,
            gr = NULL,
```

```

        observed_responses = cal_data,
        method="Nelder-Mead")

cal

#apply calibrated release model
sim_cal <- release_model(cal_data,
                        k=cal$par[1],
                        Cpw=cal$par[2])

#Calculate model efficiency for calibrated model
EF_cal <- NSE(sim_cal$pred_nh4, sim_cal$nh4)

#plot modeled v. measured for calibration data
p1 <- ggplot(sim_cal)+
  geom_point(aes(x = time,y = nh4),shape = 20)+
  geom_line(aes(x = time,y = pred_nh4))+
  geom_text(aes(label = paste("k =", round(cal$par[1],3), ", Cpw =", round(cal$par[2],1), ", NSE =",
round(EF_cal,2), sep = ""), x = 5, y = 16),
           position = position_dodge(0.9))+
  lims(y = c(0,18))+
  labs(y = expression(NH[4]-N~concentration~(mg/L)), x = "Time (Days)",
       title = paste("Treatment =", sim_cal$treat[1], "mg/L", sep = ""))+
  theme_bw()

ggsave(filename = paste0("figs/p", z, ".png"), plot = p1, width = 12, height = 10, dpi = 300, units = "cm")

results <- data.frame(matrix(vector(), 0, 6,
                            dimnames=list(c(), c("Run", "Treatment", "Eu", "k","Cpw","EF"))),
                    stringsAsFactors=F)
results[1,] <- c(cal_data$run[1],cal_data$treatment[1],cal_data$eu[1],cal$par[1],cal$par[2], EF_cal)
return(results)
}

```

APPENDIX E: CHAPTER IV SUPPLEMENTAL INFORMATION

Table E.1: Monthly average water quality data at Walnut Cove.

year_month	ID	NO3 grab	NH4 grab	Temp	Do	Do_per	pH	Scond	don	on	nh4n	no3n	tdn	tn
6/1/2019	IN	0.3	6.7	26.6	1.8	23.5	7.6	422.0	2.3	3.6	6.6	0.1	9.0	10.3
6/1/2019	OUT1	0.2	4.6	23.7	0.2	2.5	6.9	397.7	1.8	3.0	4.8	0.1	6.7	8.3
6/1/2019	OUT2	0.2	6.8	25.5	0.4	5.4	6.9	433.1	2.0	3.4	6.9	0.1	9.0	13.5
7/1/2019	IN	0.1	4.2	27.0	0.2	2.2	7.1	419.1	1.9	3.9	4.9	0.0	6.8	8.8
7/1/2019	OUT1	0.2	4.1	23.8	0.1	1.6	6.9	418.1	2.1	2.9	4.2	0.0	6.4	6.9
7/1/2019	OUT2	0.1	6.2	26.9	0.5	6.7	6.9	443.6	1.9	2.0	7.0	0.0	8.9	9.1
8/1/2019	IN	0.2	1.1	25.2	1.1	13.2	7.1	391.1	1.2	NA	1.3	0.0	2.6	NA
8/1/2019	OUT1	0.1	1.9	22.8	0.3	3.4	7.0	409.1	1.3	NA	2.2	0.0	3.5	NA
8/1/2019	OUT2	0.1	3.0	25.8	0.6	7.8	7.0	416.4	1.3	NA	4.0	0.0	5.3	NA
9/1/2019	IN	0.1	1.4	24.2	0.3	3.7	6.9	442.5	1.6	2.4	1.9	0.0	3.5	4.5
9/1/2019	OUT1	0.1	0.7	21.5	0.4	4.1	6.8	447.7	1.4	2.2	0.9	0.0	2.3	3.2
9/1/2019	OUT2	0.1	2.9	23.9	0.8	10.2	6.9	457.5	1.4	2.4	3.4	0.0	4.8	5.9
10/1/2019	IN	0.3	3.7	15.6	0.6	5.3	7.0	474.5	1.3	2.1	3.9	0.2	5.5	7.3
10/1/2019	OUT1	0.2	2.1	13.7	0.7	6.6	6.8	470.3	0.8	1.6	2.8	0.0	3.6	5.1
10/1/2019	OUT2	0.2	3.0	14.8	1.8	17.8	6.9	473.9	0.9	2.5	3.6	0.1	4.5	6.6
11/1/2019	IN	1.6	6.3	10.1	1.7	15.0	7.1	444.0	1.5	2.8	8.5	1.3	11.4	12.7
11/1/2019	OUT1	1.1	5.6	8.4	1.0	8.8	6.6	456.3	1.1	1.7	7.0	1.1	9.2	9.9
11/1/2019	OUT2	0.5	6.0	9.8	3.8	33.5	6.9	435.7	0.7	2.4	8.1	0.3	9.1	11.0
12/1/2019	IN	0.9	10.5	6.0	3.5	28.4	7.3	433.1	1.0	1.8	10.5	0.8	12.3	13.4
12/1/2019	OUT1	1.5	9.2	4.2	1.0	7.6	6.9	425.5	0.6	1.4	8.8	1.3	10.8	11.7
12/1/2019	OUT2	0.6	10.6	4.8	5.7	44.6	7.1	432.6	0.5	1.9	10.3	0.4	11.2	12.2
1/1/2020	IN	0.8	9.7	8.0	4.1	35.0	7.3	390.5	1.2	2.0	10.1	0.5	11.8	12.5
1/1/2020	OUT1	3.0	4.7	5.6	2.1	17.3	6.9	350.2	1.0	1.7	6.8	1.8	9.6	9.6
1/1/2020	OUT2	0.5	9.1	5.6	6.2	49.7	7.1	382.5	0.8	4.9	9.7	0.4	10.9	14.7
2/1/2020	IN	0.7	3.8	10.7	11.6	105.8	7.5	181.8	1.0	1.7	2.1	0.4	3.5	4.3
2/1/2020	OUT1	2.1	0.5	7.9	3.8	32.0	6.6	160.9	0.9	1.5	1.0	0.9	2.8	3.0
2/1/2020	OUT2	0.7	3.5	9.7	6.1	55.0	6.8	184.7	1.0	2.5	1.5	0.6	3.1	5.0
3/1/2020	IN	0.4	2.2	14.9	10.5	102.3	8.1	222.2	1.4	4.1	1.0	0.6	3.0	5.7
3/1/2020	OUT1	0.2	0.3	12.6	2.4	21.5	6.7	202.8	1.2	2.3	0.1	0.8	2.1	3.2
3/1/2020	OUT2	0.3	2.5	12.5	6.1	54.7	7.2	227.5	2.1	6.0	1.2	0.5	3.8	7.7
6/1/2020	IN	0.2	0.4	27.1	1.7	22.0	7.6	292.8	NA	NA	NA	NA	NA	NA
6/1/2020	OUT1	0.2	2.4	21.1	0.3	3.0	6.7	327.0	NA	NA	NA	NA	NA	NA
6/1/2020	OUT2	0.3	1.6	27.8	1.0	13.2	6.9	309.7	NA	NA	NA	NA	NA	NA
7/1/2020	IN	0.3	2.5	28.1	0.3	3.8	7.1	398.1	NA	NA	NA	NA	NA	NA
7/1/2020	OUT1	0.3	3.8	24.1	0.3	3.5	6.7	420.8	NA	NA	NA	NA	NA	NA
7/1/2020	OUT2	0.3	2.7	31.8	0.5	7.2	6.8	398.3	NA	NA	NA	NA	NA	NA

8/1/2020	IN	0.1	4.7	26.9	0.3	3.4	7.0	432.2	NA	NA	NA	NA	NA	NA
8/1/2020	OUT1	0.1	4.7	23.6	0.5	6.0	6.8	394.6	NA	NA	NA	NA	NA	NA
8/1/2020	OUT2	0.1	4.4	31.1	2.3	31.4	6.9	372.8	NA	NA	NA	NA	NA	NA
9/1/2020	IN	0.2	6.7	22.3	0.6	6.5	7.0	441.8	0.9	2.2	6.7	0.1	7.8	9.3
9/1/2020	OUT1	0.1	6.1	19.0	0.2	2.2	6.8	440.6	1.2	1.8	6.0	0.0	7.3	8.1
9/1/2020	OUT2	0.1	7.2	22.6	1.5	17.7	7.1	471.4	1.2	4.5	6.9	0.1	7.9	11.6
10/1/2020	IN	0.4	6.7	17.2	0.4	4.5	7.0	425.7	0.8	2.0	7.5	0.2	8.5	9.8
10/1/2020	OUT1	0.1	6.4	15.1	0.3	3.4	6.8	427.5	0.4	1.0	6.8	0.0	7.2	7.8
10/1/2020	OUT2	0.1	6.2	19.3	13.5	36.0	7.1	436.7	0.5	1.8	6.3	0.0	6.8	8.1
11/1/2020	IN	0.3	5.0	12.9	2.4	22.2	7.0	303.5	0.8	2.1	4.9	0.2	5.8	7.2
11/1/2020	OUT1	0.2	4.4	10.0	0.8	6.8	6.8	304.1	0.4	0.7	5.4	0.1	5.9	6.3
11/1/2020	OUT2	0.3	4.6	14.0	4.2	40.3	7.0	308.8	0.5	1.7	4.4	0.2	5.1	6.3
12/1/2020	IN	0.3	4.3	8.2	14.9	130.8	7.9	201.9	0.9	1.8	4.7	0.1	5.7	6.6
12/1/2020	OUT1	0.7	3.5	6.1	5.8	51.0	7.0	160.7	0.9	1.3	4.3	0.1	5.2	5.6
12/1/2020	OUT2	0.7	3.1	8.1	10.7	103.7	7.5	158.4	1.3	1.9	3.7	0.2	5.1	5.6
1/1/2021	IN	0.2	10.3	6.6	5.8	48.1	7.5	362.0	0.9	2.8	10.5	0.1	11.5	13.6
1/1/2021	OUT1	0.4	8.7	4.2	4.6	36.9	7.4	344.2	0.8	1.1	8.7	0.3	9.8	10.3
1/1/2021	OUT2	0.4	8.3	7.9	8.6	73.6	7.5	338.0	0.6	1.8	8.0	0.4	9.1	10.4
2/1/2021	IN	0.2	9.0	8.2	8.7	74.1	7.7	351.0	1.9	5.1	8.7	0.1	10.7	14.0
2/1/2021	OUT1	0.5	7.9	6.8	5.0	41.0	7.4	341.9	1.3	2.8	7.7	0.4	9.5	11.0
2/1/2021	OUT2	0.3	8.2	8.7	8.1	69.7	7.6	337.3	1.3	3.9	7.8	0.3	9.4	12.2
3/1/2021	IN	0.2	10.7	16.0	6.1	63.7	7.7	355.1	3.5	7.4	9.8	0.8	14.0	18.0
3/1/2021	OUT1	0.6	8.4	12.7	5.9	57.9	7.5	333.5	2.1	4.2	7.3	0.6	10.0	12.1
3/1/2021	OUT2	0.4	9.4	16.4	5.4	56.1	7.5	338.2	2.4	8.3	9.0	0.2	11.6	17.5
5/1/2021	IN	0.3	4.2	21.6	3.7	41.1	8.0	371.4	3.1	8.3	4.2	0.1	7.4	13.1
5/1/2021	OUT1	0.4	3.9	15.7	0.3	3.3	6.7	381.5	2.6	6.6	3.6	0.0	6.3	10.9
5/1/2021	OUT2	0.3	6.8	19.8	1.5	16.7	7.3	404.6	2.3	10.4	6.6	0.1	9.0	17.3

Table E.2: Estimated monthly loading (in g)

ID	month	nh4n	no3n	don	on	tdn	tn	NO3 grab	NH4 grab
IN	2019-06	95149.13	1480.65	34018.01	55380.18	130647.8	151607.9	4280.055	94376.53
IN	2019-07	52720.89	219.9454	19838.42	45616.63	72779.26	98950.31	1404.157	45392.13
IN	2019-08	17691.24	622.5952	13961.53	37175.88	32275.36	75021.83	1830.976	16677.41
IN	2019-09	9805.667	41.02901	8362.94	12713.69	18209.64	23188.03	592.4403	7030.414
IN	2019-10	56020.52	3634.793	14985.72	26097.96	74641.03	89311.5	7733.169	54006.84
IN	2019-11	115912.6	19514.26	23559.07	43171.86	158985.9	179564.4	21900.48	88663.34
IN	2019-12	179785.7	13365.47	17647.33	34459.18	210798.5	232065.4	14679.23	173024
IN	2020-01	157779.9	8136.186	17687.6	32212.23	183603.7	198394.1	11130.05	156492.6
IN	2020-02	81676.17	9332.182	21917.58	33678.66	112925.9	126407.5	15104.36	81606.63
IN	2020-03	16249.5	6473.286	17390.77	50064.16	40113.56	73829.91	4562.871	38126.48
IN	2020-04	29181.86	5653.952	17309.82	51654.56	52145.63	88066.56	3390.128	43881.74
IN	2020-05	69821.75	7818.587	28105.17	87014.84	105745.5	168142.6	5900.439	32825.78
IN	2020-06	52159.68	3640.932	15866.78	50910.37	71667.4	109206.9	2628.403	9640.59
IN	2020-07	47287.42	1966.377	11273.43	37605.77	60527.23	89055.99	2142.471	24027.39
IN	2020-08	92836.63	1982.849	17754.84	61800.39	112574.3	160838.7	1336.216	65984.35
IN	2020-09	73215.42	1038.052	7946.397	20947.21	82199.87	97782.72	2087.939	68216.92
IN	2020-10	87201.51	3253.192	9501.867	25149.25	99956.57	116749.4	5125.49	82646.4
IN	2020-11	90189.77	3447.492	11729.95	36880.19	105367.2	130840.8	4914.748	79349.15
IN	2020-12	106532.8	2136.897	14831.36	36708.73	123501	147070.7	5647.688	85794.48
IN	2021-01	121193.1	1183.6	10552.95	34195.25	132929.7	159546.6	2258.395	114349.7
IN	2021-02	181892	2279.098	37653.56	99279.26	221824.7	285554.7	4443.053	185160.5
IN	2021-03	169398.9	13975.18	60423.58	130000.6	243797.6	315894.5	18087.28	181534.2
IN	2021-04	48066.55	52301.03	33827.04	84614.3	134194.6	188089.4	47299.39	46449.79
IN	2021-05	32299.98	829.0204	24157.62	63166.2	57286.62	99481.72	2255.396	30481.85
OUT1	2019-06	72465.89	1021.607	27947.72	46259.78	101435.2	129963.4	3740.359	68479.25
OUT1	2019-07	51492.23	166.0502	21179.89	30644.81	72838.17	77622.57	2133.656	49017.42
OUT1	2019-08	29332.1	201.0657	15422.52	29315.64	44955.69	62437.77	1822.564	31329.8
OUT1	2019-09	3861.556	40.4382	5787.812	9743.738	9689.807	13748.45	639.1086	2994.412
OUT1	2019-10	46665.88	559.704	9132.794	19773.14	56358.38	68640.15	2943.341	44758.97
OUT1	2019-11	98913.14	16066.95	14323.1	24244.13	129303.2	139019.2	16039.35	81533.97
OUT1	2019-12	159031.2	23147.35	12020.33	25756.53	194198.9	210418.5	29470.42	157907.5
OUT1	2020-01	127509.1	25155.85	15389.22	27805.5	168054.2	175935.9	44562.93	99379.72
OUT1	2020-02	39508.35	32607.04	18859.54	33176.22	90974.94	101208.4	51481.37	16854.75
OUT1	2020-03	6322.961	8372.171	13860.42	26396.96	28555.55	41397.52	3659.657	5747.341
OUT1	2020-04	20370.85	7843.116	15292.28	29817.11	43506.25	58840.99	3600.126	17300.98
OUT1	2020-05	66040.82	12444.92	29650.58	59186.78	108136.3	140180	6980.278	50297.3
OUT1	2020-06	43965.52	4629.495	14128.54	28849.31	62723.55	79080.36	3342.994	37059.76
OUT1	2020-07	41886.56	2323.751	10257.38	21460.55	54467.68	67210.54	2197.371	36625.68
OUT1	2020-08	90674.36	1958.523	17489.8	37588.68	110122.7	133526.6	1376.839	72919.46
OUT1	2020-09	70275.69	273.9064	8975.013	16186.55	79524.61	88097.93	1535.271	67480.46

OUT1	2020-10	93500.57	258.9024	5865.036	12007.17	99624.51	105527.4	1475.697	92324.02
OUT1	2020-11	104801.6	2231.692	10267.95	16382.35	117301.3	125480.1	5201.33	79782.04
OUT1	2020-12	109027	2743.423	16367.79	20361.02	128138.3	133031.4	15166.82	79306.5
OUT1	2021-01	105434.6	3391.531	9500.902	10004.07	118327	121978.2	5452.103	100543.2
OUT1	2021-02	171664.3	9320.334	30168.88	66361.71	211153.5	248889.5	10600.25	174947.7
OUT1	2021-03	130899	10060.64	37584.71	73289.32	178544.4	214429.2	10316.34	149751.7
OUT1	2021-04	37895.31	5420.751	23143.85	41333.45	66459.91	85056.14	5269.813	39765.86
OUT1	2021-05	22003.51	203.0857	16318.7	41628.44	38525.29	66786.74	2077.654	21935
OUT2	2019-06	89753.09	1325.396	31777.9	52520.16	122856.4	198345.2	3252.421	93884.56
OUT2	2019-07	64576.93	233.9285	17606.18	18115.24	82417.04	80831.28	1351.223	63436.86
OUT2	2019-08	45428.74	530.4264	14852.29	23380.75	60811.46	75044.92	1419.071	39222.93
OUT2	2019-09	14039.53	188.5808	5735.743	9873.414	19963.86	24418.19	460.3161	11428.93
OUT2	2019-10	49180.55	763.1713	8566.648	29577.32	58510.37	80008.5	2905.842	44180.36
OUT2	2019-11	110683.4	5262.609	11173.63	32868.86	127119.7	149795.1	7036.066	85558.93
OUT2	2019-12	182428.8	7047.859	8832.524	41545.06	198309.2	225950	10049.93	178556.5
OUT2	2020-01	148211.7	5626.536	10762.38	66425.65	164600.6	220717.6	8234.714	141070.8
OUT2	2020-02	71493.95	10863.13	18277.76	61424.37	100634.8	147483.6	14698.4	76898.98
OUT2	2020-03	18596.42	6207.613	25908.32	74820.96	50712.36	100462.6	2936.013	42128.14
OUT2	2020-04	31436.21	5716.148	26667.44	83565.58	63819.8	122568.9	2813.731	53034.76
OUT2	2020-05	75450.73	8503.229	45302.87	153711.3	129256.8	242582.8	6542.094	57109.38
OUT2	2020-06	48063.13	3554.988	22183.66	81193.05	73801.78	136113.2	3209.26	20441.96
OUT2	2020-07	41859.27	1995.488	15374.05	60826.11	59228.81	107656.9	2036.018	24167.17
OUT2	2020-08	95743.14	2646.541	28288.91	121899.3	126678.6	227270.7	1847.852	69464.15
OUT2	2020-09	71154.37	696.7375	4466.778	35642.46	76317.89	109146.8	1195.018	72785.11
OUT2	2020-10	79760.36	808.3612	7338.368	25399.92	87907.09	105986	2313.499	84950.93
OUT2	2020-11	90789.8	4670.317	7053.974	33631.74	102514.1	128731.7	5655.647	80249.27
OUT2	2020-12	93313.47	4175.193	22321.79	35063.75	119810.4	131398.7	16031.23	65893.85
OUT2	2021-01	113837.1	5784.222	9899.424	24587.42	129520.7	145592.6	6638.088	110957.1
OUT2	2021-02	184608.4	6191.474	30124.38	93077.73	220924.2	287668	7902.984	193520.8
OUT2	2021-03	179529.1	3536.877	48227.8	161404.9	231293.7	345599.1	9675.31	197079.2
OUT2	2021-04	62460.6	12246.37	30258.5	81057.65	104965.5	155281.9	18756.01	62528.35
OUT2	2021-05	48406.76	585.8474	16962.69	74077.03	65955.29	124771.3	2329.372	47013.38

Example of R Code for load analysis

```
# Load Analysis for June 19 through May 2021
# Objective: Average flow during the weekly composite sample
rm(list = ls())

# load packages
library(readxl)
library(ggpmisc)
library(dplyr)
library(ggpubr)
library(lubridate)
library(tidyverse)
library(data.table)
library(RiverLoad)

?method6

#####
# load in data
#####
# load in grab sample data
raw <- read_excel("data/raw/wq/grab_samp.xlsx")

# MDL is 0.03, if concentrations is below MDL, then bump up to MDL (mainly for nitrate and on)
# for(i in 1:nrow(raw)){
#   if(raw$NO3[i] <= 0.23){
#     raw$NO3[i] <- runif(1,min=0,max=0.23)
#   }
#   if(raw$NH4[i] <= 1){
#     raw$NH4[i] <- runif(1,min=0,max=1)
#   }
# }

raw$NO3 <- round(raw$NO3,2)
raw$NH4 <- round(raw$NH4,2)

# remove discrete nitrate dosing samples and midpoint samples
data <- raw %>%
  filter(no3_dosing <= 0.1 | no3_dosing >= 1.5) %>%
  filter(ID != "MID1") %>%
  filter(Date >= "2019-06-01") %>%
  select(-no3_dosing, -Isco, -Time_Win)

data_nit <- data %>%
  select(Date, ID, NO3, NH4) %>%
  dplyr::rename(datetime = Date)

#####
#                               load in data                               #
#####

conc <- read.csv("data/raw/wq/wc_comp.csv")

#filter to include only wk_comp samples
wq <- conc %>%
  mutate(start_date = as.POSIXct(conc$start_date, format = "%m/%d/%Y"),
         datetime = as.POSIXct(conc$end_date, format = "%m/%d/%Y")) %>%
  subset(location == "IN" | location == "OUT1" | location == "OUT2") %>%
  subset(type == "wk_comp" | type == "daily") %>%
  subset(filter != "DUP" & filter != "UF") %>%
  filter(start_date >= "2019-06-01") %>%
  mutate(don = tkn-nh4n,
         tdn = tkn+no3n) %>%
  select(location, start_date, datetime, nh4n, no3n, don, tdn) %>%
```

```

group_by(location, start_date, datetime) %>%
dplyr::summarise(across(where(is.numeric), ~ mean(.x, na.rm = TRUE)))

#####
# filter to include only wk_comp samples for unfiltered
wq_uf <- conc %>%
  mutate(start_date = as.POSIXct(conc$start_date, format = "%m/%d/%Y"),
         datetime = as.POSIXct(conc$end_date, format = "%m/%d/%Y")) %>%
  subset(location == "IN"|location == "OUT1"|location=="OUT2") %>%
  subset(type == "wk_comp") %>%
  subset(filter == "UF" & filter != "DUP") %>%
  filter(start_date >= "2019-06-01") %>%
  mutate(on = tkn-nh4n,
         tn = tkn+no3n) %>%
  select(location,start_date,datetime, on, tn) %>%
  group_by(location, start_date, datetime) %>%
  dplyr::summarise(across(where(is.numeric), ~ mean(.x, na.rm = TRUE)))

# wq_uf <- na.omit(wq_uf)

wqc <- left_join(wq, wq_uf, by = c("location","start_date","datetime"), keep = FALSE)

# break out weekly composite sampling by day
wq_daily <- wqc %>%
  expand(datetime = seq(start_date, datetime, by="1 day"), nh4n, no3n,don, on, tdn, tn) %>%
  dplyr::rename(ID = location) %>%
  mutate(datetime = as.Date(datetime)) %>%
  group_by(ID, datetime) %>%
  dplyr::summarise(across(where(is.numeric), ~ mean(.x, na.rm = TRUE)))

dates <- data.frame(seq(as.Date('2019-06-01'), as.Date('2021-05-31'), by = 'days'))
x <- c("datetime")
colnames(dates) <- x

dates <- dates %>%
  mutate(inlet = rep("IN",nrow(dates)),
         outlet1 = rep("OUT1",nrow(dates)),
         outlet3 = rep("OUT2",nrow(dates))) %>%
  gather(key = "location", value = "ID", -datetime) %>%
  select(datetime,ID)

wq_daily_all <- dates %>%
  left_join(., wq_daily, by = c("datetime","ID"))

# calculate removal rates for NH4N, NO3N, and TDN
dat <- wq_daily_all %>%
  full_join(., data_nit, by = c("datetime", "ID")) %>%
  mutate(datetime = as.POSIXct(datetime))

# Plot data for chapter 4
plot_dat <- dat %>%
  ungroup() %>%
  gather(key = "nut", value = "conc", -ID, -datetime) %>%
  mutate(year = year(datetime),
         datetime = as.Date(datetime))

m_rate_names <- list("NH4" = "Ammonium-N","NO3" = "Nitrate-N","nh4n" = "ammonium","no3n" = "nitrate",
                   "don" = "Dissolved organic nitrogen", "on" = "organic nitrogen", "tdn" = "TDN","tn" =
"TN")

m_rate_labeller <- function(variable,value){
  return(m_rate_names[value])
}

# time series
ggplot(plot_dat[!is.na(plot_dat$conc),],aes(x = datetime, y = conc, color = ID))+
  geom_point()+

```

```

geom_line()+
facet_wrap(~nut, ncol =1, labeller = m_rate_labeller)+
labs(x = "", y = expression(Concentration~(mg~L^{-1}))) +
theme_bw()+
scale_x_date(date_breaks = "3 month", date_labels = "%m-%y")+
scale_color_manual(name = "Location", labels = c("IN","OUT1","OUT2"), values = c("grey80","steelblue2",
"orangered3"))

plot_dat %>%
mutate(ID =as.factor(ID),
      nut = as.factor(nut))%>%
group_by(ID,nut) %>%
summarise(num = n_distinct(conc,na.rm=TRUE))

# Boxplot
ggplot(plot_dat, aes(x = nut, y = conc, fill = ID))+
geom_boxplot() +
stat_summary(fun=median, aes(group=ID), geom="point", size=3,show.legend = FALSE,
position=position_dodge(.75))+
stat_summary(fun=median, geom="text", show.legend = FALSE,
            vjust=-0.7, aes(group=ID, label=round(.y.., digits=1)), position=position_dodge(0.75))+
theme_bw()+
labs(y = expression(Median~monthly~concentrations~(mg~N~L^{-1})), fill = "Location", x = "")+
scale_x_discrete(labels = c("NH4" = "Ammonium-N", "NO3" = "Nitrate-N", "tn" = "TN", "tdn" = "TDN"))+
scale_fill_manual(values = c("grey80","steelblue2", "orangered3"))

# Summary Statistics
dat %>%
mutate(year_month = lubridate::floor_date(datetime, "month")) %>%
select(-datetime) %>%
gather(key = "pollutant",value = "conc", -year_month, - ID) %>%
group_by(ID, pollutant, year_month) %>%
dplyr::summarise(conc = median(conc, na.rm = TRUE)) %>%
group_by(ID,pollutant) %>%
dplyr::summarise(median = median(conc, na.rm = TRUE),
                iqr = IQR(conc, na.rm = TRUE))

mon_dat <- dat %>%
mutate(year_month = lubridate::floor_date(datetime, "month")) %>%
select(-datetime) %>%
group_by(year_month,ID) %>%
dplyr::summarise(nh4 = median(NH4, na.rm = TRUE),
                no3 = median(NO3, na.rm = TRUE),
                tdn = median(tdn, na.rm = TRUE),
                tn = median(tn, na.rm = TRUE)) %>%
filter(ID != "IN")

write.csv(mon_dat, "data/clean/ch4/mon_dat.csv")

#####
# inlet samples
in_wq <- subset(dat, ID == "IN")
in_wq <- in_wq[,-c(2)]

in_wq %>%
gather(key = "nut", value = "conc", -datetime)%>%
ggplot()+
geom_point(aes(x = datetime, y = conc, color = nut))+
geom_smooth(aes(x = datetime, y = conc, color = nut), se = FALSE, span = 0.4)

# outlet 1 samples
out1_wq <- subset(dat, ID == "OUT1")
out1_wq <- out1_wq[,-c(2)]

# outlet 2 samples
out2_wq<- subset(dat, ID == "OUT2")

```

```

out2_wq <- out2_wq[,-c(2)]
## Water Balance
wb <- read.csv("data/clean/daily_wb.csv")
wb$datetime <- as.POSIXct(wb$date, format = "%Y-%m-%d")

# filter flow data to pre cleanout data
wb <- wb %>%
  filter(datetime >= "2019-06-01" & datetime <= "2021-05-31")

temp <- wb %>%
  select(datetime, W_temp)%>%
  group_by(month = lubridate::floor_date(datetime, "month"))%>%
  summarise(mean = mean(W_temp, na.rm = TRUE),
            sd = sd(W_temp, na.rm = TRUE))

# Cell 1 monthly means
in1_flow <- wb %>%
  select(datetime, inlet1) %>%
  dplyr::rename(flow = inlet1) %>%
  mutate(flow = flow/86400,
         datetime = as.Date(datetime),
         datetime = as.POSIXct(datetime))

# in1 <- monthly.mean(in1_flow, "sd") %>%
# mutate(flow=flow*86400)

out1_flow <- wb %>%
  select(datetime, out1) %>%
  dplyr::rename(flow = out1) %>%
  mutate(flow = flow/86400,
         datetime = as.Date(datetime),
         datetime = as.POSIXct(datetime))

monthly.mean(out1_flow, "sd") %>%
  mutate(flow=flow*86400)

# Cell 2 monthly means
in2_flow <- wb %>%
  select(datetime, inlet2)%>%
  dplyr::rename(flow = inlet2) %>%
  mutate(flow = flow/86400,
         datetime = as.Date(datetime),
         datetime = as.POSIXct(datetime))

# in2 <- monthly.mean(in2_flow, "sd") %>%
# mutate(flow=flow*86400)

out2_flow <- wb %>%
  select(datetime, out2) %>%
  dplyr::rename(flow = out2) %>%
  mutate(flow = flow/86400,
         datetime = as.Date(datetime),
         datetime = as.POSIXct(datetime))

monthly.mean(out2_flow, "sd") %>%
  mutate(flow=flow*86400)

# in1$flow-in2$flow

#####
#Flow weighted averages
#####
# create vector for results
result <- data.frame(cell = c("cell1","cell1","cell2","cell2"), loc =
c("inlet","outlet","inlet","outlet"),
                    on = c(0,0,0,0), nh4 = c(0,0,0,0), no3 = c(0,0,0,0), tn = c(0,0,0,0))

```

```
# from this setup, in the output lists, nh4 is 1, no3 is 2, on is 3, and tn is 4
```

```
# Cell 1
```

```
#####
```

```
# Inlet
```

```
union <- left_join(in1_flow,in_wq)
union
```

```
in1.month<-method6(union, 8, "month")
```

```
in1.df <- as.data.frame(in1.month)
```

```
in1.df <- setDT(in1.df, keep.rownames = "month")[]
```

```
in1.df <- in1.df %>%
  mutate(ID = "IN")
```

```
in1.year <- method6(union, 8, "year")
```

```
in1.year <- as.data.frame(in1.year)
```

```
in1.year <- setDT(in1.year, keep.rownames = "year")[]
```

```
in1.year <- in1.year %>%
  mutate(ID="IN")
```

```
#in1.df <- in1.df %>%
```

```
# mutate(don = don/1000,
#         nh4n = nh4n/1000,
#         no3n = no3n/1000,
#         on = on/1000,
#         tn = tn/1000,
#         tdn = tdn/1000)
```

```
write.csv(in1.df, "data/clean/ch4/in1.csv")
```

```
## Outlet
```

```
union<-left_join(out1_flow, out1_wq)
```

```
out1.month<-method6(union, 8, "month")
```

```
out1.df <- as.data.frame(out1.month)
```

```
out1.df <- setDT(out1.df, keep.rownames = "month")[]
```

```
out1.df <- out1.df %>%
  mutate(ID = "OUT1")
```

```
# yearly
```

```
out1.year <- method6(union, 8, "year")
```

```
out1.year <- as.data.frame(out1.year)
```

```
out1.year <- setDT(out1.year, keep.rownames = "year")[]
```

```
out1.year <- out1.year %>%
  mutate(ID="OUT1")
```

```
#out1.df <- out1.df %>%
```

```
# mutate(don = don/1000,
#         nh4n = nh4n/1000,
#         no3n = no3n/1000,
#         on = on/1000,
#         tn = tn/1000,
#         tdn = tdn/1000)
```

```

write.csv(out1.df, "data/clean/ch4/out1.csv")

#####
# Cell 2
#####
## Inlet
union <- left_join(in2_flow,in_wq)
union

in2.month<-method6(union, 8, "month")

in2.df <- as.data.frame(in2.month)

in2.df <- setDT(in2.df, keep.rownames = "month")[]

in2.df <- in2.df %>%
  mutate(ID = "IN")

#yearly
in2.year <- method6(union, 8, "year")

in2.year <- as.data.frame(in2.year)

in2.year <- setDT(in2.year, keep.rownames = "year")[]

in2.year <- in2.year %>%
  mutate(ID="IN")

#in2.df <- in2.df %>%
# mutate(don = don/1000,
#         nh4n = nh4n/1000,
#         no3n = no3n/1000,
#         on = on/1000,
#         tn = tn/1000,
#         tdn = tdn/1000)

write.csv(in2.df, "data/clean/ch4/in2.csv")

## Outlet
union <- left_join(out2_flow,out2_wq)
union

out2.month<-method6(union, 8, "month")

out2.df <- as.data.frame(out2.month)

out2.df <- setDT(out2.df, keep.rownames = "month")[]

out2.df <- out2.df %>%
  mutate(ID = "OUT2")

out2.year <- method6(union, 8, "year")

out2.year <- as.data.frame(out2.year)

out2.year <- setDT(out2.year, keep.rownames = "year")[]

out2.year <- out2.year %>%
  mutate(ID="OUT2")

```

Example of R Code for monthly analysis

```
# Author: Brock Kamrath
# Date: 5/15/2021
# Objective: WB, Concentration, and Load Analysis for Chapter 4
rm(list = ls())

# load packages
library(ggplot2)
library(dplyr)
library(tidyverse)
library(lubridate)
library(colortools)
library(readxl)
library(gridExtra)

#####
#                               load in grab data                               #
#####
raw <- read_excel("data/raw/wq/grab_samp.xlsx")

# MDL is 0.03, if concentrations is below MDL, then bump up to MDL (mainly for nitrate and on)
# for(i in 1:nrow(raw)){
#   if(raw$NO3[i] <= 0.23){
#     raw$NO3[i] <- runif(1,min=0,max=0.23)
#   }
#   if(raw$NH4[i] <= 1){
#     raw$NH4[i] <- runif(1,min=0,max=1)
#   }
# }

raw$NO3 <- round(raw$NO3,2)
raw$NH4 <- round(raw$NH4,2)

# remove discrete nitrate dosing samples and midpoint samples
data <- raw %>%
  filter(no3_dosing <= 0.1) %>%
  filter(ID != "MID1") %>%
  filter(Date >= "2019-06-01") %>%
  select(-no3_dosing, -Isco,-Time_Win) %>%
  group_by(year_month = lubridate::floor_date(Date, "month"), ID) %>%
  dplyr::summarise(across(where(is.numeric), ~ mean(.x, na.rm = TRUE)))

data_nit <- data %>%
  select(year_month,ID, NO3, NH4, Temp, Do, Do_per, pH,Scnd)

#####
#                               load in comp data                               #
#####

conc <- read.csv("data/raw/wq/wc_comp.csv")

#filter to include only wk_comp samples
wq <- conc %>%
  mutate(start_date = as.POSIXct(conc$start_date, format = "%m/%d/%Y"),
         datetime = as.POSIXct(conc$end_date, format = "%m/%d/%Y")) %>%
  subset(location == "IN"|location == "OUT1"|location=="OUT2") %>%
  subset(type == "wk_comp" | type == "daily") %>%
  subset(filter != "DUP" & filter != "UF") %>%
  filter(start_date >= "2019-06-01") %>%
  mutate(don = tkn-nh4n,
         tdn = tkn+no3n) %>%
  select(location,start_date,datetime, don, nh4n, no3n, tdn) %>%
  group_by(location, start_date, datetime) %>%
  dplyr::summarise(across(where(is.numeric), ~ mean(.x, na.rm = TRUE)))
```

```

#####
# filter to include only wk_comp samples for unfiltered
wq_uf <- conc %>%
  mutate(start_date = as.POSIXct(conc$start_date, format = "%m/%d/%Y"),
         datetime = as.POSIXct(conc$end_date, format = "%m/%d/%Y")) %>%
  subset(location == "IN"|location == "OUT1"|location=="OUT2") %>%
  subset(type == "wk_comp") %>%
  subset(filter == "UF" & filter != "DUP") %>%
  filter(start_date >= "2019-06-01") %>%
  mutate(on = tkn-nh4n,
         tn = tkn+no3n) %>%
  select(location,start_date,datetime, on,tn) %>%
  group_by(location, start_date, datetime) %>%
  dplyr::summarise(across(where(is.numeric), ~ mean(.x, na.rm = TRUE)))

# wq_uf <- na.omit(wq_uf)

wqc <- left_join(wq, wq_uf, by = c("location","start_date","datetime"), keep = FALSE)

# break out weekly composite sampling by day
wq_daily <- wqc %>%
  expand(datetime = seq(start_date, datetime, by="1 day"), don, on, nh4n, no3n, tdn, tn)
#####

# DON cannot be negative, if concentrations is below 0, then set to 0.01 (mainly for nitrate and on)
for(i in 1:nrow(wq_daily)){
  if(wq_daily$don[i] <= 0){
    wq_daily$don[i] <- 0.01
  }
}

# widen data for use in parametric tests
mon_wide <- wq_daily %>%
  group_by(year_month = lubridate::floor_date(datetime, "month"), location) %>%
  dplyr::summarise(don = mean(don, na.rm= TRUE),
                 on = mean(on, na.rm= TRUE),
                 nh4n = mean(nh4n, na.rm= TRUE),
                 no3n = mean(no3n,na.rm = TRUE),
                 tdn = mean(tdn, na.rm=TRUE),
                 tn = mean(tn, na.rm = TRUE)) %>%
  dplyr::rename(ID = location) %>%
  mutate(year_month = as.Date(year_month))

#####
wq_mon <- left_join(data_nit, mon_wide, by = c("ID","year_month"))
wq_mon$tn[is.nan(wq_mon$tn)]<-NA

#remove april 2021 - nitrate dosing study
wq_mon <- wq_mon[-c(61:63),]

write.csv(wq_mon,"data/clean/ch4/wq_mon.csv")

inlet <- wq_mon %>%
  filter(ID == "IN")

out1 <- wq_mon %>%
  filter(ID == "OUT1")

out2 <- wq_mon %>%
  filter(ID == "OUT2")

#summarise values
wq_mon %>%
  select(-year_month) %>%
  group_by(ID) %>%
  summarise(across(where(is.numeric), ~ mean(.x, na.rm = TRUE)))

```

```

wq_mon %>%
  select(-year_month) %>%
  group_by(ID) %>%
  summarise(across(where(is.numeric), ~ sd(.x, na.rm = TRUE)))

wq_mon_plot <- gather(wq_mon, key = "pollutant", value = "conc", -year_month, -ID)

season <- c(rep("Spring",3),rep("Summer",9),rep("Fall",9),rep("Winter",9),
           rep("Spring",3), rep("Summer",9),rep("Fall",9),rep("Winter",9),
           rep("Spring",3))

#Summarise by season
wq_seasonality <- wq_mon %>%
  add_column(season) %>%
  gather(key = "pollutant", value = "conc", -year_month, -ID, -season) %>%
  group_by(ID, season, pollutant) %>%
  dplyr::summarise(mean = mean(conc, na.rm = TRUE),
                  sd = sd(conc, na.rm=TRUE),
                  min = min(conc, na.rm=TRUE),
                  max = max(conc, na.rm = TRUE),
                  n = n_distinct(conc, na.rm = TRUE))

# Summarise by overall for the entire two year period
wq_overall <- wq_mon_plot %>%
  group_by(ID, pollutant) %>%
  dplyr::summarise(mean = mean(conc, na.rm = TRUE),
                  sd = sd(conc, na.rm=TRUE),
                  min = min(conc, na.rm=TRUE),
                  max = max(conc, na.rm = TRUE),
                  n = n_distinct(conc, na.rm = TRUE))

#####
# Nitrogen species plots
wq_mon <- wq_mon %>%
  add_column(season) %>%
  mutate(season = as.factor(season))

#nitrate plots
pl_no3 <- wq_mon_plot %>%
  filter(pollutant == "NO3") %>%
  ggplot(aes(as.Date(year_month), conc, color = ID))+
  geom_point()+
  geom_line()+
  lims(y = c(0,5))+
  labs(y = "", x = "")+
  scale_color_manual(values=c("grey50", "dodgerblue4", "orangered1"))+
  scale_x_date(date_breaks = "3 month", date_labels = "%m-%y") +
  theme_classic()+
  theme(text = element_text(size = 14))

pb_no3 <- wq_mon %>%
  filter(ID != "IN") %>%
  ggplot(aes(ID, NO3, fill = ID)) +
  geom_boxplot(outlier.shape = NA, coef = 0, show.legend = FALSE) +
  geom_point(aes(fill=ID, group=year_month), size=2, shape=21, show.legend = FALSE)+
  geom_line(aes(group=year_month)) +
  theme(legend.position = "none")+
  lims(y = c(0,5))+
  labs(y = expression(NO[3]~-N~(mg~L^{-1})), x = "")+
  scale_fill_manual(values=c("dodgerblue4", "orangered1"))+
  theme_classic()+
  theme(text = element_text(size = 14))

grid.arrange(pb_no3, pl_no3, nrow=1, widths = c(1,2))

```

```

#ammonium plots
pl_nh4 <- wq_mon_plot %>%
filter(pollutant == "NH4") %>%
  ggplot(aes(as.Date(year_month), conc, color = ID))+
  geom_point()+
  geom_line()+
  labs(y = "", x = "Date")+
  lims(y = c(0,20))+
  scale_color_manual(values=c("grey50", "dodgerblue4", "orangered1"))+
  scale_x_date(date_breaks = "3 month", date_labels = "%m-%y") +
  theme_classic()+
  theme(text = element_text(size = 14))

pb_nh4 <- wq_mon %>%
  filter(ID != "IN") %>%
  ggplot(aes(ID, NH4, fill=ID)) +
  geom_boxplot(outlier.shape = NA, coef = 0, show.legend = FALSE) +
  geom_point(aes(fill=ID, group=year_month), size=2, shape=21, show.legend = FALSE)+
  geom_line(aes(group=year_month)) +
  theme(legend.position = "none")+
  lims(y = c(0,20))+
  labs(y = expression(NH[4]~N~(mg~L^{-1})), x = "")+
  scale_fill_manual(values=c("dodgerblue4", "orangered1"))+
  theme_classic()+
  theme(text = element_text(size = 14))

grid.arrange(pb_nh4, pl_nh4, nrow=1, widths = c(1,2))

# dissolved organic nitrogen plots
pl_don <- wq_mon_plot %>%
  filter(pollutant == "don") %>%
  ggplot(aes(as.Date(year_month), conc, color = ID))+
  geom_point()+
  geom_line()+
  lims(y = c(0,20))+
  labs(y = "", x = "")+
  scale_color_manual(values=c("grey50", "dodgerblue4", "orangered1"))+
  scale_x_date(date_breaks = "3 month", date_labels = "%m-%y") +
  theme_classic()+
  theme(text = element_text(size = 14))

pb_don <- wq_mon %>%
  filter(ID != "IN") %>%
  ggplot(aes(ID, don, fill=ID)) +
  geom_boxplot(outlier.shape = NA, coef = 0, show.legend = FALSE) +
  geom_point(aes(fill=ID, group=year_month), size=2, shape=21, show.legend = FALSE)+
  geom_line(aes(group=year_month)) +
  theme(legend.position = "none")+
  lims(y = c(0,15))+
  labs(y = expression(DON~(mg~L^{-1})), x = "")+
  scale_fill_manual(values=c("dodgerblue4", "orangered1"))+
  theme_classic()+
  theme(text = element_text(size = 14))

grid.arrange(pb_don, pl_don, nrow=1, widths = c(1,2))

# organic nitrogen plots
pl_on <- wq_mon_plot %>%
  filter(pollutant == "on") %>%
  ggplot(aes(as.Date(year_month), conc, color = ID))+
  geom_point()+
  geom_line()+
  lims(y = c(0,15))+
  labs(y = "", x = "Date")+
  scale_color_manual(values=c("grey50", "dodgerblue4", "orangered1"))+

```

```

scale_x_date(date_breaks = "3 month", date_labels = "%m-%y") +
theme_classic()+
theme(text = element_text(size = 14))

pb_on <- wq_mon %>%
  filter(ID != "IN") %>%
  ggplot(aes(ID,on, fill=ID)) +
  geom_boxplot(outlier.shape = NA, coef = 0,show.legend = FALSE) +
  geom_point(aes(fill=ID,group=year_month),size=2,shape=21,show.legend = FALSE)+
  geom_line(aes(group=year_month)) +
  theme(legend.position = "none")+
  lims(y = c(0,15))+
  labs(y = expression(ON~(mg~L^{-1})), x = "")+
  scale_fill_manual(values=c("dodgerblue4","orangered1"))+
  theme_classic()+
  theme(text = element_text(size = 14))

grid.arrange(pb_on,pl_on,nrow=1,widths = c(1,2))

# total dissolved nitrogen plots
pl_tdn <- wq_mon_plot %>%
  filter(pollutant == "tdn") %>%
  ggplot(aes(as.Date(year_month), conc, color = ID))+
  geom_point()+
  geom_line()+
  lims(y = c(0,20))+
  labs(y = "", x = "")+
  scale_color_manual(values=c("grey50","dodgerblue4","orangered1"))+
  scale_x_date(date_breaks = "3 month", date_labels = "%m-%y") +
  theme_classic()+
  theme(text = element_text(size = 14))

pb_tdn <- wq_mon %>%
  filter(ID != "IN") %>%
  ggplot(aes(ID,tdn, fill=ID)) +
  geom_boxplot(outlier.shape = NA, coef = 0,show.legend = FALSE) +
  geom_point(aes(fill=ID,group=year_month),size=2,shape=21,show.legend = FALSE)+
  geom_line(aes(group=year_month)) +
  theme(legend.position = "none")+
  lims(y = c(0,20))+
  labs(y = expression(TDN~(mg~L^{-1})), x = "")+
  scale_fill_manual(values=c("dodgerblue4","orangered1"))+
  theme_classic()+
  theme(text = element_text(size = 14))

grid.arrange(pb_tdn,pl_tdn,nrow=1,widths = c(1,2))

# total nitrogen plots
pl_tn <- wq_mon_plot %>%
  filter(pollutant == "tn") %>%
  ggplot(aes(as.Date(year_month), conc, color = ID))+
  geom_point()+
  geom_line()+
  lims(y = c(0,20))+
  labs(y = "", x = "Date")+
  scale_color_manual(values=c("grey50","dodgerblue4","orangered1"))+
  scale_x_date(date_breaks = "3 month", date_labels = "%m-%y") +
  theme_classic()+
  theme(text = element_text(size = 14))

pb_tn <- wq_mon %>%
  filter(ID != "IN") %>%
  ggplot(aes(ID,tn, fill=ID)) +
  geom_boxplot(outlier.shape = NA, coef = 0,show.legend = FALSE) +
  geom_point(aes(fill=ID,group=year_month),size=2,shape=21, show.legend = FALSE)+

```

```

geom_line(aes(group=year_month)) +
theme(legend.position = "none")+
lims(y = c(0,20))+
labs(y = expression(TN~(mg~L^{-1})), x = "")+
scale_fill_manual(values=c("dodgerblue4","orangered1"))+
theme_classic()+
theme(text = element_text(size = 14))

grid.arrange(pb_tn,pl_tn,nrow=1,widths = c(1,2))

grid.arrange(pb_no3,pl_no3,
pb_nh4,pl_nh4,
nrow = 2, widths = c(1,2))

grid.arrange(pb_don,pl_don,
pb_on,pl_on,
nrow = 2, widths = c(1,2))

grid.arrange(pb_tdn,pl_tdn,
pb_tn,pl_tn,
nrow=2,widths = c(1,2))

grid.arrange(pb_nh4, pb_no3,
pb_don, pb_on,
pb_tdn, pb_tn,
nrow = 3)

#####
# Water quality plots
#temperature plots
pl_temp <- wq_mon_plot %>%
  filter(pollutant == "Temp") %>%
  ggplot(aes(as.Date(year_month), conc, color = ID))+
  geom_point()+
  geom_line()+
  lims(y = c(0,35))+
  labs(y = "", x = "")+
  scale_color_manual(values=c("grey50","dodgerblue4","orangered1"))+
  scale_x_date(date_breaks = "3 month", date_labels = "%m-%y") +
  theme_classic()+
  theme(text = element_text(size = 14))

pb_temp <- wq_mon %>%
  filter(ID != "IN") %>%
  ggplot(aes(ID,Temp, fill=ID)) +
  geom_boxplot(outlier.shape = NA, coef = 0,show.legend = FALSE) +
  geom_point(aes(fill=ID,group=year_month),size=2,shape=21,show.legend = FALSE)+
  geom_line(aes(group=year_month)) +
  theme(legend.position = "none")+
  lims(y = c(0,35))+
  labs(y = expression(Water~temperature~(degree~C)), x = "")+
  scale_fill_manual(values=c("dodgerblue4","orangered1"))+
  theme_classic()+
  theme(text = element_text(size = 14))

grid.arrange(pb_temp,pl_temp,nrow=1,widths = c(1,2))

#dissolved oxygen plots
pl_do <- wq_mon_plot %>%
  filter(pollutant == "Do") %>%
  ggplot(aes(as.Date(year_month), conc, color = ID))+
  geom_point()+
  geom_line()+
  labs(y = "", x = "")+
  lims(y = c(0,15))+
  scale_color_manual(values=c("grey50","dodgerblue4","orangered1"))+
  scale_x_date(date_breaks = "3 month", date_labels = "%m-%y") +

```

```

theme_classic()+
theme(text = element_text(size = 14))

pb_do <- wq_mon %>%
  filter(ID != "IN") %>%
  ggplot(aes(ID,Do, fill=ID)) +
  geom_boxplot(outlier.shape = NA, coef = 0,show.legend = FALSE) +
  geom_point(aes(fill=ID,group=year_month),size=2,shape=21,show.legend = FALSE)+
  geom_line(aes(group=year_month)) +
  theme(legend.position = "none")+
  lims(y = c(0,15))+
  labs(y = expression(DO~(mg~L^{-1})), x = "")+
  scale_fill_manual(values=c("dodgerblue4","orangered1"))+
  theme_classic()+
  theme(text = element_text(size = 14))

grid.arrange(pb_do,p1_do,nrow=1,widths = c(1,2))

# pH plots
p1_ph <- wq_mon_plot %>%
  filter(pollutant == "pH") %>%
  ggplot(aes(as.Date(year_month), conc, color = ID))+
  geom_point()+
  geom_line()+
  lims(y = c(6,9))+
  labs(y = "", x = "")+
  scale_color_manual(values=c("grey50","dodgerblue4","orangered1"))+
  scale_x_date(date_breaks = "3 month", date_labels = "%m-%y") +
  theme_classic()+
  theme(text = element_text(size = 14))

pb_ph <- wq_mon %>%
  filter(ID != "IN") %>%
  ggplot(aes(ID,pH, fill=ID)) +
  geom_boxplot(outlier.shape = NA, coef = 0,show.legend = FALSE) +
  geom_point(aes(fill=ID,group=year_month),size=2,shape=21,show.legend = FALSE)+
  geom_line(aes(group=year_month)) +
  theme(legend.position = "none")+
  lims(y = c(6,9))+
  labs(y = expression(pH), x = "")+
  scale_fill_manual(values=c("dodgerblue4","orangered1"))+
  theme_classic()+
  theme(text = element_text(size = 14))

grid.arrange(pb_ph,p1_ph,nrow=1,widths = c(1,2))

# Specific conductivity plots
p1_sc <- wq_mon_plot %>%
  filter(pollutant == "Scond") %>%
  ggplot(aes(as.Date(year_month), conc, color = ID))+
  geom_point()+
  geom_line()+
  labs(y = "", x = "Date")+
  scale_color_manual(values=c("grey50","dodgerblue4","orangered1"))+
  scale_x_date(date_breaks = "3 month", date_labels = "%m-%y") +
  theme_classic()+
  theme(text = element_text(size = 14))

pb_sc <- wq_mon %>%
  filter(ID != "IN") %>%
  ggplot(aes(ID,Scond, fill=ID)) +
  geom_boxplot(outlier.shape = NA, coef = 0,show.legend = FALSE) +
  geom_point(aes(fill=ID,group=year_month),size=2,shape=21,show.legend = FALSE)+
  geom_line(aes(group=year_month)) +

```

```

theme(legend.position = "none")+
labs(y = expression(Specific~conductivity~(mu~S~cm^{-1})), x = "Sampling Station")+
scale_fill_manual(values=c("dodgerblue4","orangered1"))+
theme_classic()+
theme(text = element_text(size = 14))

grid.arrange(pb_temp,pl_temp, pb_do,pl_do, pb_ph,pl_ph,
pb_sc,pl_sc,nrow=4,widths = c(1,2))
#####

# Statistical Analysis between outlet 1 and outlet 2

t.test(wq_mon$NH4,wq_mon$nh4n, paired = TRUE, na.rm = TRUE)
t.test(wq_mon$NO3,wq_mon$no3n, paired = TRUE, na.rm = TRUE)

#t.tests between outlets (paired by month)
#####
# Nitrogen concentrations

#Nitrate
t.test(out1$NO3,out2$NO3, paired = TRUE)

#Ammonium
t.test(out1$NH4,out2$NH4, paired = TRUE)

#dissolved organic nitrogen
t.test(out1$don,out2$don, paired = TRUE)

#organic nitrogen
t.test(out1$on,out2$on, paired = TRUE)

#total dissolved nitrogen
t.test(out1$tdn,out2$tdn, paired = TRUE)

#total nitrogen
t.test(out1$tn,out2$tn, paired = TRUE)

#####3
# water quality parameters

#temperature
t.test(out1$Temp,out2$Temp, paired = TRUE)

#dissolved oxygen
t.test(out1$Do,out2$Do, paired = TRUE)

#pH
t.test(out1$pH,out2$pH, paired = TRUE)

#specific conductivity
t.test(out1$Scond,out2$Scond, paired = TRUE)

ggplot(wq_mon,aes(x = pH, y= Do, ))+
  geom_point(aes(shape = ID))+
  geom_smooth(method = "lm",se=FALSE)+
  facet_wrap(~season)

#####
# Nitrogen species plots
wq_mon %>%
  ungroup() %>%
  select(ID, season, NO3, NH4, tn) %>%
  gather(key = "n_species", value = "conc", -ID, -season) %>%
  group_by(ID, season) %>%

```

```

ggplot(aes(season, conc, fill = ID)) +
  stat_summary(geom = "bar", fun = mean, position = "dodge") +
  stat_summary(geom = "errorbar", fun.data = mean_se, position = "dodge")+
  stat_summary(geom = "text", fun = mean, aes(label= round(..y..,1)), position = "dodge")+
  facet_wrap(~n_species)

library(plyr)
library(ggplot2)

dat <- wq_mon %>%
  ungroup() %>%
  select(ID, season, NO3, NH4) %>%
  gather(key = "n_species", value = "conc", -ID, -season) %>%
  group_by(ID, season, n_species) %>%
  dplyr::summarise(mean = mean(conc, na.rm = TRUE),
                  sd = sd(conc, na.rm = TRUE))

dat = within(dat, {
  mean_mpg_string = sprintf('%0.1f', mean)
})

nitrogen_names <- list(
  'NH4' = expression(NH[4]~-N),
  'NO3' = expression(NO[3]~-N)
)

nit_labeller <- function(variable,value){
  return(nitrogen_names[value])
}

ggplot(dat, aes(x = season, y = mean)) +
  geom_bar(aes(fill = ID), stat = "identity", position = "dodge") +
  geom_text(aes(label = mean_mpg_string, group = ID), position = position_dodge(width = 1),
            vjjust = -0.5, size = 3)+
  facet_wrap(~n_species, labeller = nit_labeller)+
  labs(y = expression(Average~seasonal~concentration~(mg~L^{-1})), x = "")+
  scale_fill_manual(values=c("grey50","dodgerblue4","orangered1"))+
  theme_classic()

wq_mon %>%
  ungroup() %>%
  select(ID, season, NO3, NH4, don, on, tdn, tn) %>%
  gather(key = "n_species", value = "conc", -ID, -season) %>%
  group_by(ID, season) %>%
  summarise(mean = mean(conc, na.rm = TRUE),
            sd = sd(conc, na.rm = TRUE))

```

APPENDIX F: CHAPTER V SUPPLEMENTAL INFORMATION

Pilot NO₃-N dosing studies at Walnut Cove

In the first stage, influent nitrate concentrations were increased via calcium nitrate additions to the duckweed collector pond influent just upstream of the wetland cells. The duckweed collector pond was dosed with 22.7 kg (50-lb) per day of YaraLiva Tropicote 15.5-0-0 dry slow-release calcium nitrate (Ca(NO₃)₂) fertilizer (Oslo, Norway). The fertilizer was mixed into the wastewater as it entered the duckweed collector pond for 20-30 minutes until all visible calcium nitrate pellets had dissolved. This process was completed every day during each five-day period. Each bag contained 14.5% NO₃-N, which resulted in 3.2 kg-N d⁻¹ of NO₃-N added to the influent waste stream during the short-term studies (1.6 kg-N d⁻¹ to each cell).

Data Collection

In the first stage, water quality samples were collected using composite flow-based sampling. For the first dosing run (9/21/2020 to 9/28/2020), a 350 mL sample was collected for every 37,850 L (10,000 gallons) of water that passed over the sharp-crested weirs. At an initial influent flow rate (Q_{in}) of 190 Lpm (273 m³ d⁻¹), this sampling scheme was designed to collect a sample every 3 hours. Two samples were composited in each bottle. Each bottle represented a 6-hour period. Therefore, each 700 mL sample represented 75,710 L (20,000 gallons). For the second dosing run (10/26/2020 to 11/2/2020), the flow-based sampling scheme was adjusted to reduce sample processing time. In this run, a 200 mL sample was collected for every 45,420 L (12,000 gallons) of water that passed into and out of the wetland cells. At an initial Q_{in} of 265 Lpm (380 m³ d⁻¹), this sampling scheme was predicted to collect a sample every 3 hours. Four samples were composited in each bottle with each bottle representing a 12-hour period. Therefore, each 800 mL sample represented 181,700 L (48,000 gallons). In both runs, sampling

was conducted over eight days to account for travel time through each cell (dosing only occurred for 5 days). For the first dosing run, a review of the concentration data from the eight-day sampling period (9/21/2021 – 9 /28/2021) showed that samples taken during the last two days of the dosing period were no longer influenced by the dosing due to a precipitation event on the fifth day of nitrate dosing. Therefore, the dataset was truncated to six days (9/21/21 – 9/26/21) by removing the last 8, 9, and 10 samples from the inlet, outlet1, and outlet 2 sampling locations.

Hydrology and Hydraulics

The mean daily influent flows to each cell during the dosing runs ranged from 297 to 401 $\text{m}^3 \text{d}^{-1}$ (0.08 to 0.11 MGD), which were slightly below the mean daily influent flow of 480 $\text{m}^3 \text{d}^{-1}$ (0.12 MGD) for the period from September 2020 through April 2021 (Table F.1). Outflows were greater than inflows for each period. Cumulative P and ET totals were approximately equal for the first two dosing runs. Because P fell over a larger area, the runoff area to the cells was greater than surface area due to side slopes, this was expected. During the third dosing run, cumulative ET eclipsed P. This was expected to result in lower outflows than inflows. Outflow estimates eclipsing inflow estimates during this period suggested slight flow estimate errors, slight ET estimate errors, or both. However, these slight estimation errors should not substantially influence removal estimates during the period.

Table F.1: Hydrologic results during the first two dosing runs.

Dosing Run	$Q_{\text{in}} (\text{m}^3 \text{d}^{-1})$	P (mm)	ET (mm)	Cell 1 $Q_{\text{out}} (\text{m}^3 \text{d}^{-1})$	Cell 2 $Q_{\text{out}} (\text{m}^3 \text{d}^{-1})$
9/21/20 to 9/26/20	297 ± 114	23	17	309 ± 137	283 ± 131
10/26/20 to 11/2/20	401 ± 122	28	28	475 ± 142	454 ± 127

The hydraulic conditions based on the tracer tests conducted in the fall 2020 and spring 2021 are reported. The hydraulic parameters varied slightly within each cell, between the fall 2020 and the spring 2021 tracer tests. These variations were likely caused by temporal changes in site factors that influenced flow patterns, such as mean water depth, influent flow rate, and vegetation density. Even with this variability, tracer test results showed that hydraulic conditions were consistently better in cell 1 than cell 2.

Table F.2: Hydraulic conditions within the two FWS CW cells at the Walnut Cove WWTP during the three nitrate dosing periods. The values of N and e were used as part of equations 5.4 and 5.5 to estimate a nitrate removal rate constant for the site.

Dosing Run	Wetland	Water depth (m)	N	e	τ (d)	HLR_e ($m\ d^{-1}$)
9/21/20 to 9/26/20	Cell 1	0.18	5.8	0.52	3.6	0.05
	Cell 2	0.15	3.9	0.38	2.6	0.06
10/26/20 to 11/2/20	Cell 1	0.18	5.8	0.52	2.8	0.07
	Cell 2	0.15	3.9	0.38	2.0	0.07
3/21/21 to 4/20/21	Cell 1	0.18	8.1	0.37	1.9	0.09
	Cell 2	0.12	2.2	0.17	0.9	0.14

Water Quality parameters

For each dosing run, temperature, DO, and pH measurements were taken during each site visit at each sampling location. Water temperature, DO, and pH were important for evaluating wetland nitrogen removal performance because biological nitrogen transformation rates have been inextricably linked to these water quality parameters (Bachand & Horne, 1999b; Kadlec & Wallace, 2009; Mitsch & Gosselink, 2015; Vymazal, 2007).

Mean water temperatures for the dosing periods ranged from 14 to 22 °C, with water temperature increasing through cell 2 and decreasing through cell 1 (Table 5.3). Based on these values, water temperatures were always above the minimum temperature for biological nitrogen

processing (5 °C), but below the optimal temperature ranges for denitrification (60-75 °C) and nitrification (30-40 °C) (Vymazal, 2007). Mean DO concentrations for the first stage dosing periods ranged from 0.2 to 4 mg L⁻¹. Again, values increased through cell 2 and decreased through cell 1. These values were in the expected range for a constantly saturated high nutrient FWS CW and favorable for anaerobic conditions within the detritus substrate. With DO concentrations near or below 1.5 mg L⁻¹, nitrification rates were likely to be severely reduced at in cell 1. DO concentrations above 1.5 mg L⁻¹ at the outlet of cell 2 allowed for the possibility of nitrification in cell 2. During the third dosing run, DO concentrations were substantially increased with the mean inlet concentration above saturation (10.1 mg L⁻¹) and mean outlet concentrations in the 3-5 mg L⁻¹ range. These values indicated a high potential for nitrification in both cells during this period. Mean pH values showed a similar trend to temperature and DO, with near neutral values (6.8 - 7.2), an increase through cell 2, and a decrease through cell 1 during the first two dosing runs. These values were within optimal ranges for nitrification and denitrification (Vymazal, 2007). Then, for the third dosing run, the pH values increased substantially, with a mean inlet pH value of 8.6. Taken together, these values suggested that the wetland environment was conducive to denitrification and unfavorable for nitrification during the first dosing stage (runs 1 and 2), but these conditions changed in stage 2.

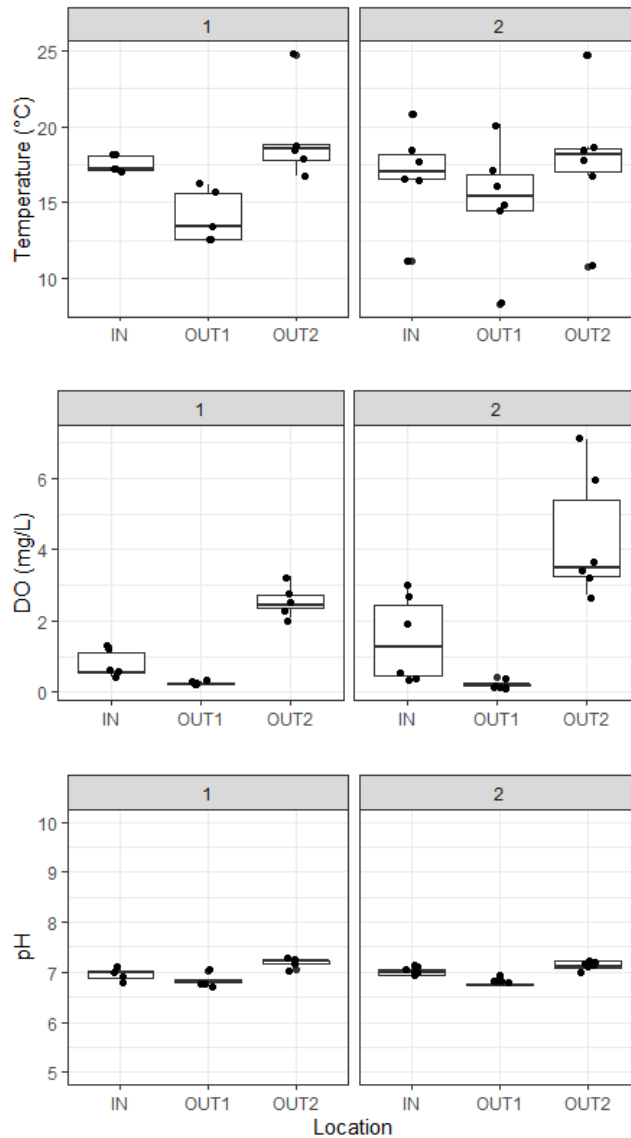


Figure F.1: Water quality parameters for nitrate dosing tests 1 and 2.

Table F.3: Mean values for temperature, dissolved oxygen, and pH for each dosing run. Mean values calculated from measurements taken during site visits.

Dosing Run	Location	Temperature (°C)	DO (mg L ⁻¹)	pH
9/21/20 to 9/28/20	Inlet	17.5	0.8	7.0
	Outlet 1	14.1	0.2	6.8
	Outlet 2	19.3	2.6	7.2
10/26/20 to 11/2/20	Inlet	16.8	1.5	7.0
	Outlet 1	15.1	0.2	6.8
	Outlet 2	17.8	4.3	7.1

Results

The measured influent nitrate load during the dosing study was 14.4 kg, which corresponded to 87% of the actual load added (16.5 kg). Because the influent waste stream was split equally into both cells, the influent nitrate load to each cell was assumed to be 7.2 kg. The effluent nitrate loads from cells 1 and 2 were 0.95 and 1.81 kg, respectively. Using this data, the nitrate load was reduced by 87% in cell 1 and 75% in cell 2. The areal mass removal rates over the eight-day study period were $39.4 \text{ g-N m}^{-2} \text{ yr}^{-1}$ and $34.0 \text{ g-N m}^{-2} \text{ yr}^{-1}$ for cell 1 and cell 2, respectively.

The measured influent nitrate load during the dosing study was 10.9 kg, which corresponded to 67% of the actual load added (16.5 kg). Because the influent waste stream was split equally into both cells, the influent nitrate load to each cell was assumed to be 5.4 kg. The effluent nitrate loads from cells 1 and 2 were 0.8 and 2.1 kg, respectively. Using this data, the nitrate load was reduced by 85% in cell 1 and 61% in cell 2. The areal mass removal rates over the eight-day study period were $29.3 \text{ g-N m}^{-2} \text{ yr}^{-1}$ and $21.1 \text{ g-N m}^{-2} \text{ yr}^{-1}$ for cell 1 and cell 2, respectively.

R code for Chapter V analysis

```
# Author: Brock Kamrath
# Objective: ON, NH4, NO3, and TN concentration and load analysis
# Date: 06/24/2021

library(tidyverse)
library(readxl)

data_raw <- read_excel("data/raw/comp_data3.xlsx",
                      sheet = "r_data")

# make "data a list
data <- list()

# create cleaned dataset with on conc and loads in kg/d
data_cn <- data_raw %>%
  mutate(on = tkn-nh4,
         on_kg = (on*flow)/1000,
         nh4_kg = (nh4*flow)/1000,
         no3c_kg = (no3c*flow)/1000,
         tnc_kg = (tnc*flow)/1000) %>%
  select(loc, sample, flow, on, nh4, no3c, tnc, on_kg, nh4_kg, no3c_kg, tnc_kg)

# first list in data (inlet1)
data[[1]] <- data_cn %>%
  filter(loc == "IN")

# second list in data (out1)
data[[2]] <- data_cn %>%
  filter(loc == "OUT1")

# third list in data (inlet2)
data[[3]] <- data_cn %>%
  filter(loc == "IN")

# fourth list in data (out2)
data[[4]] <- data_cn %>%
  filter(loc == "OUT2")

# create dataframes to contain concentration results (conc_result) and load results (load_result)
conc_result <- data.frame(cell = c("cell1", "cell1", "cell2", "cell2"), loc =
  c("inlet", "outlet", "inlet", "outlet"),
  on = c(0,0,0,0), nh4 = c(0,0,0,0), no3 = c(0,0,0,0), tn = c(0,0,0,0))

load_result <- data.frame(cell = c("cell1", "cell1", "cell2", "cell2"), loc =
  c("inlet", "outlet", "inlet", "outlet"),
  on = c(0,0,0,0), nh4 = c(0,0,0,0), no3 = c(0,0,0,0), tn = c(0,0,0,0))

# for loop to calculate concentration and load dynamics
for(j in 1:4){
  data_new <- data[[j]]
  for(i in 1:4){
    conc_result[j,i+2] <- round(weighted.mean(data_new[,i+3], data_new[,3], na.rm = FALSE), digits =1)
    load_result[j,i+2] <- round(sum(data_new[,i+7]), digits =1)
  }
}

conc_result
load_result
```

APPENDIX G: CHAPTER VI SUPPLEMENTAL INFORMATION

Table G.1: NPDES data for Danbury WWTP in 2019.

<i>YEAR</i>	<i>MONTH</i>	<i>DAYS</i>	<i>FLOW_MGD</i>	<i>NH4_MAX</i>	<i>FLOW_GPD</i>	<i>FLOW_LPD</i>	<i>NH4_KG</i>
2019	1	31	0.0313	4.03	31300	118470.5	14.80
2019	2	28	0.0635	0.819	63500	240347.5	5.51
2019	3	31	0.0288	14.4	28800	109008	48.66
2019	4	30	0.0291	13.1	29100	110143.5	43.29
2019	5	31	0.0315	3.16	31500	119227.5	11.67
2019	6	30	0.0398	1.89	39800	150643	8.54
2019	7	31	0.0463	2.56	46300	175245.5	13.91
2019	8	31	0.0587	0.405	58700	222179.5	2.79
2019	9	30	0.0643	0.444	64300	243375.5	3.24
2019	10	31	0.0437	0.467	43700	165404.5	2.39
2019	11	30	0.0344	0.335	34400	130204	1.30
2019	12	31	0.0313	0.393	31300	118470.5	1.44

Table G.2: Grab Sample data for Danbury WWTP collected by Dr. Burchell's team.

<i>SITE</i>	<i>DATE</i>	<i>YEAR</i>	<i>MONTH</i>	<i>TKN</i>	<i>NH4N</i>	<i>NO3N</i>	<i>TN</i>	<i>TP</i>	<i>COD</i>
DWTP	1/11/2019	2019	1	1.35	1.17	22.52	23.87	1.76	
DWTP	1/25/2019	2019	1	0.43	0.38	17.05	17.49	1.58	
DWTP	2/22/2019	2019	2	1.59	0.34	18.42	20.02	4.2	
DWTP	3/8/2019	2019	3	0.93	0.67	16.98	17.91		
DWTP	3/29/2019	2019	3	13.72	13.3	7.53	21.25		114.61
DWTP	4/12/2019	2019	4	19.5	15.4	1.03	20.53	1.93	
DWTP	4/22/2019	2019	4	0.68	1.44	12.86	13.54	3.12	108
DWTP	5/10/2019	2019	5	5.4	3.98	6.37	11.77		
DWTP	5/24/2019	2019	5	3.42	2.86	5.73	9.15		
DWTP	6/21/2019	2019	6	3.33	2.25	8.13	11.46	2.18	
DWTP	6/28/2019	2019	6	0.31	0.89	11.44	11.75		
DWTP	7/19/2019	2019	7	1.87	3.93	12.12	13.99		
DWTP	7/26/2019	2019	7	0.78	0.45	12.5	13.28		
DWTP	8/13/2019	2019	8	0.61	0.14	11.2	11.81		
DWTP	8/23/2019	2019	8	0.26	0.32	13	13.26		
DWTP	9/6/2019	2019	9	0.36	0.39	13.6	13.96	7.23	
DWTP	9/27/2019	2019	9	0.93	0.29	14.9	15.83	6.54	
DWTP	10/11/2019	2019	10	0.68	0.23	16.63	17.31		
DWTP	10/25/2019	2019	10	0.28	0.22	20.03	20.31	4.74	
DWTP	11/8/2019	2019	11	0.1	0.16	18.8	18.9	3.45	
DWTP	11/22/2019	2019	11	0.13	0.24	18.7	18.83		
DWTP	12/6/2019	2019	12	0.31	0.14	16.5	16.81		
DWTP	12/16/2019	2019	12	0.15	0.13	9.85	10		

R Code for Chapter IV analysis

```
# Author: Brock Kamrath
# Date: 7/21/21
# Objective: Run an uncertainty analysis for each month using
# the values found at Walnut Cove

# Clear the workspace
rm(list=ls(all=TRUE))
set.seed(0874)

# Load packages
library(tidyverse)
library(sensitivity)
library(readxl)
library(lubridate)

# danbury temperature and flow data from 2016-2020
data <- read_excel("Ph.D/Walnut_Cove/danbury_flows/Danburyflowsandtemp.xlsx")

#####3
# check danbury data plots
ggplot(data)+
  geom_density(aes(temp))

ggplot(data)+
  geom_density(aes(temp, color = period))

g_data <- data %>%
  filter(period == "g")

ng_data <- data %>%
  filter(period == "ng")
#####

# number of runs
n <- 5000

# fifty fifty split for temperature data
w <- rbinom(n, 1, 0.5)

# k 20 values with a range from 0.068 (25 m/yr) to .16 (60 m/yr) - uniform distribution
k20 <- runif(n, min=0.068, max = 0.16)

# N values from 1 to 10 - uniform distribution
N <- runif(n, min = 1, max = 10)

# temperature from 0 to 30 deg C
temp <- runif(n, min = 0, max = 30)

# constant removal rate of 0.1 (90% removal)
rem <- rep(0.1, n)

ggplot()+
  geom_density(aes(temp))

# blank vector for y
y <- rep(0,n)

# blank vector for k
k <- rep(0,n)
```

```

# meat and potatoes evaluation using the arrenhius and TIS model
for(i in 1:n){
  k[i] <- k20[i]*1.106^(temp[i]-20)
  y[i] <- (((rem[i])^(-1/N[i]))-1)*(N[i]/k[i])
  y[i] <- (y[i]*0.003785*10^6)/10000
}

# summary of y values ( y is in ha/MGD - see Jasper, 2014)
summary(y)
shapiro.test(y)

ggplot()+
  geom_density(aes(y))

ggplot()+
  geom_point(aes(x = k, y= y))

# Create an area value for different flows at danbury - Blocked out, doesn't make sense
# Qin <- rnorm(n, mean = 0.033, sd = 0.01)
# Area <- Qin*y

# summary(Area)
#ggplot()+
#  geom_density(aes(Area))

ggplot()+
  geom_point(aes(x = temp, y = log(y)))+
  geom_smooth(aes(x = temp, y = log(y)),method = "lm")+
  labs(x = expression(paste('Temperature (',degree,'C',sep='')), y = expression(ln(A[90]^1)))+
  lims(y = c(-1,5))+
  theme_classic()

slr <- lm(log(y) ~ temp)
summary(slr)

# prediction of y (1/q) in ha/MGD using Danbury data
pred_ha_MGD <- predict(slr, newdata=data)

# bind the column
data <- cbind(data,pred_ha_MGD)

#convert from log back to actual value
data$pred_ha_MGD <- exp(data$pred_ha_MGD)

min(data$pred_ha_MGD, na.rm=TRUE)
max(data$pred_ha_MGD, na.rm=TRUE)
mean(data$pred_ha_MGD, na.rm=TRUE)
sd(data$pred_ha_MGD, na.rm=TRUE)
n_distinct(data$pred_ha_MGD, na.rm=TRUE)

# calculate area needed by multiplying the predicted y (pred_ha_MGD) by the observed monthly flow (MGD)
data$area90 <- data$flow*data$pred_ha_MGD

summary(data$area90)

# Plot using area (ha) and months for Danbury
data %>%
  ggplot()+
  geom_point(aes(x = month(date, label=TRUE, abbr=TRUE), y = area90))+
  geom_smooth(aes(x = month(date), y = area90))+
  lims(y = c(0,1.25))+
  theme_bw()+
  labs(x="Month", y = expression(Area[90]~(ha)))

# Plot using predicted area (ha) per 1 MGD of flow and months for Danbury
data %>%

```

```

ggplot()+
  geom_point(aes(x = month(date, label=TRUE, abbr=TRUE), y = pred_ha_MGD))+
  geom_smooth(aes(x = month(date), y = pred_ha_MGD))+
  lims(y = c(0,35))+
  theme_bw()+
  labs(x="Month", y = expression(A[90]^1~(ha~MGD^-1)))

#####3
# area for 50%
# constant removal rate of 0.1 (90% removal)
rem <- rep(0.5, n)

# blank vector for y
y <- rep(0,n)

# blank vector for k
k <- rep(0,n)

# meat and potatoes evaluation using the arrenhius and TIS model
for(i in 1:n){
  k[i] <- k20[i]*1.106^(temp[i]-20)
  y[i] <- (((rem[i])^(-1/N[i]))-1)*(N[i]/k[i])
  y[i] <- (y[i]*0.003785*10^6)/10000
}

# summary of y values ( y is in ha/MGD - see Jasper, 2014)
summary(y)
sd(y)
shapiro.test(y)

ggplot()+
  geom_density(aes(y))

ggplot()+
  geom_point(aes(x = k, y= y))

# Create an area value for different flows at danbury - Blocked out, doesn't make sense
# Qin <- rnorm(n, mean = 0.033, sd = 0.01)
# Area <- Qin*y

# summary(Area)
#ggplot()+
# geom_density(aes(Area))

ggplot()+
  geom_point(aes(x = temp, y = log(y)))+
  geom_smooth(aes(x = temp, y = log(y)),method = "lm")+
  labs(x = expression(paste('Temperature (',degree,'C',sep='')), y = expression(ln(A[50]^1)))+
  lims(y = c(-1,5))+
  theme_classic()

max(temp)
slr <- lm(log(y) ~ temp)
summary(slr)

# prediction of y (1/q) in ha/MGD using Danbury data
pred50_ha_MGD <- predict(slr, newdata=data)

# bind the column
data <- cbind(data,pred50_ha_MGD)

```

```

# Convert back to actual value
data$pred50_ha_MGD <- exp(data$pred50_ha_MGD)

# calculate area needed by multiplying the predicted y (pred_ha_MGD) by the observed monthly flow (MGD)
data$area50 <- data$flow*data$pred50_ha_MGD

summary(data$pred50_ha_MGD)
summary(data$pred_ha_MGD)

# Plot using area (ha) and months for Danbury
data %>%
  ggplot()+
  geom_point(aes(x = month(date, label=TRUE, abbr=TRUE), y = area90))+
  geom_smooth(aes(x = month(date), y = area90))+
  geom_point(aes(x = month(date, label=TRUE, abbr=TRUE), y = area50), shape = 3)+
  geom_smooth(aes(x = month(date), y = area50), color = "black", linetype = 2)+
  lims(y = c(0,1))+
  theme_bw()+
  labs(x="Month", y = expression(Area~(ha)))

# Plot using predicted area (ha) per 1 MGD of flow and months for Danbury
data %>%
  ggplot()+
  geom_point(aes(x = month(date, label=TRUE, abbr=TRUE), y = pred_ha_MGD))+
  geom_smooth(aes(x = month(date), y = pred_ha_MGD))+
  geom_point(aes(x = month(date, label=TRUE, abbr=TRUE), y = pred50_ha_MGD), shape = 3)+
  geom_smooth(aes(x = month(date), y = pred50_ha_MGD), linetype = 2)+
  lims(y = c(0,35))+
  theme_bw()+
  labs(x="Month", y = expression(A[50/90]^1~(ha~MGD^-1)))

```